City Research Online

City, University of London Institutional Repository

Ethnic differences in the spatial distribution of macular pigment and its association with foveal anatomy

Irene Ctori

Doctor of Philosophy

City University London

Division of Optometry and Visual Science

March 2016

.

THE FOLLOWING PREVIOUSLY PUBLISHED PAPER HAS BEEN REDACTED FOR COPYRIGHT REASONS:

This page is intentionally left blank

TABLE OF CONTENTS

List of Tables

7

List of Figures

against retinal eccentricity (x-axis), indicated by the red line. The shaded grey area schematically represents one CoR above and below the exponential fit to the data (grey dashed line). According to the objective profile classification, d) shows an exponential profile; e) shows a ring-like profile, whereby MPOD at 0.8º is more than 1 CoR above the exponential fit line and f) shows that although image c) was subjectively classified as a central dip, central MPOD is not more than 1 CoR below the exponential fit line and is therefore objectively classified as an exponential profile.

This page is intentionally left blank

Acknowledgements

First and foremost I would like to express my special appreciation and huge gratitude to my supervisor Dr Byki Huntjens. With endless enthusiasm you gave me continuous support and allowed me to grow as a research scientist. I have truly enjoyed my experience throughout this process. Thank you.

For this thesis, I would like to thank Professor Chris Hull for the astute comments and suggestions. Your advice on the statistical analysis was particularly helpful.

I gratefully acknowledge Professor John Barbur for use of the Macular Assessment Profile test and Carl Zeiss Meditec for use of the IOLMaster. In addition, I thank the TwinsUK registry at St Thomas' Hospital London for access to the twin data and Dr Omar Mahroo for visual classification of macular pigment spatial profiles based on fundus autofluorescence scan images.

I am especially indebted to all the volunteers that took time out of their busy day to take part in the research study. It was a pleasure to meet you all and I still smile at some of the amusing tales you told me.

Mum and Dad, from a very young age you instilled in me a thirst for knowledge and a desire to always achieve the best that I can. Words cannot express how grateful I am to you both, and also to my mother-in-law and father-in-law for all of your help over the years.

Lastly, I would like to thank my family for their never-ending love and encouragement. To my children Alex and Katerina, I hope I have inspired you to never stop learning and to always follow your dreams. And to my husband Peter, thank you for faithfully supporting me to follow mine.

This page is intentionally left blank

Declaration

17

I hereby grant powers of discretion to the University Librarian to allow this thesis to be copied in whole or in part without further reference to the author. This permission covers only single copies made for study purposes, subject to normal conditions of acknowledgement.

This page is intentionally left blank

Abstract

Macular pigment (MP) at the centre of the retina is thought to serve a protective function shielding the photoreceptors from damaging effects of blue light. The amount of MP and its spatial density distribution across the macula i.e. its spatial profile varies among individuals. Lower levels of MP and certain MP spatial profile phenotypes are believed to be associated with increased risk of age-related macular degeneration (AMD). There is suggestion that MP spatial profiles differ between ethnicities, with non-exponential profiles occurring more frequently in non-whites. This may explain some of the ethnic variations seen in AMD prevalence. However, previous investigations have used several methodologies to measure MP. In addition, inconsistent MP spatial profile definitions have been used; thus comparing data between studies is difficult. Nevertheless, it has been hypothesised that variations in MP spatial distribution could be due to differences in foveal architecture, in particular at the foveal centre where MP levels peak.

A study was designed to investigate the effect of ethnicity on MP spatial density distribution and its relation to foveal architecture. The influence of known risk factors for AMD was also considered. Young (18 to 39 years), healthy volunteers of white (n = 76), South Asian (n = 80) and black (n = 70) ethnic origin were recruited to take part. MP measurements were obtained using a method based on heterochromatic flicker photometry (HFP) and foveal morphology measurements were taken from optical coherence tomography (OCT) scans. The coefficients of repeatability of each of these were confirmed in a sub-study. A systematic objective MP spatial profile classification technique was implemented throughout. The feasibility of applying this to MP measurements obtained with different techniques such as HFP and fundus autofluorescence (FAF) was also explored in a sub-study.

The results showed that measures of MP optical density (MPOD) over the central retinal area were statistically significantly increased in South Asian and black compared to white subjects, whereby ethnicity explained around 10% of the variation (P < 0.0005). Non-exponential MP spatial profiles (ring-like and central dip respectively) were significantly more prevalent in South Asian and black compared with white subjects (χ^2 (4, n = 226) = 13.4, P = 0.009). Integrated MPOD up to 1.8º was significantly increased in ring-like and central dip compared to exponential profiles (P < 0.0005) irrespective of ethnicity. South Asian and black individuals presented thinner central retinas and wider foveas compared to white individuals (P < 0.0005). However, while accounting for these ethnic variations, foveal architecture provided no predictive values for the MP spatial profile phenotype.

Key of abbreviations

AMD	age-related macular degeneration
ANCOVA	analysis of covariance
ANOVA	analysis of variance
AREDS	Age-Related Eye Disease Study
BMI	body mass index
CAREDS	Carotenoids and Age-Related Eye Disease Study
CFF	critical flicker frequency
CFT	central foveal thickness
CH	choroid
cHFP	customized HFP
CoR	Coefficient of Repeatability
DZ	dizygotic
ETDRS	Early Treatment Diabetic Retinopathy Study
ELM	external limiting membrane
FAF	fundus autofluorescence
FR	fundus reflectometry
GCL	ganglion cell layer
HFP	heterochromatic flicker photometry
HPLC	high performance liquid chromatography
HRA	Heidelberg retina angiograph
INL	inner nuclear layer
IPL	inner plexiform layer
IRL	inner retinal layer
IS	inner segments
K	keratometry
L	lutein
LoA	limits of agreement
logMAR	logarithm of minimal angle of resolution
LW	long wavelength
MAP	Macular Assessment Profile

Md	median
MFT	minimum foveal thickness
MP	macular pigment
MPOD	macular pigment optical density
MSE	mean spherical error
meso-Z	meso-zeaxanthin
MZ	monozygotic
OCT	optical coherence tomography
ONL	outer nuclear layer
OPL	outer plexiform layer
OS	outer segments
PR	photoreceptor layer
RNFL	retinal nerve fibre layer
RPE	retinal pigment epithelium
RRS	resonance Raman spectroscopy
RT	retinal thickness
SD	standard deviation
SD-OCT	spectral domain optical coherence tomography
SW	short wavelength
UV	ultraviolet
VDU	visual display unit
Z	zeaxanthin

This page is intentionally left blank

Thesis synopsis

The candidate Irene Ctori (IC) carried out a thorough review of current literature relating to the variation of macular pigment (MP) with ethnicity and its association with foveal architecture. The first chapter begins with an outline of the composition of the carotenoids that constitute macular pigment (MP) and a summary of its function and anatomical location. The concentration of MP is measured in vivo as MP optical density (MPOD) and is a measure of the amount of blue light attenuation by MP. Methods of measuring MPOD in vivo vary considerably. The most widely used techniques, including assumptions, limitations and disadvantages are briefly reviewed in Chapter 1, with more detail provided on the subjective psychophysical test used in the research study.

Variations in the classification of MP spatial density profile phenotype across the literature are also described in Chapter 1, demonstrating the difficulties in comparing findings between studies due to inconsistent interpretation of data. It is known that MPOD typically peaks at the centre of the fovea, while following an exponential decline away from it. There have been numerous reports of deviations away from an exponential decline e.g. a secondary peak manifesting as a ring-like structure. These rings are usually located between 0.5º and 1.2º away from the centre of the fovea. As well as ring-like structures, dips at the centre of the MP spatial density distribution have been identified. However, there is currently no consensus on a universal classification system, mainly because the definitions of profiles vary among studies. Notwithstanding, presence of non-exponential profiles has been demonstrated using subjective psychophysical methods such as heterochromatic flicker photometry (HFP), as well as objective fundus autofluorescence (FAF). It must be kept in mind that the classification of spatial profiles is often purely based on visual deviations from an expected exponential curve and it has been questioned whether the ring-like structure is a real perturbation or whether it is a result of an artefact of the MP measurement technique. The amplitude of deviations away from an exponential fit is often small and may not be statistically reliable. Nevertheless, there has been great interest in understanding the relevance of the MP spatial density distribution over the central retina, for example in relation to age-related macular degeneration (AMD) and dietary intake of carotenoids. Chapter 1 concludes with a consideration of the factors that may influence inter-individual variations in MP and its spatial profile.

An investigation of the repeatability of MPOD measurements obtained using two different MPOD measuring techniques (HFP and FAF imaging), is presented in Chapter 2. The first investigation based on HFP methods included MPOD data collected by the candidate IC (n = 26) combined with data collected from an additional fourteen individuals as part of a previous study (Huntjens et al., 2014). The second investigation included MPOD data for forty subjects acquired using two-wavelength FAF imaging collected as part of a separate study (Hammond et al., 2012) in which IC was not involved. The candidate IC carried out the data analysis described in Chapter 2. For each subject (n = 40 for each technique), point MPOD measurements at several retinal eccentricities were used to determine a two-dimensional MP spatial profile, to which a systematic objective profile phenotype classification was applied, based on the repeatability coefficient of the instrument. Our research group reported this classification method describing exponential, ring-like and central dip profiles in a recently published article, included in the Appendix 6.1 (Huntjens et al., 2014). The reproducibility of spatial profile phenotyping is also reported in this chapter. In addition, results of a study whereby existing twin MPOD data (Tariq et al., 2014) were re-analyzed by the candidate IC to investigate the feasibility of applying the objective classification system to MPOD data obtained by FAF imaging is included in Chapter 2. The findings show that while the systematic objective MP spatial profile classification is highly reproducible, there are some shortcomings when applying this to MPOD data obtained using FAF imaging. An alternative approach to report an integrated MPOD measurement that captures information regarding the amount of MP over the foveal area is recommended for future studies. Calculation and repeatability of integrated MPOD measurements are described in detail within this chapter.

To our knowledge there are no reports comparing differences in MP spatial profile phenotypes between ethnic groups. One of the main aims of this research study was to investigate variations in MPOD and its presentation as different spatial profiles phenotypes among three ethnic groups: white, South Asian and black. Ethnicity for the purpose of this research project was classified according to the criteria used by the Office for National Statistics (Office for National Statistics, 2013). The choice of ethnicities to include in the study was based on the three largest ethnic groups in England and Wales. According to data from the 2011 census for England and Wales the largest representation of 86% of the population (around 48 million people in 2011) are those of white ethnicity. The next largest group accounting for 5.5% of the population is formed from those of South Asian ethnicity,

including Indian, Bangladeshi and Pakistani. Individuals of black ethnicity (African and Caribbean) represent 2% of the population (Office for National Statistics, 2011). An added benefit of selecting these three ethnic groups is the limited research on the comparison of MP and its spatial profile among these ethnicities.

Chapter 3 presents a study (conducted solely by the candidate IC) investigating variations in MP and its spatial density distribution, among the three aforementioned ethnic groups. Approximately seventy-five young, healthy subjects for each of three ethnic groups were included in the study. MPOD was measured using a HFP based method. The influences of known risk factors for AMD such as age, gender and smoking status were included in the data analysis. Differences in MP spatial profile prevalence between the ethnicities are described. The results showed that as well as increased central and integrated MPOD, non-exponential spatial profiles were more prevalent in the non-white ethnic groups.

The cause of variations in MPOD among different ethnic groups may be due to variations in foveal anatomy. Chapter 4 describes an investigation of the relationship between the amount of MP present and its spatial profile phenotype with foveal architecture among the three ethnic groups. The candidate IC carried out all investigations described in Chapter 4. Foveal morphology measurements were taken from SD-OCT scans acquired using the Spectralis device (Heidelberg Engineering, Germany). Several parameters, such as foveal width, central retinal thickness and gradient of the foveal pit profile slope were included in data analysis. With the recent introduction of new Spectralis software (version 6.0c) that allowed the measurement of individual retinal layer thickness, the correlation between individual retinal layers relative to the location of MPOD measurement was also assessed. In addition, Chapter 4 includes details of two additional studies in relation to this: 1) the effect of ocular magnification on SD-OCT scans acquired using the Spectralis instrument (Ctori et al., 2014) (Appendix 6.2), and 2) repeatability of individual retinal layer thickness and foveal width measurements (Ctori and Huntjens, 2015) (Appendix 6.3).

Chapter 5 summarises the conclusions of the investigations from previous chapters. A section is dedicated to future studies following the work described. The participant information sheet, consent form and health questionnaire are included in Appendix 6.4, 6.5 and 6.6. A list of publications and presentations produced by the candidate

IC is also provided in Appendix 6.7. All statistical analysis described within this thesis was conducted by the candidate IC.

The key objectives of this work were to:

1. Establish the repeatability of MPOD measurements and reproducibility of MP spatial profile classification obtained by either objective or subjective methods;

2. Investigate the feasibility of implementing a method of classifying the MP spatial profile that can be applied to any method of measuring MPOD;

3. Describe variations in MP spatial density distribution among three ethnic groups;

4. Verify the optimum method of obtaining foveal measurements using the Spectralis SD-OCT device taking into account ocular magnification;

5. Evaluate the repeatability of foveal measurements derived from the Spectralis SD-OCT device;

6. Explore the hypothesis that foveal anatomy influences the distribution of MP with emphasis on the potential impact of ethnicity.

The major findings of the thesis are:

1. Deviations away from an exponential decline in MPOD from the centre of the fovea are real and reproducible;

2. In the absence of a classification method that can be applied to all techniques of measuring MPOD we recommend that an integrated value of MPOD be reported to allow for comparisons between studies;

3. Ethnicity plays an important part in variations observed between MP spatial profiles. The amount of MP over the central retina area varies between different ethnic groups, whereby it is lower in white compared to non-white ethnic groups. Non-exponential profiles are more common in certain ethnic groups. It is therefore important to report and consider ethnicity in future studies;

4. The effect of ocular magnification on lateral Spectralis SD-OCT scan measurements is minimized when corneal curvature data is included during scan acquisition;

5. Foveal measurements including individual retinal layers at the centre of the fovea and up to 5° eccentricity are highly repeatable;

6. While accounting for ethnic variations in retinal anatomy, foveal architecture provided no predictive values for the MP spatial profile or indeed average or integrated MP over the central retina.

1 Background: Macular pigment, its measurement, spatial density distribution and inter-individual variations

1.1 Macular pigment

The macula is an avascular, horizontally oval area around 5 to 6mm in diameter, located at the centre of the posterior pole of the retina. It subtends approximately 15° to 20° of the visual field and is responsible for central high-resolution vision. In the middle of the macula, the fovea occupies an area of around 1.85mm diameter, corresponding to 5° of the visual field, with the foveola located centrally occupying about 0.35mm (Figure 1). The area immediately surrounding the foveola is known as the parafovea and beyond this is the perifovea (Bron et al., 1997).
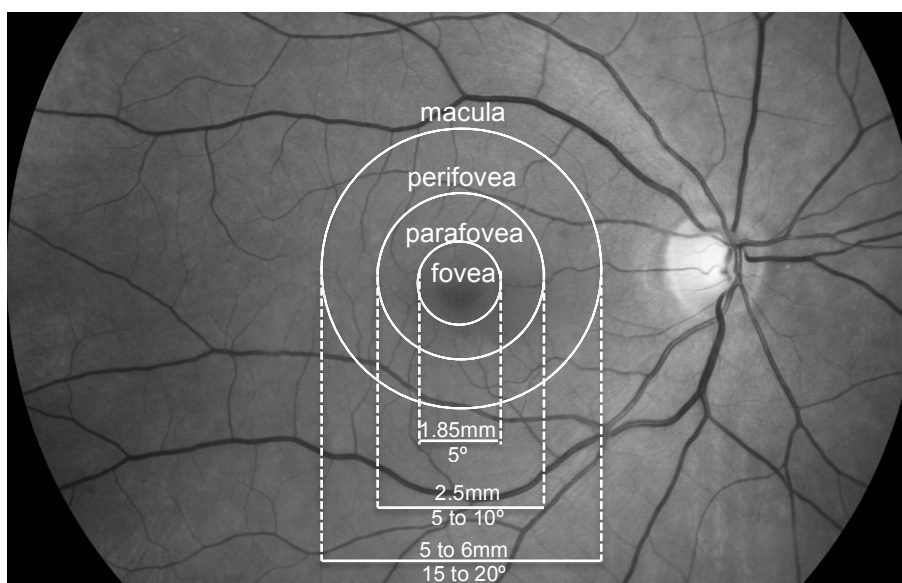
Figure 1 Fundus image of the right eye showing macular dimensions (not to scale). Image adapted from retinagallery.com.

The characteristic yellow colour at the centre of the fovea is due to the presence of macular pigment (MP), composed of the carotenoids lutein (L), zeaxanthin (Z) and meso-zeaxanthin (meso-Z). Carotenoids have been identified in human ocular tissues such as the crystalline lens (Yeum et al., 1995) and the retina (Bernstein et al., 2001). While L and Z are detectable throughout the retina, meso-Z is the only carotenoid found exclusively in the macula (Snodderly et al., 1984a, Snodderly et al., 1984b, Bone et al., 1988). Chemical analysis by high performance liquid chromatography (HPLC) has been used on donor human retinas to confirm that MP comprises the carotenoids L, Z, and meso-Z (Bone et al., 1988, Handelman et al., 1988, Bone et al., 1993). The chemically identical isomers L and Z are also known as xanthophyll carotenoids.

Humans and primates rely solely on dietary sources of L and Z since carotenoids cannot be synthesized *de novo.* A marked deficiency of MP in macaque monkeys has been demonstrated following a carotenoid-deprived diet (Malinow et al., 1980, Neuringer et al., 2004). In contrast, it is thought that meso-Z is formed in the retina (Bone et al., 1993). Investigations involving human subjects have confirmed that only L and Z are found in blood plasma. The lack of meso-Z in the blood implies that it is metabolized in the retina or is a conversion product (Bone et al., 1993). Such a transformation is viable since the three carotenoids have very similar chemical structures (Figure 2) (Bone et al., 1993).
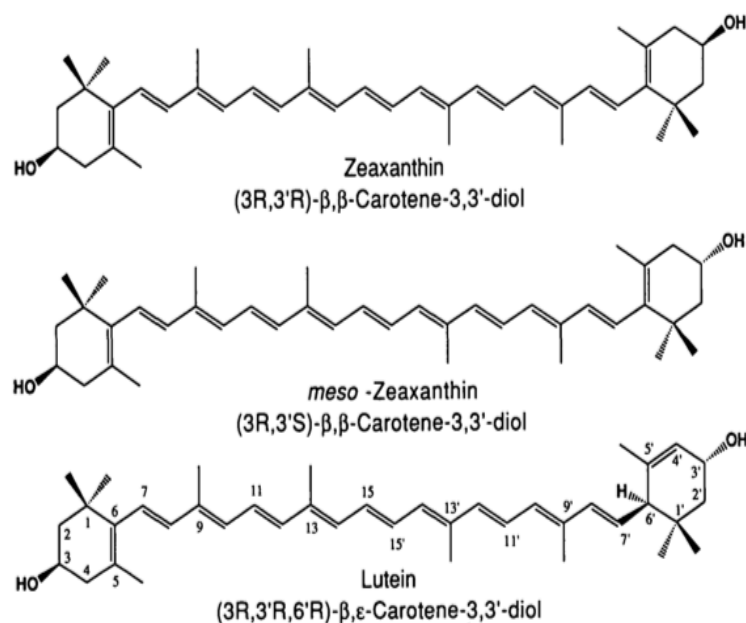
Figure 2 The chemical structures of lutein, zeaxanthin and meso-zeaxanthin (from Bone et al., 1993).

While L exceeds Z in blood plasma, the combined Z stereoisomers exceed L in the retina. This provides further support of the hypothesis that meso-Z is a derivative of L formed by chemical processes within the retina itself (Bone et al., 1993, Bone et al., 1997). In vitro studies on the distribution of MP have shown that the concentration of Z in the foveal region is approximately twice that of L (Bone et al., 1988, Handelman et al., 1988, Snodderly et al., 1991, Bone et al., 1997). This ratio changes with eccentricity, so that beyond the fovea, L dominates with a ratio of L:Z exceeding 2:1 at the periphery of the macula as shown in Figure 3 (Bone et al., 1988, Handelman et al., 1988, Landrum, 2001).
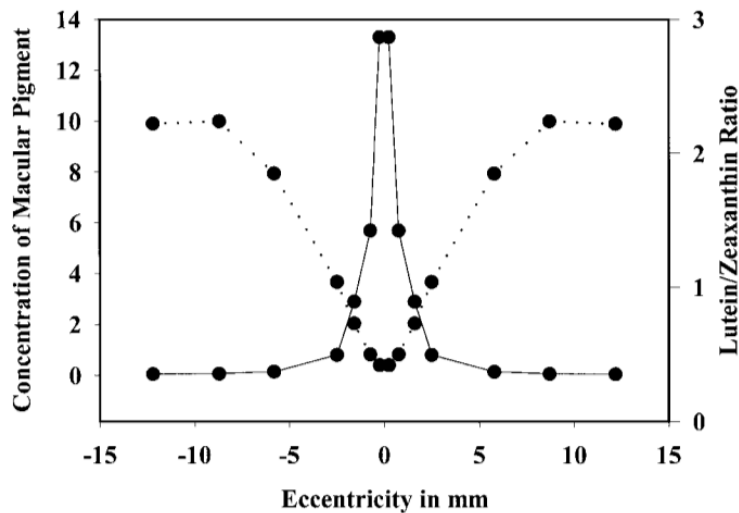
Figure 3 Concentration of MP in the human macula as measured by HPLC (solid line). The ratio of lutein: zeaxanthin plotted against eccentricity from the fovea indicated by the dotted line. From Landrum and Bone (2001).

This finding has been confirmed in vivo, in which the level of Z dropped below the level of L at about 2° retinal eccentricity (van de Kraats et al., 2008). It is thought that isomerase catalyses the reaction of L into meso-Z, although this process is not straightforward. This process appears to occur selectively in the inner annulus of the macula nearer the fovea, where the meso-Z:Z ratio is high and the L:Z ratio is low. The hypothesis that L is converted to meso-Z is supported by the finding of a low concentration of L in the central region of the retina compared to the reverse situation in the outer annulus (Bone et al., 1997). Furthermore, the variation in (L + meso-Z):Z ratio across the retina is thought to be due to the location of the isomerase catalyst in the cone cell axons, resulting in a reduced conversion rate of L to meso-Z with eccentricity from the fovea (Bone et al., 1997). Nonetheless, it must be noted that the hypothesis that meso-Z is derived solely from L has been challenged (Bhosale et al., 2007). Indeed, it has been recommended that the presence of meso-Z in foodstuffs be further investigated using modern techniques (Nolan et al., 2013).

1.1.1 Functions of macular pigment

The macular carotenoids potentially play an important role in the protection of the retina. This has drawn particular interest with regards to age-related macular degeneration (AMD), especially because of the paucity in treatment options for the condition. AMD is one of the leading causes of irreversible blindness in the Western

World (Pascolini and Mariotti, 2012, Bourne et al., 2013) and remains one of the leading causes of certified visual loss in England and Wales (Bunce and Wormald, 2006, Bunce et al., 2010). The condition is characterized by a degenerative disorder of the central area of the retina causing significant visual loss (Bird et al., 1995). The findings of a recent population study based on nine hundred and sixty-three participants suggested that cumulative ocular exposure to blue light is associated with increased prevalence of AMD (Delcourt et al., 2014). Chronic light exposure has been implicated with the incidence of early stage AMD (Cruickshanks et al., 1993, Cruickshanks et al., 2001, Tomany et al., 2004) and late stage AMD (Hirakawa et al., 2008). MP is thought to protect the macular region by filtering harmful blue light (Junghans et al., 2001, Barker et al., 2011, Bone et al., 2012). Lower levels of MP are therefore believed to be associated with an increased prevalence of AMD (Beatty et al., 2001, Nolan et al., 2007b, Obana et al., 2008).

The cornea absorbs most ultraviolet (UV) light below 295nm. The crystalline lens absorbs UVA (280 to 315nm) and UVB (315 to 400nm) light (Boettner and Wolter, 1962) so that almost all UV light is absorbed before it reaches the retina (Weale, 1988). However, the retina remains vulnerable to the damaging effects caused by the products of photochemical reactions following the absorption of high energy, short wavelength (SW) blue light of 400 to 500nm. A recent study attempted to quantify the cumulative light distribution on the retina in an attempt to establish whether the macula is exposed to a greater flux of light compared to the surrounding retina. Although there were limitations in the methodology encountered by the use of a scene camera as an imaging photometer, the results were interesting. Levels of light appeared to peak in the macula in some individuals undertaking certain tasks, for example computer work. It seems that in these scenarios there would be an increased likelihood of damage to the macula, although this may be mitigated by the presence of MP (Bone et al., 2012). The high concentration of the carotenoids at the macula overlying the central photoreceptors suggests that MP serves some critical function by shielding the macula from continuous exposure to light.

MP maximally absorbs SW blue light at 454nm (Snodderly et al., 1984b, Bone et al., 1992). The absorption spectra of the individual carotenoids L, Z and meso-Z vary slightly, so that in combination, a wider range of wavelength light incident on the retina is attenuated. This enables MP to filter out harmful visible blue light between 400 to 500nm (Junghans et al., 2001). In particular, the anatomical positioning of MP within the retinal layers places it in an ideal position to protect the underlying photoreceptor

cells (Snodderly et al., 1984a, Trieschmann et al., 2008). The orientation of L and Z parallel to the plane of the cell membrane, enhanced by the additional perpendicular orientation of L, allows MP to absorb light from all directions (Sujak et al., 1999). Indeed, this dual orientation of L has been suggested as the reason why L has a greater filter efficacy than Z (Junghans et al., 2001). It is notable that the filtering effects of MP are not uniform across the macula due to the variation in its topographic distribution. Since MP levels peak in the central retina at the macula, blue-light absorption is greatest at this location (Stringham et al., 2006). Despite this uneven distribution of MP, the visual system employs a compensation mechanism involving an increased gain of the s-cone pathway so that sensitivity to wavelengths of light remains constant across the retina (Werner et al., 2000, Rodriguez-Carmona et al., 2006, Stringham et al., 2006).

As well as acting as an optical filter, MP quenches toxic antioxidants and neutralizes active free radicals formed by oxidative stress (Khachik et al., 1997, Kim et al., 2006), thus preventing their capacity to damage the retina. It is thought that oxidative stress is one of the main pathogenic factors involved in AMD (Khandhadia and Lotery, 2010, Brantley et al., 2012, Jarrett and Boulton, 2012). The likelihood of degenerative macular disease may therefore be reduced with increased MP levels (Beatty et al., 2000b, Jarrett and Boulton, 2012). Indeed there is evidence to suggest that the antioxidant activity of L and Z is greater than its blue light filtering capacity. In a previous investigation, reduced retinal damage from acute blue light exposure was demonstrated in primate retinas with MP compared to those without any MP. Biochemical measurements indicated that this reduction in damage by L and Z was brought about more by protection against photochemical reactions via antioxidant activity than by their blue light filtering capacity. In addition, it was also proposed that the same protective mechanisms of L and Z against the acute effects of blue light are likely to take place with chronic exposure (Barker et al., 2011).

Many factors such as age, inflammation and smoking promote oxidative damage. In addition, photochemical reactions have been shown to be a cause of oxidative stress (Beatty et al., 2000b). The retina is particularly vulnerable to oxidative stress due to the constant exposure to visible light. In addition, the high oxygen consumption levels of the retina and therefore the high levels of oxygen in the retina also promote oxidative damage. Furthermore, polyunsaturated fatty acids in the inner segments of the photoreceptors are especially vulnerable to oxidative stress (Beatty et al., 2000b, Organisciak and Vaughan, 2010). Oxidative processes result in the formation of

reactive oxygen intermediates including free radicals and singlet oxygen. Reactive oxygen intermediates are highly reactive molecules, atoms or ions that target mitochondria and lipids. The location of MP within the lipid membranes of the human retina places the carotenoids in an ideal position to act as lipid antioxidants. Moreover, it has been suggested that the chemical structure of the carotenoids, specifically the presence of the hydroxyl groups, plays a role in their antioxidant activity (Khachik et al., 1997). Together with lipid antioxidant capabilities, L and Z provide direct neuroprotection of the photoreceptors (Kim et al., 2006, Chucair et al., 2007). The location of MP overlying the central photoreceptors places it ideally for this role. In addition, the association of L and Z with xanthophyll-binding proteins appears to enhance synergistically the antioxidant activity (Bhosale and Bernstein, 2005). When the antioxidant capability of the macular carotenoids has been compared, meso-Z has been shown to be a more robust antioxidant than Z, while Z is more potent than L (Sujak et al., 1999, Bhosale and Bernstein, 2005, Kim et al., 2006).

Besides the protective function of the macular carotenoids, there has been speculation as to the potential effect of MP on visual performance. It has been proposed that visual acuity is enhanced by the absorption of SW light by MP, hence reducing chromatic aberration and potential image degradation (Wooten and Hammond, 2002). To test the plausibility of the *acuity hypothesis,* gap acuity, hyperacuity and levels of MP were measured in a study including eighty healthy young subjects. Different responses were elicited by performing the acuity tests under different illumination conditions. These included a mid-yellow illumination not absorbed by MP and a perceptual white light illumination, with a blue component that is absorbed by MP. The results showed no correlation between MP levels and hyper-acuity or gap acuity. Furthermore, there was no significant difference in response between the different illumination conditions and it was therefore concluded that since MP did not appear to provide an optical function, it was more likely to serve a biological purpose (Engles et al., 2007). In contrast to this, a statistically significant moderate positive correlation ($r = 0.3$, $P < 0.01$) was found between MP and best-corrected visual acuity in a study involving one hundred and forty-two young healthy subjects (Loughman et al., 2010). In addition, increased MP was associated with improved contrast sensitivity at intermediate spatial frequencies, in both photopic and mesopic conditions (Kvansakul et al., 2006, Loughman et al., 2010).

It has been shown that variations in the amount of MP present may be correlated with some optical factors of visual function resulting in enhanced visual performance. Given that MP attenuates the amount of incident SW light on the central retina, the effect of

MP on the photophobic reaction has been investigated. A decreased photophobic reaction (measured as less squinting) was reported in subjects with higher MP levels (Stringham et al., 2003, Stringham et al., 2004). The authors considered this an enhancement to visual performance since there was less discomfort in response to a bright light stimulus in those with increased MP. In addition, laboratory data have indicated that increased MP is associated with a reduction in discomfort glare. This is known as the *glare hypothesis* and may be due to veiling luminance filtering by MP, thereby increasing comfort. In addition, photostress recovery was found inversely related to MP (Stringham and Hammond, 2007, Stringham and Hammond, 2008). Although it is an attractive proposition that MP plays a role in diminishing glare discomfort, it must be noted that these effects were demonstrated in an artificial laboratory environment. Consequently the results may not be applicable or valid in an ecological sense (Stringham and Hammond, 2007, Stringham and Hammond, 2008). To this aim, a more recent study re-examined the variation of MP on the immediate effects on visual function on a sample of one hundred and fifty healthy individuals. Glare disability and photostress recovery were measured using carefully selected stimuli that matched the midday sunlight spectrum and were therefore considered ecologically valid. Increased MP was associated with improved photostress recovery, glare disability and chromatic contrast (Hammond et al., 2013). These findings are not consistent across the literature however (Loughman et al., 2010). The contradictory evidence regarding the effect of MP on visual performance may be explained by the variations in methodology used in different studies, illustrating the difficulties in applying the results of visual performance tasks in laboratory settings to everyday life.

1.1.2   Anatomical location of macular pigment within the retina

The fovea is critical for high-resolution visual acuity and colour vision. The accumulation of the xanthophyll carotenoids within the fovea places MP in an ideal location to act as a blue light filter. The exact location of MP within the retinal layers has drawn much interest due to its potential putative role against AMD. The morphology of the individual layers of the retina has been identified by histological examination (Hendrickson, 1992, Hendrickson et al., 2012) as presented in Figure 4.

The outer retina includes the retinal pigment epithelium (RPE), overlying the choroid, and the photoreceptor outer segments (OS) and inner segment (IS) layers. The

external limiting membrane (ELM) separates the outer and inner retinal layers. The inner retina includes the following: the outer nuclear layer (ONL), containing a single row of cone cell bodies near the ELM and multiple rows of deeper rod cell bodies; the outer plexiform layer (OPL), hosting the Henle fibres (unmyelinated photoreceptor axons); the inner nuclear layer (INL), containing the cell bodies of horizontal, bipolar cells, Müller glia and amacrine cells; the inner plexiform layer (IPL); the ganglion cell layer (GCL); and the nerve fibre layer (NFL) (Hendrickson et al., 2012).
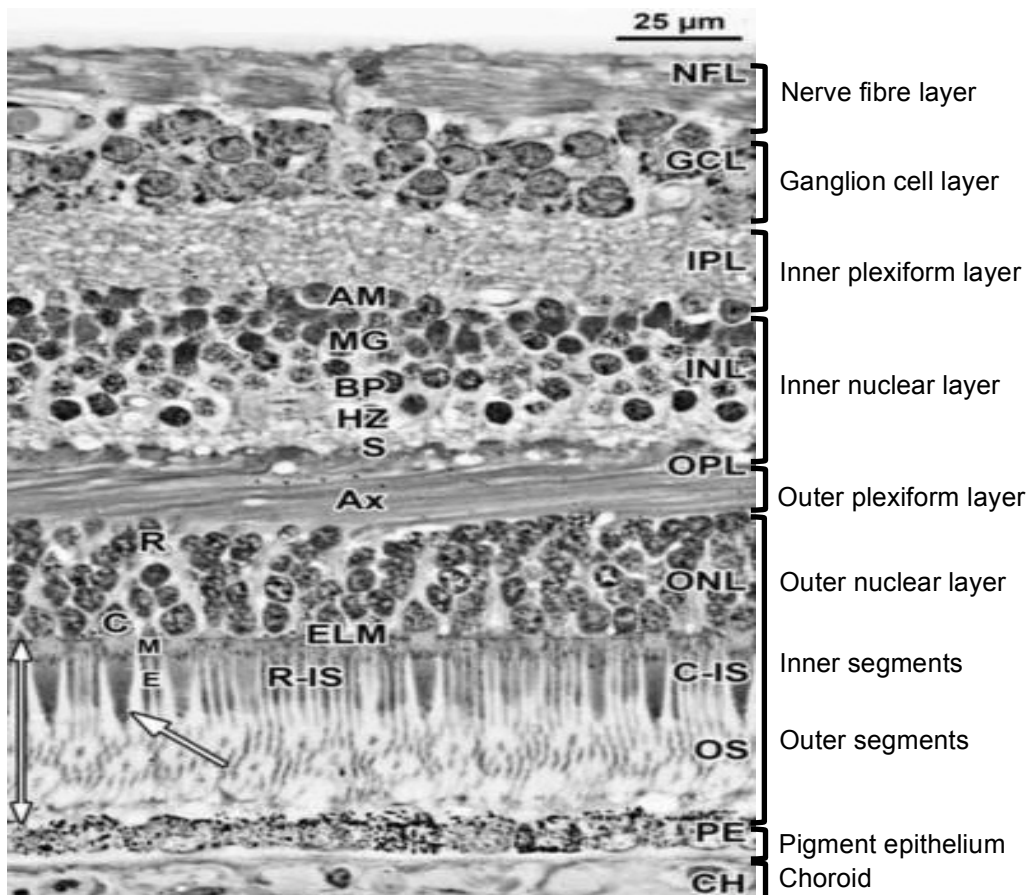
Figure 4 Layers and histology of normal adult human retina at 2mm nasal from the fovea centre. Adapted from Hendrickson et al. (2012). Abbreviations: choroid (CH); pigment epithelium (PE); outer segments (OS); cone inner segments C-(IS); rod inner segments (R-IS); inner segment ellipsoid (E) and myeloid (M); external limiting membrane (ELM); outer nuclear layer (ONL); cone cell bodies (C); rod cell bodies (R); outer plexiform layer (OPL); photoreceptor axons (Ax); synaptic layer (S); inner nuclear layer (INL); horizontal cells (Hz); bipolar cells (BP); Müller glia (MG); amacrine cells (AM); inner plexiform layer (IPL); ganglion cell layer (GCL); nerve fibre layer (NFL).

Histological studies of primate retinas have shown that the highest concentrations of MP are present in the photoreceptor axons (layer of the fibres of Henle) at the fovea

and in the inner plexiform layer outside the foveola as shown in Figure 5 (Snodderly et al., 1984a, Snodderly et al., 1984b). The authors postulated that a vertical band of MP at the centre of the fovea was caused by axons from the outermost cones passing through the ONL. It was thought that the first horizontal band of MP was a result of the photoreceptor axon layer and that MP in the second horizontal layer was caused by interneurones within the IPL. More recent histological examinations of the human retina have confirmed that indeed MP concentration in the human retina is primarily located in the inner retinal layers. In the parafoveal region MP has been identified between the cell nuclei of the nuclear layer where fibres from the outer plexiform layer have horizontal extensions into the inner nuclear layer synapsing onto bipolar cells (Trieschmann et al., 2008). In addition, It was hypothesised that MP is also located within the Müller cell cone, an inverted conical area of Müller cells (Gass, 1999) based on evidence that the Müller cells interleaved amongst the cone photoreceptors contain macular carotenoids (Gass, 1999, Powner et al., 2010).
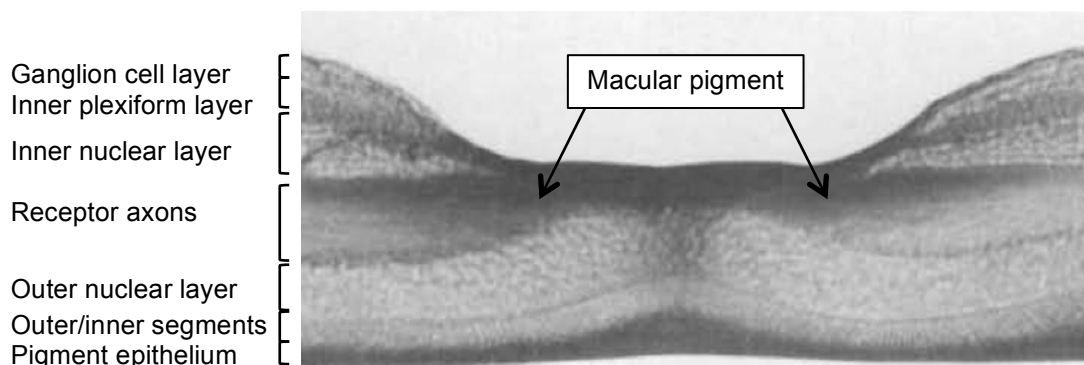
Figure 5 Photograph of histological section of the human retina taken in blue light (adapted from Snodderly et al., 1984a). MP absorbs blue light so that the anatomical location of MP is shown as dark areas, as indicated by the arrows.

Over thirty years ago it was suggested that the spatial distribution of MP might be attributed to its position within the individual retinal layers (Snodderly et al., 1984a, Snodderly et al., 1984b). The original 1984 Snodderly model described high concentrations of carotenoid in the inner retina. Given the association of MP with Müller cells it is plausible that the distribution of Müller cells across the retina may explain the distribution of MP across the central retina. Müller cell somata have been identified close to the foveal and parafoveal regions, with the concentration of Müller cells decreasing with increasing distance from the fovea. In addition, Müller cell processes are thinner and longer in the central retina compared to the periphery (Distler and Dreher, 1996). The 1984 Snodderly model also described the presence of

secondary peaks of MP in the plexiform layers (Snodderly et al., 1984a, Snodderly et al., 1984b). The association of MP with Müller cells may explain these secondary peaks caused by Müller cell side branches into the two plexiform layers.

The anatomical location of MP is crucial to its protective role as a blue light filter and an antioxidant described in section 1.1.1. Its preceptoral positioning within the inner retina places MP in an ideal position to act as an optical filter. However, in order for its antioxidant role to be fulfilled, MP must be located close to sites that are particularly vulnerable to oxidative stress. It had previously been proposed that the macular carotenoids are associated with photoreceptor type i.e. rod versus cone. As the L:Z ratio followed the same pattern as the rod: cone ratio when plotted as a function of eccentricity (Figure 3), it was thought that L is associated with rods and Z with cones (Bone et al., 1988). On the other hand, it was postulated that the distribution of L and Z was due to the relationship of the carotenoids with specific cone types, as both L and Z exist in the rod-free fovea (Snodderly et al., 1991). However, the presence of L and Z has been determined in the human retinal pigment epithelium in the rod outer segment (Rapp et al., 2000) thus indicating that the association of the carotenoids with photoreceptor type is not straightforward. Outside the fovea within the rod outer segments there is a greater combined L and Z concentration in the perifovea than the peripheral retina (Rapp et al., 2000). The finding of MP within the rod outer segments supports the hypothesis that MP plays an anti-oxidant role in the macula since the rod outer segments have been identified as a site susceptible to oxidative stress (Jin et al., 2001). Furthermore, within the retinal cell membranes, the orientation angles of L and Z vary, such that Z adopts a vertical orientation whereas L has two orthogonal orientations both parallel and perpendicular to the plane of the cell membrane. It is thought that this variation in positioning is thought to play a role in the protective efficacy of L and Z (Sujak et al., 1999).

1.2 Measurement of macular pigment optical density and its spatial profile

The distribution of MP in the retina has been determined by microspectrophotometry and two-wavelength microdensitometry analysis of donor primate maculae (Snodderly et al., 1984a, Snodderly et al., 1984b) and confirmed by HPLC on human donor retinas (Bone et al., 1988). Since in vitro methods are not appropriate for widespread use, various in vivo methods of measuring MP have been developed based on either subjective or objective techniques. The concentration of MP, measured in vivo as MPOD, is a measure of the amount of blue light attenuation by the macular carotenoids. MPOD serves as a surrogate optical indicator of carotenoid levels in the eye. Methods of measuring MPOD in vivo vary considerably. In order to compare findings from studies measuring MPOD using different methods it is important to understand the basis and limitations of the underlying principles of each technique. A thorough review of these has been conducted previously (Howells et al., 2011). A brief account of the most widely used techniques is provided in the following sections, with a more detailed description of the Macular Assessment Profile (MAP) test used to measure MPOD in the studies included within the thesis is provided in section 1.2.1.2. This includes the general principles of the MAP test and comparisons with other techniques.

1.2.1 Subjective psychophysical techniques

Subjective psychophysical methods require a response from the subject. Several tests exist, such as threshold spectral sensitivity (Pease et al., 1987), colour matching (Davies and Moreland, 2002) and motion photometry (Moreland, 2004, Bartlett and Eperjesi, 2011). These methods are time-consuming and generally difficult to perform so are not widely employed. The more commonly used subjective psychophysical techniques incorporate HFP, a well-accepted, non-invasive, in vivo technique. It does not require pupil dilation or photopigment bleaching and the equipment is less expensive relative to objective techniques.

1.2.1.1 Heterochromatic flicker photometry

The concept of HFP is based on the spectrally selective properties of MP (Snodderly et al., 1984b, Junghans et al., 2001). There is no "gold standard" for a single HFP method and many variations in methodology exist. In general, an optical system is used to

create two rapidly alternating beams of light, creating a high frequency flicker. The first beam is a monochromatic or spectrally narrow SW beam. This is the test wavelength and is set close to the maximum absorption of MP at around 460nm (i.e. blue). The second beam is of long wavelength (LW) from the region of the visible spectrum that is not absorbed by MP. The latter constitutes the reference wavelength, typically around 540nm (i.e. green) (Snodderly et al., 1984b, Stockman and Sharpe, 2000). During HFP techniques the intensity of the SW test beam is altered to eliminate the subject's perception of flicker. This is repeated at a parafoveal location where MP is assumed to be negligible (Snodderly et al., 1984a, Snodderly et al., 1984b, Bone et al., 1988, Berendschot and van Norren, 2006). The log ratio of the luminance required to null the flicker at both locations is calculated to give a measure of MPOD.

Throughout HFP methods, it is important for the stimulus to have an appropriate flicker frequency to allow the subject to determine a null point where no flicker is perceived. Nonetheless, the flicker frequency varies according to the chosen technique, ranging from 12 to 18Hz for foveal measurements and 7 to 13Hz for parafoveal measurements (Hammond and Caruso-Avery, 2000, Nolan et al., 2004, Snodderly et al., 2004, Engles et al., 2007, Iannaccone et al., 2007, Canovas et al., 2010). A customized HFP (cHFP) technique was described in the Carotenoids and Age-Related Eye Disease Study (CAREDS) (Snodderly et al., 2004). This encompassed determination of the critical flicker frequency (CFF) for the foveal and parafoveal regions, followed by application of an algorithm to allow the examiner to determine the best flicker frequency for performing HFP for each subject. The flicker frequency subsequently used for cHFP was 11.5 ± 2.5Hz in the fovea and 7.3 ± 2.6Hz in the parafovea. As it has been demonstrated that the CFF significantly declines with age (r = -0.56, P < 0.0005) it is considered desirable to individually determine the CFF to ensure as narrow a null zone as possible of around 0.15 log units (Hammond and Wooten, 2005). Several research groups have adopted the cHFP approach in their investigations of MPOD (Hammond and Wooten, 2005, Stringham and Hammond, 2007, Nolan et al., 2008, Stringham and Hammond, 2008, Stringham et al., 2008, Connolly et al., 2010, Loane et al., 2010). It has since been incorporated into the methodology of the MPS 9000 device, also known as the M:Pod or the QuantifEYE (Topcon, Newbury, UK) used to measure MPOD (Bartlett et al., 2010b).

1.2.1.2   The Macular Assessment Profile test

Instrumentation used to implement HFP techniques varies considerably. Complex Maxwellian viewing systems have been employed that require the subject to use a dental bite bar to maintain steady alignment of the incoming light (Hammond and Fuld, 1992). Simple free view systems have since been developed that do not require such steady alignment, and are more portable and easier to use (Wooten et al., 1999, Beatty et al., 2000a). A study of MPOD measured with a table-top device incorporating LEDs compared to a traditional Maxwellian viewing method revealed a high correlation between the two systems (r = 0.95, P value not provided) indicating that use of a free view set up does not affect accuracy of MPOD measurements (Wooten et al., 1999).

Alternative methods have also been developed. A Visual Display Unit (VDU) can be incorporated, whereby the SW test beam and the LW reference beam are derived from the phosphor outputs of a colour monitor (Moreland et al., 2001). However, some limitations do arise from the use of a VDU such as the low luminous output of the SW phosphor. In addition, VDU based HFP techniques may underestimate peak MPOD values due to the wider SW test output beam of the VDU compared to methods utilizing a narrow SW test beam (Moreland et al., 2001). A review of the validity of various in vivo methods of MPOD measurement reported that the narrower the bandwidth of the SW test output, the more accurate the results (Hammond et al., 2005).

The MAP test is a subjective psychophysical method of measuring MPOD. It was devised to overcome some of the issues inherent in using a VDU (Schalch et al., 2004, Barbur et al., 2010). As with other subjective HFP techniques, pupil dilation is not required and as such the test is non-invasive. Table 1 provides a summary of the key differences in technique between the MAP test and other optically based HFP methods. The MAP test is operated on the Eizo T566 monitor (a 17" cathode ray tube screen, driven at a frame rate of 140Hz) with the capacity to generate a high luminous output over a defined region of the display surface. This region is a carefully calibrated rectangular band subtending 16° by 8° at the subject's eye. Displaying the stimulus within a rectangular band allows the background luminance to remain steady at about 54cd.m^{-2} as seen through the notch filter (described below). The steady luminance is derived from the output of the phosphors (24cd.m^{-2} red, 24 cd.m^{-2} green and 6 cd.m^{-2} blue). The red and green phosphor output contributes a mean luminance of 16cd.m^{-2} to the LW reference beam, whereas the blue output provides a constant 2cd.m^{-2}. As well as ensuring that the subject always sees the stimulus, since it appears darker than the

background, this display arrangement provides background light adaptation, which improves the flicker sensitivity (Peachey et al., 1992). This is important as incomplete light adaptation can lead to inaccurate MPOD measurements (Barbur et al., 2010).

	MAP test	Maxwellian view	Free view
Paper	Barbur et al. (2010)	Wooten et al (1999)	Wooten et al. (1999)
Viewing system	VDU based	Complex optical system	Simplified optical system
Test stimuli	Phosphors of the colour monitor	Single xenon arc light source	LEDs with suitable peak wavelength
Use of filters	"Notch" filter to increase separation between SW and LW beams	Interference filters to produce background and reference fields	None, as LEDs produce near monochromatic light
Method of flicker production	Rapid sinusoidal modulation	Rotating mirror to produce square wave alternation	Square wave current pulses
Beam width	Wide: light enters through whole pupil	Narrow: light must pass pupil centre	Wide: light enters through whole pupil
Central stimulus	Circular 0.36° diameter stimulus	Circular 1° diameter stimulus	Circular 1° diameter stimulus
Parafoveal reference	Average of 6.8° and 7.8° eccentricities	6° in temporal retina	4° in temporal retina
Flicker rate	17Hz	12Hz foveal 6Hz parafoveal	15 Hz foveal 7Hz parafoveal
Half bandwidth	±28nm	±7nm	±20nm
Short wavelength	450nm	460nm	470nm
Long wavelength	560nm	550nm	570nm
Head stabilisation	Chin-rest and forehead bar	Dental bite-bar	Chin-rest and forehead bar
Working distance	70cm	33cm	33cm

Table 1 Summary of the key differences between the MAP test and optically based HFP methods.

Like other tests employing HFP techniques, the MAP test is based on the spectrally selective properties of MP. Two beams of light are produced optically by the phosphors of the MAP test display unit. In order to achieve the desired SW test beam and LW reference beam, the MAP test utilizes a "notch" optical filter, which is placed in front of the test eye, perpendicular to the direction of viewing (Barbur et al., 2010). The filter has a narrow absorption band (peaking at ~520nm) and so produces a larger separation between the SW test beam and the LW reference beam. By using the "notch" filter, the SW test beam is derived only from the blue phosphor of the VDU (peaking at around 450nm which is maximally absorbed in the central retina by MP) with a half maximum spectral width of ±28nm. The LW reference beam that is not absorbed by MP (Snodderly et al., 1984b) is composed of filtered red and green phosphor outputs (Rodriguez-Carmona et al., 2006). Alternating the SW test and LW reference beams at a frequency of 17Hz produces the test stimulus. When the luminance of the test and reference beams is not equal, a counter phased sinusoidal pattern is produced and the stimulus appears to flicker (Snodderly et al., 1984a, Bone and Landrum, 2004). A larger difference in luminance yields a stronger sensation of flicker. The LW reference beam has a constant modulation depth of 12.7%. This means that when the SW test beam has zero modulation, the subject observes a strong flicker produced solely by the LW reference beam. It has been reported that this makes it an easier task for the subject and in turn improves the accuracy of the test (Rodriguez-Carmona et al., 2006). Furthermore, the constant modulation depth of the LW reference beam consists of 18% modulation from the red phosphor output and 9% from the green. It is thought that the green component allows both middle wavelength m-cones and long wavelength sensitive l-cones to contribute to the detection of both beams (Barbur et al., 2010). The relative contribution of the different cone photoreceptors will be discussed further in section 1.2.1.3.

The MAP test measures MPOD at 0°, 0.8°, 1.8°, 2.8° and 3.8° eccentricity from the fovea. The central stimulus employed in the MAP test is a disc of 0.36° diameter (Figure 6a) and is considered to provide the MPOD at 0° (Barbur et al., 2010). The peripheral stimuli employed in the MAP test are sectors of an annulus presented concentric to the fovea (Figure 6b and 6c). At the 0.8°, 1.8° and 2.8° locations, a static mirror symmetric stimulus is presented at the corresponding location in the visual field to minimize the subject's tendency to saccade to the flickering peripheral target (Figure 6b). The MAP test has the capacity to support stimuli presented along any selected meridian. Notwithstanding, since MP spatial profiles have been shown to be radially symmetrical (Hammond et al., 1997c, Putnam and Bassi, 2015) all measurements

reported in the studies included within this thesis were performed with the stimulus centred along the horizontal meridian as shown in Figure 6.
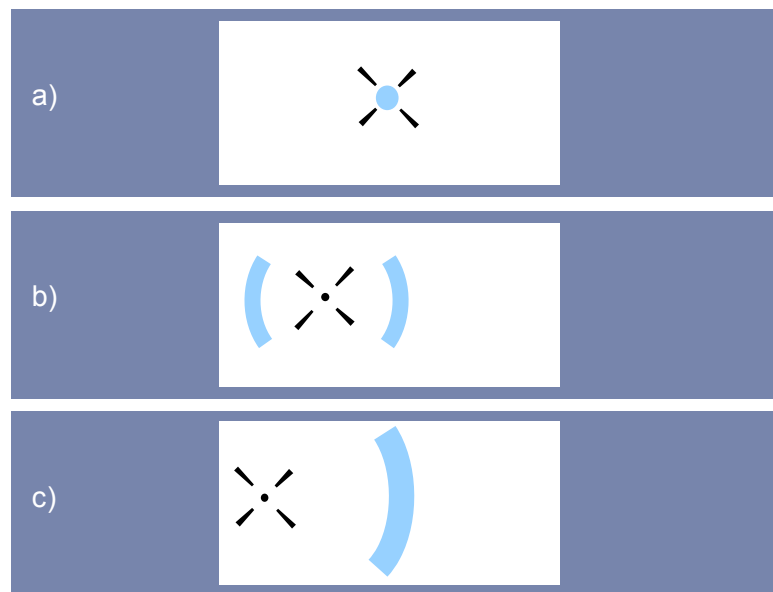
Figure 6 MAP test screen output (not to scale, adapted from Barbur et al. 2010). Examples of the rectangular band displayed on the VDU for mean MPOD assessment: a) at the fovea: a central circular flickering stimulus of 0.36° diameter; b) at 1.8° eccentricity: the symmetrical mirror image of the sector annulus stimulus does not flicker but aims to minimize the subject's tendency to saccade towards the flickering stimulus and so aids steady fixation; and c) at 7.8° eccentricity: note the sector annulus stimulus is larger for more eccentric locations. The dot with surrounding guides act as a fixation point in b) and c).

During the MAP test, the luminance of the test beam is altered until the perception of flicker is cancelled or minimized. In order to ascertain the range of luminance for which the perception of flicker is absent, the MAP test calculates a low and a high threshold using a modified staircase double reversal technique. The average of the low and high values is computed to give the luminance of the test beam required to cancel the reference beam i.e. the flicker null point. The test is repeated in a random order eight times (four high and four low thresholds) at each eccentricity and the average is calculated to give the mean luminance of the SW test beam required to achieve the flicker null point. The modulation of the LW beam, the pre-receptoral absorption of light, the size of the pupil and the sensitivity of the retina and the visual pathways remain constant at each retinal location being measured. The intensity of the SW test beam is the only parameter that changes. MPOD is calculated by comparing the mean

luminance adjustment of this SW light in the central retina to a reference point in the peripheral retina,

$$MPOD = log_{10}\left(L_i/L_0\right) \qquad (1)$$

where L_i is the mean luminance of the SW test beam at location i and L_0 is the average of the test beam luminance of the 6.8° and 7.8° peripheral locations where MP levels are thought to be negligible (Snodderly et al., 1984a, Snodderly et al., 1984b, Bone et al., 1988, Berendschot and van Norren, 2006). In addition, the average luminance of the SW test beam required to null the flicker at the 6.8° and 7.8° locations provides a measure of the absorption of blue light by the crystalline lens. The average lens transmittance of blue light can be derived from:

$$T_{AV} = \frac{\int_{380}^{760} T_L(\lambda)SW(\lambda)d\lambda}{\int_{380}^{760} SW(\lambda)d\lambda} \qquad (2)$$

where $T_L(\lambda)$ is the spectral transmittance of the lens and $SW(\lambda)$ is the wavelength radiance distribution of the test beam.

A photometric model has been developed to convert the measured MPOD to the corresponding peak optical density taking into account the width of the SW output (Barbur et al., 2010). This computation is automatically applied to the output produced by the MAP test for all MPOD measurements.

1.2.1.3 Assumptions, limitations and disadvantages of the principles of heterochromatic flicker photometry

The principles of HFP used to measure MPOD are based on several assumptions. In the first instance, the results are assumed independent of the effects of absorption or light scatter by the ocular media through use of a peripheral reference measurement locus as well as a reference LW beam (Wooten et al., 1999, Ciulla et al., 2001b, Bone and Landrum, 2004, Barbur et al., 2010). This has been demonstrated practically through use of neutral density filters over a 2-log unit range yielding no difference in MPOD measurements (Hammond et al., 1997b). In addition, the lack of effect of reduced retinal illuminance caused by increased crystalline lens optical density was

confirmed in a control experiment whereby changes in the background radiance, over a 1-log unit range simulating a dense to a clear crystalline lens, had no significant effect on MPOD values (Wooten et al., 1999).

Traditionally the parafoveal reference location is set at around 7° (Beatty et al., 2001, Delori et al., 2001a, Snodderly et al., 2004, Liew et al., 2005, Iannaccone et al., 2007, Nolan et al., 2008, Barbur et al., 2010, Canovas et al., 2010, Raman et al., 2011, Yu et al., 2012) where MP levels are presumed negligible (Bone et al., 1988, Berendschot and van Norren, 2006). The peripheral reference location used in the MAP test is provided by the average of the test beam luminance required to null flicker at the 6.8° and 7.8° eccentricities. The assumption that MP levels are negligible at this peripheral location is reasonable based on microspectrophotometry in cadaver eyes (Handelman et al., 1991, Snodderly et al., 1991, Bernstein et al., 1998). It is noteworthy that the peripheral reference location varies according to the HFP technique employed, with reports of less eccentric reference loci at 4° (Hammond and Caruso-Avery, 2000, Ciulla et al., 2001a, Hammond et al., 2002, Tang et al., 2004) or 5.5° (Hammond et al., 1996c). It has been shown that MPOD levels are likely to be underestimated when an insufficiently eccentric reference locus is used (Loane et al., 2007). When a reference point at 8° is used, MPOD may be under-estimated by around 4% (Hammond et al., 1997c), rising to almost 30% for a 4° reference point and up to 80% if a 2° reference point is used (Robson et al., 2003). In any event, foveal MPOD will be underestimated in individuals with a broad lateral distribution of MP exceeding the traditional reference location (Bhosale et al., 2007). The use of an appropriate peripheral reference point is particularly important in studies involving the use of L and/or Z supplements. An increase of 0.01 log units in MPOD in the equatorial retina was demonstrated in supplemented eyes, resulting in up to a 10-fold increase in peripheral MP levels. In these eyes, an underestimation of 10% to 30% of foveal MPOD was deemed possible by using the traditional 7° peripheral reference location of current HFP methods (Bhosale et al., 2007).

As well as the potential effect of an insufficiently peripheral parafoveal reference location, there are other factors that need to be taken into account when interpreting MPOD measurements obtained via different HFP techniques or instruments. Variations in stimulus size may cause difficulties when comparing results between studies, whereby a smaller foveal stimulus size yields a larger peak MPOD measurement (Hammond et al., 1997c, Barbur et al., 2010). Inconsistent interpretation of the actual point location of MPOD measurement due to the *edge hypothesis* remains another

source of debate. It has been suggested that during flicker photometry, MPOD is being measured at the edge of the flickering stimulus and not averaged across the entire test field (Werner et al., 1987). The *edge hypothesis* was tested by comparing MPOD measured using a small target comprising an annulus of 12 minutes of arc presented at 0.5° eccentricity with that obtained from a 1° diameter target presented centrally. A significantly high correlation was demonstrated (r = 0.91, P < 0.0005). These findings support the edge hypothesis since the 1° diameter target was assumed to measure MPOD at the edge of the target i.e. at 0.5°. In addition, the edge effect remained when the whole MP distribution was tested (Hammond et al., 1997c). Conversely, MPOD measured using a large central stimulus corresponded with that obtained using an annular stimulus at half the stimulus radius (Bone and Landrum, 2004). It may well be the case that flicker detection is dependent on a mechanism sensitive to both edge and local flicker. Furthermore, these mechanisms may work in isolation or together (Robinson and de Sa, 2012) so that the exact location of MPOD measurement by HFP is not straightforward. With regards to the MAP test, the geometry of the stimuli employed have been designed to ensure full spatial summation for flicker detection at each retinal test location (Barbur et al., 2010).

Another influencing factor that needs to be considered when using HFP to measure MPOD is the relative spectral sensitivity due to the distribution of photoreceptors across the retina. Rods and SW sensitive cones (s-cones) are found at the parafovea and peripheral retina, but not at the fovea, where m-cones and l-cones predominate (Curcio et al., 1990, Curcio et al., 1991, Roorda and Williams, 1999). The ratio of m- to l-cones remains constant across the central retina (Cicerone and Nerger, 1989, Nerger and Cicerone, 1992) and should therefore not affect MPOD measurements. The potential contribution of the rods and s-cones is minimised during HFP techniques by presenting the stimulus on a bright white background creating photopic conditions so that the rods are suppressed (Bone and Landrum, 2004). Alternatively, a blue adaptive background is used to suppress the response from the s-cones and rods, thus isolating a response from the m- and l-cones (Wooten et al., 1999). During the MAP test the background has been calibrated to ensure an adaptive background luminance (Barbur et al., 2010). In addition, the rod and s-cone response is further excluded through use of a flicker rate that is above their CFF, while remaining lower than the CFF of m- and l-cones (Nolan et al., 2004). A frequency of 17Hz is used during the MAP test for all retinal test locations. This is within the range used in previous HFP studies (Nolan et al., 2004, Hammond and Wooten, 2005).

Measuring MPOD by HFP has been validated by comparing the in vivo spectral absorbance and spatial distribution against an ex vivo template (Werner et al., 1987, Bone and Landrum, 2004, Hammond et al., 2005, Wooten and Hammond, 2005). More recently, newer HFP techniques have been validated by comparison with older established methods (Wooten et al., 1999, Beatty et al., 2000a). Validation of the MAP test and the photometric model used to convert MPOD values has been reported (Barbur et al., 2010). This was carried out by comparing results of the MP spatial profile to those obtained by the modified motion photometry method that employs a narrow SW beam at 460nm and is therefore considered to measure the peak MPOD (Moreland, 2004).

One of the main disadvantages of HFP is that the method is subjective and demands good cooperation and fixation (Canovas et al., 2010). The task can be difficult to perform and is unsuitable for individuals with poor visual acuity and learning difficulties. Some subjects find that Troxler's effect causes the peripheral target to fade (de Kinkelder et al., 2010). In addition, HFP can be a time-consuming task, particularly if a complete MPOD distribution is required involving several measurements. With this in mind various objective techniques have been developed to measure MPOD.

1.2.2   Objective techniques

Objective techniques of measuring MPOD include fundus autofluorescence (FAF) (Delori et al., 2001b, Wustemeyer et al., 2003, Egan et al., 2009) fundus reflectometry (FR) (van de Kraats et al., 2008), resonance Raman spectroscopy (RRS) (Bernstein et al., 1998, Hogg et al., 2007), and steady state visual evoked potentials (Robson and Parry, 2008). A brief description of the two most widely used objective techniques, FAF and FR, follows with emphasis on the limitations of each process for measuring MPOD.

1.2.2.1   Fundus autofluorescence

The method of FAF was selected as the most suitable for quantitative analysis of MP for subjects of the Age-Related Eye Disease Study 2 (AREDS2) (Bernstein et al., 2012). As with HFP, the technique of FAF to measure MPOD has been validated by comparison with in vitro MP spectral absorption curves (Delori et al., 2001b). The

technique of FAF is based on the autofluorescence of lipofuscin (Delori et al., 1995). Lipofuscin is a photoreceptor waste product located in the retinal pigment epithelium (Kennedy et al., 1995). Lipofuscin emits light between 520-800m when excited by light of wavelengths 400 to 590nm (Delori et al., 1995). Light within the absorption range of MP entering the eye will be absorbed by the carotenoids before it encounters lipofuscin. Consequently, there is less lipofuscin autofluorescence at the macula compared to the retinal periphery. Levels of MP can be measured by analysis of FAF images, either by one- or two- wavelength imaging. The one-wavelength technique uses a standard 488nm argon single wavelength to obtain images (Robson et al., 2003, Trieschmann et al., 2003). However, the non-uniform distribution of lipofuscin (Delori et al., 2001a) influences the output of the one-wavelength method, with higher lipofuscin levels resulting in increased autofluorescence and therefore overestimation in MPOD measurements (Delori et al., 2001b, Trieschmann et al., 2006). This problem is dealt with during two-wavelength FAF by the addition of a second longer excitation wavelength at 514nm that is not absorbed by MP. In any event, since the two wavelengths used do not match the maximum and minimum absorption of MP, a correction is applied for MPOD calculation (Delori et al., 2001b). Additionally, a common barrier filter blocking wavelengths shorter than 560nm (i.e. corresponding to the peak absorption of MP) is incorporated into the measuring system for single-pass measurement.

Typically, FAF is performed using a modified scanning laser ophthalmoscope. An example of this is the Heidelberg Retina Angiograph (HRA, Heidelberg engineering, Heidelberg). MPOD is measured in one of two ways. The supplied software calculates MPOD by comparing autofluorescence at the fovea to that at a parafoveal reference point (Delori et al., 2001b); for two-wavelength FAF, MPOD is measured by digital subtraction of the second image produced by the additional longer wavelength (Trieschmann et al., 2006). Alternatively, one or two wavelengths are used to take a series of up to 32 images that are aligned and averaged to create MP density maps. The intensity of a greyscale map is generated via digital subtraction of the images obtained at the two wavelengths via specialised inbuilt software (Wustemeyer et al., 2003).

The technique of FAF is based on the assumption that there are no fluorophores anterior to MP. Measurements of MPOD will be slightly underestimated if fluorophores exist anterior to the MP, although the incorporation a second wavelength reduces this effect (Delori et al., 2001b, Delori et al., 2006). Another consideration is the absorption

of light by the visual pigments whereby light is absorbed at 440nm (s-cones), 543nm (m-cones and 566nm (l-cones) (DeMarco et al., 1992). It follows that the visual pigments will absorb light at the wavelengths employed by the FAF technique at 488nm and 512nm. It has been shown that absorption at 488nm is 62% of the m-cone peak density and 91% at 514nm and for the l-cones it is 0.32% at 488nm and 0.64% at 514nm (Berendschot and van Norren, 2006). Complete photoreceptor bleaching is therefore desirable to eliminate this potential contamination of MPOD measurement, causing a reduced MPOD. Nonetheless it has been demonstrated that incomplete bleaching is unlikely to have a significant effect, whereby no significant effect of the absorption of light by the visual pigments on the MP distribution has been shown (Berendschot and van Norren, 2006, Delori et al., 2006). It is also presumed that the absorption of light by retinal blood and retinal pigment epithelium (RPE) melanin as well as the photoreceptor pigments has a negligible effect on MPOD measurement (Delori et al., 2001b, Delori et al., 2006). Indeed it has been demonstrated that variations in MP profiles as measured by two-wavelength FAF are unlikely to be caused by the effects of absorption by the RPE or the crystalline lens (Delori et al., 2006). Finally, similar to the principles of HFP, it is assumed there is no or little MP at the peripheral measurement location (section 1.2.1.3)

1.2.2.2 Fundus reflectometry

The technique of measuring MP in vivo by FR is based on the comparison of light reflected from the fovea to that reflected by a peripheral area (Berendschot et al., 2003, Berendschot and van Norren, 2004). This technique has been validated by demonstrating a good match of MPOD measured by FR in vivo with the spectral curve of MP ex vivo (Delori et al., 2001b). Light entering the eye passes through the ocular media (cornea, crystalline lens and vitreous), retina and choroid. A small amount of incoming light is reflected at interfaces of layers with different refractive indices, mainly at the inner limiting membrane, outer segments of photoreceptors and choroid (Hammer and Schweitzer, 2002). As with HFP two wavelengths of light are used, one corresponding to that absorbed by MP (488nm) and one that is not (514nm) (Delori et al., 2001b). The difference in reflectance between the two measurement sites indicates the amount of MP present. An alternative FR technique incorporates spectral analysis. This is based on an optical model of light transmission through the eye, using the spectral absorption of MP (Berendschot and van Norren, 2004). This method allows

calculation of the density of the lens, melanin and blood as well (Berendschot and van Norren, 2005, Kanis et al., 2007).

The instrumentation used to carry out FR varies. It can be carried out with a modified fundus camera (Delori and Pflibsen, 1989); a customised scanning laser ophthalmoscope (Berendschot and van Norren, 2005); a purpose built instrument such as the foveal reflection analyser (Kanis et al., 2007); or the MP reflectometer (van de Kraats et al., 2006). As with FAF, a correction needs to be applied to account for the discrepancy between the wavelengths employed (488 and 514nm) and the maximum and minimum MP absorptions. Of note, some FR techniques do not include comparison with a peripheral reference point so that the output is a combination of MPOD as well as lens optical density (Berendschot and van Norren, 2005).

The basis of FR is that the spectral properties of the ocular tissues across the area being measured are homogenous (Delori et al., 2001b). As with FAF, photoreceptor bleaching is necessary to prevent absorption of light by the cone and rod photopigments. Even if complete bleaching is not achieved, any residual rod photopigment (rhodopsin) has been found to have little effect on MPOD measurement by FR (Delori et al., 2001b). The set up of the apparatus must ensure that light scatter, by the crystalline lens or other pre- or intra-retinal structures, is controlled for, whereby the use of the peripheral reference site minimises this effect (Delori et al., 2001b). As with the comparison techniques described for both HFP and FAF methods, it is assumed there is negligible MP at the peripheral reference location. There is general consensus that during FR the average MPOD across an area is being measured (Berendschot and van Norren, 2005).

1.2.2.3 Disadvantages of objective methods of measuring macular pigment optical density

While objective techniques of measuring MPOD offer a quick test time that can be performed in most individuals, there are some disadvantages. Photoreceptor pigment bleaching is required and the bright light levels used during the procedure can be uncomfortable for the subject. In addition, mydriasis is required. This may create a problem in subjects in whom the pupil does not dilate sufficiently either due to age or disease (Bremner and Smith, 2006). As a consequence, a non-mydriatic device has

been developed for FAF (Sharifzadeh et al., 2006) and has subsequently been selected as the most suitable way of measuring MP and its distribution in sub-study of AREDS2 (Bernstein et al., 2012). A modified fundus camera for measuring MPOD by FR that eliminates the requirement of pupil dilation and photoreceptor bleaching has also been described (Bone et al., 2007). Another disadvantage of objective methods compared to HFP is that clear optical media are necessary for adequate image quality during FAF (Canovas et al., 2010). In addition, FR and RRS results are detrimentally affected by changes in the ocular media (Howells et al., 2011). Finally, the major disadvantage of objective methods of measuring MPOD is that the instruments are expensive. Moreover, the modified confocal scanning laser ophthalmoscope employed for FAF is not yet commercially available.

1.2.3 Agreement between macular pigment optical density measurements obtained using subjective and objective techniques

Peak MPOD, the MP spatial profile and the lateral extent of MP have been shown to vary greatly among individuals (Hammond et al., 1997c, Berendschot and van Norren, 2006, Delori et al., 2006, Nolan et al., 2008, Raman et al., 2011). The reported differences may be due to the methods used to measure MPOD. In a study including thirty individuals, HFP, FAF and FR techniques were all used to measure MPOD. A significant correlation was demonstrated between HFP and FAF (r = 0.77, P < 0.0005) and between HFP and FR (r = 0.61, P < 0.0005) (Delori et al., 2001b). Similar investigations have yielded comparable results, whereby correlation was used as a measure of agreement (Liew et al., 2005, Berendschot and van Norren, 2006, van de Kraats et al., 2006, Bone et al., 2007, van der Veen et al., 2009b, Canovas et al., 2010). Notably, a recent study showed similar results using both correlation and accuracy as measures of agreement (Dennison et al., 2013). However, measurements obtained by subjective and objective techniques are not interchangeable, especially when the different methods are not measuring MPOD at the same retinal location (Delori et al., 2001b). With this in mind, a study was conducted to compare MPOD values obtained by both HFP and FAF at the same retinal locations at 0.25°, 0.50°, 1.00° and 1.75° retinal eccentricity in ten individuals (Canovas et al., 2010). There was a significant positive correlation in MPOD measured at 0.25º (r = 0.56, P = 0.017) and almost all other measurement locations between the two methods. However, mean MPOD at

0.25° measured by FAF was 0.54 ± 0.11 compared to 0.37 ± 0.07 by HFP. Indeed, MPOD was consistently higher when measured by FAF at all locations (P < 0.001). It has been suggested that the secondary effects of artefacts may potentially influence objective measurement of MPOD whereby absorption of the photopigments and RPE melanin as well as the effects of stray light play a role in accuracy of MPOD determination as discussed in section 1.2.2.3.

1.2.4 Measurement of macular pigment spatial density distribution

The spatial density distribution profile of MP can be established with HFP based methods by taking several MPOD measurements at increasing eccentricity locations relative to the fovea. One way of achieving this is by presenting foveal test stimuli of increasing diameters. This method is based on the *edge hypothesis* in which the perceived flicker of a (circular) stimulus is detected by receptors at the edge of the stimulus (Werner et al., 1987). More commonly, eccentric measurements are obtained by presenting a small circular stimulus so that it is viewed eccentrically, at various retinal locations (Bone and Landrum, 2004). The macular densitometer, a HFP based device that presents stimuli in free view via LEDs (Wooten et al., 1999) has been modified to measure MPOD at retinal eccentricities of 0.25º, 0.5º, 1º, 1.75º, 3º and 5º, relative to a peripheral reference location at 7º (Nolan et al., 2008, Kirby et al., 2010). Central MPOD measurements at 20' and 30' have also been obtained using this device (Stringham and Hammond, 2007). Regarding VDU-based HFP techniques, several eccentric MPOD measurements can be achieved by presenting a series of annular stimuli of varying diameters whilst the subject fixates centrally, as is the case with the MAP test (Barbur et al., 2010). Aside from two-dimensional representations, high-resolution optical imaging techniques such as FAF and FR provide three-dimensional representations of topographical variations in MPOD. Analysis of the MP density maps and radial density profiles allows analysis of the overall MP spatial profile (Elsner et al., 1998, Berendschot and van Norren, 2006, Delori et al., 2006, Dietzel et al., 2011b). The following section describes inter-individual variations observed in the spatial density distribution of MP.

1.3   Spatial density distribution of macular pigment

The concentration of MP peaks towards the centre of the fovea. There is evidence for this from histology and HPLC studies of primate and human retinas ex vivo (Snodderly et al., 1984a, Snodderly et al., 1984b, Handelman et al., 1988, Trieschmann et al., 2008) as well as evidence from clinical studies involving the measurement of MPOD in vivo by subjective psychophysical HFP (Hammond et al., 1997c, Delori et al., 2001b, Nolan et al., 2008, Barbur et al., 2010, Yu et al., 2012) and objective imaging methods such as FAF (Delori et al., 2001b) and FR (Berendschot and van Norren, 2006).

Peak MPOD may be a poor predictor of the total amount of MP present (Robson et al., 2003). It is therefore important to consider the overall distribution of MP and not a single central measurement of MPOD. Typically, the spatial density distribution of MP has a central peak, with a sharp decline in MPOD with eccentricity from the centre of the fovea (Snodderly et al., 1984a, Bone et al., 1988, Hammond et al., 1997c, Nolan et al., 2008). It has been shown that an exponential function describes the MP spatial profile well. A best fit exponential curve fit better described the averaged MPOD of thirty-two subjects ($R^2 = 0.99$) compared to a Gaussian function ($R^2 = 0.93$) (Hammond et al., 1997c). Given that the distribution of MP typically follows an exponential decline with eccentricity, it has been suggested that it is possible to predict MPOD at any retinal eccentricity based on a single central measurement, described by:

$$MPOD = A(10^{-0.42x}) \tag{3}$$

where A is the amplitude of the central MPOD measurement and x is the retinal eccentricity in degrees (Hammond et al., 1997c). However, as well as single central peaks accompanied by a monotonic exponential decline in MPOD with eccentricity, there are reports of secondary peaks in the MP spatial profile. These give rise to a ring-like structure of MP centred on the fovea whereby an annulus of higher MPOD is superimposed on a central exponential-distribution (Berendschot and van Norren, 2006, Delori et al., 2006).

The overall data distribution of MP taking the presence of secondary peaks into account was investigated in a study involving both FAF and FR methods to examine the distribution of MPOD in fifty-three subjects (aged 50 ± 17 years). The spatial profile was described as a combination of an exponentially decaying function of eccentricity

together with a Gaussian-distributed ring (Berendschot and van Norren, 2006). The MP distribution was best described by

$$MPOD(x) = A_1(10^{-\rho_1 x}) + A_2(10^{-\rho_2(x-x_2)^2}) \tag{4}$$

where x is the eccentricity, A_1 and A_2 are the amplitudes of the exponential and Gaussian distributions respectively, ρ_1 and ρ_2 represent the peakedness and x_2 is the eccentricity at which the Gaussian distribution peaks. In the absence of a ring-like structure A_2 is equal to zero so that the data is described by the exponential fit alone (Equation 3).

The ring-like structure described by the Gaussian fit can be considered a positive deviation away from the exponential fit. The retinal eccentricity at which this deviation occurs varies. Using two-wavelength FAF, the peak MP of the ring identified in seventy-three participants was located at a minimum eccentricity of 0.48º and a maximum of 0.85º (Dietzel et al., 2011). Similar locations of a secondary peak in MPOD between 0.6° and 1.2° eccentricity measured in vivo have also been described using a variety of instruments, including subjective MPOD measurements (Hammond et al., 1997c, Kirby et al., 2009) as well as objective FAF methods (Berendschot and van Norren, 2006, Delori et al., 2006)

The various different MP spatial profile phenotypes have been described as typical exponential or as atypical, including ring or ring-like, secondary peaks and bimodal distributions. The spatial distribution of MP across the central retina has been shown to vary considerably among healthy individuals. Using HFP, the MP spatial distribution of thirty-two Caucasian subjects was best described by an exponential fit (Hammond et al., 1997c). However, the authors also discovered that about 40% of subjects presented secondary peaks, defined as increments greater than 0.05 optical density units from the exponential fit, at 1° and 2°. More recent investigations have reported the presence of a ring-like MP spatial profile in a significant proportion of healthy subjects. Using objective two-wavelength FAF techniques, the prevalence of a ring-like structure was reported to be almost 20% among three hundred and sixty-nine participants (Dietzel et al., 2011b), 26% among three hundred and fourteen female twins (Tariq et al., 2014), 23% in seventy-nine individuals (Meyer zu Westrup et al., 2014) and over 50% in forty subjects (Delori et al., 2006).

The existence of different types of MP distributions is supported by the different presentations of Maxwell's spot, an entopic phenomenon elicited by the presence of MP. Subjects displaying a secondary peak in their MP distribution have described the visualization of Maxwell's spot as a dark ring, with or without a central spot (Delori et al., 2006). The high degree of inter-ocular symmetry of the MP spatial profile phenotypes also suggests that different phenotypes are a real phenomenon. The presence or absence of a ring-like MP distribution measured by two-wavelength FAF was highly symmetrical in 85% of the two hundred and two pairs of eyes investigated (P < 0.0005). In addition, the eccentricity at which the minimum and maximum of the ring occurred was highly symmetrical (Spearman's r = 0.89, P < 0.0001) (Dietzel et al., 2011b).

As well as exponential (i.e. monotonic) and ring-like MP spatial profiles there are also reports of "intermediate distributions" in which there is no secondary peak, but instead a plateau on the slope of the distribution (Figure 7c). These "intermediate" or "plateau" profile phenotypes have been identified by subjective visual analysis of MP density maps produced by two-wavelength FAF obtained under mydriasis (Dietzel et al., 2011b, Tariq et al., 2014). Another description of MP profile types has also been offered. The profile was classified as either presenting a monotonic decline from the centre to the periphery of the fovea, or demonstrating a central dip in a study investigating the relationship between these specific MP spatial profiles and risk factors for AMD. The central dip profile was defined by MPOD (measured by HFP) being lower at 0.25° than at 0.50° and then declining steadily to the periphery (Kirby et al., 2010).
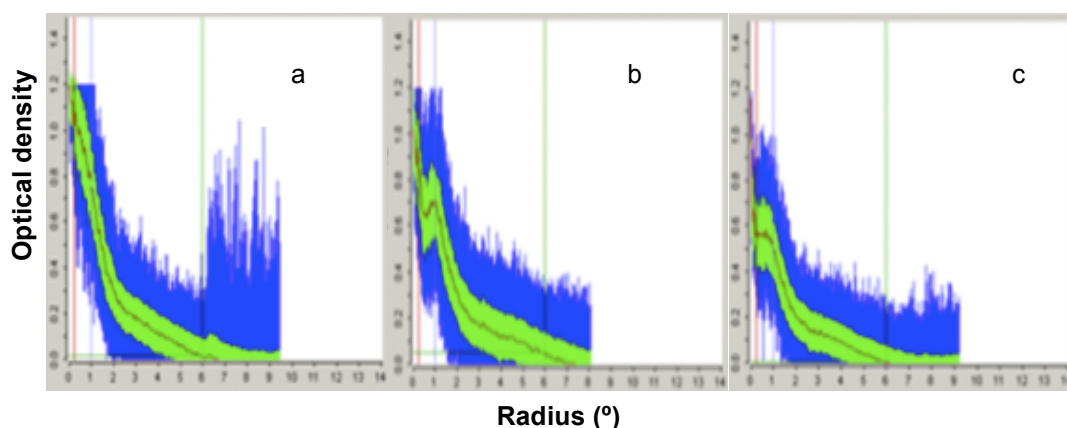
Figure 7 MP density maps to show examples of a) monotonic decline with no secondary peak; b) bimodal distribution with a ringlike structure; and c) an intermediate distribution with a plateau in the slope (Dietzel et al., 2011b).

The relevance of the spatial distribution of MP is that certain profile types appear to be more prevalent in healthy eyes compared to eyes with signs of AMD. This has

generated interest in the importance of the MP spatial profile with suggestion that the presence of a ring-like structure of MP may play a role in the protection of the eye against AMD. In a study of three hundred and sixty-nine participants of the Muenster Aging and Retina Study the presence of an annulus of increased MPOD was three times less common in eyes with presence of AMD compared to healthy eyes (Dietzel et al., 2011b). However, a relationship between MP profile type (typical exponential versus atypical central dip) and the three established risk factors for AMD: family history of AMD, cigarette smoking and increasing age was not found in a study of four hundred and eighty-four healthy individuals (Kirby et al., 2010). This brings about the following question: is the presence of ring-like MP structure a protective feature, or a consequence or part of sequelae of developing AMD? An understanding of the spatial distribution of MP in healthy eyes is required In order to answer this question.

1.3.1   Classification of the macular pigment spatial profile

It is apparent from the literature that the classification of MP spatial profile phenotypes other than "typical" exponential varies across the literature including descriptions of "atypical" bi-modal (Delori et al., 2006), secondary peaks (Hammond et al., 1997c, Kirby et al., 2009), parafoveal ring or ring-like (Berendschot and van Norren, 2006, Dietzel et al., 2011b), shoulders or flanks (Snodderly et al., 1984a), and central dips (Kirby et al., 2010). It remains that the comparison of MP spatial density distribution between studies is complicated when different phenotype classification methods are employed (Hammond et al., 1997c, Delori et al., 2006, Kirby et al., 2009).

There is currently no consensus on a classification system for MP profiles and various definitions and criteria have been used. The mathematical analysis of a combination of an exponential and Gaussian fit to the data distribution has been described (Equation 4) (Berendschot and van Norren, 2006). Analysis of MP using grey scale values derived from FAF images has also been used in the past to characterize four different MP spatial profile types: Type 1, showing high levels of central MP; Type 2, displaying lower central MP and a shallower curve progression; Type 3, with only central MP present and no surrounding MP; and Type 4 presenting with no enhanced central MP and only peripheral MP observed (Trieschmann et al., 2003). An alternative approach of analysing MPOD plotted against eccentricity following digital subtraction of two-wavelength FAF and FR images has been described, involving analysis of secondary

maxima-minima pairs (Delori et al., 2006). Subjective visual assessment of FAF images has also been implemented as a classification method of analysing FAF images (Tariq et al., 2014). Using HFP methods to measure MPOD, an atypical MP profile has been assigned when MPOD at 0.25º does not exceed MPOD at 0.5º as measured by cHFP by more than 0.04 density units (Nolan et al., 2012a).

As well as a difference in classification criteria employed across different studies, the measurement points vary according to measurement technique. HFP methods rely on a two dimensional evaluation of MPOD along a single meridian, whereas objective imaging methods may average the data obtained at a given radius. Nonetheless, a high correlation of MPOD measurements obtained along different meridians has been shown (Hammond et al., 1997c, Robson et al., 2003, Delori et al., 2006) despite reports of both horizontal elliptical MP distributions (Delori et al., 2006) and circularly symmetrical distributions (Hammond et al., 1997c). Using HFP methods, mean MPOD taken in the four quadrants (nasal, temporal, superior and inferior) at 1º eccentricity was not statistically significantly different ($P < 0.42$) (Hammond et al., 1997c) and in a recent study a high level of symmetry was demonstrated among the four quadrants measured at 2º ($r = 0.96$) (Putnam and Bassi, 2015). This suggests that data taken from a single meridian is likely to represent the distribution of MP in all quadrants. It also implies that data from different meridians can be averaged to characterize the spatial distribution (Delori et al., 2006).

It has been questioned whether the existence of different MP spatial profile phenotypes is real or a product of measurement error. If classification of the MP spatial profile is based on deviations away from an exponential fit to the data (Berendschot and van Norren, 2006) or an increase in MPOD relative to central MPOD (Nolan et al., 2012a) the reliability of the MPOD measurement must be considered. However, repeatability of MPOD measurements varies depending on the instrument employed (Snodderly et al., 2004, Tang et al., 2004, de Kinkelder et al., 2010). It is therefore important to consider the repeatability of MPOD measurements according to the instrument used. The repeatability of MPOD at different eccentricities should also be taken into account, although test-retest repeatability of MPOD measurements are often carried out only at a single 0.5° location for HFP methods (Snodderly et al., 2004, Tang et al., 2004, Bartlett et al., 2010a, de Kinkelder et al., 2010) or at 0.5° and 2° eccentricity using two-wavelength FAF (Trieschmann et al., 2006).

1.4   Factors associated with inter-individual variations in macular pigment

As well as the variations in MP density distribution patterns, there are wide inter-individual variations in levels of MPOD measured at all retinal eccentricities (Figure 8) (Hammond and Caruso-Avery, 2000, Ciulla et al., 2001a, Delori et al., 2001b, Liew et al., 2005, Nolan et al., 2007a, Kirby et al., 2010).
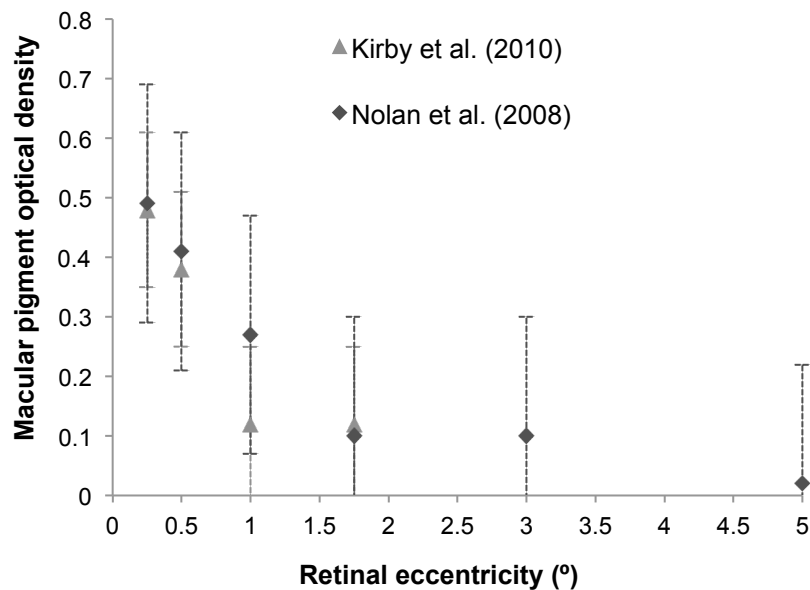
Figure 8 Graph to show MPOD (mean ± SD) at several retinal eccentricities from the centre at 0.25° to 5°. The error bars indicate inter-individual variation for each eccentricity. Data derived from two large studies involving eight hundred and twenty-four (Nolan et al., 2007b) and four hundred and eighty-four healthy individuals (Kirby et al., 2010).

Values of MPOD at 0.5° have been shown to vary between 0 to around 1 (Hammond et al., 1997c, Nolan et al., 2007b, Kirby et al., 2010). The reason for the large variations in measured MPOD has yet to be determined. There has been interest in the potential association of MPOD with risk factors for AMD in a white population (Nolan et al., 2007b) as well as an Indian population (Raman et al., 2012b) whereby there appears to be an interaction between established risk factors for AMD and MP levels. It has been reported that MPOD may be affected by age (Beatty et al., 2001, Ciulla and Hammond, 2004, Berendschot and van Norren, 2005, Nolan et al., 2010), gender (Hammond et al., 1996a), iris colour (Hammond et al., 1996b, Ciulla et al., 2001a) and modifiable factors such as diet (Hammond et al., 1997a, Bone et al., 2000, Mares et al., 2006, Nolan et al., 2007a) and smoking status (Hammond et al., 1996c, Kirby et al., 2010, Nolan et al., 2012b, Raman et al., 2012a). Ethnicity may also play a role (Beatty

et al., 2001, Nolan et al., 2007b). As well as the risk factors for AMD, it has also been hypothesised that anatomical correlates i.e. foveal architecture may play a role in governing MP levels and its spatial distribution (Liew et al., 2006, Nolan et al., 2008, Kirby et al., 2009). These factors will be discussed further below.

Despite the wide inter-individual differences observed in MPOD, correlation in MPOD levels between the right and the left eye has been shown to be high. Inter-ocular concordance has been demonstrated by biochemical HPLC techniques (Handelman et al., 1988), HFP methods (Hammond and Fuld, 1992, Snodderly et al., 2004, Lam et al., 2005, Iannaccone et al., 2007), motion photometry techniques (Robson et al., 2003), objective imaging by FR (Kanis et al., 2007) and FAF methods (Dietzel et al., 2011a). In a sample of three hundred and sixty-nine individuals, measurements of peak MPOD at 0° using FAF objective methods were 0.71 ± 0.23 and 0.72 ± 0.21 for the right and left eye respectively (Spearman's r = 0.91, P < 0.0001) (Dietzel et al., 2011b). In addition, MPOD measured by HFP at different retinal eccentricities has been shown to have high concordance between the right and left eye (Yu et al., 2012). It must be noted that not all studies have found this high level of inter-ocular agreement. One explanation for asymmetry may be increasing age (Snodderly et al., 2004). Lower visual acuity (less than 6/12 Snellen equivalent) in one eye may also result in poor concordance in MPOD between the eyes (Snodderly et al., 2004). Ocular pathology in one eye may also result in asymmetrical MP levels with suggestions that over 34% relative inter-ocular differences in MPOD might indicate pathology (Kanis et al., 2007).

1.4.1   Age

The effect of age on MP levels has been investigated. L and Z have both been detected in prenatal eyes at around twenty weeks gestation (Bone et al., 1988). The presence of carotenoid in the retina shortly after birth has been demonstrated whereby a visible yellow spot forms at around six months post-natal (Bone et al., 1988, Handelman et al., 1988). A HPLC investigation of eighty-seven donor human retinas ranging from 3 to 95 years old found no effect of age on levels of L and Z present. While there was a predominance of Z in the majority of retinas (90%), L was the most prominent carotenoid present in all retinas under 2 years of age (Bone et al., 1988). The finding of more L and less meso-Z in infant compared to adult retinas was confirmed in a later study (Bone et al., 1997). Nonetheless, beyond the infant years

there is evidence that MPOD does not change as a function of age (Werner et al., 1987). No systematic variation in MPOD with age was found even when elderly subjects with cataracts and AMD were considered (Ciulla and Hammond, 2004). The results of a study based on longitudinal data collected over a time span of 1 to 16 years from a sample of ten individuals found no change in MPOD (measured by HFP) with age (Hammond et al., 1997c). There was no evidence of an age-related decline in MPOD at 0.5º measured by HFP in two hundred and twenty-two individuals aged 79 ± 3.2 years of age (Iannaccone et al., 2007) or in a larger sample of one thousand six hundred and ninety-eight women aged 53 to 86 years (r = -0.03, P value not given) (Mares et al., 2006). This finding was confirmed in a study of MPOD in patients with and without wet AMD in an Indian population (Raman et al., 2012a). Likewise, there was no association of age with MPOD measured at 0.25°, 0.5°, 1.0° or 1.75° in a study including four hundred and eighty-four Caucasian individuals aged 18 to 70 years (Kirby et al., 2010). This finding was confirmed in a more recent study of ninety-eight individuals aged 19 to 71 years (O'Beirne, 2014).

However, there are inconsistencies in the findings of the effect of age on MPOD with an age related decline reported in some studies (Hammond and Caruso-Avery, 2000, Beatty et al., 2001, Lam et al., 2005) and even a slight increase of MPOD at 0.5º and 2º reported in one study (Dietzel et al., 2011b). The results of The Irish Longitudinal Study on Ageing (TILDA) found a moderate decline in MPOD at 0.5° measured by HFP associated with increasing age (r = -0.25, P = 0.045) based on seventy-nine individuals aged 65 ± 11 years (Nolan et al., 2010). MPOD has been found to decline in South Asian subjects over 40 years of age (Raman et al., 2011). Kirby et al. (2010) reported a weak negative association between age and MPOD measured at 0.25º by HFP methods in males (r = -0.146, P = 0.049) compared to females. The authors postulated that this was likely due to gender differences in the transport and metabolism of the carotenoids. It is possible that the inconsistencies in reports of the effect of age on MPOD and its distribution are a result of subject selection and sample size. While no relationship of MPOD (measured by HFP) with age was demonstrated in one hundred and ten elderly subjects aged 72 ± 8 years, the sample included a small number of individuals with cataracts and AMD and many of these subjects were taking dietary supplements that may have influenced the results (Ciulla and Hammond, 2004). In addition, the method of MPOD measurement may skew findings and result in the discrepancies between studies (Ciulla and Hammond, 2004). MPOD was independent of the effect of age when measured objectively by FR, but showed a slight decrease when the same subjects were examined using HFP (Berendschot and van Norren,

2005). The variations due to measurement techniques have been described in section 1.2.3. Crystalline lens optical density may influence MPOD measured by RRS. The potentially confounding effect of lens yellowing was removed in a recent study whereby MPOD was measured by RRS in one hundred and forty-four patients with non-tinted intra-ocular implants following cataract surgery. Age was found to significantly affect MPOD, with a decline of 10% per decade reported based on patients over the age of 50 (Obana, 2014). Another confounding factor may be ethnicity. In a study of fifty-nine healthy subjects aged 35.6 ± 11.4 years of varied ethnic backgrounds, an inverse age-related trend in MPOD at 0.25° (r = -0.252, P = 0.049), 1° (r = -0.278, P = 0.033) and 3° (r = -0.284, P = 0.030) was reported. Interestingly, this effect was not demonstrable after adjustment for ethnicity (Nolan et al., 2008). This finding suggests that ethnicity may play a greater role in inter-individual variations in MPOD than age.

The effect of age on MP spatial distribution has also been investigated. The spatial profile remained stable in four individuals tested over a period of 4 to 14 months (Hammond et al., 1997c). No dependence on age of MP spatial profile type measured by two-wavelength FAF was found in individuals less than 60 years of age (Delori et al., 2006). Similarly, in a sample of fifty-three individuals aged 50 ± 17 years, there was no association between age and the presence of a secondary peak in the MP spatial profile (Berendschot and van Norren, 2006). This is in agreement with a more recent study of older individuals aged 62 to 85 years (Dietzel et al., 2011b). In contrast, other researchers have reported that subjects presenting with the typical exponential MP spatial profile tended to be younger (5 ± 12 years) and that older subjects were more likely to exhibit a central dip in their profile (Kirby et al., 2010). This finding is supported by a study of two hundred and eighty-one healthy Chinese subjects aged 17 to 85 years, whereby there was an age-related decline in MPOD at 0.25º (r = -0.165, P = 0.014), but not at 0.5º (r = -0.025, P = 0.68), 1º (r = -0.053, P = 0.38), or 1.75º (r = 0.094, P = 0.15) eccentricities (Yu et al., 2012). Nonetheless, the authors noted that only 6.3% of the reduced central MPOD could be explained by increasing age. Likewise, in a study of two hundred and one healthy adults aged 20 to 95 years, age significantly predicted the MPOD value in a simple linear regression model that took into account age and iris colour. Since age only predicted 5% of the variation in MPOD (R^2 = 0.048), it was concluded that a number of variables are likely to play a role in the large range of MPOD values among individuals (Abell et al., 2014).

1.4.2   Gender

Investigations of the effect of gender on central MP levels have yielded inconsistent results. An early study reported significant sex differences in central MPOD (measured by HFP using a 1° test stimulus), whereby MPOD was 38% higher in forty healthy males compared to forty-eight healthy females (P < 0.001) (Hammond et al., 1996a). Mean MPOD measured by FR was also found to be significantly higher by 13% in males (n = 177) compared to females (n = 199) (Broekmans et al., 2002). On the other hand, females were found to have significantly higher MPOD at 0.5° (0.27 ± 0.17, n = 50) compared to males (0.18 ± 0.15, n = 29, P = 0.032) (Nolan et al., 2010). Similar findings have been reported by more recent investigations (Nolan et al., 2012b, Abell et al., 2014, Kyle-Little et al., 2014). It remains that the effect of gender on MPOD levels is not conclusive.

There are also conflicting reports as to whether gender has an association with the shape of the MP spatial distribution. It has been speculated that women are more likely to present with a bi-modal MP distribution. This was based on the findings of an investigation of a Caucasian sample of forty-one subjects (mean age 49 ± 15 years) using FAF methods (Delori et al., 2006). Similarly, a more recent study involving a much larger sample of three hundred and sixty-nine individuals (mean age 71.6 years) and employing FAF methods also found that females were more likely to present with a ring-like MP distribution, whereby a ring-like distribution was found in 25% females compared to 11% males (P = 0.004) (Dietzel et al., 2011b). In contrast, other investigators have found no evidence to support a gender influence on the presence of a secondary peak in the MP spatial profile. This has been reported in studies using objective FAF as well as FR techniques (Berendschot and van Norren, 2006) and also when HFP methods have been employed to measure the distribution of MP (Kirby et al., 2010). It has been hypothesised that differences in lipid metabolism between males and females may influence the accumulation of L and Z (Nolan et al., 2004).

1.4.3   Iris colour, sunlight exposure, skin type and hair colour

The relationship between iris colour and MP levels has been investigated in the past. Using HFP, MPOD at 0.5° was significantly higher in individuals with brown or black eyes (0.38 ± 0.24) compared to green or hazel (0.32 ± 0.15) and blue or grey eyes

(0.25 ± 0.20, P < 0.02) despite similar diet and blood carotenoid concentrations among the three groups (Hammond et al., 1996b). Ethnicity did not appear to play a role in this relationship hence it was suggested that MPOD might be determined by another genetic component or an environmental factor such as light exposure and oxidative stress. The investigators postulated that the increased light transmittance and subsequent increase in oxidative stress associated with a light coloured iris (van den Berg et al., 1991) resulted in a depleted MPOD. Increased MPOD (at 0.5º and 1º, measured by cHFP) in subjects with dark compared to light eyes was confirmed in a more recent study of four hundred and eighty-four healthy individuals of Caucasian ethnicity (Kirby et al., 2010). No relationship between MP spatial profile type, based on the presence or absence of a central dip, and iris colour was reported. However, the effect of iris colour on MPOD values is not consistent across the literature. No significant effect of eye colour on MPOD was established in the CAREDS ancillary study involving one thousand six hundred and ninety-eight women (Mares et al., 2006) or in an investigation of MP levels of two hundred and one healthy Australian adults (Abell et al., 2014).

It has also been suggested that increased sunlight exposure is a risk factor for developing AMD (Fletcher et al., 2008, Hirakawa et al., 2008). A significant association between extended sunlight exposure in the summer and the 10-year incidence of early age-related maculopathy was reported in the Beaver Dam Eye Study (Tomany et al., 2004). However, it is important to note that an adequate history of sun exposure is difficult to capture via a questionnaire. In addition, skin type and hair colour may be confounding factors although this relationship is not straightforward. An association between skin prone to sunburn and AMD was established in a study of four hundred and forty-six white subjects with end stage AMD (Khan et al., 2006a). On the other hand, while no relationship between eye or hair colour and late AMD was established, modest associations with early AMD were determined in a recent investigation examining the effects of sunlight exposure, eye and hair colour and genetics on the incidence of AMD based on almost five thousand persons tested over a 20 year period (Klein et al., 2014). Nonetheless, few studies have reported on the effect of sunlight exposure and MPOD. A reduced MPOD was found in subjects with a higher UV index (r = -0.341, P = 0.007) so that MPOD was almost 47.5% lower in those with the highest level of UV exposure (Raman et al., 2012b). This finding could not be confirmed in a later study though (Howells et al., 2013). Further work is warranted to explore the potential effect of sunlight exposure, skin type and hair colour on MP levels.

1.4.4   Heritability

A genetic component governing levels of MP has been suggested (Hammond et al., 1995, Loane et al., 2010, Hammond et al., 2012, Hogg et al., 2012) although it is likely that a number of variables other than genetics are involved (Hammond et al., 1995, Hogg et al., 2012). Nonetheless, the genetic influence on MPOD levels is complex. For example, there is evidence that MPOD levels are influenced by gene variants related to carotenoid metabolism in healthy individuals, but not in those with advanced neovascular AMD (Feigl et al., 2014). Classic twin studies have been used to examine the heritability of MPOD levels. Peak MPOD has been shown to be a heritable feature when measured by FAF (Liew et al., 2005, Hogg et al., 2012) or by HFP methods (Liew et al., 2005). On the other hand, it was reported that the MP spatial profile (as represented by the width of the spatial distribution profile curve at half its peak) was not a heritable feature among forty-three twin pairs (Hogg et al., 2012). The authors concluded that MP distribution may be more influenced by environmental or lifestyle risk factors such as diet (Hogg et al., 2012). However, there were limitations in the study as a result of using one-wavelength FAF. In contrast, the ring-like MP distribution was found to be highly heritable in a recent twin study including one hundred and fifty-seven twin pairs (Tariq et al., 2014) in which MPOD was measured by two-wavelength FAF and the spatial profile determined by subjective visual analysis. The differences in measurement methods and in classification between the two studies may explain the conflicting findings and as such requires further work.

1.4.5   Diet and body mass index

It is known that MPOD correlates with both dietary intake and blood serum concentration of L and Z in healthy individuals (Bone et al., 2000, Ciulla et al., 2001a, Nolan et al., 2007a). A stronger relationship between MPOD at 0.5º measured by HFP and serum concentration of L and Z compared to dietary intake of L and Z was demonstrated in one thousand six hundred and ninety-eight females taking part in the Carotenoids in Age-related Eye Disease Study (CAREDS) (Mares et al., 2006). The intake of other dietary components, such as polyunsaturated fat, was shown to be an additional factor that may influence L and Z uptake. Furthermore, it has been demonstrated that dietary modifications can augment MP levels (Hammond et al.,

1997a). What is more, supplementation with L and Z improves MP levels among patients with early AMD (Ma et al., 2012).

There is also evidence that carotenoid metabolism and its genetic coding plays a role in how MP is deposited in the retina (Meyers et al., 2013), and it has been suggested that uptake and transport of L and Z may be affected by abnormalities in carotenoid metabolism (Wang et al., 2007). Moreover, variations in genetic coding for the retinal carotenoid binding proteins involved and affinity of L and Z to the lipoproteins involved in their transport may govern the delivery site for the carotenoids (Bhosale and Bernstein, 2005, Wang et al., 2007). However, the process of carotenoid metabolism is complex, involving competitive uptake of L and Z associated with beta-carotene (Fernández-García et al., 2012). In addition, the isomerisation of L to meso-Z at the centre of the fovea is a poorly understood mechanism (Bone et al., 1993, Bone et al., 1997) but may be responsible for increased MPOD at 0.8° resulting in the appearance of ring-like MP profiles.

Nonetheless it remains that analysis of the individual concentration of effect of L and Z is difficult because dietary databases report concentrations of L and Z combined together (Johnson et al., 2010). Despite the findings of an association between MP levels and dietary and blood serum levels of L and Z, the results of an early study of nineteen healthy individuals showed that approximately half (55%) of the variability in L and Z serum concentration can be explained by a subject's dietary intake of L and Z. Furthermore, it was proposed that 30% of the variability in MPOD could be explained by serum levels of L and Z (Bone et al., 2000). In an investigation of a large sample of women involved in the CAREDS ancillary study (n = 1,698), it was reported that a lower amount of MPOD variability of just 12% could be explained by dietary, health and lifestyle factors. It was therefore concluded that there appeared to be other important predictors of MPOD (Mares et al., 2006).

Obesity has been associated with an increased risk of developing AMD (Clemons et al., 2005, Chakravarthy et al., 2010). Few studies have specifically investigated the hypothesis that body mass index (BMI) is related to retinal carotenoid concentration. Nonetheless, a significant inverse relationship between BMI and body fat percentage and MPOD (measured at 1° by HFP) has been demonstrated (n = 680, r = -0.12, P < 0.0008) (Hammond et al., 2002). This was explained in part by differences in the dietary patterns between the obese and non-obese subjects. However, weight loss in a sample of one hundred and four obese subjects (defined as BMI ≥ 28kg/m^2)

significantly increased MPOD measured by cHFP despite no significant alteration to blood serum carotenoid concentration over the study period (Kirby et al., 2011). An inverse relationship between BMI and MPOD was also reported in a study of sixty-two Indian subjects (r = -0.387, P = 0.002) (Raman et al., 2012a). The investigators concluded that this could be due to competitive uptake of the carotenoids between the retina and adipose tissue. These findings indicate that BMI should therefore be taken into account when exploring inter-individual differences in MPOD.

1.4.6 Smoking status

Smoking is one of the established risk factors for developing AMD (Clemons et al., 2005, Khan et al., 2006b, Chakravarthy et al., 2010). For this reason there has been interest in the effect of smoking status on the levels and distribution of MP. A significant inverse association between MPOD and the average number of cigarettes smoked per day has been demonstrated (r = -0.498, P < 0.001) (Hammond et al., 1996c). More recently, current smokers were reported to present with lower MPOD measured at a single eccentricity at 0.5º (n = 614, 0.18 ± 0.12) than past smokers (n = 1710; 0.21 ± 0.16, P < 0.001) or individuals that had never smoked (n = 1957; 0.21 ± 0.17, P < 0.001) as measured by cHFP (Nolan et al., 2012b). The finding of an inverse association of smoking and MPOD at 0.5º was confirmed in a study of an Indian population, whereby smokers had 30% significantly lower MPOD than non-smokers (Raman et al., 2012a).

As well as point measurements of MPOD at a single retinal eccentricity, it has been questioned whether the lateral extent of the MP spatial profile is related to variables such as smoking status, with a narrower average half-width indicated in heavy smokers compared to non-smokers (Hammond et al., 1997c). However, there is a lack of agreement regarding smoking status and MP spatial profile type. Non-smokers were determined as more likely to have a ring-like MPOD presentation (Dietzel et al., 2011b). It has also been reported that non-smokers (defined as those that had never smoked) were less likely to have a central dip in the MP spatial profile with 8.8% of non-smokers exhibiting a central dip compared to 18.8% of current smokers. However, no statistically significant difference in smoking status and MPOD area, or MPOD at each eccentricity tested was established (Kirby et al., 2010). No effect of smoking status on MPOD values was determined in a more recent investigation of MPOD measured by

HFP in two hundred and one Australian adults although the number of smokers included in the study was not reported (Abell et al., 2014).

1.4.7   Ethnicity

Lower levels of MP are believed to be a risk factor for the development of AMD (Beatty et al., 2001, Nolan et al., 2007b). Epidemiological studies have highlighted a number of risk factors that may be associated with progression of AMD, with smoking, previous cataract surgery and a family history of AMD identified as consistent risk factors (Chakravarthy et al., 2010). A less consistent risk factor is ethnicity (Schachat et al., 1995, Friedman et al., 2004, Bressler et al., 2008, Chang et al., 2008, Chakravarthy et al., 2010, Klein et al., 2011). Prevalence of early AMD has been reported to range across different ethnicities from 2.4% in black to around 6% in whites (Klein et al., 2006, Klein et al., 2013). Other studies have found a similar prevalence of early AMD in Asian Chinese or Japanese people compared to whites (Chen et al., 2008, Kawasaki et al., 2008, Kawasaki et al., 2010), while prevalence of early AMD in Asian Indians has been found to be lower at 2.7% (Nangia et al., 2011). Furthermore, the leading cause of blindness among white persons older than 40 years of age in the United States is AMD (54.4%), but in African persons it is only 4.4% (Congdon et al., 2004). Visual impairment caused by AMD in Indian populations has also been reported to be lower than white populations (Nirmalan et al., 2004, Nangia et al., 2011), whereas visual impairment in Japanese populations has been estimated to be 10.9% (Yamada et al., 2010). This indicates the possibility that protective genetic variants may exist among different ethnicities.

Ethnic differences in central MPOD have been investigated, although data regarding non-white subjects is limited. Most MP studies in the past were derived mainly from white non-Hispanic participants (Hammond et al., 1995, Beatty et al., 2001, Nolan et al., 2004, Nolan et al., 2007a, Nolan et al., 2008, Kirby et al., 2010) and only a few are derived solely from other ethnic backgrounds such as Chinese (Tang et al., 2004, Lam et al., 2005, Yu et al., 2012) and South Asian (Raman et al., 2011). A graph summarising the results of several investigations of MPOD in different ethnicities is presented in Figure 9. The graph shows a general trend towards non-white ethnic groups presenting with lower MPOD at all eccentricities. However, there is difficulty in

comparing findings between studies when different methodologies are employed, as explained in section 1.2.3
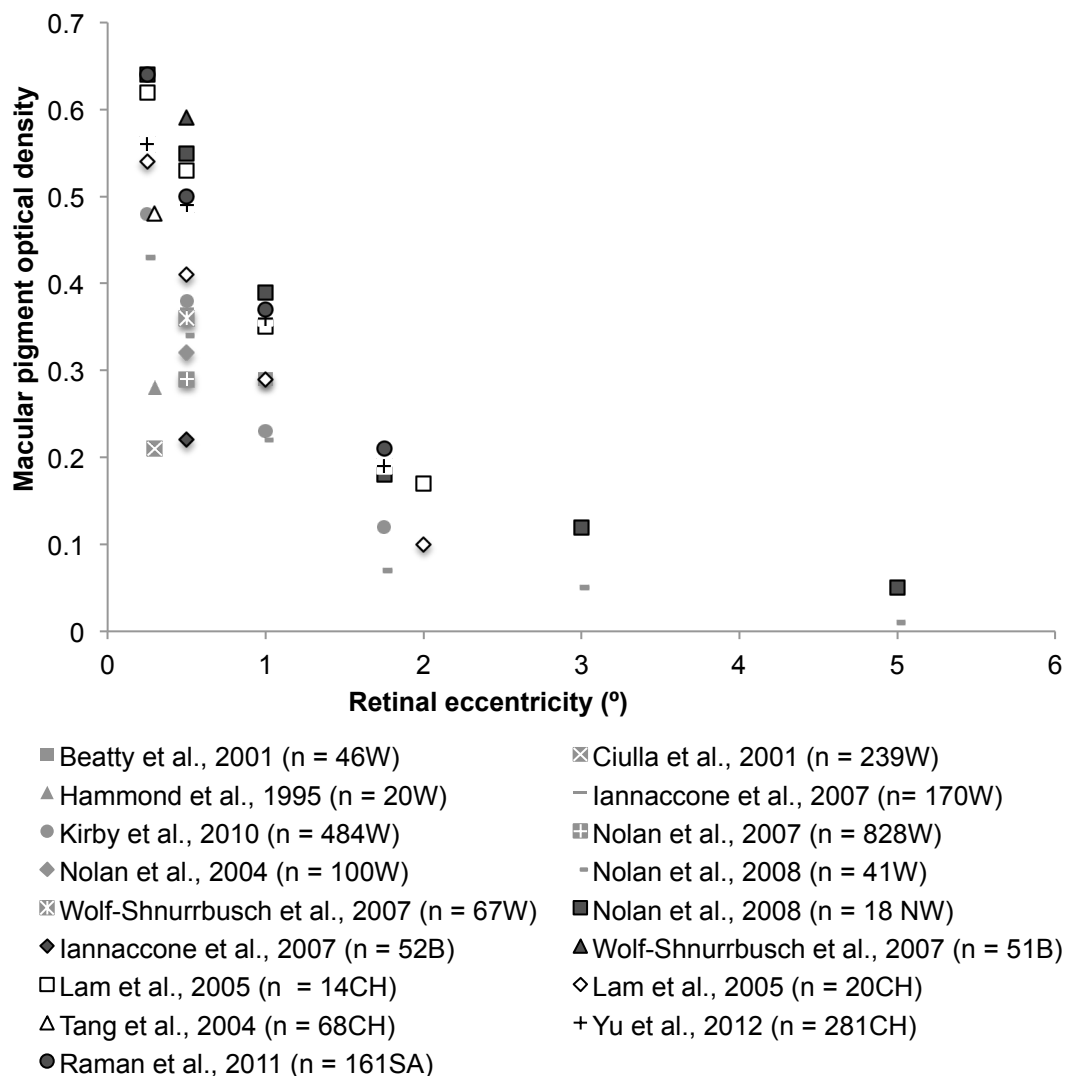
Figure 9 Graph to show variations in MPOD at different eccentricities derived from multiple studies. Abbreviations: W = white, NW = non-white, B = black, CH = Chinese, SA = South Asian.

Few investigations have compared MPOD between ethnic groups using the same measurement technique within a single study. Nonetheless, results from these few studies indicate that white subjects appear to demonstrate lower central MPOD than non-whites. In a recent report a lower mean central MPOD was found in white individuals (0.33 ± 0.13) compared to South Asians (0.43 ± 0.14, P = 0.0005) (Howells et al., 2013). Mean central MPOD was also reduced in white subjects (0.36 ± 0.13) compared to those of African American descent (0.59 ± 0.14, P < 0.0005) (Wolf-Schnurrbusch et al., 2007) supporting previous findings (Ciulla et al., 2001a). The

finding of lower MPOD in black subjects is not consistent though. A lower MPOD was reported in black participants (0.22 ± 0.23, n = 52) compared to whites (0.37 ± 0.19, n = 106, P = 0.0002) among a biracial sample with mean age of 79.1 ± 3.2 years with no ocular disease. This finding could not be explained by correlates such as lutein supplementation and the authors concluded that further work was required to establish normative MPOD data for the black ethnicity group.

There have been reports of an association between ethnicity and MP spatial profile type. Secondary peaks occurred in 86% of Black subjects compared to 68% of white (non-Hispanic) healthy subjects aged 35 to 49 years (P < 0.0001) (Wolf-Schnurrbusch et al., 2007). It seems that there is an increased prevalence of secondary peak profiles reported in ethnicities with lower prevalence of AMD, whereby prevalence of early AMD was reported to be 2.4% in blacks compared to 6% in whites in the Multi-Ethnic Study of Atherosclerosis (Klein et al., 2013). This suggests that the ring-like structure may play a putative role against AMD. However, the finding of an association between ethnicity and the MP spatial profile is not consistent across the literature (Nolan et al., 2008) although this study included a limited number of non-whites. An investigation was carried out in an attempt to further understand the effect of ethnicity on MP and its spatial distribution and is presented in Chapter 3.

1.4.8 Foveal anatomy

Based on histological analysis of primate retinas, it was suggested that the anatomical location of MP might be attributed to its position within the individual retinal layers, since the highest concentrations of MP were measured in the photoreceptor axons at the fovea and in the inner plexiform layer outside the foveola (Snodderly et al., 1984a, Snodderly et al., 1984b) (section 1.1.2). This brings about the following questions. Could the presence of a ring-like MP structure be due to anatomical differences amongst individuals? Can the existence of different MP density distribution phenotypes be explained by variations in the foveal architecture? With the arrival of sophisticated retinal imaging techniques such as OCT, it has become possible to investigate the hypothesis that individual variations in the presentation of MP profiles are due to differences in the foveal architecture, such that retinal thickness, foveal width, and foveal pit slope may play a role in the distribution of MP across the retina (Liew et al., 2006, Nolan et al., 2008, Kirby et al., 2009).

1.4.8.1   Retinal thickness and macular pigment levels

The relationship between central retinal thickness and MPOD has been investigated previously. MPOD was measured by HFP at 1° retinal eccentricity in three hundred and six healthy females aged 17 to 50 years. For each subject foveal measurements were taken from Stratus OCT (Carl Zeiss Meditec, Inc., Dublin, CA) scans. These included average retinal thickness across the central 1000µm (corresponding to around 3.3° retinal eccentricity) and central foveal thickness, taken as the average retinal thickness at the intersection of six radial scans. A thicker retina was associated with higher MPOD in the central 1° field, for both central foveal thickness (178 ± 23µm, r = 0.28, P < 0.0001) (example shown in Figure 10) and average central retinal thickness (212 ± 19µm; r = 0.29, P < 0.0001) (Liew et al., 2006). The finding of a positive significant correlation between MPOD and central foveal thickness was also reported in a later study (van der Veen et al., 2009c).
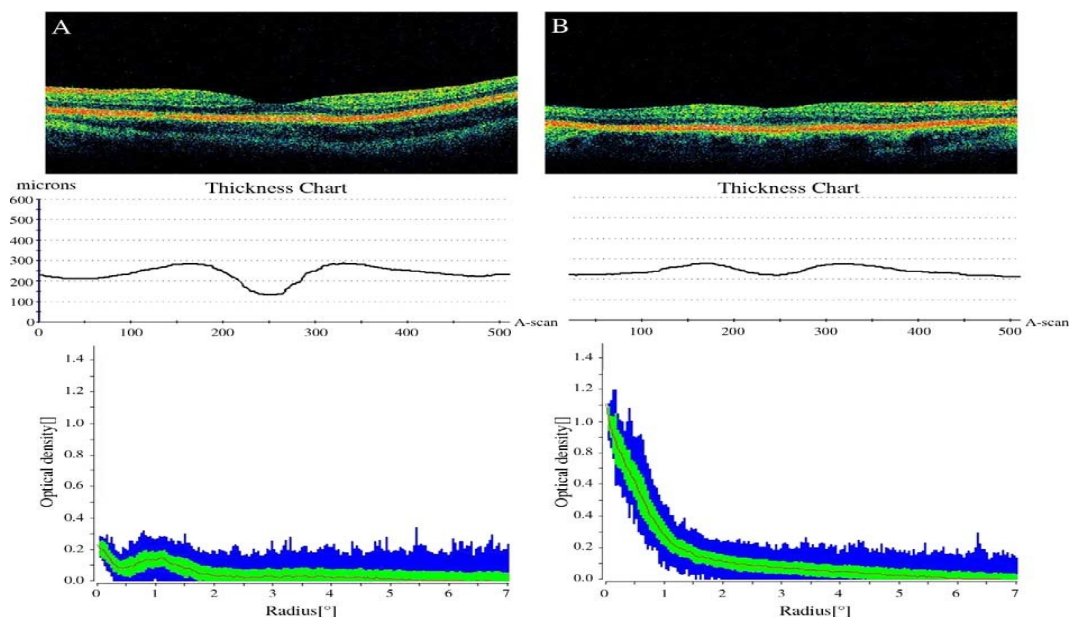
Figure 10 Example of differences in retinal anatomy and MPOD (Liew et al., 2006). OCT images are shown at the top, with the corresponding retinal thickness maps below. MPOD as measured by autofluorescence is shown at the bottom. Subject A has a thinner central retina and lower central MPOD levels compared to subject B.

Nonetheless, the finding of a thicker retina in association with higher MPOD is not consistent across the literature (Kirby et al., 2009). In a study of thirty-seven Caucasian individuals aged 18 to 74 years, no significant correlation between the average macular retinal thickness in the central 1000µm diameter zone (210 ± 28µm) and peak MPOD (r = -0.04, P = 0.82) was found. Additionally, average foveal retinal thickness at the

intersection of six radial scans (175 ± 34µm), was not related to MPOD (r = 0.05, P = 0.78). The conclusion was that foveal anatomy does not play a strong role in establishing the amount of MP present (Kanis et al., 2007).

A lack of association between MPOD measured at the 0.5º retinal location and minimum foveal thickness at the intersection of six radial scans as well as central foveal thickness averaged over the central 1000µm foveal diameter and was also reported in a group of fifty-nine normal subjects (r = 0.03, P = 0.81 and r = -0.08, P = 0.57, respectively) (Nolan et al., 2008). As the study sample included forty-one white and eighteen non-white individuals (including Indian, Asian, Hispanic and black ethnicity) the data was also analysed for white versus non-white individuals. While the lack of correlation remained for the white subjects, a significant positive correlation was found between minimum foveal thickness and MPOD at 0.25º and 0.5º in the non-white group (r = 0.59 and r = 0.67 respectively, P < 0.01). However, no significant correlation between MPOD at either eccentricity and the average foveal thickness across the central 1000µm foveal diameter was determined. Further investigation of the association of retinal thickness with MPOD is necessary, in particular taking into account the potential influence of ethnicity.

1.4.8.2   Foveal width and macular pigment levels

During its early development the foveal pit is formed by peripheral displacement of the inner retinal layers. After birth, the photoreceptors migrate inwards, a process that dramatically increases foveal cone density to 208 200/mm^2 for a 37-year old adult (Yuodelis and Hendrickson, 1986). The width of the fovea is determined by the diameter of the foveola as well as the surrounding parafoveal band. The elevated sides of the foveal depression are due to piling up of the inner retinal layers, formed during early development. At the centre of the foveal pit, the foveola is a rod-free zone located in the photoreceptor layer consisting of cone axons and Müller cell cytoplasm (Yuodelis and Hendrickson, 1986, Hendrickson et al., 2012). It has been shown in the monkey retina that length of the Henle fibres vary with foveal eccentricity and are longer in the centre compared to the peripheral retina (Distler and Dreher, 1996). A wider foveal pit may therefore represent longer central photoreceptor axons and therefore increased storage capacity for MP. This hypothesis was explored in a study involving fifty-nine normal subjects aged between 18 and 60 years. Foveal measurements were taken

from OCT scans obtained using the Stratus OCT (Nolan et al., 2008). Foveal width (measured from crest to crest) was found to be positively related to averaged MPOD taken as the mean of MPOD at 0.25°, 0.5°, 1°, 1.75° and 3° retinal eccentricity (r = 0.32, P = 0.01). Foveal width was also positively correlated with integrated MP across the fovea (r = 0.32, P = 0.01). In the same study, MP measures were also compared to foveal parameters separately for whites (n = 41) versus non-whites (n = 18). Foveal width and average MP remained positively significantly correlated for both the white and the non-white subjects (r = 0.28 and r = 0.26 respectively, P = 0.01). The authors proposed that their findings supported the theory that a wider fovea supports more cone axons and therefore more storage capacity for MP. However, a positive significant correlation between foveal width and MPOD is not a consistent finding (van der Veen et al., 2009c) although this may be due to the smaller sample size included in the latter study or the comparison of foveal width with a single measure of MPOD at 1° retinal eccentricity.

1.4.8.3   Foveal anatomy and the macular pigment spatial profile

Previous investigations have found that a secondary peak MP spatial profile may be related to the foveal morphology (Kirby et al., 2009). It was suggested that the increased likelihood of a secondary peak spatial profile in women might be due to a larger foveal depression compared to men (Delori et al., 2006). Although, foveal anatomy was not directly investigated in the study involving forty-one white subjects, the foveal reflex from reflectance images was analysed. The mean radius of the reflex (corresponding with the radius of curvature of the inner limiting membrane surface) was found to be greater in women (1185µm) than in men (744µm, P value not given). The authors concluded that this was consistent with a broader foveal depression and concluded that foveal morphology may play a role in the occurrence of a secondary peak MP spatial profile. Such a relationship is likely to be complex however due to the possible differences in foveal pit morphology associated with gender and ethnicity (Ooto et al., 2011, Wagner-Schuman et al., 2011).

The potential influence of foveal width on the MP spatial profile type has also been considered (Kirby et al., 2009). The MP spatial profile was measured using the Macular Densitometer device based on HFP in a small study of sixteen healthy subjects. Two groups were compared based on the subjects' MP profile shape. The first group

comprised those exhibiting a typical exponential decline in the MP spatial profile (n = 9) and the second group consisted of those with an atypical spatial profile, defined as those with a MP spatial profile displaying secondary peaks (n = 7). Foveal morphology measurements were taken subjectively from OCT scans obtained by the Topcon 3-D OCT 1000 (Topcon Corp., Tokyo, Japan) using the built-in calliper function. Mean foveal width, measured as a straight line from nerve fibre layer to nerve fibre layer on either side of the foveal depression, was found to be significantly greater in the atypical group (1915 ± 161µm) compared to the typical exponential group (1306 ± 246µm, P < 0.001). While there was a difference in MPOD at 0.25° eccentricity between the typical group (0.58 ± 0.21) and the atypical secondary peak group (0.38 ± 0.19) this did not reach statistical significance (P = 0.086). This was also the case at the 0.5° retinal eccentricity (Kirby et al., 2009). This finding suggests that a wider fovea in the atypical group is not associated with increased MPOD. It may therefore be the case that the overall profile of the foveal pit as described by its width has a greater influence on the overall shape of the MP distribution profile rather than discrete or averaged MPOD values. It would be valuable to explore this hypothesis in a larger sample size.

Differences in foveal width and foveal pit depth have been demonstrated, resulting in variations in the foveal pit profile slope among individuals (Kirby et al., 2009). Given that MPOD typically exhibits a sharp exponential decline with eccentricity from the fovea (section 1.3) it is not unreasonable to look for a correlation between the gradients of the MP profile slope and the foveal pit profile slope. In a study investigating the association between foveal anatomy and MP spatial profile type, a statistically significant relationship was not found between the foveal pit profile slope and the MP profile slope between 0.25° and 0.5° (r = 0.303, P = 0.254) although when an outlier >3SD above the mean was removed, a positive and significant relationship was established (r = 0.591, P = 0.02) (Kirby et al., 2009). When the analysis was repeated separately for typical exponential and atypical secondary peak MP spatial profile groups a positive and significant relationship between the foveal pit profile slope and the MP profile slope was only determined in the atypical group (r = 0.821, P = 0.023). Although the atypical profile group was predominantly female and since females have been found to have wider foveas (Delori et al., 2006), the gender association was not deemed significant. Rather, the presence or absence of a secondary peak was deemed the group membership variable, as males with a secondary peak also tended to have wider foveas. The authors proposed that the finding of a steeper MP profile slope in association with a steeper foveal depression was due to compression of the

inner plexiform and cone axon layers of the retina. Since these layers host MP, this would result in a steeper decline in MPOD from the centre of the fovea.

The relationship between the distribution of MP and foveal morphology is complex and as such warrants further research to evolve our understanding of inter-individual variations. One of the aims of this research study was to explore the possibility that variations in foveal anatomy, as measured from OCT scans, explain the variations seen in MP spatial profile phenotypes. Specifically, the purpose of the study was to investigate the relationship between MPOD at several retinal eccentricities and thickness of the total and inner retinal layer at corresponding locations. The association of foveal width and volume with MP spatial profile type was also explored. In addition, the correlation between the slope of the foveal pit and the slope of the MP distribution among different spatial profile phenotypes was investigated. Given that foveal anatomy may be influenced by ethnicity, the study included individuals from three different ethnic backgrounds (white, South Asian and black) to allowing comparisons to be drawn.

2 Repeatability of macular pigment optical density measurement and its spatial profile: a comparison of objective and subjective methods

2.1.1 Introduction

Previous investigations of the spatial density distribution of MP have used several different methodologies to measure MPOD, which causes inconsistencies when comparing data between studies (Chapter 1, section 1.2.3). Furthermore, the classification of spatial profile phenotypes varies across the literature (Chapter 1, section 1.3.1). There is currently no consensus on a single classification system for MP spatial profiles. Various techniques have been described including objective analysis of secondary maxima-minima pairs (Delori et al., 2006) and mathematical analysis of a combination of an exponential and Gaussian fit to the data distribution (Berendschot and van Norren, 2006). Quantification analysis of MP derived from FAF images has been used in the past to characterize different MP spatial profile phenotypes (Trieschmann et al., 2003) as well as subjective visual assessment of two-wavelength FAF scan images (Tariq et al., 2014). Nevertheless, the presence of a ring-like structure or a secondary peak within the MP spatial profile has been demonstrated by subjective HFP methods (Hammond et al., 1997c, Kirby et al., 2009, Kirby et al., 2010) as well as objective imaging by two-wavelength FAF (Berendschot and van Norren, 2006, Delori et al., 2006, Dietzel et al., 2011b, Tariq et al., 2014).

It has been questioned whether the ring-like structure is a real perturbation or whether it is a result of measurement error, noise in the data, or an artefact of the MPOD measurement method (Delori, 2004). In a preliminary investigation, mapping of the MP spatial profile between sessions was shown to be reliable in four subjects tested by HFP (Hammond et al., 1997c). Reproducibility of the MP spatial profile was also investigated in sixteen healthy individuals in a later study in which MPOD was measured using the Macula Densitometer™ device based on cHFP, where it was concluded that peaks and valleys in the MP spatial profile were not due to measurement error (Kirby et al., 2009). Of note, the amplitude of deviations away from an exponential fit to the data are often small and may not be statistically reliable (Hammond et al., 1997c). Furthermore, repeatability of MPOD measurements varies depending on the instrument employed (Snodderly et al., 2004, Tang et al., 2004, de Kinkelder et al., 2010). Moreover, test-retest repeatability of MPOD measurements are often carried out only at a single 0.5° location for HFP methods (Snodderly et al., 2004, Tang et al., 2004, Bartlett et al., 2010a, de Kinkelder et al., 2010) or at 0.5° and 2° eccentricity using two-wavelength FAF (Trieschmann et al., 2006). If MP spatial profile classification is based on deviations from an exponential fit to the data (Berendschot

and van Norren, 2006, Nolan et al., 2008, Huntjens et al., 2014) or an increase relative to central MPOD (Nolan et al., 2012a) it is important to consider the reliability of the MPOD measurement not only according to the instrument used, but the repeatability of the MPOD measurement at the different retinal eccentricities tested.

A single central MPOD measurement may be a poor predictor of the total amount of MP present (Robson et al., 2003). For this reason, along with point measures of MPOD at single retinal eccentricities and subsequent MP spatial profile phenotyping, various approaches at averaging the MPOD across an area of the retina have been presented. The averaged MPOD value calculated from MPOD at 0.25º, 0.5º, 1º, 1.75º and 3º has been reported in the past (Nolan et al., 2008). An alternative approach has been to calculate the area under the exponential curve fit to a subject's MP spatial distribution data (Nolan et al., 2008). A variation of this was to determine integrated MP by calculating the area of MPOD under the spatial profile curve created by plotting discrete MPOD values (y-axis) against the respective retinal eccentricity in degrees (x-axis) using the trapezoidal rule (Kirby et al., 2010). Indeed calculating the area under the MP profile curve as a means of quantifying the total quantity of MP present has been applied to MP data obtained by two-wavelength FAF too (Hammond et al., 2012). This integrated value provides information as to the overall quantity of MP present across the macula as opposed to measurement at a single retinal eccentricity. This is a useful indicator to consider as it has been shown that the overall amount of MP present varies according to its density distribution (Trieschmann et al., 2003).

Aside from the amount of MP over a defined area there has been interest in the lateral extent of the MP distribution. This has been shown to vary among individuals, with widths ranging from 200μm up to 900μm reported in human histological studies (Trieschmann et al., 2008). The lateral extent of the MP spatial profile measured in vivo can be described by the half-width of the exponential distribution i.e. the retinal eccentricity where the MPOD is at half its maximum (Hammond et al., 1997c). Although averaged and integrated MPOD measures as well as the lateral extent of the MP spatial density distribution have been described in the literature, the repeatability of these measures has not been previously reported.

Aim

The first aim of this study was to investigate repeatability of discrete point MPOD measurements from 0° to around 4° retinal eccentricity using the psychophysical MAP test based on HFP (Chapter 1, section 1.2.1.2). This was also done for MPOD measurements obtained by the two-wavelength FAF imaging technique (Chapter 1, section 1.2.2.1). Repeatability statistics for the following MPOD measures were also established:

- MPODav: an averaged MPOD measure corresponding to the average blue light transmittance (Tav) over a given area (Huntjens et al., 2014);
- MPODint: a measure of the integrated MPOD based on the area under the MPOD distribution curve; and
- Lateral extent of the MP spatial distribution represented by the retinal eccentricity where MPOD was at half its peak value.

In addition, the hypothesis that a single central MPOD measure is a poor predictor of the total amount of MP present was tested by calculating the correlation of MPOD at 0°, 0.8° and 1.8° with the total amount of MP present, as represented by MPODint.

The second aim of the investigation was to explore the feasibility of applying a consistent mathematical objective method of classifying an individual's MP spatial profile phenotype (as exponential, ring-like or central dip) from data obtained by the HFP and the FAF techniques. This classification system (described in detail in section 2.1.2) has been previously reported by our research group, Appendix 6.1 (Huntjens et al., 2014). In addition, the two-wavelength FAF scan images were visually inspected to subjectively classify MP spatial profiles (Dietzel et al., 2011b, Tariq et al., 2014). Agreement of objective MP spatial profile classification between visits for each instrument was calculated. This was compared to agreement of MP spatial profiling between FAF scans as determined by subjective visual inspection.

As an extension to the repeatability study, both profiling methods (objective based on deviations from the exponential fit and subjective visual inspection) were applied to existing twin MP data for one hundred and fifty-seven twin pairs. Concordance of the ring-like profile was calculated for monozygotic (MZ) and dizygotic (DZ) twin pairs and compared to previously obtained data.

2.1.2   Methods

Phase 1: Macular Assessment Profile test repeatability study

Ethical approval for the study was obtained from the Optometry Research & Ethics Committee at City University London and written informed consent (Appendix 6.5) was obtained from all subjects, conforming to the tenets of the Declaration of Helsinki. The MAP test repeatability study took place at the Division of Optometry and Visual Science. Investigator IC (Irene Ctori) recruited a total of twenty-six healthy volunteers from the student population between October 2013 and December 2013. Data collected from an additional fourteen individuals as part of a previous study between October 2010 and November 2010 (Huntjens et al., 2014) was also included in the present investigation. This data had been collected using the same protocol and methods as the current study.

Visual acuity was assessed using a logMAR (logarithm of minimal angle of resolution) EDTRS chart at 4m under standard testing conditions. This was carried out monocularly using the subject's habitual refractive correction with either contact lenses or spectacles where necessary. Inclusion into the study was based on a logMAR visual acuity of 0.3 log units or better in the eye being tested, consistent with the minimum requirement for reliable MPOD measurement (Nolan et al., 2007a, Nolan et al., 2009). All participants completed a health and lifestyle questionnaire (Appendix 6.6). The questionnaire was designed to collect demographic data. Its rationale is explained in more detail in section 3.1.2. Exclusion criteria were: ocular pathology including age-related macular degeneration, previous laser eye surgery and medication that may affect retinal function e.g. hydroxychloroquine used for the treatment of inflammatory conditions such as rheumatoid arthritis and systemic lupus erythematosus.

By default, measurements were taken for the right eye unless it did not meet the inclusion criteria, in which case the left eye was used. MPOD in log units was measured using the MAP test. The principles of the MAP test have been described in detail in Chapter 1, section 1.2.1.2. The MAP test was repeated for all participants within two weeks of the first visit by the same investigator following the same protocol throughout.

Macular Assessment Profile test method

Calibration of the Eizo T566 display screen used for the MAP test was carried out prior to the start of data collection to ensure the appropriate luminance levels were being used. The display screen was switched on 30 minutes prior to calibration. An LMT 1009 luminance meter was used together with the luminance calibration programme. The luminance versus the applied voltage relationship for each electron gun was measured automatically at 8 voltage steps of the 1024 steps of the 10-bit graphics card.

The same protocol was maintained throughout the study. The MAP test was performed monocularly in a dark room, at a distance of 70cm from the display screen to the eye. The subject's habitual distance correction was used. If the participant wore glasses it was ensured that the spectacle lenses were not tinted. Room lights were switched off prior to explaining the MAP test procedure during which the investigator provided a uniform introduction to the test for each participant. A period of at least five minutes was allowed to ensure dark adaptation, consistent with the procedures used with other optical HFP methods (Werner et al., 1987, Beatty et al., 2000a, Bone and Landrum, 2004, Putnam and Bassi, 2015). The participant was positioned with their chin on a chinrest and forehead against a headrest bar so that the outer canthus was aligned to the appropriate height, indicated by a marker on the side of the viewing station. The "notch" filter (Chapter 1, section 1.2.1.2) was positioned in front of the test eye so that the participant was looking through it for the duration of the test.
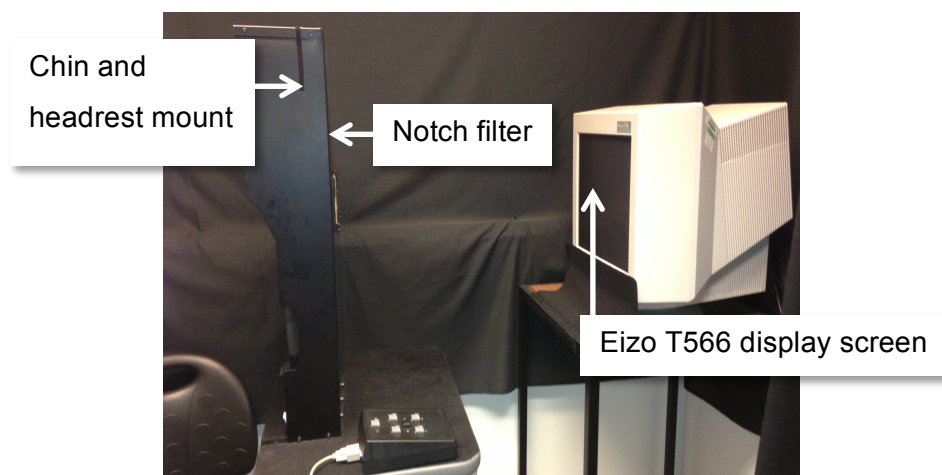
Figure 11 Photograph of the MAP test arrangement. The subject sits on the left placing their chin on the chin rest and forehead against the headrest within the mount. The subject views the display screen at a distance of 70cm looking through the notch filter positioned in front of the test eye.

The MAP test software randomly sequences the order of stimulus location presentations to each subject. For the 0° stimulus location, the participant was asked to look directly at the central disc stimulus. For the six peripheral stimulus locations (at 0.8°, 1.8°, 2.8°, 3.8°, 6.8°, 7.8° eccentricity), participants were instructed to look at a black fixation spot in the centre of four target lines and the stimulus was presented peripheral to this (Chapter 1, Figure 6). The stimulus was presented as short bursts of flicker of approximately 0.5 seconds duration (Rodriguez-Carmona et al., 2006). A low threshold and high threshold was determined for each spatial location and this was repeated four times. For the lower threshold, the test beam luminance was set to zero so that the stimulus flickered strongly. The investigator adjusted the intensity of the SW beam in small increments until the subject reported no perception of flicker. The higher threshold was established by increasing the luminance of the test beam until the subject reported maximal flicker. The investigator then reduced the luminance of the test beam until the subject reported no flicker. A modified staircase double-reversal method was used to determine all thresholds. If a subject found it difficult to null the flicker, for example those with high flicker sensitivity, the investigator aimed to establish where flicker was minimal. Regular breaks were given during the test. A single reversal technique was only adopted if patient fatigue meant the double reversal technique was not possible. Subjects were encouraged to blink throughout the test to minimize the Troxler effect (de Kinkelder et al., 2010). In order to assess repeatability, the MAP test was repeated within seven to fourteen days adopting the same procedure as above for the second visit.

Phase 2: Two-wavelength fundus autofluorescence repeatability study

Approval to re-analyze two-wavelength FAF images acquired for a previous study (Hammond et al., 2012) was obtained from the TwinsUK Resource Executive Committee (TREC) of St Thomas' Hospital, London. Two-wavelength FAF imaging was previously carried out as part of a Twin heritability study described in detail elsewhere (Hammond et al., 2012) that included three hundred and fourteen healthy female twin volunteers aged 16 to 50 years, recruited from the TwinsUK registry at St Thomas' Hospital (London, UK). In brief, following mydriasis, two-wavelength FAF imaging was performed on both eyes of each participant using a modified confocal scanning laser ophthalmoscope (Heidelberg Engineering, Heidelberg, Germany) providing high-resolution images at 488 and 514nm wavelengths. The intensity of a greyscale map, generated by digital subtraction of the images obtained at the two wavelengths, was

proportional to the MPOD at each retinal location. The instrument's software generated a plot of MPOD against eccentricity by averaging MPOD measurements at each retinal location (Wustemeyer et al., 2003).

Data analysis for the present study took place at the Department of Ophthalmology, Kings College London, St Thomas' Hospital Campus, London. Only subjects that had two scans taken within a single visit were eligible for inclusion into the repeatability study. For each of the two FAF scans performed within a single visit, the MPOD profile was generated using the automated "find fovea" function available within the instrument's software. This was done as an attempt to have a consistent approach to locating the fovea (Sasamoto et al., 2010) rather than manually placing the cursor at the perceived centre of the fovea. If this function did not locate the fovea but instead located a blood vessel, the scan was disregarded for the repeatability study. When the "find fovea" function did locate the fovea, the linear intensity graph was inspected to ensure that the linear graph was maximally converged; if manually moving the centre of the scan in any direction away from the automatic foveal centre location decreased the convergence (i.e. more separation between the lines), the scan was not selected for further analysis and the subject was not eligible for inclusion. Two suitable scans taken from a single eye for each of forty participants were identified.

Phase 3: Two-wavelength fundus autofluorescence twin heritability study

An extension of the repeatability study was to assess concordance of the MP spatial profile phenotype between MZ and DZ twins. For this, MPOD was quantified from all base-line FAF scans for each of the three hundred and fourteen participants from the Twin Study Database. If the find fovea function did not automatically locate the fovea, a cursor was manually positioned at the centre of the MPOD reflex and the position adjusted to achieve maximal convergence of the output of the linear graph as explained above.

Classification of MP spatial profiles phenotypes

A MP spatial profile phenotype was assigned to each participant's MPOD data set obtained at each visit for the MAP test obtained during the Phase 1 study, or for each FAF scan evaluated during the Phase 2 and Phase 3 studies. This was achieved by

plotting MPOD against retinal eccentricity for each subject. For the MAP test data this was based on MPOD at 0º, 0.8º, 1.8º, 2.8º and 3.8º derived directly from the instrument's output. For each FAF image, the radial intensity graph incorporated in the Heidelberg software (identified according to the method described) was used to extract MPOD values at 0°, 0.1°, 0.8°, 1.8°, 2.8° and 3.8° (Figure 12). An additional measure of MPOD at 0.1° was included due to poor repeatability of the central 0° measurement, which is explained further in the results (Table 4) and discussion. An exponential curve was fitted to the MPOD data up to 3.8º allowing the exponential function to float, rather than assuming a fixed negligible value at the peripheral reference location (Putnam and Bassi, 2015).
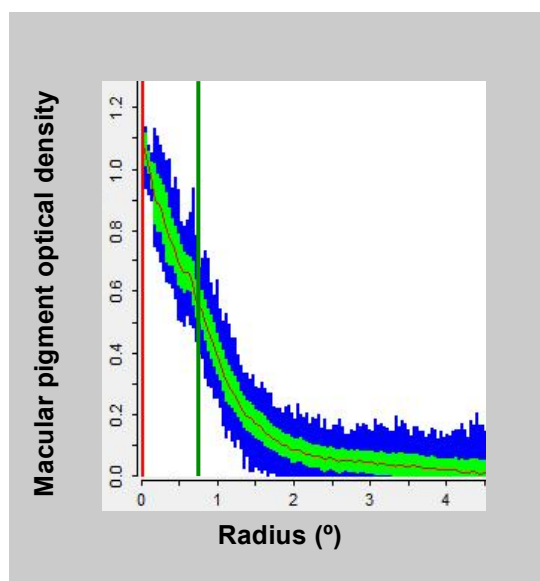
Figure 12 Example of two-wavelength fundus autofluorescence radial intensity graph. The green vertical line was positioned at the required retinal eccentricity on the x-axis (shown at 0.8° in the example) and the corresponding MPOD value (y-axis) displayed in a separate window (not shown) was recorded.

Classification of the MP spatial profile was based deviations away from an exponential fit of the data distribution while taking into account the instrument's measurement error for each retinal location tested, as determined by the repeatability study. The following protocol was implemented: an exponential profile was assigned if the measured MPOD value at 0°, 0.8° and 1.8° was within the 95% confidence limits of the value predicted by the fitted exponential curve. Profiles with MPOD values deviating greater than one CoR above the exponential fit at 0.8° or 1.8° were assigned a ring-like classification. A deviation more than one CoR below the expected value at 0° was classified as a central dip as shown in Figure 13 (Huntjens et al., 2014).
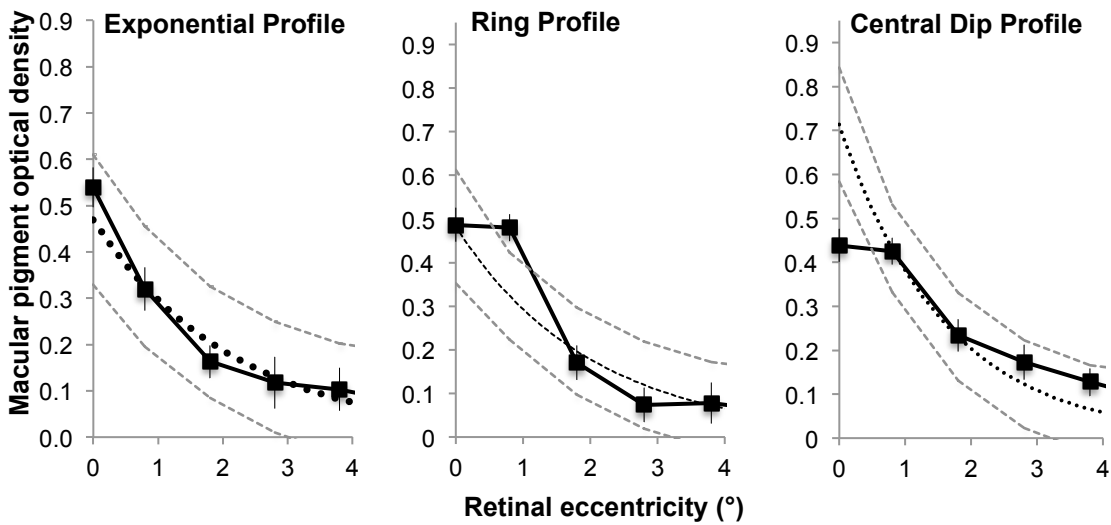
Figure 13 MPOD distribution as a function of eccentricity for three participants tested using the MAP test to show an example of the exponential, ring-like, and central dip profile. All three graphs include the mean absolute MPOD values ± SD of eight measurements (four low and four high thresholds) at 0, 0.8, 1.8, 2.8 and 3.8° retinal eccentricities. The black dotted line represents the exponential curve fitting to the mean absolute MPOD values. The grey dashed lines represent the MAP test measurement error according to eccentricity away from the exponential curve. Note the MPOD at 0.8° in the ring-like profile presents more than one coefficient of repeatability (CoR) above the expected exponential curve at 0.8°. The MPOD at 0° in the central dip profile shows more than one CoR below exponential curve.

As well as the discrete MPOD values measured at single retinal eccentricities the integrated blue light transmittance (Tav) and corresponding average MPOD (MPODav) were also calculated for each data set (Huntjens et al., 2014). MPODav is a single value representing an average MPOD value over a given area. At each retinal eccentricity measured by the MAP test, the transmittance (T_i) is a measure of the SW blue light-filtering capacity of the MP at that location (i) and is given by:

$$T_i = 10^{-\text{MPOD}_i} \tag{5}$$

The value of T_i was plotted on the y-axis against retinal eccentricity on the x-axis (Figure 14). Calculating the volume of each quasi-cylinder (with height T_i and radius according to the aperture size) and dividing by the surface area of the aperture gives the integrated transmittance over that area.
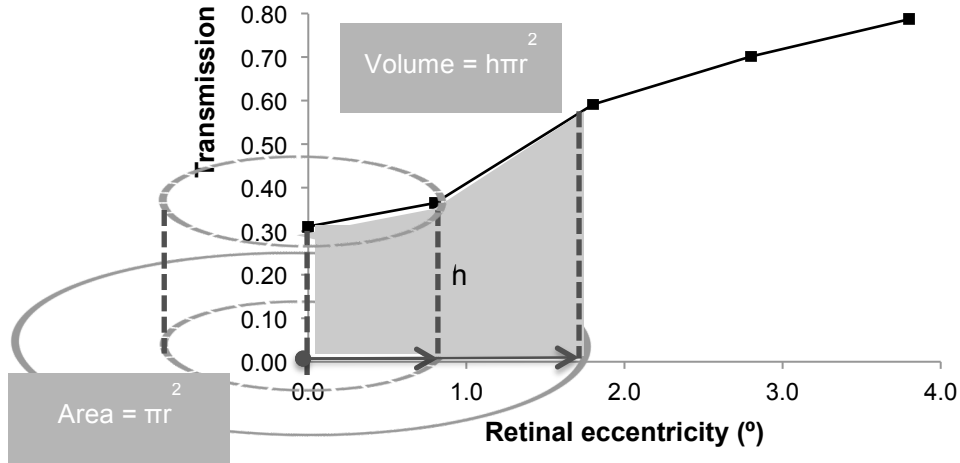
Figure 14 Graph to show transmission of blue light (y-axis) versus retinal eccentricity (x-axis). The grey circles schematically illustrate the area over which integrated transmission of MP was calculated.

The integrated transmittance Tav was calculated up to 1.8º corresponding to a 3.6° diameter circular aperture using the formula:

$$T_{AV(0-1.8)} = \frac{0.5(T_0+T_{0.8})(\pi 0.8^2-0)+0.5(T_{0.8}+T_{1.8})(\pi 1.8^2-\pi 0.8^2)}{\pi 1.8^2} \tag{6}$$

where T_0 = 10^-MPOD at 0°, $T_{0.8}$ = 10^-MPOD at 0.8°, and $T_{1.8}$ = 10^-MPOD at 1.8°. The value of Tav (0-1.8) was used to calculate an average MPOD between 0° and 1.8°:

$$MPOD_{AV(0-1.8)} = -log_{10}T_{AV(0-1.8)} \tag{7}$$

Values of MPODav (0 to 3.8º) were calculated in a similar manner. Average MPOD over a weighted area means that as the area increases, the transmissibility increases and MPODav decreases.

A measure of the integrated MPOD over an area, represented by "MPODint", was also calculated for each participant's MPOD data set. This was done using the same approach detailed by Kirby et al. (2010). However, rather than calculating the area under the curve up to the peripheral reference point based on assumed MPOD of zero at this location, the area was calculated up to the most eccentric point measured by the MAP test not including the reference point (i.e. up to 3.8º) (Figure 15).
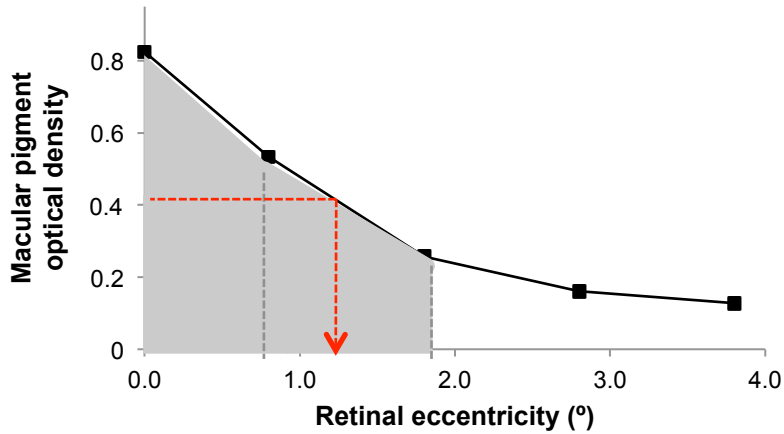
Figure 15 MPODint (0 to 1.8) shown by shaded grey area represents integrated area under the curve according to the trapezium rule. The red arrow indicates the x-value at half peak MPOD.

The trapezium rule was used in a two-dimensional or rectangular coordinate system to calculate the MPODint between 0º and 1.8º. (The area under the curve from 0º to 3.8º, i.e. MPODint (0 to 3.8) was calculated in a similar way).

$$MPODint\ (0\ to\ 1.8)$$
$$= \{[(MPOD_0 + MPOD_{0.8})/2]{\times}0.8\} + \{[(MPOD_{0.8} + MPOD_{1.8})/2]{\times}1.0\}$$

(8)

The lateral extent of the MP distribution, represented by the half width at peak MPOD, was determined for each subject based on the exponential curve fit to the MPOD data (Hammond et al., 1997c). This was calculated in an excel spreadsheet as the retinal eccentricity where MPOD was at half its peak value, shown graphically in Figure 15.

As well as the objective classification system described, a subjective classification method was used to assess the MP spatial profile from FAF images. Experienced investigator (OM) visually inspected each FAF image for the presence of a ring-like pattern or central dip as described in a previous study (Tariq et al. 2014). Each FAF image was inspected in a random order, blind to the results of the first scan and blind to the objective classification. Examples of the three MP spatial profile types as identified by visual inspection are presented in Figure 16.
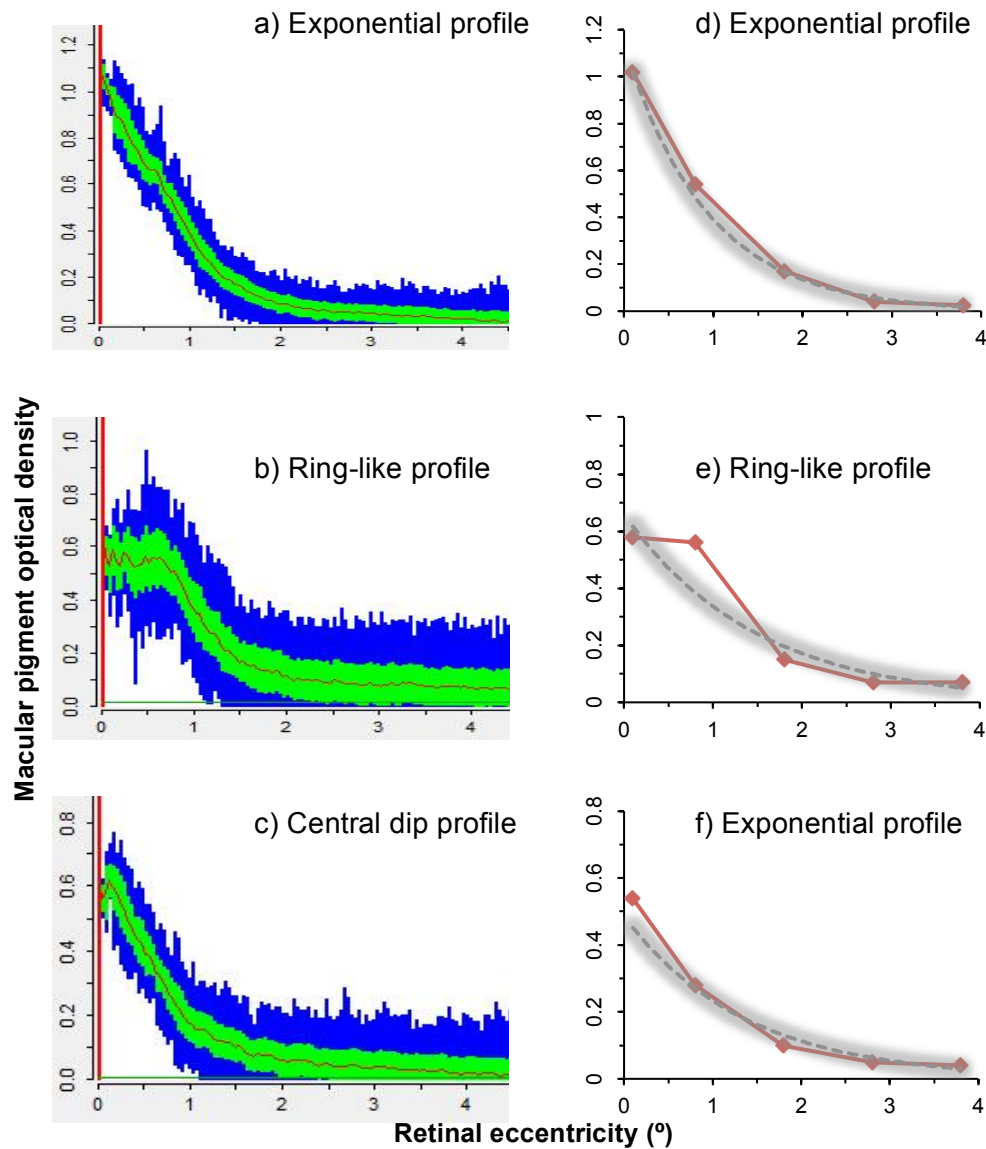
Figure 16 Examples of the three MP spatial profile phenotypes as classified by subjective visual inspection of fundus autofluorescence images shown on left hand side: a) exponential profile; b) ring-like profile and c) central dip profile. The graphs on the right show the corresponding MPOD data (y-axis) plotted against retinal eccentricity (x-axis), indicated by the red line. The shaded grey area schematically represents one CoR above and below the exponential fit to the data (grey dashed line). According to the objective profile classification, d) shows an exponential profile; e) shows a ring-like profile, whereby MPOD at 0.8° is more than 1 CoR above the exponential fit line and f) shows that although image c) was subjectively classified as a central dip, central MPOD is not more than 1 CoR below the exponential fit line and is therefore objectively classified as an exponential profile.

Statistical analysis

All statistical analyses were performed using SPSS version 22.0 for Windows (SPSS Inc., Chicago, USA). Values in the text and tables are presented as mean ± standard deviation (SD). MPOD measurements are in log units. The Coefficient of Repeatability (CoR) was calculated as: CoR = 1.96s, where s is the SD of the difference between pairs of MPOD measurements between visits one and two (Bland and Altman, 1986). Limits of Agreement (LoA) were determined as the mean difference between pairs of MPOD measurements ± CoR. The LoA indicate the range within which 95% of the differences between measurements will lie (Bland and Altman, 1986, Bland and Altman, 1999, McAlinden et al., 2011). Agreement of classification of the MP spatial profile was evaluated by the overall percentage of agreement between visits or scans and by the Kappa measure of agreement, κ (Landis and Koch, 1977, Sim and Wright, 2005). Case-wise concordance for presence of a ring-like or central dip profile was calculated separately for MZ and DZ twins as: 2C/(2C + D), where C is the number of twin pairs concordant and D the number discordant (Tariq et al., 2014).

Sample size calculation

An a priori power statistics analysis revealed that a sample size of forty subjects was required for each repeatability study. This was calculated using G*Power 3.1 with power set at 80% and a statistical significance level of α = 0.05 (Faul et al., 2007, Faul et al., 2009) This calculation was based on a paired t-test, with an effect size of 0.45 based on an estimated mean difference in MPOD of 0.05 with SD of difference between measurements of 0.11 (Huntjens et al., 2014).

2.1.3   Results

Phase 1: Macular Assessment Profile test repeatability study

The mean age of the forty participants for the MAP test study was 24 ± 6.0 years. Mean MPOD at 0° was 0.57 ± 0.23 for the first and 0.58 ± 0.23 for the second visit, which was not statistically significantly different (dependent samples t-test, P = 0.12). A CoR of 0.12 was calculated. Mean MPOD for all spatial locations, MPODav, MPODint

and x at half peak MPOD and the corresponding CoR values are presented in Table 4 and Table 5. The lower and upper 95% LoA, mean difference between visits and the variance are also presented. Bland-Altman plots for the 0° and 0.8° locations are shown in Figure 17. The mean standard error of MPOD measured at all retinal eccentricities locations was 0.05. This was based on eight measurements per eccentricity within a single session (four low threshold and four high threshold).

The frequency distributions of the three different spatial profile types (exponential, ring-like and central dip) are shown in Table 2. The overall percentage of agreement of objective classification of the MP spatial profile between MAP test visits was 95%, with a κ-value of 0.89 (95% confidence interval 0.74 to 1.00, P < 0.0005).

	Spatial profile phenotype					
	Exponential		Ring-like		Central dip	
	%	(n)	%	(n)	%	(n)
Visit 1	70	(28)	17.5	(7)	12.5	(5)
Visit 2	75	(30)	15	(6)	10	(4)

Table 2 Frequency distributions of the three different MP spatial profile phenotypes (exponential, ring-like and central dip) among the forty participants in the Phase 1 Map test study.

As well as individual subject MP spatial profile phenotyping according to the classification criteria, an analysis was conducted to assess how well an exponential profile described the averaged subjects' MPOD data profile. The coefficient of determination, R^2 of the averaged subjects' profile data (i.e. MPOD measured at 0º, 0.8º, 1.8º, 2.8º and 3.8º) and a first order decreasing exponential profile, was calculated in an excel spreadsheet. A very high correlation of R^2 = 0.98 was found demonstrating that the exponential model explained almost all of the variation in the data.

To explore how well a single MPOD measurement correlated with the overall amount of MPOD, the association between MPOD at 0º, 0.8º and 1.8º with MPODint and MPODav was calculated and is presented in Table 3. Correlation of MPOD at each single eccentricity with MPODint and MPODav was strong in each case. A Fisher r to z transformation was applied to assess the significance of the difference between the

correlation coefficients. This showed that the relationship was significantly stronger for MPOD at 0.8º compared to 0º as indicated by -1.96 < z < -1.96 in each case (P < 0.05).

	MAP test			FAF scan		
	MPOD at 0º	MPOD at 0.8º	MPOD at 1.8º	MPOD at 0º	MPOD at 0.8º	MPOD at 1.8º
	R^2	R^2	R^2	R^2	R^2	R^2
MPODint (0 to 1.8)	0.86	0.96	0.70	0.83	0.95	0.76
MPODint (0 to 3.8)	0.77	0.91	0.78	0.80	0.94	0.82
MPODav (0 to 1.8)	0.73	0.91	0.85	0.67	0.97	0.87
MPODav (0 to 3.8)	0.49	0.66	0.70	0.60	0.84	0.90

Table 3 Correlation of MPOD at single central eccentricities with integrated MPODint and MPODav (0 to 3.8º) and (0 to 1.8º).

Phase 2: Two-wavelength fundus autofluorescence repeatability study

The mean age of the forty female participants in the FAF study was 39 ± 8.6 years. The mean MPOD at 0° was 0.57 ± 0.22 for the first scan and 0.57 ± 0.21 for the second, which was not statistically significantly different (dependent samples t-test, P = 0.86). A CoR of 0.23 was calculated. At 0.1° the CoR was 0.15 and reduced to ≤ 0.06 from 0.8° and beyond (Table 4). Further analysis of additional MPOD data values obtained at 0.2º and 0.5º retinal eccentricities revealed a CoR of 0.12 and 0.06 respectively. To maintain consistency with the Phase 1 data, these additional MPOD data values were not used to derive averaged or integrated MPOD or for spatial profile classification. MPODav, MPODint and x value at half peak MPOD and the corresponding CoR values are presented in Table 5. The lower and upper 95% LoA, mean difference between visits and the variance are also presented. Bland-Altman plots for the 0° and 0.8° locations are shown in Figure 17.

Eccentricity (°)	Mean ± SD	Mean ± SD	CoR	Mean difference	Upper limit of agreement	Lower limit of agreement	Variance (%)
MAP test	**Visit 1**	**Visit 2**					
0	0.57 ± 0.23	0.58 ± 0.23	0.12	-0.016	0.11	-0.14	5.5
0.8	0.49 ± 0.20	0.48 ± 0.19	0.12	0.005	0.12	-0.11	3.9
1.8	0.25 ± 0.12	0.25 ± 0.12	0.14	0.002	0.14	-0.14	1.4
2.8	0.14 ± 0.07	0.15 ± 0.07	0.11	-0.013	0.10	-0.12	0.5
3.8	0.10 ± 0.07	0.11 ± 0.06	0.11	-0.001	0.11	-0.11	0.3
FAF imaging	**Scan 1**	**Scan 2**					
0	0.57 ± 0.22	0.57 ± 0.21	0.23	-0.006	0.22	-0.24	4.8
0.1	0.55 ± 0.21	0.54 ± 0.19	0.15	0.009	0.16	-0.14	4.6
0.2	*0.51 ± 0.19*	*0.51 ± 0.18*	*0.12*	*0.002*	*0.18*	*-0.06*	*3.7*
0.5	*0.39 ± 0.15*	*0.38 ±0.15*	*0.06*	*0.01*	*0.08*	*-0.03*	*2.1*
0.8	0.34 ± 0.12	0.33 ± 0.12	0.06	0.006	0.09	-0.03	1.4
1.8	0.10 ± 0.04	0.09 ± 0.04	0.04	0.003	0.04	-0.03	0.2
2.8	0.05 ± 0.02	0.05 ± 0.02	0.03	0.004	0.03	-0.02	0.05
3.8	0.04 ± 0.01	0.03 ± 0.02	0.03	0.002	0.02	-0.02	0.02

Table 4 Mean MPOD ± SD measured by the Macular Assessment Profile (MAP) test for each visit and fundus autofluorescence (FAF) imaging for each scan. Repeatability measures for both instruments according to the retinal eccentricity measured are also displayed.

Eccentricity (°)	Mean ± SD	Mean ± SD	CoR	Mean difference	Upper limit of agreement	Lower limit of agreement	Variance (%)
MAP test	Visit 1	Visit 2					
MPODav (0 to 1.8)	0.37 ± 0.14	0.37 ± 0.14	0.11	0.00	0.11	-0.11	2.1
MPODav (0 to 3.8)	0.19 ± 0.07	0.19 ± 0.07	0.04	0.00	0.08	-0.09	0.5
MPODint (0 to 1.8)	0.79 ± 0.31	0.79 ± 0.30	0.09	0.00	0.18	-0.18	9.8
MPODint (0 to 3.8)	1.10 ± 0.43	1.11 ± 0.41	0.16	-0.01	0.30	-0.33	18.6
x value at half peak MPOD	1.61 ± 0.58	1.70 ± 0.71	0.42	-0.09	0.72	-0.91	34.0
FAF imaging	Scan 1	Scan 2					
MPODav (0 to 1.8)	0.24 ± 0.07	0.23 ± 0.07	0.04	0.00	0.05	-0.04	0.5
MPODav (0 to 3.8)	0.09 ± 0.03	0.09 ± 0.03	0.03	0.00	0.03	-0.02	0.1
MPODint (0 to 1.8)	0.53 ± 0.18	0.52 ± 0.17	0.10	0.01	0.11	-0.09	3.1
MPODint (0 to 3.8)	0.65 ± 0.22	0.63 ± 0.21	0.14	0.02	0.15	-0.12	4.6
x value at half peak MPOD	0.78 ± 0.23	0.74 ± 0.18	0.32	0.04	0.36	-0.28	4.4

Table 5 Mean ± SD of: averaged MPOD over an integrated area (MPODav); integrated MPOD area under the curve (MPODint); and the x-value at half peak MPOD as measured by the Macular Assessment Profile (MAP) test for each visit and fundus autofluorescence (FAF) imaging for each scan. Repeatability measures for each MPOD parameter are provided.
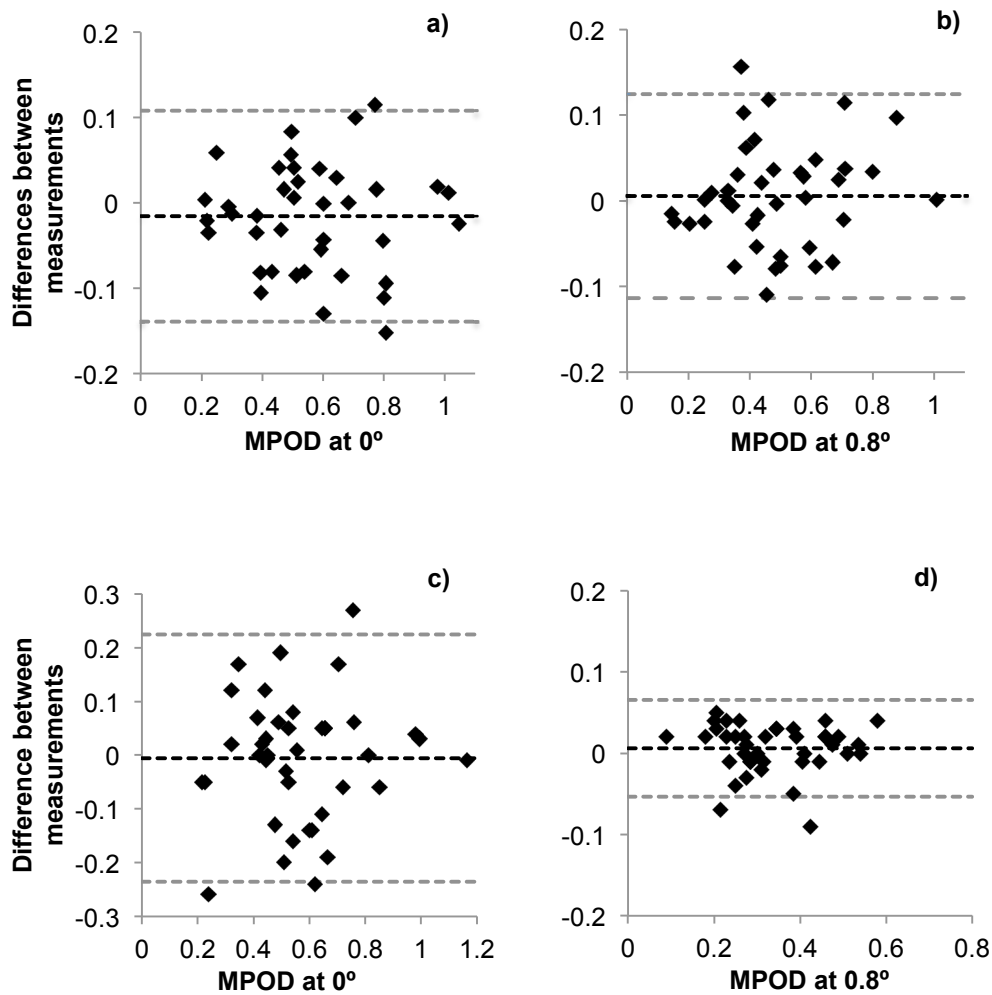
Figure 17 Bland-Altman plots to show repeatability of MPOD measurements. The upper plots show difference in MPOD measurements between visits using the Macular Assessment Profile (MAP) test results a) at 0° and b) at 0.8°. The lower plots show difference in MPOD measurements between fundus autofluorescence (FAF) scans c) at 0° and d) at 0.8°. Black dashed line represents the mean of the two measurements. Grey dashed lines indicate the upper and lower Limits of Agreement indicating the range within which 95% of the differences between measurements are expected to lie.

The frequency distribution of the three different spatial profile types is presented in Table 6. The overall percentage of agreement of objective classification of the MP spatial profile between each pair of FAF scans was 93% with a κ-value of 0.85 (95% confidence interval 0.69 to 1.00, P < 0.0005). Subjective visual classification of the MP spatial profile between FAF scans resulted in 73% overall percentage agreement, and a κ-value of 0.48 (95% confidence interval 0.23 to 0.73, P < 0.0005). The agreement between the objective and subjective classification methods for all 80 FAF scans

resulted in overall percentage agreement of 60%, with a κ-value of 0.23 (95% confidence interval 0.04 to 0.42, P = 0.02). Of note, in a separate analysis the addition of MPOD data points at 0.2º and/or 0.5º did not significantly alter the MP spatial profile classification and agreement.

	Spatial profile phenotype					
	Exponential		**Ring-like**		**Central dip**	
	%	**(n)**	**%**	**(n)**	**%**	**(n)**
Objective spatial profiling						
Scan 1	52.5	(21)	47.5	(19)	0	(0)
Scan 2	60.0	(24)	40.0	(16)	0	(0)
Subjective visual spatial profiling						
Scan 1	62.5	(25)	30	(12)	7.5	(3)
Scan 2	57.5	(23)	35	(14)	7.5	(3)

Table 6 Frequency of MP spatial profile phenotypes determined by objective and subjective classification of MPOD measured using fundus autofluorescence (FAF). Results presented as %, with the actual number in brackets.

As with the Phase 1 data, the R^2 value between the averaged subjects' profile data (MPOD at 0.1º, 0.8º, 1.8º, 2.8º and 3.8º) and a first order decreasing exponential profile was very high (R^2 = 0.96).

In agreement with results of the Phase 1 study, whilst the relationship between MPOD at each single eccentricity with MPODint and MPODav was strong it was significantly stronger for MPOD at 0.8º compared to 0º (P < 0.05) (Table 3).

Phase 3: Two-wavelength fundus autofluorescence twin heritability study

The mean age of the three hundred and fourteen twins (157 pairs) was 39 ± 8.8 years. Analysis of MP spatial profile phenotype among the twins revealed that overall prevalence of the exponential profile by objective classification was 71% and the ring-like profile was 29%. No central dip profiles were identified by the objective classification method (Table 7). Case-wise concordance was calculated as 0.74 for MZ and 0.36 for DZ twins. According to visual subjective profiling, 64% presented with an

exponential profile while 27% had ring-like and 9% central dip profiles. Case-wise concordance was recalculated for subjective profile classification resulting in 0.80 for MZ and 0.41 for DZ twins when the central dip was combined with the ring-like profiles.

	Spatial profile phenotype					
	Exponential		Ring-like		Central dip	
	%	(n)	%	(n)	%	(n)
Visual assessment (Tariq et al., 2014)	*59*	*(187)*	*26*	*(81)*	*0*	*(0)*
Objective spatial profiling	71	(223)	29	(91)	0	(0)
Subjective visual spatial profiling	64	(201)	27	(85)	9	(28)

Table 7 Prevalence of MP spatial profile phenotypes determined by objective and subjective profiling. Original study results (Tariq et al., 2014) provided for comparison.

A further analysis was carried out to assess how well a single measure of MPOD describes the overall amount of MP present, based on a larger sample size (n= 314). Mean ± SD MPOD at 0.1º, 0.8º and 1.8º and correlation with MPODint and MPODav (0 to 3.8) is presented in Table 8.

			Correlation with MPODint (0 to 3.8)		Correlation with MPODav (0 to 3.8)	
	Mean	SD	r	R^2	r	R^2
MPOD at 0.1º	0.58	0.18	0.80	0.64	0.61	0.37
MPOD at 0.8º	0.34	0.13	0.95	0.90	0.83	0.70
MPOD at 1.8º	0.10	0.05	0.91	0.84	0.05	0.00

Table 8 Correlation of MPOD at single central eccentricities with integrated MPODint (0 to 3.8º) and MPODav (0 to 3.8º) among the participants of the Twin study (n = 314).

Comparisons of the correlation coefficients showed a significant difference in correlation between the MPOD at 0.1º and 0.8º correlations with MPODint (0 to 3.8) (z = -9.14, P < 0.0005) and between the 0.1º and 1.8º correlations with MPODint (0 to 3.8) (z = -5.35, P < 0.0005) (Figure 18 a and b). Results were very similar for MPODav (0 to 3.8) and when the analysis was repeated using one twin of each twin pair and also when the group was split according to spatial profile group.
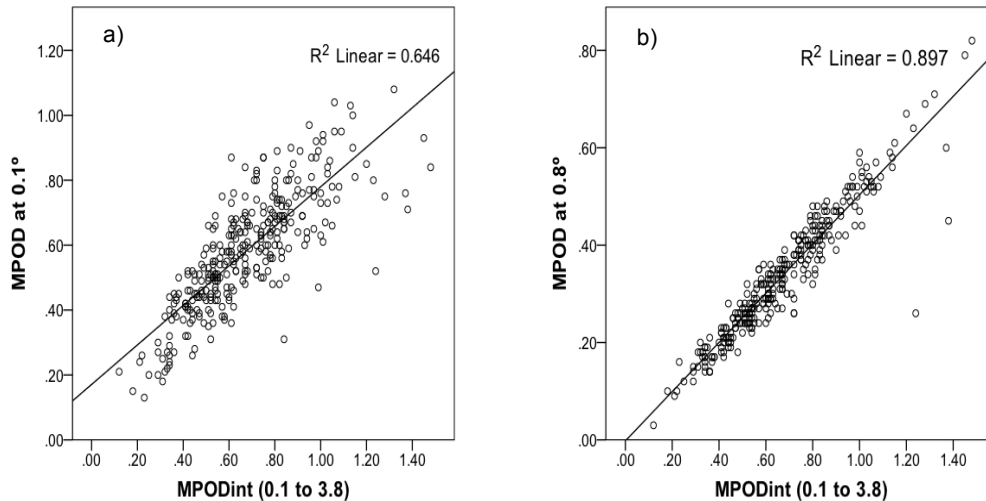
Figure 18 a) Correlation between a single central MPOD at 0.1° and the integrated area under the curve, MPODint (0 to 3.8); b) Correlation between a single central MPOD at 0.8° and the integrated area under the curve, MPODint (0 to 3.8).

2.1.4   Discussion

The between-visit repeatability of MPOD measured using the MAP test based on subjective HFP was investigated. Bland Altman analysis showed good inter-visit agreement between corresponding MPOD measurements at each retinal spatial location. The mean difference in MPOD between visits was less than 0.02 log units for all spatial locations indicating an excellent level of repeatability (Table 4). The CoR values indicate the amount of variation that can exist between MPOD measurements representing "noise". Good repeatability of MPOD measurements was demonstrated at all retinal eccentricities tested. Previous investigations of test-retest repeatability measurements of MPOD by HFP methods have yielded varying CoR values depending on the device used. A summary of these is provided in Table 9. At the 0.5° test location a CoR of 0.12 was reported using a customized LED device (Tang et al., 2004), 0.18 using the QuantifEye device (de Kinkelder et al., 2010) and 0.19 using the Macular Densitometer™ (Snodderly et al., 2004). The poor repeatability (CoR = 0.33) of the MPS 9000 MP screener based on HFP (Bartlett et al., 2010b) was the subject of debate whereby the instrument's designers reported a CoR of 0.15, claiming that operator error was the main cause of the discrepancy (Murray et al., 2011). In other cases, potential fading of the central stimulus due to the Troxler effect and conceptual difficulties in identification of central minimum flicker has been described when MPOD

at 0.5° was measured using the Macuscope™ resulting in poor repeatability (CoR of 0.32) (de Kinkelder et al., 2010) and 0.45 (Bartlett et al., 2010a). However, this effect is avoided during the MAP test as the stimulus is presented in short bursts of approximately 0.5 seconds duration (Rodriguez-Carmona et al., 2006). The improved repeatability of the MAP test compared to the Macuscope™ may also be partly due to the number of measurements taken within each session for each retinal location (eight compared to five respectively). It appears that when several measurements are repeated within a single session and then averaged, the CoR improves.

The Pearson product moment correlation coefficient has often been reported in repeatability studies to indicate agreement between visits (Table 9). Variations range from strong positive, r = 0.97 (van der Veen et al., 2009a) to more moderate correlations, r = 0.49 (Hagen et al., 2010). Although this method of assessing agreement may be misleading (Bland and Altman, 1986), it has been included in Table 9 to allow comparisons with previous investigations. Consistent with our findings, a lower correlation between visits of MPOD at increasing eccentricity away from the fovea has been reported (Snodderly et al., 2004, Lam et al., 2005). One possible explanation is that subjective recognition of the flicker null point becomes more difficult at peripheral eccentricities. In a MPOD repeated measures study using the MacuScope™ flicker photometer, it was commented that the poor correlation of MPOD levels between visits (r = 0.50) was due to participants' difficulties in identifying the point at which no flicker was perceived (Hagen et al., 2010). The authors suggested following a standardised explanation protocol prior to testing each subject. It follows that, as with all HFP methods, given the subjective nature of the MAP test it is important the subject understands and performs the test correctly. In addition, care should be taken in giving the same explanation and repeated instructions to all subjects to reduce investigator bias.

As well as between-visit repeatability, measurement of MPOD using the MAP test was shown to be highly reliable as indicated by the mean within session standard error of 0.05 density units obtained for all retinal eccentricities tested. This value is based on data collected across four low and four high threshold measurement repetitions for MPOD at each eccentricity tested, averaged across all participants. The value obtained compares well to reports from studies using alternative HFP based methods although this is usually based on a single central location at 0.5° (Hammond et al., 1997c, Tang et al., 2004, van der Veen et al., 2009a).

Study	n	HFP device	Test location (°)	Reference location (°)	Repeatability statistics r	CoR
Hammond et al. (1997)	32	Three-channel optical system	0.5	5.5	0.91	0.16
Snodderly et al. (2004)	48	Macular Densitometer™	0.25	7	0.86	
			0.5		0.90	0.19
			1		0.86	
			1.75		0.68	
Tang et al. (2004)	6	Customised LED device	0.5	4		0.12
Lam et al. (2005)	9	Macular Densitometer™	0.25	7	0.72	
			0.5		0.68	
			1		0.63	
			2		0.45	
van der Veen et al. (2009)	11	MPS 9000	0.5	8	0.97	
Bartlett et al. (2010a)	40	MPS 9000	0.5	8		0.30
Bartlett et al. (2010b)	38	MacuScope™	0.5	8		0.45
Hagen et al. (2010)	24	MacuScope™	0.5	8	0.49	
de Kinkelder et al. (2010)	23	MacuScope™	0.5	8		0.32
de Kinkelder et al. (2010)	20	MPS 9000	0.5	6		0.18
Current study	**40**	**MAP test**	**0**	**Average of 6.8 and 7.8**	**0.96**	**0.12**
			0.8		**0.93**	**0.12**
			1.8		**0.66**	**0.14**
			2.8		**0.49**	**0.11**
			3.8		**0.57**	**0.11**

Table 9 Summary of results from heterochromatic flicker photometry based repeatability studies. Results of the current study are included for comparison. The correlation between visits Pearson's r and/or the Coefficient of Repeatability (CoR) are provided.

The effect of head movements on measurement of MPOD was considered in an early study describing a free-view desktop device based on subjective HFP (Wooten et al., 1999). Even when subjects were misaligned by to 1.5cm to the left or the right (the maximum lateral movement before the stimulus was no longer in view) there was no effect on MP values. A forward or backwards movement of up to 10cm in either direction also had no effect. During the MAP test lateral movements are limited to around 2cm in either direction by the size of the notch filter, which is approximately 4cm^2 in size. In addition, constant contact with the forehead rest throughout the test minimises any forward or backwards movement by the subject. Head movements were therefore not expected to have any effect on MPOD measurement.

As a subjective method, HFP relies upon the cooperation of the subject to maintain fixation and be able to perform the test. Thus, another potential source of error during the MAP test is fixational eye movements resulting in poor retinal stabilisation. If the test eye is not steady, then the centre of the stimulus at 0°, or the fixation stimulus for all other eccentricities will not fall on the fovea and MPOD may consequently be over- or under- estimated. The effect of eye movements on MPOD measurements has been assessed previously. During a repeatability study of MPOD measurement by HFP methods, a bite bar and headrest assembly was used to stabilize the subject's head position while the pupil location was monitored for correct stimulus alignment (Snodderly et al., 2004). The inter-visit correlation coefficients reported are of a similar order to the current findings even though eye movements are not recorded during the MAP test. This indicates that precise monitoring of eye movements is not necessary during HFP methods. Notwithstanding, it has been suggested that good correspondence in MPOD measurements taken at more central retinal eccentricities between visits indicates good fixation (Hammond et al., 1997c). With regards to the MAP test, the small size of the central stimulus (0.36º diameter) has been chosen to minimise the potential effects of eye movements while ensuring adequate spatial sampling accuracy (Barbur et al., 2010). In order to further minimise the effect of eye movements during each test, repeated instruction was given by the investigator to maintain steady fixation for each stimulus presentation.

Analysis and interpretation of MPOD measurements varies across the literature and differences in discrete MPOD measurements at a single retinal eccentricity, rather than an integrated MPOD measure, are often reported (Stringham and Hammond, 2007). What a single eccentricity measurement does not capture however is the distribution of MP or the overall amount of MP present over a defined area. In a study of MP

distribution measured by both FR and two-wavelength FAF techniques, the quotient of an integrated measure of MP within the ring structure (based on the Gaussian-distributed ring) compared to the amount of MP present within the main exponential structure was used to quantify the prominence of the ring-like structure (Berendschot and van Norren, 2006). The mean ring index for each of these techniques (0.43 ± 0.32 and 0.35 ± 0.38 respectively) appears to show a large variability as indicated by the SD. This implies that in some individuals the prominence of the ring was more pronounced than in others. A different approach was adopted in the present study. Rather than the prominence of any ring-like structures, in order to quantify the amount of MP present over the central retinal area, including the location of any ring-like structures, integrated MP from 0º to 1.8º and from 0º to 3.8º was calculated using the trapezium rule applied to each participant's MPOD data distribution. The advantage of this method is that the integrated measure captures the total amount of MP present over an area and allows comparisons between individuals to be drawn regardless of the spatial distribution phenotype. In addition, the calculation of correlation between MPOD at 0.1º, 0.8º and 1.8º and MPODint (0 to 3.8) demonstrated that while there is a strong correlation between the central MPOD measurement and the total amount of MP present, this relationship is significantly stronger for single MPOD measurements at 0.8º and 1.8º (P < 00005). A single central MPOD measurement does not sufficiently predict the overall amount of MP present.

There are no previous descriptions of the repeatability of integrated measures of MPOD. The advantage of using these parameters is that despite the high CoR for MPOD at 0.1º when using FAF, this is not reflected by the CoR for MPODav or MPODint. Since averaging MPOD over the central 1.8º or 3.8º, or an integrated measure incorporating the area under the curve captures information regarding the overall distribution of MP, it is proposed that the MPODav or MPODint measures are a better indicator of the amount of MP present as opposed to a single eccentricity MPOD measurement and is therefore are appropriate parameters to report in future studies.

There are few reports describing repeatability of MPOD measurements quantified from FAF scans at locations close to the foveal centre. The test-retest reproducibility of two-wavelength FAF for MPOD averaged over a 2º diameter sampling area was around 0.05 density units in an earlier study (Delori, 2004). Nevertheless, the results of the present study demonstrate a large variation in the repeatability coefficient for MPOD measurements quantified from FAF scans at 0° compared to 0.8° retinal eccentricity (Table 4). Maybe somewhat surprisingly, repeatability of foveal MPOD measurements

using the FAF imaging technique produced a relatively high CoR of 0.23 compared to 0.12 using the HFP method. The large CoR value may be due to incorrect alignment or poor fixation. Indeed, feasibility of MP quantification using a grey scale analysis of FAF images obtained from two different instruments (HRA2 and S3300 Spectralis HRA-OCT, Heidelberg Engineering, Heidelberg, Germany) was evaluated in an investigation including thirty-four normal subjects (Delori et al., 2011). Several technical modifications were suggested to reduce measurement errors, including implementing new alignment software as well as correction of the data to compensate for the absorption of the ocular media. Although such a correction algorithm was not applied to the absolute measure of MPOD in the current study, the prevalence of significant lens opacity in the study cohort would be expected to be low given the average age of 40 years. Nonetheless, repeatability of MPOD as measured by FAF showed an improved CoR of 0.15 for MPOD at 0.1° and excellent within-session repeatability of around 0.05 from 0.8° and beyond. These findings are consistent with previous investigations whereby high repeatability was demonstrated using the two-wavelength FAF imaging method to measure MPOD (Trieschmann et al., 2006). In addition, there was a reduced variance of MPOD at the central (0.1°) and peripheral locations (Table 4) compared to the variance of ±6.9% at the fovea and ±2.7% peripherally at 7° to 9° eccentricity found in a repeatability study including twelve subjects using the S3300 Spectralis HRA-OCT (Delori et al., 2011). These findings indicate that measurement error has little influence on MPOD measurements quantified from the two-wavelength FAF imaging technique employed in the current study at eccentricities other than at 0°.

The derivation of measures of MPOD and its spatial distribution from a single FAF image has been demonstrated in the past. In a recent classical twin study the MP spatial profile measured by one-wavelength FAF was quantified by fitting a best-fit curve to a single (horizontal) meridian MPOD data distribution and the resultant width at half peak measure assessed (Hogg et al., 2012). The authors concluded that relative peak MPOD was genetically influenced, whereas the spatial profile was not. However, difficulties identified in the study were limitations of the one-wavelength FAF method caused by heterogeneous distribution of lipofuscin fluorophores (Trieschmann et al., 2006), as explained in Chapter 1, section 1.2.2.3. A strength of the present study is that MPOD measurements were acquired by two-wavelength FAF which was shown to be a more accurate method (Trieschmann et al., 2006). In contrast to the study by Hogg et al. (2012), MP quantification in the current study was based on the average of MPOD in all directions from the foveal centre and not just a single meridian, although it has been shown that the distribution of MP is radially symmetrical (Hammond et al.,

1997c, Robson et al., 2003). Quantification analysis of MP derived from FAF images has also been used to characterize different MP spatial profile types. Four phenotypes of MP distribution were proposed in a study of four hundred eyes including two hundred and fifty-three with and one hundred and forty-seven without AMD (Trieschmann et al., 2003). The profile types were described as: type 1, intense central and paracentral MP; type 2, less intense central and paracentral MP; type 3, only central MP; and type 4, only paracentral MP. However, measurement error and repeatability of these profile types were not taken into account. Given the variability of the central MPOD at 0º measurement demonstrated in the current study this needs to be taken into account in future clinical studies.

During HFP methods, MPOD is measured at discrete locations. The accuracy of spatial profile mapping is dependent on the number of locations employed as well as how close the sampling areas are to one another. It has been shown that an exponential fit applied to MPOD measured centrally and a peripheral retinal location between 2.5º and 3.5º is a more accurate method than using a single central MPOD value (Hammond et al., 1997c). This implies that increasing the number of measurements between 0º and 3.8º eccentricity will increase accuracy further. The number of retinal locations tested by HFP methods is limited either by the time required to complete the test as well as the design of the instrument. However, during the present study, MPOD at single retinal eccentricities were extracted from FAF scan images and could therefore be manipulated to include more retinal locations. However, the inclusion of two additional MPOD data points at 0.2º and/or 0.5º did not significantly alter the MP spatial profile classification and agreement (data not presented).

Since repeatability of the central 0° MPOD measurement derived from two-wavelength FAF imaging was considered unacceptably poor, the more reliable MPOD measurement at 0.1° was used as the first point from which to apply the exponential fit and apply the classification protocol. Nonetheless, due to the high CoR at 0° and 0.1° relative to the more peripheral measurement locations, the objective method failed to identify any profiles as "central dip". Furthermore, while a few profiles were identified as central dips by visual inspection, objectively these were actually perturbations in the data smaller than the CoR and therefore considered a result of measurement error or noise (Figure 17). This may partly explain the inconsistent reports of central dips in the literature. In Phase 3 of the current study, three hundred and fourteen FAF images were re-analysed and MP profile type assigned by the objective technique and also by a visual inspection method. When comparing subjective visual versus objective

profiling, all central dip profiles were classified as either exponential or ring. It seems that visually, there is a tendency to overestimate the prevalence of non-exponential profiles. Additionally, even more variability in classification prevalence became apparent when the current results are compared to the original Twin study data. This is likely due to the variation in FAF scan alignment, whereby manual centration on the maximum MPOD was used in the original study instead of the find fovea function. The tendency to overestimate prevalence of central dip profiles by objective assessment was demonstrated by the findings of a recent investigation exploring the MP spatial profile in a group of ninety-five healthy Chinese subjects. Prevalence of a central dip profile was reported to be 15% compared to 85% presenting with a "typical" profile (Neelam et al., 2014). The "typical" profile described a steady exponential decline in MPOD from the centre at 0.25° to the periphery at 7°. The central dip profile was assigned to MPOD distributions in which the MPOD at 0.25° was lower than at 0.50°, with a subsequent decline to the periphery. Of note, the amount of variation required in classifying this as a real deviation is not given in the report.

To further demonstrate the variability in reporting MP spatial profile types that occurs from applying different classifications, data from a study by Kirby et al. (2009) has been re-analysed according to the classification system used in the current study (section 2.1.2). The Kirby study included sixteen individuals, nine with an exponential MP profile and seven with a ring-like profile. Deviation away from the exponential fit to the data at each retinal eccentricity tested was less than 0.05 in all but one case, and according to the re-analysis all sixteen individuals would have been classified by our classification method as presenting with exponential MP profiles. This finding highlights the discrepancies across the literature and emphasises the need for a consistent universal approach in describing the MP spatial profile phenotype.

A first order decreasing exponential function described the fit of the averaged subjects' data well, as indicated by the R^2 = 0.98 (Phase 1, MAP test data) and R^2 = 0.96 (Phase 2, FAF data). This compares well to previous work in which an R^2 of 0.99 was determined for MPOD data profiles measured by cHFP in sixty subjects (Nolan et al., 2008). While the overall MPOD profile maintains an exponential-like decline, ring-like and central dip profiles represent deviations from this fit. It has been shown that ring-like structures occur at approximately 0.7° to 0.8° eccentricity from the fovea as determined by HFP (Hammond et al., 1997c, Kirby et al., 2009, Huntjens et al., 2014) as well as FAF methods (Hammond et al., 1997c, Delori et al., 2006). However, the location of the ring-like structure does vary (Chapter 1, section 1.3). Although it is

possible to quantify MPOD at several locations from 0° to 0.8° from FAF scans, this is a time consuming task when done manually. Nonetheless, all base-line FAF scans acquired during the original Twin study were re-analysed using the objective MP profiling method. Among the three hundred and fourteen female twin participants, prevalence of the ring-like profile (29%) determined objectively compares well with the 26% reported in the original study. This finding suggests that ring-like MP structures can be identified by objective classification based on the limited eccentricities used in the analysis. Of note, in the present study a consistent method to identify the central MPOD measurement utilizing the "find fovea" function of the Heidelberg software was incorporated, whereas the original study (Tariq et al., 2014) had identified the centre of the scan as the location where MPOD was maximal. Despite this variation in methodology, prevalence of the ring MP profile by visual inspection (27%) was almost identical to that obtained in the original study (26%). With regards to heritability, based on objective MP profiling, case-wise concordance of non-exponential MP profiles was 0.74 for MZ twins; approximately double that for DZ twins. This is in accordance with the original study in which it was shown that there was greater concordance of a ring-like profile in MZ compared to DZ twins (Tariq et al., 2014), suggesting that a non-exponential MP phenotype is highly heritable.

Few studies have investigated the reproducibility of the MP spatial profile assessed between visits. In a study including sixteen individuals, nine of who presented with a "typical exponential-like profile" and seven with a "secondary peak" in their MP profile, the profile type was shown to persist on repeated testing (Kirby et al., 2009). In accordance with this, the results of the current study indicate that the methods employed for measurement and classification of the MP spatial profile are robust to test-retest variability. The objective method of classification of the MP spatial profile used in the current study is based on deviations away from an exponential fit to the data distribution taking into account the measurement error of the instrument according to the location at which MPOD is being measured (Huntjens et al., 2014). The inter-visit agreement of this method has not previously been described. The overall percentage agreement along with the κ-value has been used to describe the strength of the agreement, whereby a κ-value between 0.41 to 0.80 indicates moderate to substantial agreement and 0.81 to 1.00 indicates almost perfect agreement (Landis and Koch, 1977). Excellent agreement between visits of the objective method of MP spatial profiling measured by the MAP test was established, as indicated by the overall percentage agreement of 95% and κ-value of 0.89 (P < 0.0005). Similarly, for MPOD

measured by FAF there was excellent repeatability (93%; κ = 0.85, P < 0.0005) of profiling by objective analysis; whereas repeatability of profiling by subjective visual analysis between scans by the same investigator was lower (73%; κ = 0.48; P < 0.0005). This finding demonstrates that the objective method is a more reliable method of MP spatial profiling. Notably in a previous study the kappa measure of agreement between two graders of "ring versus no-ring" was reported as 0.705 (P-value not given), illustrating that, although this is a fast method, variability could arise with subjective classification (Tariq et al., 2014). Furthermore, our results indicate poor agreement between the objective and subjective classification method applied to the same FAF scan image (60%; κ = 0.23, P = 0.02), illustrating the difficulties in comparing studies that have employed different classification techniques. This is the first report of an objective method of classifying the MP spatial profile that has been applied to MPOD measured by different techniques.

Conclusion

The CoR value gives a limit beyond which a measurement is highly likely to be a true deviation from the model and not measurement noise. MPOD measurement error was shown to vary according to technique as well as retinal test location relative to the fovea. This finding illustrates the importance of establishing device specific CoR values. From the results, it can be concluded that with regards to the MAP test, a deviation greater than 0.12 in MPOD at 0° and 0.8° eccentricities can be considered clinically significant. With respect to the two-wavelength FAF technique, fluctuations greater than 0.12 at 0.1° and 0.08 at 0.8° are clinically significant. Improved repeatability of the measurements is achieved by integrating the MPOD over the central 2° or 4°.

The results demonstrate that the proposed objective classification method is a reliable method of MP spatial profiling that is robust to test re-test variability when MPOD measurements are obtained using a HFP based method. However, it seems that central dips are not identified when applying this objective classification method to FAF imaging, most likely due to scan alignment. This requires further investigation with instrumentation that incorporates foveal markers, for example a simultaneous OCT scan, as with the Spectralis FAF device which is soon to be commercially available (personal communication, Heidelberg Engineering July 2015). In addition, although currently there are limitations in obtaining this output manually from FAF scans,

automated quantification of MP spatial profiles may serve in the future as a potential diagnostic, prognostic and therapeutic tool for eye conditions such as AMD.

Meanwhile, in the absence of a MP profile classification system that can be used for all instruments, a consistent reporting of an integrated measure of MP: centrally up to 2º degrees and total up to 4º degrees is recommended so that comparisons can be drawn between studies.

3 Ethnic variations in macular pigment and its spatial density distribution

3.1.1 Introduction

There appears to be a relationship between the risk factors for developing AMD and the variations reported in MPOD and its spatial density distribution (Chapter 1, section 1.4). Due to the varying prevalence of AMD reported among different populations it was suggested that ethnicity might play a role with a tendency towards lower central MPOD in individuals of white compared to non-white ethnicity (Chapter 1, section 1.4.7). Many of the difficulties in comparing MPOD results between studies arising from the variations in methods and techniques employed have been explained in Chapter 1, section 1.2. Nevertheless, due to a lack of direct comparison studies variations in MPOD between ethnic populations have been reported based on results from independent investigations. Recently, there have been studies reporting on MPOD in exclusively Chinese populations born and living in their respective countries (Tang et al., 2004, Lam et al., 2005, Yu et al., 2012, Neelam et al., 2014) and it was concluded that there is no significant difference in MPOD between white and Chinese subjects (Tang et al., 2004). In contrast it seems that adult Indian subjects may demonstrate higher MPOD than white individuals (Raman et al., 2011, Raman et al., 2012b). There are no reports on MP and its spatial density distribution in persons of black ethnicity living in Africa and/or the Caribbean.

Published data specifically comparing MPOD between white and non-white ethnicities are limited and few investigations have investigated variations in MPOD between ethnic groups using the same measurement technique within a single study. Using the HFP technique, a significantly decreased mean central MPOD in white subjects (0.33 ± 0.13) versus South Asian defined as individuals from India, Pakistan and Bangladesh (0.43 ± 0.14; $P < 0.0005$), was demonstrated (Howells et al., 2013). A recent preliminary report also showed that mean MPOD measured by HFP was lower in Caucasian compared to Asian Indian individuals (Davey et al., 2014). Our research group confirmed this finding in a more recent investigation by (Huntjens et al., 2014). Lower central MPOD has also been reported in white subjects (0.36 ± 0.13) compared to black (0.59 ± 0.14, $P < 0.0005$) (Wolf-Schnurrbusch et al., 2007) and also compared to a group of non-white subjects that included Asian, black and Hispanic ethnicities (Nolan et al., 2008). Nonetheless, the finding of variations in central MPOD with ethnicity is not consistent. The results of a study where darker iris colour was linked to increased average MPOD over the central 1° area implied that central MPOD was not related to ethnicity; however, it is possible that differences in MPOD due to ethnicity

were minimized as only a small percentage of non-Caucasian (Asian and African-American) subjects were included (Hammond et al., 1996b). In contrast to the work by Wolf-Schnurrbusch et al. (2007), MPOD was reported to be 41% lower in black participants (0.22 ± 0.23, n = 35) compared to whites (0.37 ± 0.19, n = 148, P = 0.0002) among a biracial sample with mean age of 79.1 ± 3.2 years with no ocular disease (Iannaccone et al., 2007). This finding could not be explained by correlates such as lutein supplementation and the authors concluded that further work was required to establish normative MPOD data for the black ethnic group.

Many studies regarding human MPOD report variations in central MPOD values and not the overall spatial density distribution of MP. Consequently, little is known about ethnic differences in MP spatial density distribution away from the fovea. Some studies have found no relationship between ethnicity and MP spatial distribution (Hammond et al., 1996b, Hammond et al., 1997c, Nolan et al., 2008); however these included limited numbers of non-white subjects, including South Asian and black, in comparison with the white group. On the other hand, increased prevalence of a ring-like MP spatial profile has been reported in ethnicities with lower prevalence of AMD, whereby 86% of black (African) subjects presented with parafoveal MP rings versus 68% of non-Hispanic white subjects (Wolf-Schnurrbusch et al., 2007). Recent work by our research group found an increased prevalence of ring-like and central dip profiles in fifty-four young healthy South Asian subjects compared to nineteen white subjects (P = 0.008) (Huntjens et al., 2014). A comparison study of MP spatial profile phenotype prevalence among several ethnic groups has not previously been conducted to our best knowledge.

The relevance of the MP spatial profile phenotype lies with the hypothesis that some MP spatial profile phenotypes may offer an enhanced protective role over others (Dietzel et al., 2011b). While different MP spatial profile phenotypes have been explained in Chapter 1, section 1.3, there is limited work regarding the quantification of the amount of MP present in the central retinal area according to the MP spatial profile phenotype. Averaged and/or integrated MPOD measurements that represent the amount of MP over a given area have been described in Chapter 2, section 2.1.2. While no difference was found in the integrated MP (area under the curve from 0° to 7°) between a group of individuals with exponential MP spatial profiles (0.71 ± 0.42, n = 426) compared to a group presenting with a "central dip" profile (0.71 ± 0.42, n= 58) (Kirby et al., 2010), similar evaluations comparing exponential, ring-like and central dip profiles have not been described. In addition, the lateral extent of the MP distribution

may vary according to the MP spatial profile phenotype. An increased half-width eccentricity where half of the peak MPOD is reached was found in individuals presenting with a ring-like structure (1.26 ± 0.49, n = 73) compared to those with no ring-like structure (0.90 ± 0.35, n = 245, P < 0.0001) (Dietzel et al., 2011b). Nonetheless, comparisons between exponential, ring-like and central dip profiles have not been reported.

Aim

The purpose of this study was to investigate MPOD and its spatial density distribution among young (aged 18 to 39 years), healthy individuals from the three largest ethnic groups in England and Wales: whites, South Asian and black (Office for National Statistics, 2011, Office for National Statistics, 2013). As well as discrete MPOD measurements at single retinal eccentricities at 0°, 0.8°, 1.8°, 2.8° and 3.8° measured by the MAP test, averaged MPOD measures including MPODav and MPODint and were calculated and compared between the three ethnic groups. Additionally, the influence of known risk factors for AMD was considered in the investigation. These included age, gender, smoking history, BMI, eye colour, skin type and sun exposure. Country of birth and residence during childhood was also taken into account in the investigation. The prevalence of exponential, ring-like and central dip MP spatial profile phenotypes (as defined in Chapter 2, section 2.1.2) among the three ethnic groups was also investigated. Variations in the aforementioned MPOD variables as well as the lateral extent of the MP spatial density distribution described by the half-width eccentricity were also explored according to the MP spatial profile phenotype.

The current study is novel in that it explores:

- The effect of ethnicity and known risk factors of AMD on single, averaged and integrated MPOD measures within a single study; and
- The prevalence of exponential, ring-like and central dip MP spatial profiles among different ethnic groups.

The findings of the investigation will further develop the understanding of the MP spatial density distribution in healthy eyes. In addition, the results of the study will provide a normative database of MPOD measurements for young, healthy white, South Asian and black subjects living in England and Wales.

3.1.2   Methods

The investigation took place at the Division of Optometry and Visual Science, City University London. Subjects were recruited by word of mouth, via flyers distributed around the university campus and local businesses and also a local poster campaign. Study data was collected from seventy-six white, eighty South Asian and seventy black participants between October 2013 and March 2015. Ethical approval for the study was obtained from the Optometry Research & Ethics Committee and written informed consent was obtained from all subjects prior to participation, conforming to the tenets of the Declaration of Helsinki.

All participants completed a health and lifestyle questionnaire (Appendix 6.6), providing information that included ethnicity, age, gender, general and ocular health, use of medication, vitamins or MP supplementation and family history of AMD. Inclusion into the study was based on self-reported white, South Asian or black ethnicity and between 18 to 39 years of age. Classification of ethnicity was based on the criteria used by the Office of National Statistics (Office for National Statistics, 2011). The white ethnic group included English, Welsh, Scottish, Northern Irish, British, Irish, Gypsy or Irish Traveller and any other white background. The South Asian group was defined as those born in India, Pakistan, or Bangladesh, or born in the United Kingdom from Indian, Pakistani, or Bangladeshi parents. The black ethnic group included those of African or Caribbean descent. The following ethnic groups were not included in the study: mixed/multiple ethnic groups; Asian Chinese or any other Asian background not mentioned in the inclusion criteria; and all other ethnic groups.

The health and lifestyle questionnaire was also used to elicit smoking history. Non-smokers were defined as those who had never smoked. Smokers were defined as those who had smoked in the past or were current smokers (Leffondré et al., 2002). The smoking pack year was calculated using the formula: [(number of cigarettes smoked per day)(number of years smoked)/20]. This value is a numerical representation of a subject's lifetime exposure to tobacco. One pack year is defined as twenty cigarettes per day every day for a year (Leffondré et al., 2002). Information regarding the general dietary habits (meat-eater, vegetarian or vegan) over the last two years as well as average alcohol consumption (average alcohol units per week) was also gathered using the questionnaire. In addition, each participant was asked to self-report his or her eye colour as blue, grey, green, hazel, light brown or dark brown

(Seddon et al., 1990). Based on this information, iris colour was assigned as light (blue, grey) or dark (green, hazel, light or dark brown) (Klein et al., 2014). In addition, participants were required to select which of six skin type categories best described their skin type according to sun sensitivity based on the Fitzpatrick scale (Fitzpatrick, 1988). Grading of skin sun sensitivity was dichotomised to sunburn prone (types I and II) or sunburn resistant (III to VI) (Khan et al., 2006a). Data regarding each subject's ocular exposure to UV light was collected via the health and lifestyle questionnaire. This included questions regarding details of country of birth and number of years spent living outside the UK. An approximation of sun exposure was elicited from the questionnaire. The number of hours spent outdoors during the Autumn/Winter and Spring/Summer months was graded as low (less than 2 hours per day), medium (2 to 4 hours per day) or high (greater 5 hours per day) (Tomany et al., 2004, Klein et al., 2014). The use of sunglasses in bright conditions was recorded as always/mostly used or never/rarely used.

Exclusion criteria for the study were visual acuity of 0.3 logMAR or worse in the test eye, ocular pathology in the test eye, previous refractive surgery, self-reported pregnancy, current use of carotenoid supplementation, and/or medication that may affect retinal function as well as a known colour vision deficiency. All participants had their visual acuity assessed using an EDTRS logMAR chart at 4m under standard testing conditions. This was carried out monocularly using the subject's habitual refractive correction with either contact lenses or spectacles where necessary. By default, measurements were taken for the right eye unless it did not meet the inclusion criteria, in which case the left eye was used. Autorefractor measurements were obtained for each participant using the Auto Kerato-Refracto-Tonometer TRK-1P instrument (Topcon, Tokyo, Japan). The mean spherical error (MSE in dioptres) was calculated as the sphere plus half of the cylinder (Thibos et al., 1997) taken from the average of five autorefractor readings.

Each subject had his or her height and weight recorded. Height was measured with a Leicester portable height measure (Seca, Hamburg, Germany). Subjects were asked to remove footwear and stand upright with their backs to the wall. The measurement was taken with the head level and rounded to the nearest half centimetre. Weight was measured with a Seca 760 traditional spring balance (Seca, Hamburg, Germany.) positioned on a firm horizontal surface. Subjects were asked to stand on the balance with shoes and outerwear removed. Weight was recorded to the nearest half kilogram. BMI was calculated using the formula: weight (kg) divided by height (m) squared to

give the weight to height ratio (kg/m^2). BMI data was also split into two groups based on low to normal BMI ≤ 24.9, or high BMI > 25 (World Health Organization Expert Consultation, 2004, World Health Organization, 2015).

Measurement of macular pigment optical density

Measurement of MPOD was carried out using the MAP test as described in Chapter 1, section 1.2.1.2. Classification of the spatial profile phenotype was implemented according to the objective system presented in Chapter 2, section 2.1.2. MPODav, MPODint and the retinal eccentricity at half peak MPOD values were also calculated according to the methods described in Chapter 2, section 2.1.2.

Statistical analysis

All statistical analyses were performed using SPSS version 22.0 for Windows (SPSS Inc., Chicago, USA). Values in the text and tables are presented as the mean ± SD. Bootstrapped 95% confidence intervals were obtained to provide robust confidence intervals. Graphs were prepared either using SPSS version 22.0 or Microsoft Excel 2010. Error bars indicate the 95% confidence intervals. Statistical significance was accepted at the 95% confidence level ($P < 0.05$) indicated in bold type in tables.

Preliminary analyses were performed to ensure no violation of the assumptions of normality, linearity and homoscedasticity. Visual graphical assessment of histograms, boxplots, P-P and Q-Q plots (Field, 2013) of independent variables were considered prior to continuous variable data analysis. In addition to this, the Shapiro-Wilk test was used to statistically assess normality of the data distribution for small group analysis (n < 30). It has been suggested that the Shapiro-Wilk test is a preferable to the Kolmogorov-Smirnov test, due to its increased power (Razali and Wah, 2011, Ghasemi and Zahediasl, 2012).

One or two way between-groups analysis of variance (ANOVA), or the nonparametric alternative Kruskal-Wallis test was conducted to analyze differences in continuous MPOD data variables between ethnic groups. An independent student t-test or the non-parametric Mann-Whitney U test was used to explore differences in continuous data variables between dichotomised dependent data sets such as gender. Pearson's r or

the non-parametric alternative, Spearman's ρ, was used to calculate the correlation between MPOD values and continuous dependents. A Pearson Chi-squared test for independence was used to explore the relationship between categorical variables, such as MP spatial profile phenotype and ethnic grouping.

Sample size calculation

An a priori power analysis was conducted using G*Power 3.1 (Faul et al., 2007, Faul et al., 2009) revealing that a total sample size of one hundred and ninety subjects was required for the study (approximately sixty-three per group). This was based on ANCOVA fixed effects, special, main effects and interactions calculated for three groups. A power level of 80%, a statistical significance level of α = 0.05 and a medium effect size of 0.3 were used for the calculation.

3.1.3   Results

In total, two hundred and twenty-six volunteers took part in this research study with a mean age of 24.4 ± 5.7 years. The sample comprised seventy-six white, eighty South Asian and seventy black participants. The right eye fulfilled the inclusion criteria and was therefore used as the test eye in two hundred and eighteen (96%) subjects. A health and lifestyle questionnaire was used to collect demographic, lifestyle and medical history information for each subject, including risk factors for AMD such as: gender, age, smoking history, family history of AMD, BMI, eye colour, skin type and sun exposure Demographic data of the study sample are displayed in Figure 19.

Differences in MPOD variables according to ethnicity taking into account risk factors for AMD were explored. In order to establish which factors could be entered into an analysis of covariance (ANCOVA), preliminary assessments were conducted to determine whether the covariate differed according to the independent group i.e. ethnicity. If the factor significantly varied between ethnic groups then it could not be used as a covariate in the ANCOVA. The homogeneity of the regression slopes for each covariate was also examined. If there was heterogeneity of the regression slopes then the factor was not suitable as a covariate for ANCOVA. The results of these preliminary checks and decisions as to the subsequent data analyses are summarised

in Table 10. As no covariates could be entered into the ANCOVA, a two-way ANOVA was performed to explore the effect of ethnicity and gender on each of the MPOD dependent variables. The influence of age and BMI were considered separately. Smoking history, eye colour and skin type could not be used as covariates in the ethnicity evaluation (Table 11), but were analysed according to the white ethnic group alone. An evaluation of differences in MPOD parameters between individuals that had been born and lived outside the UK versus those that had not was also conducted. Table 12 provides details of the factors that were not included in the final analysis.
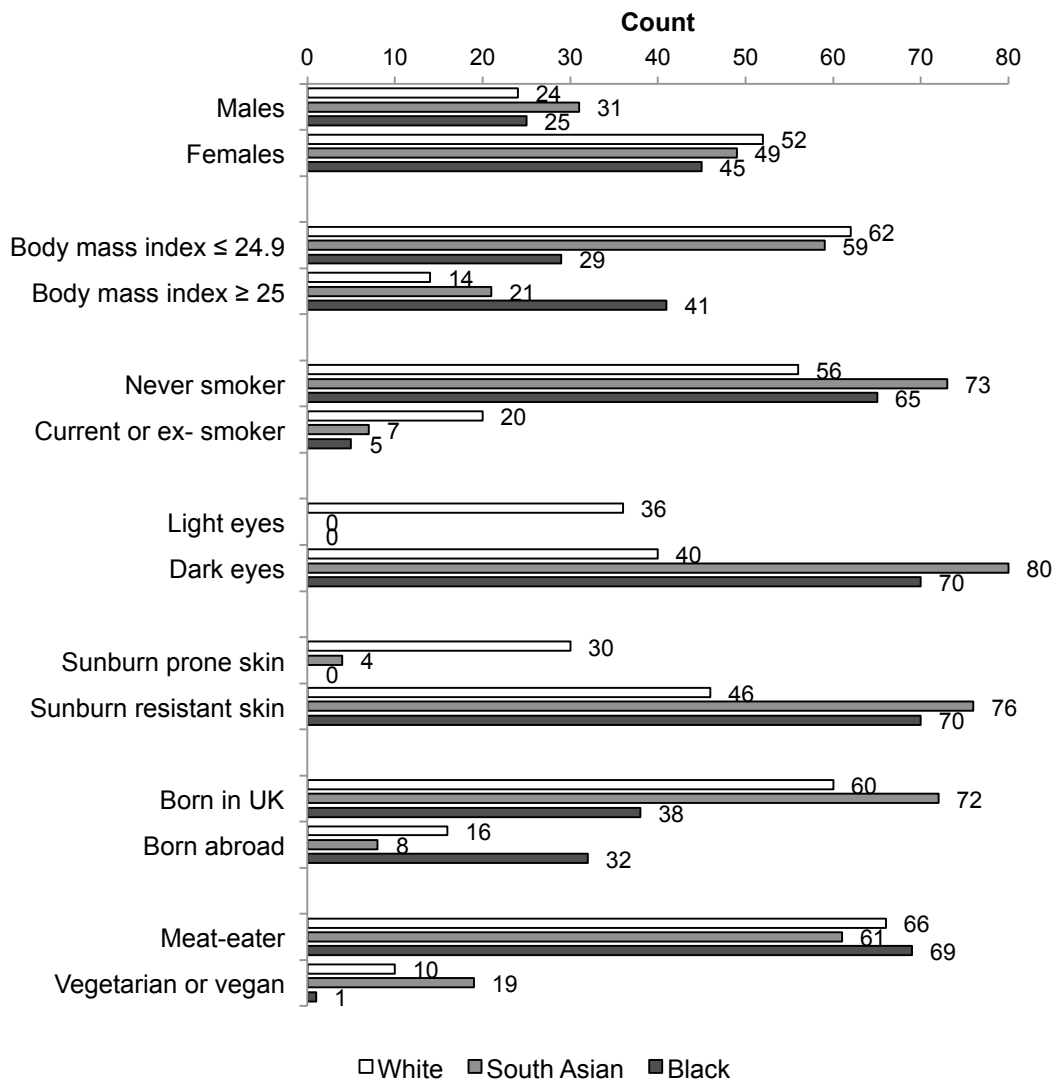
Figure 19 Demographic data of the study sample. Numbers of individuals within each category according to ethnicity are presented.

Factors	Comments
Gender	A chi-squared test for independence revealed no significant difference in the number of males and females between each ethnic group, χ^2 (2,226) = 0.88, P = 0.64.
	Gender and ethnicity used in two-way ANOVA to explore effect on MPOD variables.
Age	Kruskal-Wallis analysis revealed a statistically significant difference in age between the three ethnic groups, H(2) = 61.86, P < 0.0005.
	Heterogeneity of the regression slopes observed, so age as a covariate could not be used in ANCOVA. Association of age with MPOD variables was assessed in a separate analysis.
BMI	Kruskal-Wallis analysis determined a significant variation in BMI across the three ethnic groups, H(2) = 18.59, P < 0.005.
	Heterogeneity of the regression slopes observed, so BMI as a covariate could not be used in ANCOVA. Association of BMI with MPOD variables was assessed separately.

Table 10 Factors examined for suitability as covariates in MPOD data analysis.

Factors	Comments
Smoking history	Thirty-two subjects reported being current or ex-smokers including; twenty of white ethnicity, mean smoking pack year 0.98 ± 2.5; seven South Asian, mean smoking pack year 0.04 ± 0.2; and five black, mean smoking pack year of 0.04 ± 0.3.
	Due to small numbers of non-white individuals that were current or ex-smokers and very low smoking pack year, analysis of MPOD variables and smoking status was conducted only for the white ethnic group.
Eye colour	All participants of South Asian or black ethnicity reported having dark eyes. Analysis of MPOD variables and eye colour was conducted only for the white ethnic group.
Skin type	A total of thirty-four participants reported having sunburn prone skin types. Of these, thirty were white and four were of South Asian ethnicity. Analysis of MPOD variables and skin type was conducted only for the white ethnic group.

Table 11 Factors included in MPOD data analysis for white ethnic group only

Factors	Comments
Family history of AMD	Few participants indicated a positive family history of AMD (n = 11). Since none included a first-degree relative with AMD, family history of AMD was not included as a covariate in MPOD data analysis.
Sun exposure	Fifty-six participants (25%) had been born and spent five or more childhood years abroad (Figure 19). Although data were collected regarding winter and summer sun exposure over the last year, due to the large number of participants that had lived abroad in different climate conditions compared to the UK, the information gathered would not provide comparable cumulative lifetime sun exposure levels. It was therefore decided that sun exposure as a covariate in MPOD data analysis was of little real value and was not pursued further.
Diet	Thirty participants (13%) reported following a vegetarian or vegan diet (Figure 19). Due to the limited number, this factor was not included as a covariate in MPOD data analysis.
Alcohol consumption	Thirteen white, sixty South Asian and forty-four black individuals reported that they did not drink alcohol. Mean alcohol consumption per week was 7.0 ± 8.8 units for the white ethnic group, 1.1 ± 2.9 for the South Asian and 0.9 ± 1.7 for the black ethnic groups. Due to the low numbers this variable was not included as a covariate in MPOD data analysis.
Eye protection	Seventy-two subjects (32%) reported wearing glasses or contact lenses full time. Information regarding number of years of spectacle or contact lens use, spectacle lens coatings and contact lens type was not collected. While around 60% of all participants reported wearing sunglasses most of the time in bright conditions this was evenly spread across the three ethnic groups. For these reasons spectacle, contact lens or sunglasses use was not included as a covariate.
Mean spherical error	Mean MSE of the entire study sample was +1.28 ± 2.28DS, ranging between ±5.00DS in 96% subjects. MSE did not follow a normal distribution (whole sample and within each ethnic group). Kruskal-Wallis analysis revealed no statistically significant difference in MSE between the three ethnic groups, $H(2) = 2.97$, $P = 0.226$. Additionally, since ocular biometry does not affect MPOD, (Neelam et al., 2006) MSE was not corrected for in MPOD data analysis.

Table 12 Factors not used in the MPOD data analysis.

Effect of ethnicity and gender on macular pigment spatial distribution

Approximately one third of the entire study sample was male (n = 80) and two thirds were female (n = 146) with a similar ratio of males to females (approximately 1:2) in each ethnic group (Figure 19) (χ^2 (2,226) = 0.88, P = 0.64). Visual graphical assessment of the data distribution for the whole group, and when inspected per ethnic group, indicated a near normal distribution of each of the MPOD parameters: MPOD at 0º, 0.8º, MPODav (0 to 1.8), MPODint (0 to 1.8) and x-value at half peak MPOD. Formal Shapiro-Wilk normality testing was also conducted for the sample split by ethnicity and gender because of the smaller group sizes. This revealed no significant deviation from the normal distribution for any of the MPOD measures for male and female groups within each ethnicity and for the group as a whole (P > 0.05 for all).

A two-way between-groups ANOVA was conducted to explore the impact of ethnicity and gender on MPOD at 0º, 0.8º, MPODav and MPODint (0 to 1.8) and the x-value at half peak MPOD (Table 13). The mean, SD, minimum and maximum values of the MPOD parameters are presented in Table 14 and Table 15. The interaction between ethnicity and gender was not statistically significant in any case (P > 0.05). There was a statistically significant main effect for ethnicity for MPOD at 0º, 0.8º, MPODav and MPODint (0 to 1.8) (P < 0.0005 for all), with respective medium effect size of 0.08 to 0.12 as indicated by the partial eta squared value (Pallant, 2010). This implies that around 10% of the variance in the MPOD measurements can be explained by ethnicity.

	Ethnicity				Gender			
	F	**df**	**P value**	**Partial eta squared**	**F**	**df**	**P value**	**Partial eta squared**
MPOD at 0º	9.96	2	**< 0.0005**	**0.08**	4.63	1	**0.03**	0.02
MPOD at 0.8º	12.00	2	**< 0.0005**	**0.10**	2.49	1	0.12	0.01
MPODav (0 to 1.8)	14.30	2	**< 0.0005**	**0.12**	3.76	1	0.05	0.02
MPODint (0 to 1.8)	13.10	2	**< 0.0005**	**0.11**	3.70	1	0.06	0.02
x at half peak MPOD	4.59	2	**0.01**	**0.04**	0.01	1	0.43	0.003

Table 13 Results of the two-way ANOVA to show effect of ethnicity and gender on MPOD variables

			White			South Asian			Black			Total		
				95% Confidence Interval			95% Confidence Interval			95% Confidence Interval			95% Confidence Interval	
				Lower	Upper		Lower	Upper		Lower	Upper		Lower	Upper
MPOD at 0º	**Male**	**Mean**	**0.51**	0.44	0.59	**0.62**	0.56	0.68	**0.61**	0.53	0.70	**0.58**	0.54	0.63
		SD	**0.18**	0.12	0.23	**0.16**	0.11	0.19	**0.20**	0.15	0.24	**0.18**	0.15	0.21
	Female	**Mean**	**0.45**	0.40	0.50	**0.60**	0.55	0.65	**0.53**	0.48	0.58	**0.52**	0.49	0.55
		SD	**0.17**	0.13	0.20	**0.18**	0.13	0.22	**0.18**	0.13	0.22	**0.19**	0.16	0.21
	Total	**Mean**	**0.47**	0.43	0.51	**0.61**	0.57	0.65	**0.56**	0.52	0.61	**0.54**	0.52	0.57
		SD	**0.17**	0.14	0.20	**0.17**	0.13	0.20	**0.19**	0.16	0.22	**0.19**	0.17	0.21
MPOD at 0.8º	**Male**	**Mean**	**0.42**	0.36	0.49	**0.52**	0.46	0.59	**0.56**	0.48	0.65	**0.50**	0.46	0.55
		SD	**0.16**	0.11	0.21	**0.18**	0.12	0.24	**0.21**	0.16	0.25	**0.19**	0.16	0.22
	Female	**Mean**	**0.37**	0.33	0.41	**0.53**	0.48	0.58	**0.49**	0.44	0.55	**0.46**	0.43	0.49
		SD	**0.16**	0.12	0.18	**0.17**	0.13	0.20	**0.20**	0.14	0.24	**0.19**	0.16	0.21
	Total	**Mean**	**0.39**	0.35	0.42	**0.53**	0.49	0.56	**0.52**	0.47	0.56	**0.48**	0.45	0.50
		SD	**0.16**	0.13	0.19	**0.17**	0.14	0.21	**0.20**	0.17	0.23	**0.19**	0.17	0.21

Table 14 Mean, SD, minimum and maximum values of: MPOD at 0º and 0.8º per ethnic group and for whole study sample. Bootstrap 95% confidence intervals are also displayed.

			White			South Asian			Black			Total		
				95% Confidence Interval			95% Confidence Interval			95% Confidence Interval			95% Confidence Interval	
				Lower	Upper		Lower	Upper		Lower	Upper		Lower	Upper
MPODav	Male	Mean	**0.32**	0.27	0.36	**0.39**	0.35	0.44	**0.46**	0.39	0.53	**0.39**	0.36	0.43
(0 to 1.8)		SD	**0.11**	0.08	0.14	**0.13**	0.10	0.16	**0.17**	0.13	0.19	**0.15**	0.13	0.17
	Female	Mean	**0.29**	0.26	0.32	**0.39**	0.35	0.42	**0.39**	0.35	0.43	**0.35**	0.33	0.37
		SD	**0.11**	0.09	0.13	**0.12**	0.09	0.15	**0.15**	0.10	0.20	**0.13**	0.11	0.16
	Total	Mean	**0.30**	0.27	0.33	**0.39**	0.36	0.42	**0.41**	0.38	0.45	**0.37**	0.35	0.39
		SD	**0.11**	0.09	0.13	**0.12**	0.10	0.15	**0.16**	0.12	0.19	**0.14**	0.12	0.16
MPODint	Male	Mean	**0.68**	0.58	0.79	**0.84**	0.75	0.94	**0.92**	0.80	1.05	**0.82**	0.75	0.89
(0 to 1.8)		SD	**0.24**	0.17	0.31	**0.27**	0.18	0.33	**0.32**	0.24	0.38	**0.29**	0.25	0.33
	Female	Mean	**0.61**	0.54	0.67	**0.83**	0.77	0.90	**0.79**	0.71	0.88	**0.74**	0.69	0.78
		SD	**0.23**	0.18	0.28	**0.25**	0.19	0.31	**0.29**	0.20	0.38	**0.28**	0.23	0.32
	Total	Mean	**0.63**	0.58	0.68	**0.84**	0.78	0.90	**0.84**	0.77	0.91	**0.77**	0.73	0.80
		SD	**0.24**	0.20	0.28	**0.26**	0.21	0.30	**0.31**	0.25	0.37	**0.28**	0.25	0.32
x at half	Male	Mean	**1.62**	1.37	1.83	**1.53**	1.32	1.79	**1.88**	1.60	2.21	**1.67**	1.51	1.83
peak		SD	**0.57**	0.40	0.70	**0.67**	0.33	0.94	**0.82**	0.40	1.12	**0.70**	0.51	0.87
MPOD	Female	Mean	**1.72**	1.54	1.94	**1.60**	1.45	1.77	**1.93**	1.74	2.12	**1.74**	1.64	1.86
		SD	**0.76**	0.52	1.00	**0.56**	0.36	0.74	**0.63**	0.46	0.78	**0.67**	0.54	0.79
	Total	Mean	**1.69**	1.54	1.85	**1.57**	1.46	1.71	**1.91**	1.75	2.09	**1.72**	1.64	1.81
		SD	**0.71**	0.53	0.89	**0.60**	0.41	0.76	**0.70**	0.52	0.86	**0.68**	0.57	0.78

Table 15 Mean, SD, minimum and maximum values of MPODav and MPODint (0 to 1.8) and x value at half peak MPOD per ethnic group and for whole study sample. Bootstrap 95% confidence intervals are also displayed.

Tukey HSD post-hoc comparisons indicated that the mean MPOD values were consistently lower in the white ethnic group compared to both the South Asian and black ethnic groups ($P < 0.0005$). There was no statistically significant difference between the South Asian and black ethnic groups in any case ($P > 0.05$). The variation in MPODint (0 to 1.8) between ethnic groups and gender is displayed graphically in Figure 20. While the main effect of gender reached statistical significance for MPOD at 0º, ($F_{(1,226)} = 4.63$, $P = 0.033$), this was not the case for any of the other MPOD parameters ($P > 0.05$). In any event the effect size of gender was 0.02 or less on all MPOD variables.
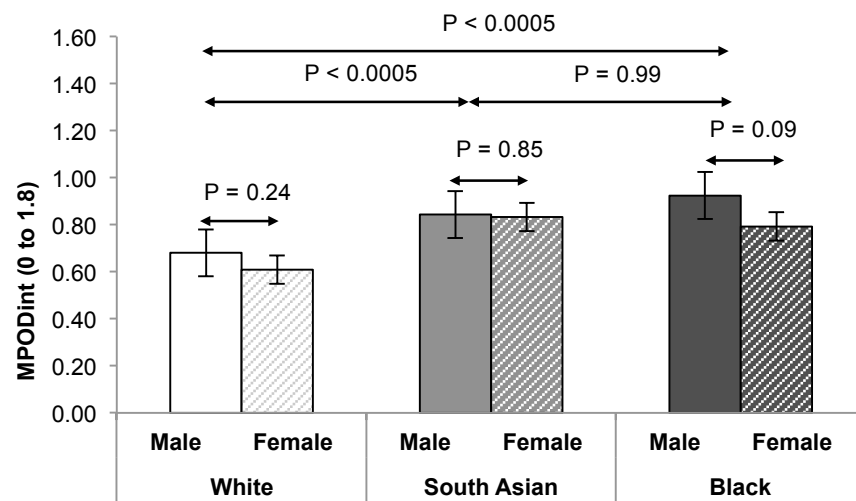
Figure 20 Variation in MPODint (0 to 1.8) between ethnic groups and gender.

The effect of country of birth on macular pigment spatial distribution

Fifty-six participants (25%) had been born and spent five or more childhood years abroad (Figure 19). One white participant was born in America and one in South Africa, and two South Asians were born in Africa. Thirty black individuals were born in Africa or the Caribbean, having spent on average 16 ± 6 years abroad. All other non-UK born participants were from Europe. Of note, the two-way ANOVA to investigate differences in MPOD parameters between ethnic groups was performed again, but with subjects that had been born and raised abroad removed from the analysis. Results were very similar to those reported above.

An independent t-test was conducted per ethnic group to investigate whether MPOD parameters varied between subjects born and raised abroad and those born and raised in the UK. Normality of the MPOD parameters being analysed was confirmed. No statistically significant difference was established in MPOD at 0º (P = 0.78), at 0.8º (P = 0.69), MPODav (0 to 1.8) (P = 0.82), MPODint (0 to 1.8) (P = 0.97) and the x-value at half peak MPOD (P = 0.64) for the black ethnic group. These findings were very similar for the white and South Asian group analysis too.

Influence of age on macular pigment spatial distribution among the three ethnic groups

The difference in age between the three ethnic groups was explored in the first instance. Mean age of the white group was 26.9 ± 5.1 years; for the South Asian group 20.1 ± 2.8 years; and for the black group 24.4 ± 5.7 years. The distribution of age across the whole sample and within each ethnic group did not follow a normal distribution. Non-parametric statistical analyses were therefore conducted for differences between groups and correlations with MPOD measures. A Kruskal-Wallis analysis revealed a statistically significant difference in age between the three ethnic groups, H(2) = 61.86, P < 0.0005. Pairwise comparisons with Bonferroni correction adjusted P-values showed that while there was a significant difference between the white and South Asian and between the South Asian and black ethnic groups (P < 0.0005), there was no significant difference in age between white and black ethnic groups (P = 0.179) (Figure 21).
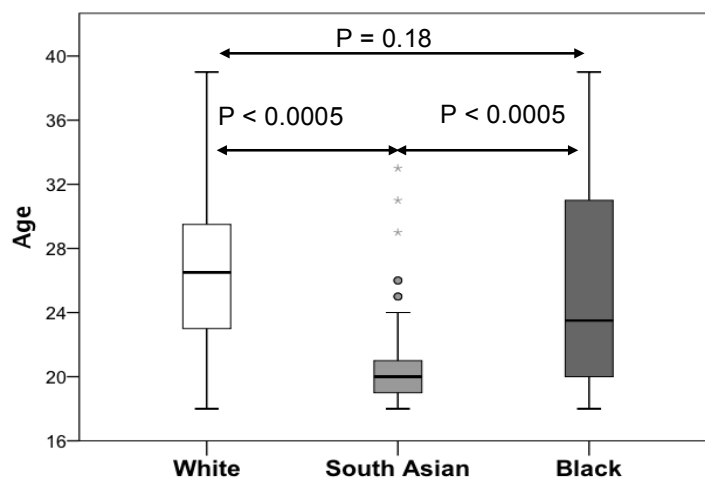
Figure 21 Boxplot to show variation in age between the three ethnic groups.

In addition the difference in age according to gender was investigated among the entire study sample. Males had a mean age of 24.5 ± 6.4 years and females 24.4 ± 5.4 years. The distribution of age within each gender group did not follow a normal distribution. A non-parametric Mann-Whitney U test indicated no statistically significant difference in age between the gender groups, U (5620) = -4.72, P = 0.64.

The relationship between MPOD at 0º and age across the whole study group was investigated using Spearman rank order correlation, ρ. No statistically significant association between MPOD at 0º and age was found (ρ = -0.10, n = 226, P = 0.15). This remained true when the same analysis was repeated for: MPOD at 0.8º and 1.8º, MPODav (0-1.8), MPODint (0 to 1.8) (Figure 22) and x-value at half peak MPOD, for the whole sample and also when repeated by ethnicity grouping (P > 0.05 for all). For this reason age was not used as a covariate in further analysis of MPOD data. In addition, analysis according to an age group e.g. bracketing 18 to 28 years and 29 to 39 years was not conducted due to the small age range among the South Asian ethnic group.
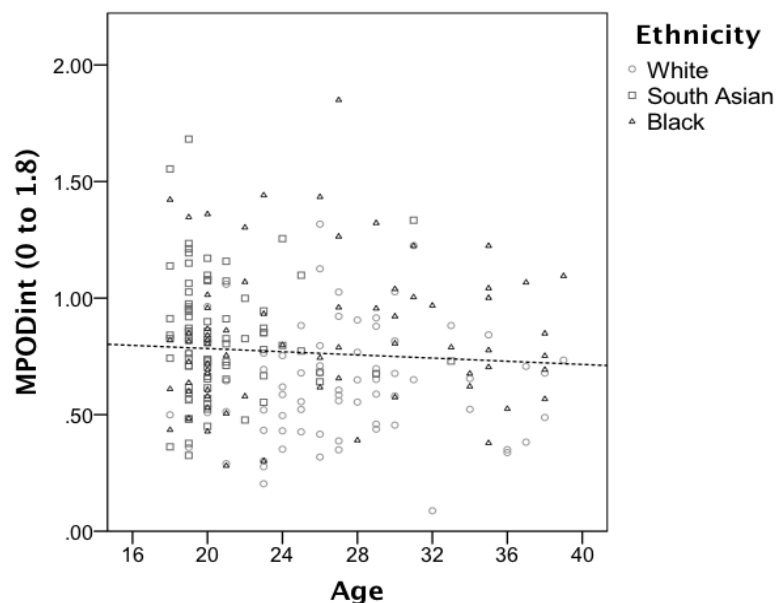
Figure 22 Scatterplot to show lack of association between age and MPODint (0 to1.8) within each ethnic group. A linear fit trend line for the whole study sample has been applied to the data.

Influence of body mass index on macular pigment spatial distribution

Before considering any association between BMI and MPOD the difference in BMI between the three ethnic groups was explored. The mean BMI of the entire study group was 23.9 ± 4.5, ranging from 14.7 to 41.5. The distribution of BMI across the whole sample and within each ethnic group did not follow a normal distribution. Non-parametric statistical analyses were therefore conducted to investigate differences in BMI between the three ethnic groups. A Kruskal-Wallis analysis determined a significant variation in BMI across the three ethnic groups, $H(2) = 18.59$, $P < 0.005$. Pairwise comparisons with Bonferroni adjusted P-values indicated a significant difference between the white (Md = 22.7 ± 3.1) and black (Md = 25.9 ± 5.3, P = 0.002) and between the South Asian (Md = 22.5 ± 4.3) and black ethnic groups (P < 0.0005). However there was no significant difference in BMI between white and South Asian groups (P = 1.00). No statistically significant correlation between BMI and MPOD measures were established when the study sample was examined as a whole and separately for each of the ethnic groups (Table 16).

In general, although not statistically significant, there appeared to be a trend towards a positive association between BMI and MPOD measures among the white ethnic group. In contrast, a negative association between BMI and all of the MPOD measures among the South Asian ethnic group was found, while there was no correlation between BMI and MPOD measures among the black ethnic group (Figure 23).

	Correlation	White	South Asian	Black	Total
MPOD at 0º	Spearman's ρ	0.21	-0.20	0.04	0.00
	P-value	0.08	0.08	0.77	0.95
MPOD at 0.8º	Spearman's ρ	0.22	-0.17	0.09	0.06
	P-value	0.06	0.13	0.47	0.40
MPODav (0 to 1.8)	Spearman's ρ	0.16	-0.16	0.10	0.07
	P-value	0.17	0.16	0.42	0.33
MPODint (0 to 1.8)	Spearman's ρ	0.19	-0.18	0.09	0.06
	P-value	0.10	0.11	0.48	0.48
x at half peak MPOD	Spearman's ρ	-0.12	-0.15	-0.08	-0.03
	P-value	0.32	0.17	0.49	0.68

Table 16 Association of body mass index and MPOD measures within each ethnic group and within the entire study group.
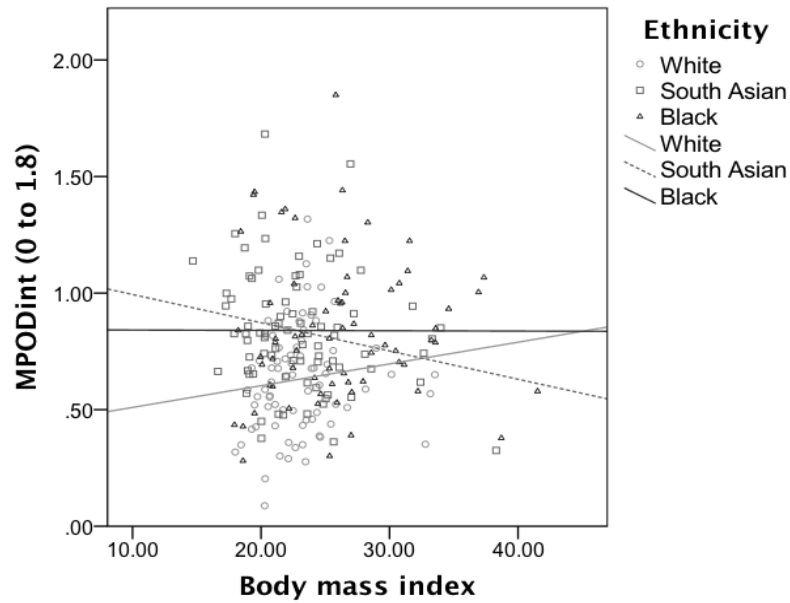
Figure 23 Scatterplot of BMI versus MPODint (0 to 1.8) per ethnic group. A linear fit trend line for each ethnic group has been applied to the data.

Influence of smoking status, eye colour and skin type on macular pigment and its spatial distribution among the white ethnic group

Among the white ethnic group fifty-six subjects reported never having smoked and twenty subjects reported being current or ex- smokers. The mean smoking pack year was 0.98 with a range from 0 to 12.00. Normality of the MPOD parameters being analysed according to smoking status was confirmed. Whilst MPOD measures were consistently higher in the never-smoker versus the current or ex-smoker groups, an independent samples t-test revealed no statistically significant difference between never smokers and current or ex-smokers with MPOD from 0º and 0.8º, MPODav and MPODint (0 to 1.8) (P > 0.05) (Table 17).

The results of the difference in MPODint (0 to 1.8) between never smokers and current or ex- smokers among the white ethnic group are presented graphically in Figure 24a. Furthermore, there was no statistically significant correlation between the smoking pack year and any of the discrete, averaged and integrated MPOD values (P > 0.05). The lack of association of the smoking pack year with MPODint (0 to 1.8) is presented graphically in Figure 24b.

		Never smoker (n = 56)			Current or ex- smoker (n = 20)					
			95% confidence interval			95% confidence interval				
			Upper	Lower		Upper	Lower	t	df	P
MPOD	Mean	**0.49**	0.44	0.54	**0.40**	0.35	0.46	1.76	74	0.08
at 0°	SD	**0.19**	0.15	0.21	**0.12**	0.07	0.15			
MPOD	Mean	**0.40**	0.36	0.45	**0.34**	0.28	0.39	1.60	74	0.11
at 0.8°	SD	**0.17**	0.14	0.20	**0.11**	0.06	0.15			
MPODav	Mean	**0.31**	0.28	0.34	**0.27**	0.23	0.31	1.35	74	0.18
(0 to 1.8)	SD	**0.12**	0.10	0.13	**0.09**	0.05	0.12			
MPODint	Mean	**0.66**	0.59	0.73	**0.56**	0.48	0.63	1.61	74	0.11
(0 to 1.8)	SD	**0.25**	0.21	0.29	**0.17**	0.09	0.23			
x: half peak	Mean	**1.69**	1.52	1.87	**1.66**	1.34	2.03	0.18	74	0.86
MPOD	SD	**0.70**	0.47	0.91	**0.75**	0.45	0.95			

Table 17 Mean ± SD of MPOD measures for never smokers versus current or ex-smokers for the white ethnic group. An independent t-test revealed no statistically significant differences between the two groups. Bootstrap 95% confidence intervals are provided in the table.
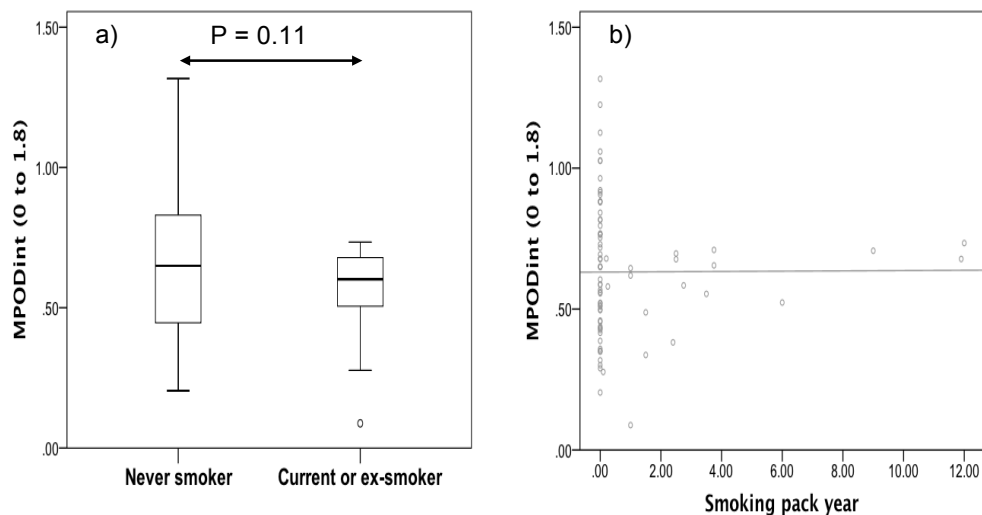
Figure 24 a) Boxplot showing variation in MPODint (0 to 1.8) between never smokers versus current or ex- smokers among the white ethnic group; b) Scatterplot to demonstrate lack of association of smoking pack year and MPODint (0 to 1.8) among the white ethnic group.

Almost half (47%) of the white participants reported having light eyes (Figure 19). Normality of the MPOD parameters being analysed according to eye colour was confirmed. Whilst MPOD measures were consistently lower in the light eye versus the dark eye group, an independent samples t-test revealed no statistically significant difference between eye colour and: MPOD at 0º and 0.8º, MPODav (0 to 1.8), MPODint (0 to 1.8) and the x-value at half peak MPOD (P > 0.05 for all) (Table 18).

		Light eyes (n = 36)				Dark eyes (n = 40)					
			95% confidence interval				95% confidence interval				
			Upper	Lower			Upper	Lower	t	df	P
MPOD	Mean	**0.44**	0.39	0.50		**0.49**	0.44	0.54	-1.32	74	0.19
at 0º	SD	**0.17**	0.11	0.21		**0.18**	0.14	0.21			
MPOD	Mean	**0.38**	0.33	0.43		**0.39**	0.34	0.44	-0.35	74	0.73
at 0.8º	SD	**0.16**	0.11	0.20		**0.16**	0.13	0.19			
MPODav	Mean	**0.29**	0.25	0.33		**0.31**	0.28	0.35	-1.06	74	0.29
(0 to 1.8)	SD	**0.11**	0.08	0.14		**0.11**	0.09	0.13			
MPODint	Mean	**0.60**	0.53	0.69		**0.66**	0.59	0.73	-0.95	74	0.34
(0 to 1.8)	SD	**0.24**	0.17	0.31		**0.23**	0.18	0.28			
x: half peak	Mean	**1.69**	1.48	1.91		**1.68**	1.47	1.94	0.00	74	1.00
MPOD	SD	**0.68**	0.38	0.97		**0.74**	0.51	0.92			

Table 18 Mean ± SD of MPOD measures for light (n= 36) versus dark eyes (n = 40) for the white ethnic group. An independent t-test revealed no statistically significant differences between the two eye colour groups.

A total of thirty white participants reported having sunburn prone skin types (Figure 19). Normality of the MPOD parameters being analysed according to skin type was confirmed. An independent samples t-test revealed no statistically significant difference between skin type among the white ethnicity group and: MPOD at 0º (P = 0.48), 0.8º (P = 0.60), MPODav (0 to 1.8) (P = 0.74), MPODint (0 to 1.8) (P = 0.61) and the x-value at half peak MPOD (P = 0.08).

Prevalence of different macular pigment spatial profile phenotypes among the three ethnic groups

When the study sample was considered as a whole, a total of one hundred and forty-eight subjects (65%) were identified as having an exponential MP spatial profile phenotype, thirty-eight subjects (17%) presented with a ring-like phenotype and forty (18%) had dip profiles. The number and percentage of individuals presenting with each MP spatial profile phenotype within the three ethnic groups and within each MP spatial profile phenotype is provided in Table 19.

Spatial profile phenotype		White	South Asian	Black	Total
Exponential	**Count**	**58**	**46**	**44**	**148**
	% within spatial profile type	39%	31%	30%	100%
	% within ethnicity	76%	58%	63%	65%
	% of total	26%	20%	20%	65%
Ring-like	**Count**	**7**	**22**	**9**	**38**
	% within spatial profile type	18%	58%	24%	100%
	% within ethnicity	9%	28%	13%	17%
	% of total	3%	10%	4%	17%
Central dip	**Count**	**11**	**12**	**17**	**40**
	% within spatial profile type	28%	30%	43%	100%
	% within ethnicity	15%	15%	24%	18%
	% of total	5%	5%	8%	18%

Table 19 Frequency of MP spatial profile phenotypes per ethnic group and for the sample as a whole.

A chi-square test for independence indicated a statistically significant association between ethnicity and presence of an exponential, ring or central dip MPOD spatial profile type (χ^2 (4, n = 226) = 13.4, P = 0.009, Cramer's V = 0.17). The majority of subjects (58%) presenting with a ring-like MP spatial profile were of South Asian ethnicity, compared to 18% of white and 24% of black participants. More black subjects (43%) presented with a dip profile compared to whites (28%) or South Asian (30%) (Figure 25).
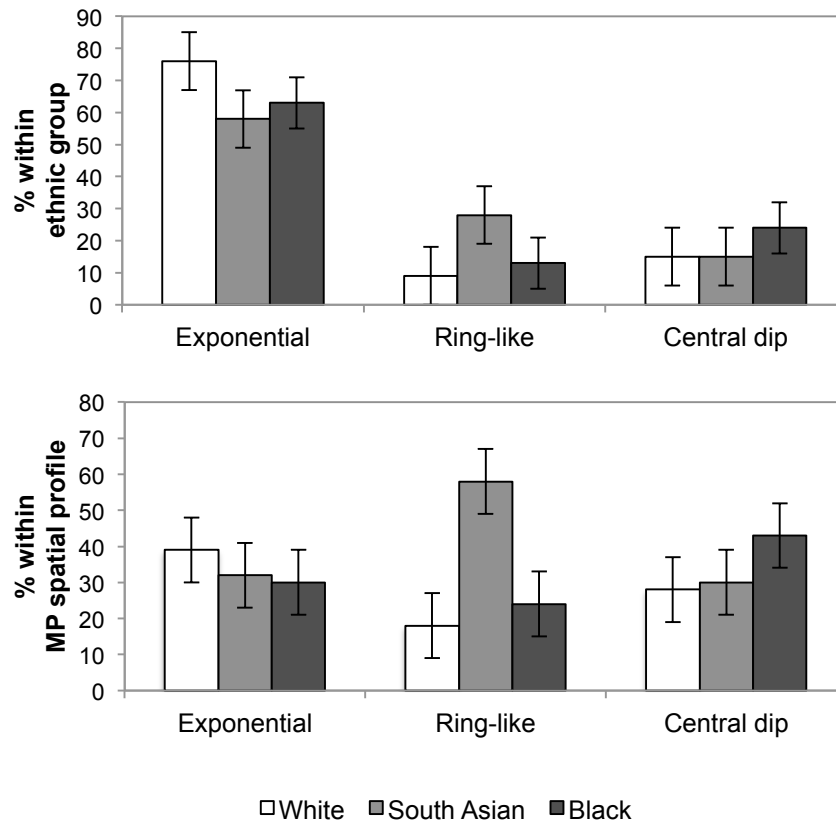
Figure 25 Frequency of individuals with exponential, ring-like or central dip MP spatial profile phenotypes within ethnic group (upper graph). Frequency of white, South Asian and black individuals within the MP spatial profile phenotype groups (lower graph).

Influence of other factors that may affect prevalence of macular pigment spatial profile phenotype

The proportion of males and females presenting with each MP spatial profile phenotype was investigated. Of the males, 60% (n = 48) presented with an exponential profile, 13.8% (n = 11) with ring-like and 26.2% (n = 21) with central dip profiles. Within the female group, 68.5% (n = 100) exhibited exponential profiles, 18.5% (n = 27) with ring-like and 13% (n = 19) with dip profiles. Although there seemed to be a greater tendency for males to present with a central dip profile compared to females, a chi-square test for independence based on the entire study sample data, just failed to reach statistical significance between gender and presence of an exponential, ring or central dip spatial profile type (χ^2 (2, n = 226) = 6.38, P = 0.06, Cramer's V = 0.17). A

formal chi-square test to examine the association between MP spatial profile phenotype and gender within each ethnic group could not be conducted due to violation of the assumption concerning minimum cell frequency within each ethnic group. The percentage within each gender group showing an exponential, ring-like and central dip profile for each ethnicity sample is presented in Figure 26. Of note, among the black ethnic group there was no association between MP spatial profile type and whether the subject had been born and raised in Africa or the Caribbean (χ^2 (2, n = 70) = 0.92, P = 0.63).
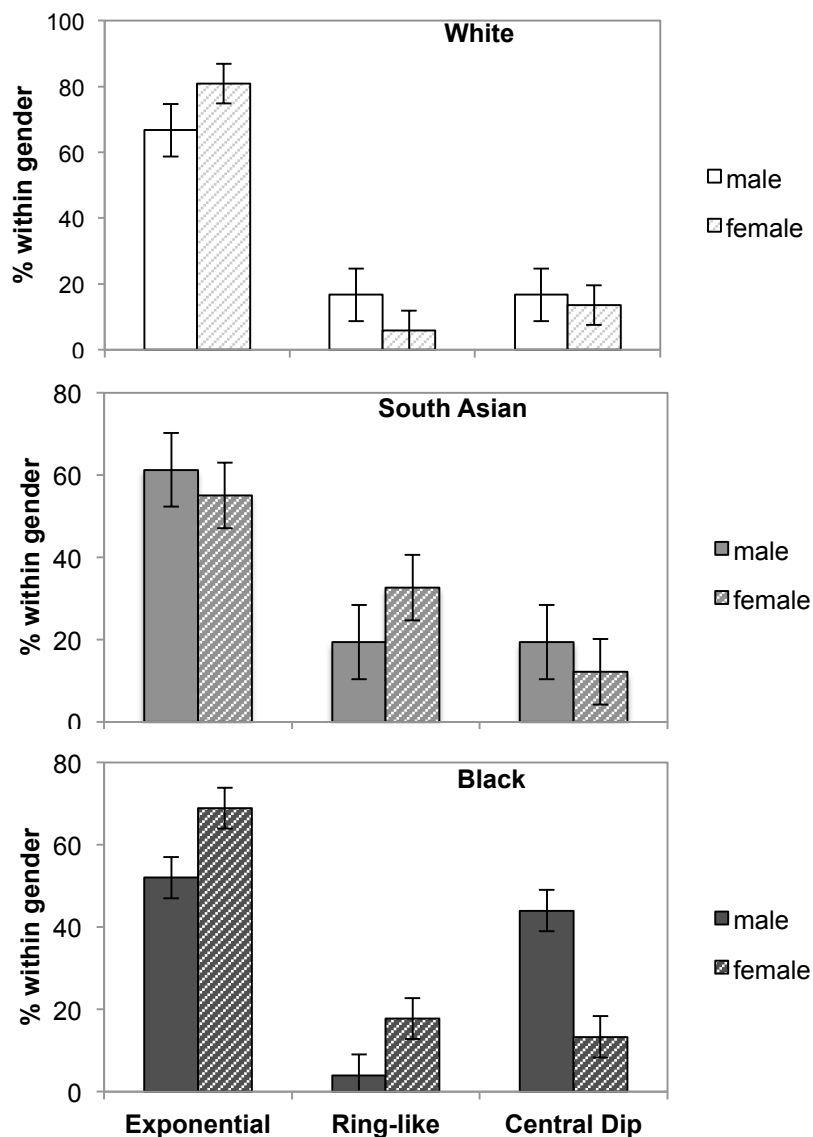
Figure 26 Bar chart to show within gender percentage of males and females presenting with exponential, ring-like or dip MP spatial profile phenotypes for each ethnic group.

The mean age according to each profile group was compared to investigate whether there was a tendency for age to influence the MP spatial profile phenotype. Within each MP spatial profile group age did not follow a normal distribution. A Kruskal-Wallis test showed no significant difference in age between the exponential (24.6 ± 5.7 years), ring-like (23.9 ± 5.8 years) and central dip groups (24.2 ± 5.7 years), (H(2) = 0.771, P = 0.68).

It was not possible to examine the prevalence of the MP spatial profile types according to BMI ≥ 25, smoking status, eye colour or skin type whilst taking into account ethnicity due to violation of the assumption concerning minimum cell frequency within each ethnic group.

Variations in macular pigment optical density according to the spatial profile phenotype

Variations in discrete MPOD measurements at single retinal eccentricities, MPODav and MPODint, and the x value at half peak MPOD according to the MP spatial profile phenotype were investigated. Visual graphical assessment (histograms, boxplots, P-P and Q-Q plots) of the MPOD data distribution per spatial profile group indicated a normal distribution of each of the MPOD parameters. There was a statistically significant difference in MPOD at the 0º, 0.8º and 1.8º retinal eccentricities measured by the MAP test between the three spatial profile groups as determined by one-way ANOVA (P < 0.0005) (Table 20). Post-hoc Tukey testing indicated that MPOD at 0º was statistically significantly lower in the exponential group (0.48 ± 0.15) compared to ring-like (0.68 ± 0.18, P < 0.0005) and dip profiles (0.64 ± 0.20, P < 0.0005) while there were no statistically significant differences between the ring-like and dip profile groups (P = 0.502). This finding remained true for MPOD at 0.8º, with lower levels in exponential (0.39 ± 0.13) compared to ring-like (0.64 ± 0.17, P < 0.0005) or dip profiles (0.63 ± 0.20, P < 0.0005). There was no statistically significant difference between the ring-like and dip profile groups (P = 0.947). In order to assess whether there was any variation in MPOD away from the centre of the fovea the difference in MPOD at 1.8º and at 2.8º was also explored. MPOD at 1.8º was lower in both the exponential (0.22 ± 0.10) and ring-like profile groups (0.22 ± 0.12) compared to the central dip profile group (0.36 ± 0.17, P < 0.0005). However, there was no significant difference in MPOD at 1.8º between the exponential and ring-like groups (P = 0.998). No significant difference in MPOD at 2.8º between the exponential and ring-like (P = 0.871) or dip profile groups

(P = 0.15) was found. Likewise, there was no difference between the ring-like and dip profile groups (P = 0.534). One-way ANOVA determined a statistically significant difference in MPODav and MPODint (0 to 1.8) between the three different MP spatial profile groups (Table 21).

		Exponential (n = 148)			Ring-like (n = 38)			Dip (n = 40)			ANOVA		
			95% confidence interval			95% confidence interval			95% confidence interval				
			Lower	Upper		Lower	Upper		Lower	Upper	F	df	P-value
MPOD at 0°	Mean	0.48	0.46	0.51	0.68	0.63	0.74	0.64	0.58	0.70	29.2	(2,223)	**< 0.0005**
	SD	0.15	0.13	0.17	0.18	0.13	0.22	0.20	0.16	0.23			
	Minimum	0.13			0.34			0.21					
	Maximum	0.99			1.16			0.97					
MPOD at 0.8°	Mean	0.39	0.37	0.41	0.64	0.59	0.69	0.63	0.57	0.69	63.9	(2,223)	**< 0.0005**
	SD	0.13	0.12	0.14	0.17	0.13	0.20	0.20	0.15	0.24			
	Minimum	0.04			0.28			0.16					
	Maximum	0.68			1.04			1.14					
MPOD at 1.8°	Mean	0.22	0.21	0.24	0.22	0.19	0.26	0.36	0.31	0.41	21.8	(2,223)	**< 0.0005**
	SD	0.10	0.09	0.11	0.12	0.08	0.15	0.17	0.13	0.21			
	Minimum	0.00			0.02			0.07					
	Maximum	0.47			0.62			0.88					
MPOD at 2.8°	Mean	0.16	0.14	0.17	0.16	0.14	0.19	0.18	0.15	0.22	1.8	(2,223)	0.175
	SD	0.08	0.07	0.09	0.09	0.06	0.12	0.11	0.08	0.14			
	Minimum	0.00			0.01			0.02					
	Maximum	0.38			0.46			0.50					

Table 20 Mean, SD, minimum and maximum values of MPOD from 0° to 3.8° for each MP spatial profile phenotype. Results of one-way analysis of variance between groups are shown. Bootstrap 95% confidence intervals are also provided.

		Exponential (n = 148)			Ring-like (n = 38)			Dip (n = 40)			ANOVA		
			95% confidence interval			95% confidence interval			95% confidence interval				
			Lower	Upper		Lower	Upper		Lower	Upper	F	df	P-value
MPODav	Mean	0.32	0.30	0.34	0.42	0.39	0.46	0.49	0.45	0.54	36.4	(2,223)	**< 0.0005**
(0 to 1.8)	SD	0.10	0.09	0.11	0.13	0.09	0.16	0.17	0.13	0.21			
	Minimum	0.03			0.17			0.16					
	Maximum	0.53			0.83			1.00					
MPODint	Mean	0.66	0.62	0.69	0.96	0.88	1.05	1.00	0.90	1.09	45.9	(2,223)	**< 0.0005**
(0 to 1.8)	SD	0.21	0.18	0.22	0.26	0.20	0.32	0.32	0.25	0.39			
	Minimum	0.09			0.44			0.30					
	Maximum	1.15			1.68			1.85					
x at half	Mean	1.83	1.72	1.96	1.46	1.33	1.61	1.52	1.41	1.63	6.9	(2,223)	**0.001**
peak	SD	0.77	0.64	0.88	0.43	0.29	0.57	0.35	0.29	0.41			
	Minimum	0.09			0.46			0.88					
	Maximum	4.48			2.89			2.26					

Table 21 Mean, SD, minimum and maximum values of MPODav, MPODint and x-value at half peak MPOD measurements for each MP spatial profile phenotype. Results of one-way analysis of variance between groups are shown. Bootstrap 95% confidence intervals are also provided.

Tukey post-hoc testing revealed that MPODav (0 to 1.8) was statistically significantly lower in the exponential (0.32 ± 0.10) compared to ring-like (0.42 ± 0.13, P < 0.0005) or dip profiles (0.49 ± 0.17, P < 0.0005) with a statistically significant difference between the ring-like and dip profile groups too (P = 0.025). Similarly, MPODint (0 to 1.8) was statistically significantly lowered in exponential (0.66 ± 0.21) compared to ring-like (0.96 ± 0.26, P < 0.0005) or dip profile groups (1.00 ± 0.32, P < 0.0005), but there was no statistically significant difference between the ring-like and dip profile groups (P = 0.724) (Figure 27).
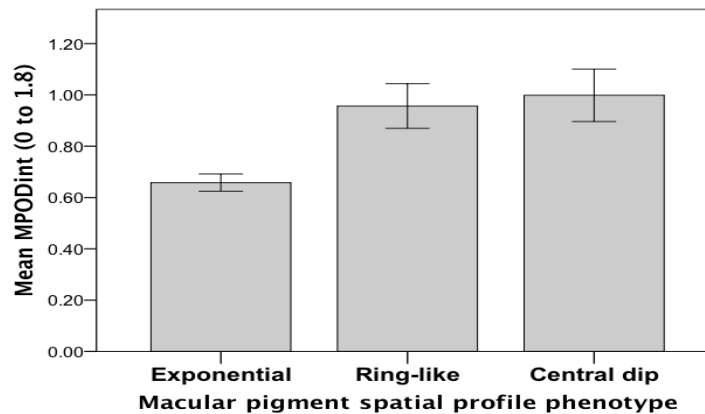
Figure 27 Bar chart to show variation in MPODint (0 to 1.8) between the three MP spatial profile groups.

There was a statistically significant difference in the x-value at half peak MPOD between profile groups as determined by one-way ANOVA. Tukey post-hoc testing showed that the x-value at half peak MPOD was statistically significantly wider in the exponential (1.83 ± 0.77) compared to the ring-like (1.46 ± 0.43, P = 0.007) or dip profile groups (1.52 ± 0.35, P = 0.022). There was no statistically significant difference between the ring-like or the dip profile groups (P = 0.928).

Variations in macular pigment optical density according to the spatial profile phenotype per ethnic group

To investigate whether there was any difference in the MPOD variables according to MP spatial profile phenotype within each ethnic group a one-way ANOVA was conducted with the data split by ethnic grouping Table 22. The results followed a similar trend to the whole group analysis whereby MPOD at 0°, 0.8°, MPODav (0 to

1.8), MPODint (0 to 1.8) were statistically significantly lower in the exponential compared to the ring-like and central dip MP spatial profile phenotypes (P < 0.05 for all). There was no statistically significantly difference in the x value at half peak MPOD between spatial profile groups within any ethnic group. The results of the analysis for variation in MPODint (0 to 1.8) between the spatial profile groups analyzed separately per ethnic group are presented graphically in Figure 28.

Ethnicity		One-way ANOVA between MP spatial profile groups		
		df	F	P-value
White	MPOD at 0º	2	6.947	**0.002**
	MPOD at 0.8º	2	17.402	**< 0.0005**
	MPODav (0 to 1.8)	2	10.521	**< 0.0005**
	MPODint (0 to 1.8)	2	12.725	**< 0.0005**
	x at half peak MPOD	2	1.961	0.148
South	MPOD at 0º	2	7.847	**0.001**
Asian	MPOD at 0.8º	2	17.525	**< 0.0005**
	MPODav (0 to 1.8)	2	10.924	**< 0.0005**
	MPODint (0 to 1.8)	2	13.088	**< 0.0005**
	x at half peak MPOD	2	2.542	0.085
Black	MPOD at 0º	2	13.385	**< 0.0005**
	MPOD at 0.8º	2	26.865	**< 0.0005**
	MPODav (0 to 1.8)	2	13.335	**< 0.0005**
	MPODint (0 to 1.8)	2	18.11	**< 0.0005**
	x at half peak MPOD	2	2.683	0.076

Table 22 Results of a one-way ANOVA to investigate the difference in MPOD variables according to MP spatial profile phenotype within each ethnic group.
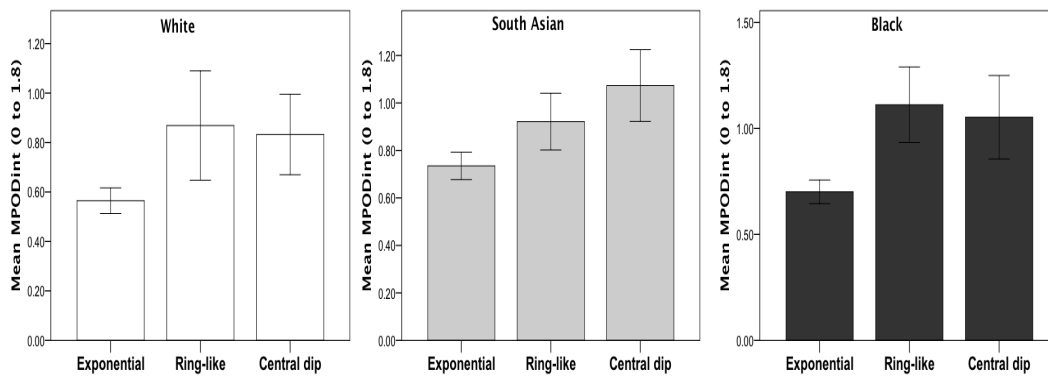
Figure 28 Bar charts to show difference in MPODint (0 to 1.8) between the MP spatial profile groups for each ethnic group.

3.1.4   Discussion

The aim of the present study was to investigate variations in MPOD and its spatial distribution among young, healthy individuals from the three largest ethnic groups in England and Wales: white, South Asian and black. White subjects, compared to South Asian and black subjects, presented with significantly lower levels of MP as represented by MPOD at 0º, 0.8º, MPODav and MPODint (0 to 1.8). No statistically significant difference was found in these MPOD variables between the non-white ethnic groups. Results of the two-way between-groups ANOVA demonstrate that around 10% of the variance in the MPOD measurements can be explained by ethnicity. This highlights the importance of taking ethnic background into account when reporting MPOD.

A single central measurement of MPOD is among the most commonly reported outcome measures in MPOD studies. For this reason variations in MPOD measured at 0º between the three ethnic groups was included in the data analysis to allow comparisons with previous studies to be drawn. There was an increased central MPOD at 0º in South Asian (0.61 ± 0.17) versus white subjects (0.47 ± 0.17, P < 0.0005). This is consistent with the findings from previous studies; an earlier investigation in which MPOD was measured using the MAP test found increased central MPOD at 0º in South Asian (0.56 ± 0.17, n = 54) compared to white subjects (0.45 ± 0.18; t (71) = 2.50, n = 19; P = 0.015) (Huntjens et al., 2014). Likewise, using the MPS 9000 (MPS Tinsley Ophthalmic, Redhill, Surrey, UK) a mean central MPOD of 0.43 ± 0.14 in one hundred and seventeen South Asian subjects, and 0.33 ± 0.13 in fifty-two white subjects was reported (P < 0.0005) (Howells et al., 2013). Overall, the lower average MPOD values per ethnic group in the study reported by Howells et al. (2013) compared with the present study are likely due to the different HFP instruments used and interpretation of their output. The MPS 9000 measures MPOD at a retinal eccentricity of 0.5º. In theory a higher MPOD at 0º would be expected assuming an exponential fit to the MPOD distribution. Indeed, the theoretical value at 0º represented by the amplitude, A, can be interpolated from Equation 3, Chapter 1, section 1.2.4. In this case, given a mean MPOD of 0.43 at 0.50º for the South Asian group in the Howell et al. (2013) study, the theoretical MPOD value at 0º would be $0.43/10^{(-0.42)*0.50} = 0.70$. Using this approach the mean MPOD of 0.33 at 0.50º for the white subjects translates into a theoretical MPOD of 0.54 at 0º. Given that the MAP test measures MPOD at 0º, it can now be seen that the results of the aforementioned studies are very similar. The

findings of the present study also compare favourably with another in which MPOD was measured in South Asian subjects. A mean central MPOD of 0.63 ± 0.16 in sixty South Asian subjects aged 20 to 29 years, and 0.72 ± 0.22 in sixty South Asian subjects aged 30 to 39 years has been reported previously (Raman et al., 2011). The central MPOD measurement was taken at a retinal eccentricity of 0.25º, as measured using the macular densitometer based on HFP. In this case, given a mean MPOD of 0.63 at 0.25º, the theoretical MPOD value at 0º would be $0.63/10^{(-0.42)*0.25} = 0.80$. Thus, it seems that the values reported by Raman et al. (2011) are indeed higher compared with the present results. Notably, in the study by Raman et al. (2011) the South Asian subjects were of South Indian origin living in India (Mumbai) whereas the South Asian subjects included in the current study were of Indian, Pakistani, and Bangladeshi descent, the majority (98%) born and living in the UK or Europe. One explanation for this may be that increased environmental sunlight exposure during childhood for subjects living in India compared to the UK contributes to increased MPOD. That said, none of the MPOD parameters showed any significant difference between subjects born and raised in the UK versus those born and raised abroad among any of the ethnic groups. This finding is of particular interest with regards to the black ethnic group, whereby almost half the group had been born and raised in Africa or the Caribbean. It seems that for the study sample, there was little environmental influence on MPOD. Given the recent reports that environmental sunlight exposure is not associated with early or late AMD (Klein et al., 2014, Yam and Kwok, 2014) this suggests that MPOD does not increase in response to increased environmental sunlight exposure. Further work is recommended to substantiate this hypothesis, including gathering detailed information regarding sunlight exposure during childhood and adult years while taking into account the country of residence and ethnicity. The country of origin and residence may also be significant because of differences in diet. For example, it has been reported that the traditional South Asian diet typically consisting of a diet rich in carotenoids may be altered after migration, particularly in young or second generation South Asians (Gilbert and Khokhar, 2008). However, dietary data was not collected for this single visit cross sectional study, which is a limitation of the investigation. Future work incorporating dietary data for different ethnic groups living in their native countries would be of great interest.

Rather than MPOD measured at a single retinal eccentricity, it is proposed that MPODav and MPODint better represent the overall amount of MP present within the central retina. The integrated transmittance of blue light over a central 0º to 1.8º area was calculated from each study participant's MPOD data and converted to an averaged

MPODav (0 to 1.8) measurement. Mean MPODav (0 to1.8) was significantly lower in white (0.30 ± 0.11) compared to South Asian (0.39 ± 0.12, P < 0.0005) or black individuals (0.41 ± 0.16, P < 0.0005). This finding compares well with earlier findings by our research group whereby MPODav (0 to 1.8) in white subjects was (0.27 ± 0.10) versus South Asians; (0.34 ± 0.09; t[71] = 3.07; P = 0.003) (Huntjens et al., 2014). The integrated area under the curve as represented by MPODint showed similar differences between the three ethnic groups. There are no previous reports of ethnic differences including the black ethnic group in these MPOD parameters.

Although the relationship between the lateral width of the MP spatial distribution and the peak MPOD value has been investigated in the past there are conflicting reports in the literature. The width of the MP distribution was significantly correlated with the peak MPOD as measured by HFP methods (n = 32, r = 0.63; P < 0.0005) implying that a wider MP distribution is anticipated in individuals with a higher peak MPOD (Hammond et al., 1997c). In contrast to this, other investigators could not confirm the relationship between the lateral extent of the MP spatial profile and peak MPOD measured by FAF and motion photometry (Robson et al., 2003) or by FR techniques (Berendschot and van Norren, 2006). In addition, the half-width peak MPOD measured by two-wavelength FAF has been shown to broaden with age (P < 0.01) although this effect was more prominent in females compared to males (P < 0.0001) (Delori et al., 2006). In the current study, the lateral extent of the MPOD distribution, represented by the retinal eccentricity corresponding to half peak MPOD, showed significant differences among the three ethnic groups. Of note, a significantly wider distribution was evident in the black compared to the South Asian ethnic groups. This finding is of interest because it implies that while MPOD measures tended to be higher in the non-white compared to the white ethnic groups, the actual spatial distribution of MPOD manifests differently among the non-white ethnic groups. Indeed, a difference in MP spatial distribution profiles between the ethnic groups was evident and is discussed further below.

The effect of various covariates on MPOD with ethnicity was explored. Although there was a statistically significant effect of gender on MPOD at 0°, the effect size was small (2%). There was no effect of gender on any other MPOD parameters. Reports of a gender association within different ethnic groups are inconsistent in the literature. While MPOD was increased in South Asian males (0.47 ± 0.13, n = 44) compared to South Asian females (0.41 ± 0.14, n = 73 (P < 0.01), this was not true for white subjects (P = 0.39) (Howells et al., 2013). No effect of gender on MPOD at 0.5° was

found in a young healthy Caucasian group (n = 46) (Kyle-Little et al., 2014). Similarly, no gender-associated difference in MPOD was ascertained in a biracial study including white (non-Hispanic) and black (African) subjects aged 35 to 49 years (Wolf-Schnurrbusch et al., 2007).

While the South Asian group was significantly younger than the white and the black ethnic groups (P < 0.0005), there was no significant difference in age between the white and black ethnic groups (P = 0.179). No effect of age on central MPOD, MPODav, MPODint, peak MPOD or the x-value at half peak MPOD measurements was demonstrable and this was the case when the group was analysed as a whole (n=226) as well as per ethnic group. Given these results, the finding of increased central MPOD in South Asian and black participants compared to the whites cannot be explained by the difference in age between the groups. It must be taken into account however that the 18 to 39 year age range was intentionally chosen as an inclusion criterion for the current study to minimise the potential confounding effect of age on any reported differences in MPOD and its spatial density distribution between the ethnic groups. Albeit inconsistent, there are previous reports of a possible negative association between age and MPOD as discussed in Chapter 1, section 1.4.1. For example, a moderate decline in MPOD at 0.5° was reported to be associated with increasing age (r = -0.251, P = 0.045) in a study of seventy-nine subjects with a mean age of 65 ± 11 years (Nolan et al., 2010). It would therefore be useful to extend the current study to include older individuals from different ethnic backgrounds.

The findings of the current study do not support the proposal that there is a negative association between increased BMI and MPOD (Chapter1, section 1.4.5). Even though BMI varied significantly among the three ethnic groups, no significant association between BMI and MPOD was established in any of the ethnic groups, consistent with a previous report comparing South Asian and white individuals (Howells et al., 2013).

Among the white ethnic group there was no difference in MPOD parameters between never smokers and current or ex-smokers. However, the latter group was relatively small and the smoking pack year was very low, which likely explains why an association was not established compared to previous studies (Chapter 1, section 1.4.6). The small number of smokers in the study sample may be reflective of the large global reduction in the estimated prevalence of daily smoking since 1980 (Ng et al., 2014).

Eye colour is associated with transmission of light through the eye, whereby more light is transmitted through light compared to dark irides (van den Berg et al., 1991). It has therefore been suggested that iris colour may influence levels of MP with higher MPOD levels reported in individuals with dark eyes (Chapter 1, section 1.4.3). However, no statistically significant difference in any of the MPOD parameters was found according to eye colour among the white ethnic group, which is in agreement with recent studies (Abell et al., 2014, Kyle-Little et al., 2014). A possible explanation of the discrepancy in findings regarding the association of MPOD and eye colour may arise due to the lack of a consistent classification system for eye colour (Mackey et al., 2011). Self-reporting of eye colour has been used in a previous investigation (Hammond et al., 1996b) as well as in the current study. An alternative approach is that a trained investigator assesses each subject's eye colour by comparing it to standard photographs (Kirby et al., 2010), although variability is still likely to result from this subjective method (Klein et al., 2014).

It has recently been reported that MPOD was 47.5% higher in subjects with a low compared to high UV index (Raman et al., 2012a). This finding could not be substantiated in the current investigation. A limitation of the study design is the imprecise measures of sunlight exposure. Detailed information regarding lifetime sun exposure in childhood and teenage years was not collected as part of the health and lifestyle questionnaire. In addition, information regarding sun exposure or sun avoidance measures taken, such as wearing a hat or seeking shade, was not gathered. Further work is warranted to establish whether there is a link between sun exposure in early life and levels of MP. Similarly, the rationale behind looking for a correlation between skin type and MPOD is the suggested association between light or sunburn prone skin and the pathogenesis of AMD (Tomany et al., 2004, Khan et al., 2006a, Klein et al., 2014). However this could not be corroborated by the current study, as there was no difference in MPOD according to skin type within the white ethnic group.

This is the first comparative study to investigate the prevalence of different MP spatial profile phenotypes in white, South Asian and black subjects. There is general agreement that MP spatial profiles follow either an exponential or non-exponential pattern. Within each ethnic group, 76% of white, 58% of South Asian and 63% of black subjects presented with an exponential MP spatial profile. Hence, the finding of an exponential profile remains the most "typical" MP spatial density distribution. Among the entire study sample, 35% overall (n = 78) presented with a non-exponential MP spatial profile. This compares well with previous reports whereby proportions ranging

from 10% (Nolan et al., 2008) and 30% (Dietzel et al., 2011b) to 50% (Berendschot and van Norren, 2006, Delori et al., 2006) of study populations have shown a deviation away from an exponential curve fit. Of note, this has been demonstrated when MP is measured by HFP (Nolan et al., 2008) as well as objective imaging techniques (Berendschot and van Norren, 2006, Delori et al., 2006, Dietzel et al., 2011b). In the aforementioned studies ethnicity was either not stated or the study included subjects of Caucasian or European descent, with the exception of the work by Nolan et al. (2008). In the latter investigation the authors reported no obvious association of ethnicity and spatial profile type, although this was not the main outcome measure. Moreover, white subjects were compared to a group of non-white individuals comprising five Indian, six Asian, three Hispanic/Spanish and four black individuals. Perhaps including several ethnicities in the non-white group may have diluted any significant associations since South Asian and black ethnicities in the current study appeared to display different spatial profile characteristics to each other.

The findings of the present study in which 9% of white compared to 28% of South Asian and 13% of black subjects presented with a ring-like MP structure; and 15% of white, 15% of South Asian and 24% of blacks presented with a central dip MP profile support the suggestion that ethnicity plays a role in the spatial distribution of MP (Wolf-Schnurrbusch et al., 2007). Our results suggest that non-exponential i.e. ring-like and central dip MP spatial profile phenotypes occur more frequently in individuals of South Asian and black ethnicity respectively, compared to white ethnicity (P = 0.009). This concurs with the previous finding of an ethnic disparity in the occurrence of MP spatial profiles, whereby a non-exponential profile was more likely in South Asian compared to white subjects (Huntjens et al., 2014). Of note, central dip MP profiles were entirely absent in the white subject group in the earlier study, but this may be due to the smaller sample size (nineteen subjects) compared to the current sample of seventy-six white subjects. There is very limited literature regarding the MP spatial profile in black subjects. Wolf-Schnurrbusch et al. (2007) showed a significantly increased frequency of a parafoveal ring in 86% healthy African compared with 68% healthy white subjects (P < 0.01). This prevalence is higher compared to the current study. However, classification of a parafoveal ring was allocated if the MPOD profile measured by two-wavelength FAF could not be approximated by a monotonic decline and a shoulder could be identified within 3º of the peak MPOD. The reliability of this seemingly subjective approach was not reported. In view of the results presented in Chapter 2, it is conceivable that the parafoveal ring group identified by Wolf-Schnurrbusch et al. (2007) could have included subjects with MP profiles that would have been defined as

central dip according to the current classification system. This illustrates the difficulty in drawing meaningful comparisons between studies. Notwithstanding, it has been proposed that a ring-like structure in MP may enhance its protective role, such that increased prevalence of ring-like MP spatial profiles was reported in healthy subjects (43%) compared to those with AMD (23%) (Dietzel et al., 2011b). Following on from this, a future study to establish the prognostic value of the MP spatial profile phenotype with regards to AMD prevalence in different ethnic populations is recommended. However, in the absence of a universally agreed spatial profile nomenclature and classification system (as discussed in Chapter 2), analysis of such work remains complicated.

There are conflicting reports as to whether gender has an association with the MP spatial profile phenotype. In 2006, Delori et al. used FAF methods to determine the MP spatial profile in a Caucasian sample (mean age 49 ± 15 years, n = 41). The ring-like MP pattern, based on the presence of secondary maximum-minimum pairs, was more pronounced in females than males (P = 0.0001) and this relationship was not affected by age (Delori et al., 2006). Likewise, a more recent study involving a much larger sample (mean age 71.6) of two hundred and twenty-seven females and one hundred and forty-two males also found that females were more likely than males to present with a ring-like MP spatial profile (P = 0.004) (Dietzel et al., 2011b). It should be noted that the ring-like profile was defined as a density profile showing a visible bimodal pattern based on the analysis of MP density maps and radial density profiles produced by FAF imaging. The amount of deviation away from a monotonic decline required to classify a ring-like or intermediate MP profile are not provided in the report. The variation in MP profile identification may contribute to the contrasting findings of the current study in which there did not appear to be a gender association with the MP spatial profile phenotype. This is in accordance with earlier work in which a similar MP profile classification method was employed, whereby presence of a ring-like MP structure was based on a deviation of MPOD ≥ 0.03 away from an exponential fit to the data as measured by FAF and FR (Berendschot and van Norren, 2006). Notwithstanding, the lack of a gender association with the MP spatial profile phenotype has also been presented by HFP studies that have used alternative profile classification methods (Hammond et al., 1997c, Kirby et al., 2009, Kirby et al., 2010).

Unsurprisingly, given the limited age range results of the current study, we found no difference in age between the three MP spatial profile groups. It remains that there is inconsistent reporting of age as a factor that may influence the spatial density

distribution of MP. A study including longitudinal data collected over 1 to 16 years from a sample of thirty-two individuals showed that the MP spatial profile remained stable with time (Hammond et al., 1997c). In addition, a lack of association of age with MP spatial profile type has been reported (Berendschot and van Norren, 2006, Delori et al., 2006). In contrast, subjects presenting with the exponential MP spatial profile were found to be younger by 5 ± 12 years compared to those presenting a central dip (Kirby et al., 2010). An increased prevalence of a central dip profile has also been reported with increasing age (Kirby et al., 2010, Neelam et al., 2014). Further work is required to examine the effect of age on the MP spatial profile type among an older cohort of different ethnic populations.

There is a lack of agreement regarding smoking status and MP spatial profile type. Recent studies have determined that never smokers were more likely to have a ring-like MPOD presentation (Dietzel et al., 2011b). Alternatively, an increased prevalence of a central dip profile has been reported in smokers compared to never-smokers with 8.8% never-smokers exhibiting a central dip in compared to 18.8% of current smokers such that it was proposed that a central dip decreased the protective role of MP (Kirby et al., 2010). It has also been reported that subjects with a higher BMI were also more likely to present with a central dip profile (Neelam et al., 2014). None of these previous findings could be confirmed in the current study.

Differences in the amount of MP represented by each of the three spatial profile phenotypes identified in the present study were explored. For whole group and per ethnic group analysis, discrete measures of MPOD at 0°, 0.8° and 1.8° showed a statistically significant difference according to MP spatial profile phenotype (P < 0.0005). In the earlier report by our research group it was proposed that a central dip profile had not lost its peak, but possibly broadened its lateral distribution (Huntjens et al., 2014). The findings of the current study revealed a narrower lateral extent, as indicated by the half peak MPOD value of the ring-like (1.46 ± 0.43°) and central dip profiles (1.52 ± 0.35°) compared to the exponential profile group (1.83 ± 0.77°). However, when the data were analysed per ethnic group there was no difference in this lateral measurement between the spatial profile types.

Irrespective of ethnicity, the integrated measures of MPODav and MPODint (0 to 1.8) were significantly increased in subjects presenting with ring-like and dip versus exponential profiles (P < 0.0005), while there was no significant difference between the two non-exponential groups. In agreement with our earlier study (Huntjens et al., 2014)

there appears to be more MP present over the central retinal area when a ring-like or central dip profile is present rather than an exponential profile. This supports the hypothesis that the presence of a central dip profile may actually offer an increased amount of MP over a central retinal area of diameter 3.6°, and therefore increased macular protection from harmful blue light (Huntjens et al., 2014). Evidence from supplementation studies has indicated that L and Z supplementation increases MPOD in the human foveal and parafoveal areas so that a central peak in MPOD may be a result of a relative enrichment of Z and a central dip profile may be representative of a relative enrichment of L (Schalch et al., 2007, Trieschmann et al., 2007, Richer, 2011). Of note, it has been suggested that L and Z supplementation might amplify, but not create non-exponential MP spatial profiles (Zeimer et al., 2012). Nonetheless, results of the present study also support the hypothesis that a central dip could be the result of a high conversion of L to meso-Z (van de Kraats et al., 2008, Connolly et al., 2010) resulting in a plateau of increased MPOD within a 3.6° central retinal area. On the other hand there has been debate surrounding the importance of a seeming lack of a central peak in "central dip" profiles. It has been postulated that the absence of a central peak in MPOD is due to an inability to convert L to meso-Z in the retina, resulting in reduced protection against AMD (Kirby et al., 2010).

Conclusions

Currently this is the sole report of variations in MPOD and its spatial distribution among young healthy individuals of white, South Asian and black ethnicity that represent the three largest ethnic groups in England and Wales. The results show that integrated measures of MP represented by MPODav and MPODint, as well as single central MPOD measurements were significantly increased in South Asian and black compared with white subjects. The lateral extent of the MP distribution appeared to be wider in the white ethnic group, suggesting that the overall MP spatial profile presented somewhat differently between the ethnic groups. Additionally, risk factors for AMD such as gender, age, and smoking status had no effect on MP or the spatial profile phenotype among the study sample. Within the black ethnic group there was no difference in MPOD parameters between those that had been born and raised in Africa or the Caribbean in comparison to those born and raised in the UK.

MP spatial profiles were classified as exponential, ring-like or central dip and the prevalence of each phenotype among the three ethnic groups was investigated. Non-

exponential MP profiles were significantly more prevalent in South Asian and black compared with white subjects. Specifically, the prevalence of a ring-like profile was increased in South Asians and a central dip was significantly increased in the black group. It was shown that integrated MPOD up to 1.8º (represented by the area under the curve, MPODint) was significantly increased in ring-like and central dip compared with an exponential profile, irrespective of ethnicity. This suggests that, similar to the ring-like MP structure, a central dip represents enhanced retinal protection from harmful blue light.

In summary,

- The overall amount of MP within the central retinal area varies between ethnic groups;
- Prevalence of MP spatial profile phenotype varies according to ethnicity;
- The amount of MP varies according to MP spatial profile phenotype irrespective of ethnicity.

The variations in MP and its spatial density distribution according to ethnicity may be explained by anatomical differences within the retina. This will be explored in the following chapter.

4 The effect of ethnicity on the association between foveal morphology and macular pigment spatial distribution

4.1   Introduction

It has been hypothesized that inter-individual variations in foveal pit morphology may play a role in the spatial distribution of MP across the retina (Delori et al., 2006, Liew et al., 2006, Nolan et al., 2008, Kirby et al., 2009). There are reports that a thicker central retina is associated with significantly higher MPOD levels (Liew et al., 2006, van der Veen et al., 2009c). However, other studies have shown a lack of correlation between central foveal thickness and MPOD (Kanis et al., 2007, Kirby et al., 2009). As well as variations in retinal thickness, it has been proposed that a wider fovea supports longer cone axons and may therefore provide more storage capacity for MP (Nolan et al., 2008), though this proposal was not supported by the results of a later study (van der Veen et al., 2009c). Additionally, a steeper incline in retinal thickness from the centre of the fovea to the periphery may result in a sharper decline in MPOD with eccentricity from the fovea, possibly due to compression of the inner plexiform and cone axon layers of the retina that host MP (Kirby et al., 2009). Few studies have reported on the variation in the inner plexiform layer specifically and its association with MPOD.

In the previous chapter it was demonstrated that MP and its spatial density distribution varies with ethnicity. Likewise, foveal morphology shows significant inter-individual variation. Central foveal thickness of healthy eyes has been found to vary between different ethnic groups whereby white subjects were found to present with thicker central foveas (208 ± 15μm, n = 60) compared to a group of non-white subjects (196 ± 15μm, P < 0.05, n = 18) (Nolan et al., 2008). In addition, African and African American (black) subjects were reported to have reduced central subfield thickness compared to white (Asefzadeh et al., 2007, Kelty et al., 2008, Kashani et al., 2010, Wagner-Schuman et al., 2011) and Indian Asian subjects were found to have a thinner central fovea than Caucasians (P = 0.04) (Pilat et al., 2014). One study reported no significant difference in central foveal thickness between Asian and black subjects, although this data was derived from a small sample of eleven subjects per ethnic group (Grover et al., 2009). Variations between males and females have also been reported, with a reduced macular thickness in females compared to males (Kelty et al., 2008, Kashani et al., 2010, Song et al., 2010, Ooto et al., 2011) although this is not a consistent finding across the literature (Grover et al., 2009, Wagner-Schuman et al., 2011). As well as variations in retinal thickness, ethnic differences in foveal width have been reported with a narrower foveal width measurement in whites compared to non-whites (Nolan et al., 2008, Wagner-Schuman et al., 2011). There are fewer reports of inter-

148

individual variations in specific retinal layers. Does the thickness of the inner plexiform layer that contains MP vary with ethnicity? Following on from this, is it possible that variations in foveal morphology (such as inner retinal layer and IPL thickness as well as foveal width) can explain some of the ethnic variation reported in MP and its spatial distribution?

Aim

The aim of the study presented in this chapter was to investigate the relationship of foveal architecture with MP parameters between young healthy white, South Asian and black subjects. Specifically, the following associations were explored:

- MPOD measured at single retinal eccentricities at 0°, 0.8° and 1.8° and the corresponding total retinal thickness, inner retinal layer thickness and IPL thickness;
- MPOD at 0° and foveal width;
- MPODint (0 to 3.8) and averaged retinal thickness across the central 1000µm, foveal width and volume;
- x value at half peak MPOD and foveal width and volume; and
- MP profile slope (0 to 0.8, 0.8 to 1.8, 1.8 to 2.8 and 2.8 to 3.8) and corresponding foveal pit profile slope.

These associations were analysed according to ethnicity, gender and MP spatial profile phenotype: exponential, ring-like and central dip. To date, this is the first report to investigate the association of foveal anatomy and MPOD among three ethnic groups in a single study. Given that prevalence of the MP spatial profile phenotype shows variations with ethnicity as discussed in the previous chapter, differences in foveal morphology according to the MP spatial profile phenotype was also examined. The findings may help to explain variations seen in spatial distribution of MP away from the fovea.

Prior to the main investigation, accuracy of foveal pit measurements was assessed. An initial study, published last year (Ctori et al., 2014), explored the effect of ocular magnification on OCT scan image size (Appendix 6.2). In addition, repeatability of axial and lateral foveal morphology measurements (Appendix 6.3) was investigated, and this was published earlier this year (Ctori and Huntjens, 2015).

4.2 The effects of ocular magnification on Spectralis spectral domain optical coherence tomography scan length

4.2.1 Introduction

OCT imaging allows non-invasive cross-sectional imaging of the human retina (Huang et al., 1991). Good correlation with retinal histology (Anger et al., 2004, Spaide and Curcio, 2011, Vajzovic et al., 2012) means that OCT imaging is used for the clinical diagnosis of a variety of ocular pathologies such as age-related macular degeneration (Regatieri et al., 2011), macular holes (Oh et al., 2010), vitreo-macular traction (Mojana et al., 2008), and glaucoma (Moreno-Montañés et al., 2010). Newer spectral domain OCT (SD-OCT) methods offer faster acquisition speed and higher image resolution compared to older time-domain OCT techniques (Nassif et al., 2004, Leung et al., 2008). Additionally, automated retinal thickness measurement techniques are a time-efficient way to investigate retinal thickness change over time (Seigo et al., 2012).

Quantitative evaluation of retinal thickness measurements in vivo, using both automatic and manual measuring techniques within the OCT software platform, is used to aid clinical diagnosis and design treatment protocols (Chiu et al., 2012, Chakravarthy and Williams, 2013, Lee et al., 2013). However, it is known that the different segmentation algorithms employed by individual OCT instruments result in variability in retinal thickness measurement. Consequently, this complicates data comparisons derived from different platforms (Carpineto et al., 2009, Folgar et al., 2014). Furthermore, ocular magnification of retinal images is affected by refractive error, corneal curvature, refractive index, axial length and anterior chamber depth (Bennett et al., 1994, Rudnicka et al., 1998). The distance of the eye to the measuring device can also influence the magnification effect (Garway-Heath et al., 1998). The optical set-up of the OCT instrument as well as the software program for calculating image size will govern image size calculation in computerized fundus imaging (Almeida and Carvalho, 2007). In the case of OCT scan images, ocular magnification may affect lateral measurements i.e. those made parallel to the retinal plane (Sanchez-Cano et al., 2008). Lateral measurements such as drusen diameter and geographical atrophy area in dry age-related macular degeneration may be used for establishing diagnosis and treatment protocols, and foveal width measurements are used in research studies. It is therefore important to consider the potential impact of ocular magnification on lateral measurements derived from OCT scan images.

It had been suggested that axial length should be taken into account when assessing the reliability of OCT data (Wakitani et al., 2003). Some studies reported an inverse correlation between retinal nerve fibre layer thickness, optic nerve head parameters and axial length (Leung et al., 2007, Rauscher et al., 2009, Odell et al., 2011, Savini et al., 2012). In contrast, other research groups found these associations became negligible when corrections accounting for axial length were applied to the measured values (Bayraktar et al., 2001, Leung et al., 2007, Savini et al., 2012) thus demonstrating the significance of taking the ocular magnification effect of axial length into account. However, not all OCT platforms account for axial length induced ocular magnification. For this reason subjects with refractive error greater than ±5.00 or ±6.00DS have been excluded from some investigations of retinal morphology to minimize potential measurement errors (Kirby et al., 2009, Menke et al., 2009).

Alternatively, various attempts have been made to correct for the magnification of an individual nominal scan length produced by the OCT instrument (Dubis et al., 2012, Savini et al., 2012). In a study by Wagner-Schuman et al., (2011) a ratio of the subject's actual axial length to that assumed by the Cirrus OCT (Carl Zeiss Meditec, Dublin, CA) was applied to lateral scan measurements. Other research groups have addressed the issue of lateral scaling by applying a correction based on the SD-OCT instrument manufacturer's formula using a modified Littman's method (Bennett et al., 1994), which incorporates individual refractive error, corneal radius and axial length (Ooto et al., 2011, Savini et al., 2012).

In contrast to other SD-OCT platforms that provide scans with a nominal scan length of 6mm (e.g. the Cirrus HD-OCT), the Spectralis (Heidelberg Engineering, Heidelberg, Germany) applies an automatic modification process to minimise the effect of ocular magnification, generating individual scan lengths based on three parameters. It assumes a non-modifiable pre-set axial length of 24.385mm based on the Gullstrand schematic eye (Atchinson and Smith, 2000) (personal communication with Heidelberg, Germany; July 2013). Secondly, by allowing the operator to focus the retinal image, the subject's refractive error is taken into account. Thirdly, a default corneal curvature i.e. keratometry (K) setting of 7.70mm equal to the K-value of Gullstrand's model eye (Atchinson and Smith, 2000) is assumed by the device, as described in its technical specifications. Alternatively, an option to use the subject's actual mean-K is provided.

Aim

A study was carried out to investigate the effect of incorporating a subject's ocular biometry measures of mean spherical error (MSE) and mean-K on the scan length obtained using the Spectralis SD-OCT versus the scan length obtained using the instrument's default K setting. Optical simulation software was used to calculate the expected scan length based MSE, mean-K and the subject's axial length. Comparisons were made between the actual and simulated scan lengths. The aim of the study was to demonstrate the benefit of acquiring Spectralis SD-OCT scans using the subject's mean-K as opposed to using the device's corneal curvature default setting.

4.2.2   Methods

The investigation took place from October 2013 to December 2013 at the Division of Optometry and Visual Science, City University London. Approval for the study was obtained from the Optometry Research and Ethics Committee City University London. Written informed consent was obtained from all subjects conforming to the tenets of the Declaration of Helsinki (Appendix 6.5). Recruitment was carried out as previously described (Chapter 3, section 3.1.2).

A total of fifty volunteers took part; all presented with logMAR visual acuity better than 0.3 log units in the eye being tested. Exclusion criteria were: ocular pathology, medication that may affect retinal function and previous laser eye surgery. By default, measurements were taken for the right eye unless it did not meet the inclusion criteria, in which case the left eye was used. Each participant had their MSE in dioptres calculated. This was done using the formula sphere plus half of the cylinder (Thibos et al., 1997), with values taken from the average of five autorefractor readings and mean-K (average of three horizontal and vertical K readings) obtained using the Auto Kerato-Refracto-Tonometer TRK-1P instrument (Topcon, Tokyo, Japan).

The Spectralis SD-OCT was used to scan the undilated test eye of each participant in a dark room (Paunescu et al., 2004, Nolan et al., 2008). Two high resolution 20° x 10° volume scans (97 B-scans 30 microns apart, ART 16 frames including 1024 A scans) were acquired for each participant. The first scan was obtained using the default corneal curvature setting of 7.70mm; while the second had the subject's mean-K

entered into the software prior to scan acquisition. The participant was instructed to look at the central fixation target while the infrared fundus image was focused with a dial corresponding to their MSE. During scan acquisition, the investigator independently monitored the participant's fixation via the live fundus image. All scans had a minimum quality level of 25 decibels, as recommended by the manufacturer's guidelines. The resulting "*default-K*" and "*mean-K*" scan length was recorded from the Spectralis mapping software, Heidelberg Eye Explorer (Version 1.7.0.0 © 2011).

Axial length was measured using the IOLMaster (Carl Zeiss Meditec, Dublin, CA, USA). This is a well-known non-contact device based on partial coherence interferometry shown to have good axial length measurement repeatability (Lam et al., 2001, Verkicharla et al., 2013). Zemax optical design software (Zemax, LLC, Redmond, WA, USA) was used for simulation of an image from a 20° SD-OCT incorporating each individual subject's MSE, mean-K and axial length data. The Gullstrand's exact model eye (Atchinson and Smith, 2000) was applied to the simulation since Spectralis software image size calculations are based on this model. Within the Zemax model, mean-K values and axial length were modified for each subject by changing the radius of curvature of the anterior corneal surface and the axial distance between posterior lens surface and retinal plane respectively. MSE was modelled as a paraxial lens immediately before the model eye. An object with a field of 10º (with respect to the optical axis, resulting in 20º overall field) was set and the size of the image at the retinal plane calculated by the software was used to represent the simulated scan length. This was compared to the default-K and mean-K scan lengths.

Statistical analysis

All statistical analyses were performed using SPSS version 21.0 for Windows (SPSS Inc., Chicago, USA). Values in the text and tables are presented as the mean (or median, Md) ± standard deviation (SD). Preliminary analyses were performed to ensure no violation of the assumptions of normality, linearity and homoscedasticity. Since Shapiro Wilk testing revealed a significant deviation from a normal distribution for scan length and MSE, Spearman's Rank Correlation Coefficient ρ was calculated to explore the correlation between default-K and mean-K with simulated scan lengths. Statistical significance was accepted at $P < 0.05$.

4.2.3   Results

A total of twenty-two males and twenty-eight females were included in the study. The mean age was 21 ± 2.9 years. Mean, minimum and maximum values of mean-K, MSE, axial length, and scan lengths are summarised in Table 23.

	Mean	SD	Minimum	Maximum
Mean keratometry, mm	7.81	0.28	7.26	8.33
MSE, DS	-1.76	2.74	-13.00	+2.00
Axial length, mm	24.01	1.36	21.41	29.04

Table 23 Summary of variations in mean keratometry, axial length and mean spherical error within the study sample.

The mean and median scan length for scans using the default-K was 6.04 ± 0.28mm, Md = 5.95mm; for the mean-K group 6.10 ± 0.33mm, Md = 6.00; and for the simulated-K group was 6.23 ± 0.38mm, Md = 6.21mm. A Wilcoxon Signed Rank Test revealed a statistically significant difference between default-K and simulated-K scan lengths ($P < 0.0005$) and between mean-K and simulated-K scan lengths ($P < 0.0005$). There was also a statistically significant difference between default-K and mean-K scan length ($P = 0.012$) (Figure 29).
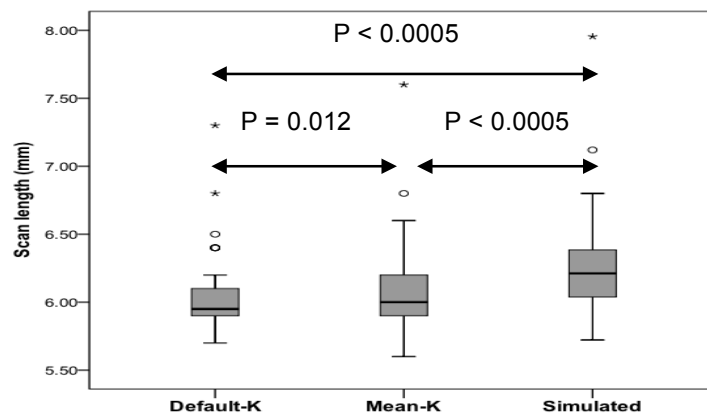
Figure 29 Box and whisker plot to show scan lengths obtained from SD-OCT scans obtained with default-K settings; mean-K values; and from software simulations incorporating axial length values. The length of each box is the interquartile range and the band inside the box represents the median. The whiskers show the smallest and largest values, with outliers indicated by the circles and extreme outliers by the asterisks.

There was a statistically significant strong positive correlation between mean-K and the simulated scan length ($\rho = 0.926$, $P < 0.0005$) and a statistically significant moderate correlation between default-K scan length and the simulated scan length ($\rho = 0.663$, $P < 0.0005$), shown in Figure 30. The effect of axial length and MSE on these relationships was explored. The correlation between mean-K and simulated scan length remained strong and statistically significant when controlling for axial length ($\rho = 0.822$, $P < 0.0005$) and for MSE ($\rho = 0.875$, $P < 0.0005$). However, the correlation was weakened for default-K measurements when controlling for axial length ($\rho = 0.473$, $P < 0.001$) and became non-significant when controlling for MSE ($\rho = 0.221$, $P = 0.128$).
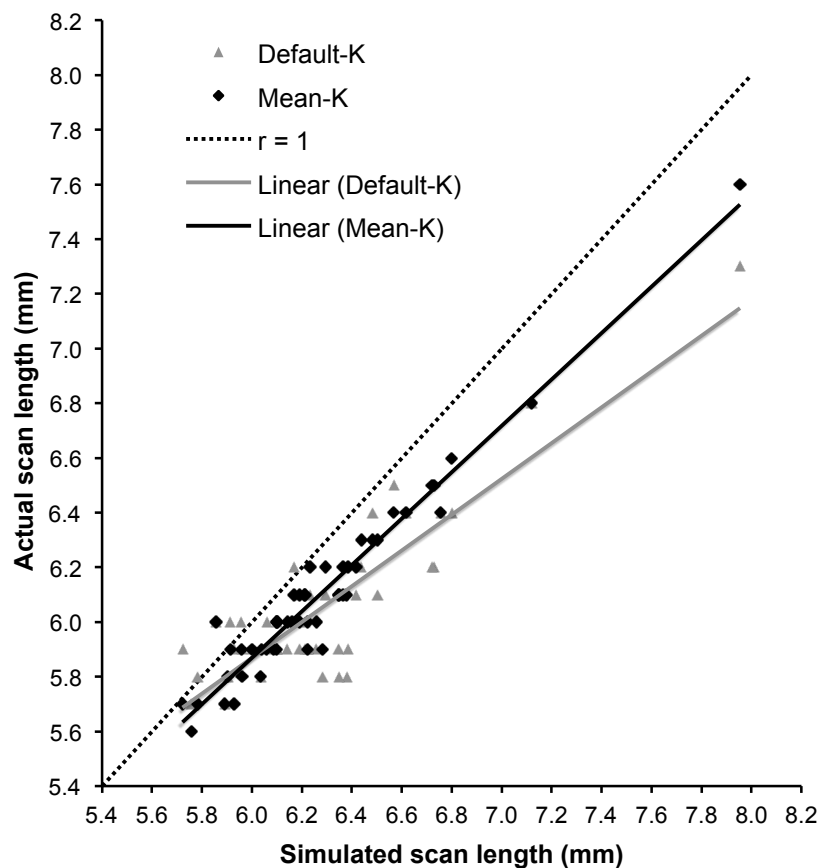
Figure 30 Scatterplot of actual scan length acquired using mean-K (black squares) and default-K (grey triangles) on the y-axis plotted against Zemax simulated scan length (x-axis). There was a statistically significant strong positive correlation between mean-K ($\rho = 0.926$, $P < 0.0005$) and default-K ($\rho = 0.663$, $P < 0.0005$) with the simulated scan length. Dashed black line represents perfect agreement, r = 1.00.

4.2.4 Discussion

The Spectralis SD-OCT generates individual scan lengths for each subject based on refractive error, corneal curvature and a non-modifiable pre-set axial length of 24.385mm based on the Gullstrand schematic eye. For each participant, Spectralis SD-OCT scan length acquired using the instrument's default-K setting of 7.70mm, versus using the subject's mean-K, was compared to a Zemax simulation software simulated scan length based on the participant's individual ocular biometry. The aim was to ascertain whether the effect of ocular magnification on SD-OCT scan length was represented more accurately using an individual's mean-K value as opposed to the Spectralis default-K setting in comparison to simulated output based on Gullstrand exact eye model (Odell et al., 2011). The study included individuals with axial length of 21.41mm to 29.04mm resulting in mean-K scan lengths ranging from 5.6 to 7.7mm (Figure 29). Whilst direct comparisons cannot be drawn from other studies with different subject demographics, similar scan lengths of 5.3 to 7.0mm have been reported whereby the nominal 6mm scan length was corrected using each subject's axial length (varying from 21.56 to 28.36mm) based on the Cirrus eye model (Odell et al., 2011). Of note, the most accurate model eye to calculate ocular magnification has yet to be determined (Almeida and Carvalho, 2007), although differences between modified Littman's technique (Bennett et al., 1994) and the Gullstrand eye model are less than 2% for axial lengths from 22 to 26.5mm (Song et al., 2011).

The correlation between mean-K and the simulated scan length ($\rho = 0.926$, $P < 0.0005$) was stronger than that between default-K scan and the simulated scan length ($\rho = 0.663$, $P < 0.0005$). The lack of perfect correlation between the mean-K and simulated scan lengths in the current study may be due to the accuracy of ocular biometry measurements obtained. The within-subject SD of K measurements have been shown to range from 0.05mm to 0.18mm depending on the instrument used (Visser et al., 2012). The TRK-1P gives repeated measurements within ±0.12DS on test eyes (personal communication with Topcon; June 2014). The repeatability of K measurements between two sessions (n = 76) indicated a mean difference of 0.04mm (data not shown). According to the Spectralis technical guidelines, a 0.1mm error in K will result in an error in lateral measurement of 0.8%. This translates to a 0.1mm change in scan length for every 0.2mm deviation from the individual's mean-K. Another consideration is that subjective refraction was not carried out to estimate MSE. However, it has been shown that using an autorefractor is an accepted method to

approximate refractive error (Pesudovs and Weisinger, 2004). In addition, there is no option to include separate horizontal and vertical K values in the Spectralis software. The mean-K value underestimates or overestimates the horizontal K value depending on whether the individual has with or against-the-rule astigmatism and this may explain the lack of perfect agreement between the mean-K and simulated scan lengths in the current study. Nonetheless, each individual's mean-K and MSE values were used for Spectralis scan acquisition as well as the Zemax simulation. Any error in these values would therefore have the same effect on both occasions. Hence, the discrepancy from perfect correlation indicating that ocular magnification is not sufficiently corrected is more likely to be caused by some other assumption built into the OCT software, or by eyes not complying with standard assumptions for example eyes that over-accommodate during imaging (Tan et al., 2004).

The influence of axial length on OCT data acquired from Spectralis SD-OCT scans involving a novel method of measuring the known distance of a sub-retinal visual implant in vivo was investigated in a recent study (Röck et al., 2014). Although the results confirmed accuracy of lateral measurements taken from Spectralis SD-OCT measurements in emmetropic, medium length eyes (22.51 to 25.5mm), the authors did recommend that caution should be taken when comparing measurements obtained from very short (< 22.5mm) or very long eyes (> 25.51mm), implying that axial length measurements were beneficial. Contrary to this, it was not deemed necessary to measure axial length to minimise lateral measurement errors resulting from not correcting for ocular magnification (Odell et al., 2011). Indeed optic nerve head area measurements obtained from Spectralis SD-OCT scans were found to be independent of axial length when transverse scaling was applied using measures of ocular biometry including K (Patel et al., 2012).

The current study showed a strong and significant positive correlation between mean-K scan length and the simulated scan length remained even after controlling for the effects of MSE ($\rho = 0.875$, $P < 0.0005$) and axial length ($\rho = 0.822$, $P < 0.0005$). What is more, the largest deviation of either mean- or default-K scan length from the simulated scan length did not belong to those with the highest MSE or those with axial length that deviated most from the Gullstrand exact eye model value of 24.385mm (Figure 30). Rather, the simulated scan length consistently overestimated the mean-K and the default-K scan length output. Nonetheless, a strong correlation between the simulated scan length and that obtained with mean-K was observed, with a consistent underestimation of around 1.0 to 1.5mm. On the other hand, scan lengths above

5.9mm produced by the default-K setting were increasingly under-estimated compared to those obtained with mean-K (Figure 30). This implies that lateral measurements of drusen size and foveal width for example are likely to be underestimated if SD-OCT scans larger than 5.9mm are obtained with the default-K setting.

Conclusion

This study provides useful information on the influence of ocular biometry measures on Spectralis SD-OCT scan length. The effect of ocular magnification on scan length appears to be better accounted for when an individual's mean-K value is incorporated into the Spectralis SD-OCT software prior to imaging as opposed to using the device's default setting. Performing scan acquisition inputting the subject's measured mean K value and the fundus image focussed according to their MSE is therefore recommended, especially when lateral retinal measurements are to be made. In addition, it is important to consistently use the individual's mean-K value for subsequent scans of the same patient for long-term monitoring in a clinical setting, for example measuring progression of non-exudative pigment epithelial atrophy. These results may be of interest for clinical trials using SD-OCT for area or lateral measurements.

4.3 Repeatability of foveal measurements using Spectralis SD-OCT segmentation software

4.3.1 Introduction

Repeatability and reproducibility of automated total retinal thickness measurements using SD-OCT have been demonstrated in healthy individuals (Wolf-Schnurrbusch et al., 2009, Tan et al., 2012) as well as those with ocular pathology (Patel et al., 2008, Krebs et al., 2011, Patel et al., 2011, Comyn et al., 2012, Pinilla et al., 2013, Bressler, 2014). This has enabled the definition of levels at which true clinical change can be distinguished from measurement variability. However, different OCT instruments employ a variety of segmentation algorithms within their software platforms so that measurements cannot be directly compared between devices (Carpineto et al., 2009, Folgar et al., 2014). It is therefore important to establish the repeatability and reproducibility of retinal measurements for each OCT device being used for clinical diagnosis and treatment protocol designs (Chiu et al., 2012, Chakravarthy and Williams, 2013, Lee et al., 2013).

According to the configuration of the Spectralis SD-OCT (Heidelberg Engineering, Heidelberg, Germany) presented in the user manual, one pixel represents 3.9µm axially and 6µm laterally (Heidelberg Engineering, 2013). It features Automatic Real Time (ART), a setting that improves image quality by averaging multiple B-scans to reduce noise and Tru-Track[TM], an eye-tracking device that improves scan reproducibility (Menke et al., 2009). Compared to other OCT instruments, the Spectralis SD-OCT presents the highest reproducibility of automated crude central foveal thickness measurement (Pierro et al., 2010, Bressler, 2014). In November 2014 Heidelberg Engineering launched an update to the Spectralis SD-OCT Heidelberg Eye Explorer mapping software (version 6.0c) that allows automatic segmentation of individual retinal layers.

Aim

The aim of the study was to report inter-investigator and inter-scan repeatability of thickness of eight individual retinal layers including the inner and outer plexiform and nuclear layers along with combined inner retinal layer thickness and overall retinal

thickness at manually derived axial and lateral foveal locations. Repeatability of foveal width measurements was also investigated. All measurements were derived from Spectralis SD-OCT scans using the newly available Spectralis retinal layer segmentation software (version 6.0c).

4.3.2   Methods

The study included forty healthy volunteers and took place at the Division of Optometry and Visual Science, City University London from October 2013 to December 2013. Approval for the study was obtained from the Optometry Research & Ethics Committee City University London. All subjects gave written informed consent conforming to the tenets of the Declaration of Helsinki (Appendix 6.5). The inclusion criterion was logMAR visual acuity better than 0.3 log units in the eye being tested. Exclusion criteria were ocular pathology including corneal disease, macular disease, medication that may affect retinal function and previous eye surgery, including refractive laser correction. For each volunteer, the eye with the best logMAR acuity was selected as the test eye. Mean spherical error (MSE), calculated as sphere plus half of the cylinder (Thibos et al., 1997) (average of five autorefractor readings), and mean keratometry measurements (average of three horizontal and vertical readings) were obtained using the Topcon TRK-1P autorefractor (Topcon, Tokyo, Japan). Two experienced investigators, Byki Huntjens (A) and Irene Ctori (B) each derived foveal measurements from Spectralis SD-OCT scans, using the techniques described below. Investigators A and B both obtained measurements from the first scan of each participant (1A and 1B respectively), and investigator B took measurements from the second scan (2B). For repeat measurements, each investigator was masked to their initial or the other investigator's results. Tomograms were measured in a random order to minimize this potential source of bias.

Spectralis SD-OCT scan acquisition

All scans were obtained without pupil dilation (Paunescu et al., 2004, Polito et al., 2005, Nolan et al., 2008) in a dark room using the Spectralis SD-OCT device. As recommended by manufacturer instructions, each participant's mean keratometry value was inserted into the Spectralis software prior to scan acquisition (Ctori et al., 2014).

Two consecutive 20° x 5° volume scans (49 B-scans 30 microns apart, ART 16 frames including 1024 A scans) were taken for the test eye within a single visit, without setting the first scan as a reference. The participant was instructed to sit back from the device between scans. The second scan was taken within minutes of the first. Each time, the investigator focused the infrared fundus image according to the participant's MSE. Central fixation was monitored via the live fundus image and scan quality was accepted above 25 decibels (dB), in accordance with the manufacturer guidelines.

Foveal measurements

Foveal measurements from each SD-OCT scan were performed using the inbuilt Spectralis mapping software, Heidelberg Eye Explorer (version 6.0c). This new Spectralis segmentation software was used to obtain individual retinal layer thickness measurements including: overall retinal thickness (RT), RNFL, GCL, IPL, INL, OPL, ONL, RPE, IRL and photoreceptor layer (PR). The IRL represents the distance from the inner to the outer ELM. Measures of foveal width were also evaluated, as well as the correlation of manual and automated measures of central retinal thickness. In addition, we explored the horizontal symmetry from the foveal centre of the thickness of the individual retinal layers.

No manual adjustments to B-scan retinal layer segmentation were made prior to measurements being taken. For each scan, the foveal centre was identified as the frame including the brightest foveal reflex (Hammer et al., 2008, Tick et al., 2011). As suggested by Mohammad *et al.,* when a bright reflex was absent or present in two or more frames, the frame containing the thickest outer segment layer was chosen (Mohammad et al., 2011). At the point where the software caliper bisected the foveal reflex, individual layer thickness (RT, RNFL, GCL, IPL, INL, OPL, ONL, RPE, IRL and PR) was recorded in microns (Figure 31A). The software displays overall retinal thickness as the vertical distance between the vitreoretinal interface and Bruch's membrane (Figure 31B).
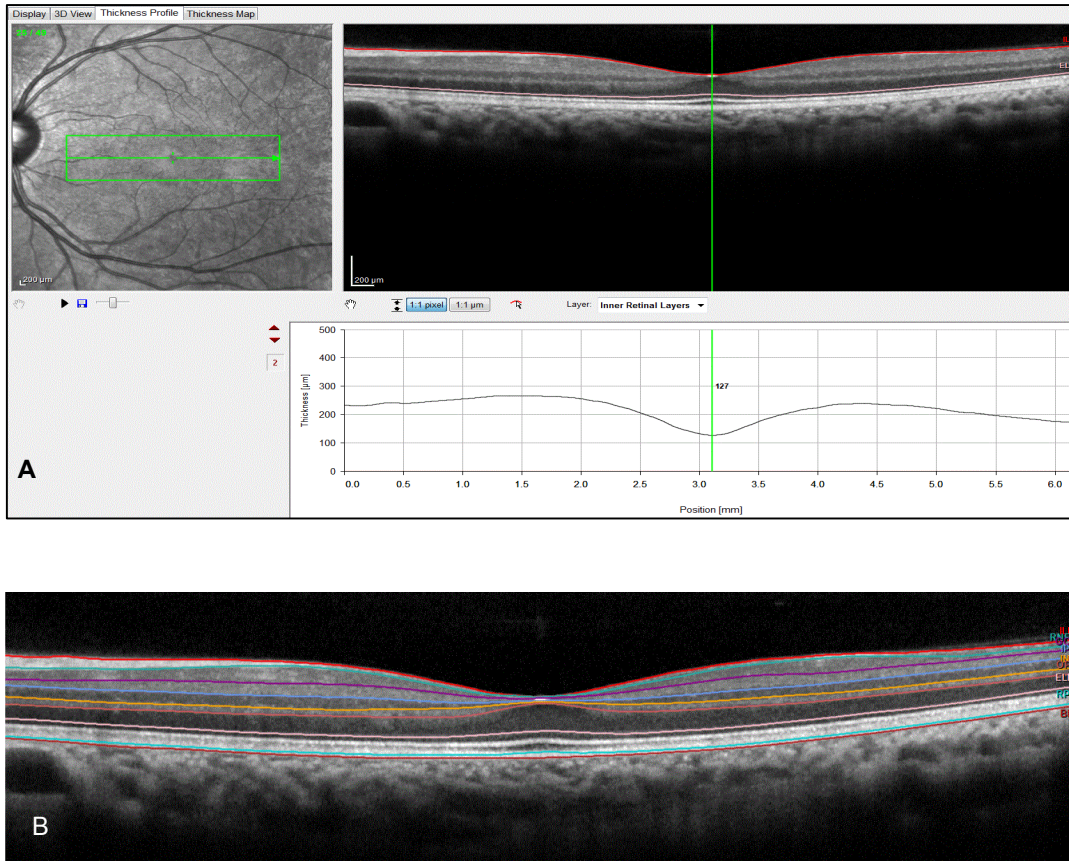
Figure 31 Central retinal thickness and layer segmentation by Spectralis SD-OCT software. The Spectralis software displays overall retinal thickness as the vertical distance between the vitreoretinal interface and Bruch's membrane. Using the thickness profile, the foveal reflex was bisected by the software caliper, and the thickness of the individual layers was recorded in microns (A). Segmentation of the individual retinal layers can be seen in the lower image (B).

Thickness of each retinal layer was also measured at 2° and 5° eccentricity away from the fovea. In order to locate these lateral positions on the tomogram, the eccentricities in degrees were converted into microns based on each individual's OCT scan length. For example, given that the scan length (in microns) generated by the Spectralis represents 20°, the lateral equivalent in microns of 2° would be given by *2*(scan length/20).* The inbuilt software caliper was set at the appropriate lateral distance perpendicular to the vertical caliper bisecting the foveal reflex and thickness of each retinal layer recorded from the retinal thickness profile (Figure 32). Lateral measurements were taken nasal to the fovea for all tomograms. In addition, temporal retinal thickness measurements were also obtained for the first scan of each participant to assess horizontal symmetry.
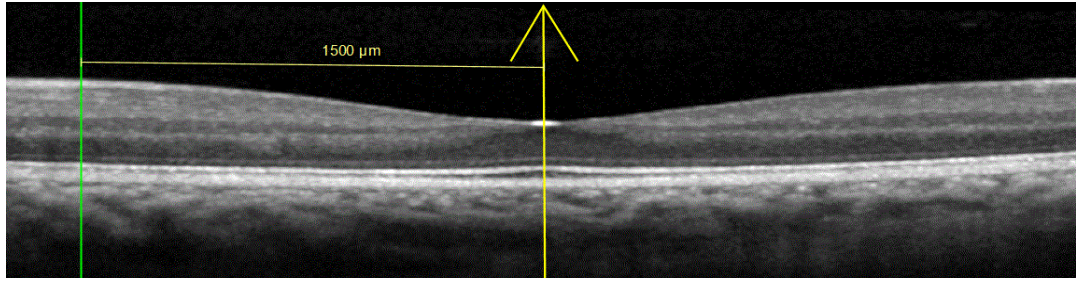
Figure 32 Positioning of software caliper for lateral retinal thickness measurement.

Using the inbuilt manual calipers, foveal width was measured in microns as the horizontal distance between foveal crests (Nolan et al., 2008, van der Veen et al., 2009c, Tick et al., 2011, Chiu et al., 2012), identified as the maximum retinal thickness nearest to the foveal reflex on the nasal and temporal side (Figure 33).
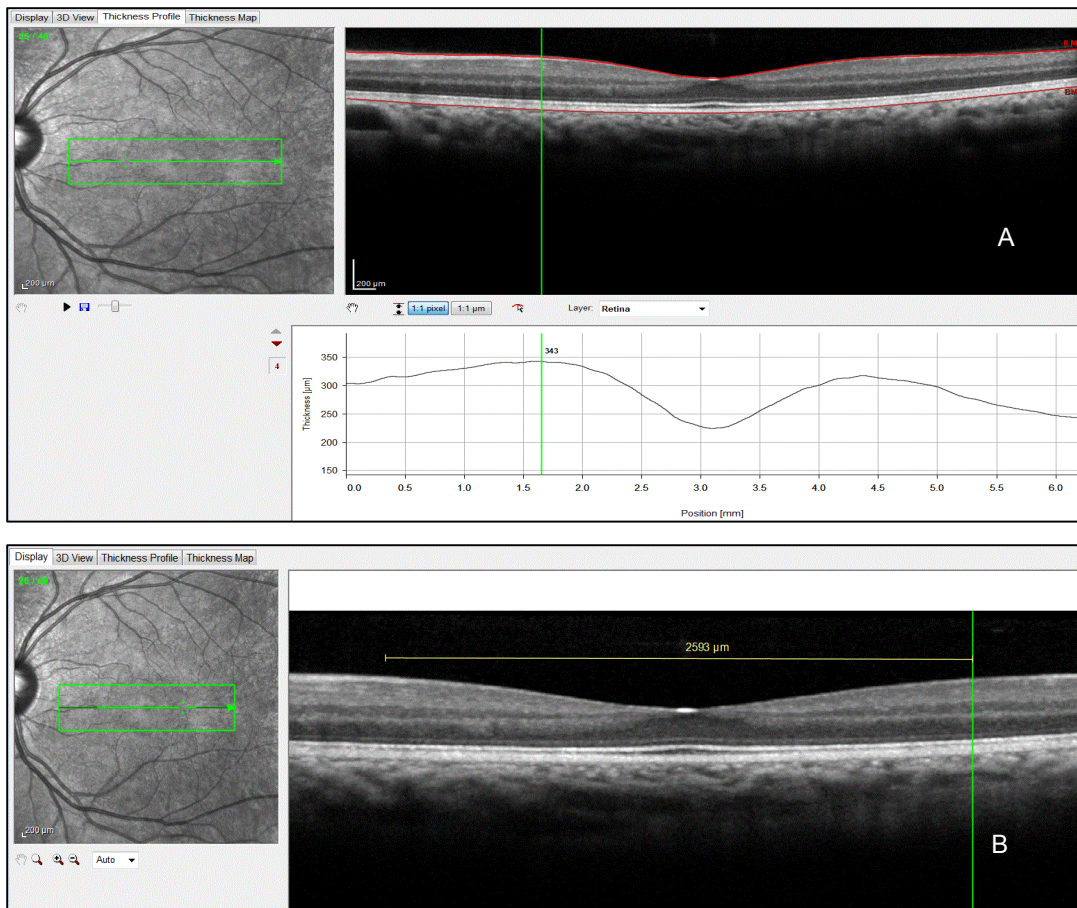
Figure 33 Measurement of foveal width. Maximum retinal thickness nearest to the foveal reflex on nasal and temporal side identified from the thickness profile. Maximum nasal thickness shown in upper image, A. Foveal width was measured in microns using the inbuilt manual calipers (B).

The Spectralis mapping software also generates automated measures of retinal thickness based on analyses of the central and inner 1000, 3000 and 6000μm subfields as defined by the Early Treatment Diabetic Retinopathy Study (ETDRS) (Early Treatment Diabetic Retinopathy Study research group, 1985). From this, the central minimum retinal thickness value was recorded as the minimum foveal thickness (MFT) for each scan. Central foveal thickness (CFT) of each retinal layer, corresponding to the average thickness of all points within the central ETDRS zone of 1000μm diameter, was also recorded.

Statistical analysis

All statistical analyses were performed using SPSS version 22.0 for Windows (SPSS Inc., Chicago, USA). Values in the text and tables are presented as the mean ± SD. Preliminary analyses were performed to ensure no violation of the assumptions of normality, linearity and homoscedasticity. Inter-investigator agreement of the thickness of each retinal layer and also foveal width measurements from the first scan (1A versus 1B) was calculated. The inter-scan CoR for the same retinal measurements taken by investigator B was also calculated (1B versus 2B). In addition, we determined the correlation of manual location of central retinal thickness (RT at 0º) and MFT using Spearman's Rank Correlation coefficient, ρ. The independent t-test was used to assess difference between nasal and temporal retinal layer thickness. Statistical significance was accepted at $P < 0.05$.

Sample size calculation

An a priori power statistics analysis was conducted using G*Power 3.1 (Faul et al., 2007, Faul et al., 2009) revealing that a total sample size of 34 subjects was required for the study. This was based on using a t-test for the difference between two dependent means (matched pairs). A power level of 80%, statistical significance level of $\alpha = 0.05$ and a moderate effect size of 0.50 were used for the calculation based on data from a previous study (Pierro et al., 2010). The aim was to recruit forty volunteers into the study to allow for unsuitable OCT scans, for example, due to poor image quality.

4.3.3   Results

The study group included forty participants (twelve males and twenty-eight females) with a mean age of 21.1 ± 3.1 years ranging from 18 to 36 years. Mean MSE was -1.70 ± 2.32DS (range -10.00DS to +0.50DS) and mean keratometry was 7.83 ± 0.30mm (range 7.16 to 9.05mm). There was no significant difference in mean image quality between scan 1 (38 ± 4dB) and scan 2 (38 ± 3dB; P = 1.00). Repeatability data (mean difference and CoR) of the thickness of individual retinal layer measurements are presented in Table 24 (inter-investigator) and Table 25 (inter-scan).

	Eccentricity from foveal centre					
	0º		2º		5º	
Retinal layer	Mean difference	CoR	Mean difference	CoR	Mean difference	CoR
Retina (total)	-0.025	0.3	-0.425	3.2	-0.075	0.5
Retinal nerve fibre layer	-0.025	0.3	0.225	3.9	-0.10	0.7
Ganglion cell layer	-0.05	0.4	-0.35	2.4	-0.025	0.3
Inner plexiform layer	0.025	0.3	-0.10	1.1	-0.025	0.3
Inner nuclear layer	0.125	1.3	-0.15	1.1	0.00	0.4
Outer plexiform layer	0.025	0.5	0.075	1.0	-0.025	0.5
Outer nuclear layer	-0.125	1.73	-0.075	2.4	0.00	0.4
Inner retinal layer	-0.025	0.7	-0.475	3.2	-0.075	0.9
Photoreceptor layer	-0.05	0.4	-0.025	1.1	0.075	0.9
Retinal pigment epithelium	0.00	0.8	0.05	1.1	0.025	0.3

Table 24 Inter-investigator agreement of thickness of retinal layers in microns. Retinal thickness refers to distance from the inner limiting membrane to the external limiting membrane. Limits of Agreement are equal to the mean difference ± Coefficient of Repeatability (CoR).

| | Eccentricity from foveal centre | | | | | | | |
| | 0º | | 2º | | 5º | | CFT | |
Retinal layer	Mean difference	CoR	Mean difference	CoR	Mean difference	CoR	Mean difference	CoR
Retina (total)	-0.35	7.4	-0.423	8.5	0.5	7.6	0.08	3.7
Retinal nerve fibre layer	0.18	3.1	0.75	8.4	-0.85	10.0	-0.05	1.6
Ganglion cell layer	-0.43	4.4	-1.00	7.1	-0.83	15.0	-0.18	1.8
Inner plexiform layer	-0.53	5.7	0.03	7.3	-0.20	9.2	-0.32	3.6
Inner nuclear layer	-0.23	5.0	0.75	9.7	0.35	14.1	-0.03	2.0
Outer plexiform layer	-0.90	8.9	-0.25	10.7	0.80	14.8	-0.2	6.0
Outer nuclear layer	1.85	14.7	0.63	13.9	-0.28	4.9	-0/05	6.9
Inner retinal layer	0.18	12.0	0.63	14.1	-0.03	8.0	-0.20	7.7
Photoreceptor layer	-0.13	13.2	0.53	12.5	1.05	7.4	0.53	4.9
Retinal pigment epithelium	0.15	11.6	0.08	8.54	0.45	4.6	0.18	2.1

Table 25 Inter-scan agreement of thickness of retinal layers in microns at 0, 2 and 5° from foveal centre. Retinal thickness refers to thickness from the inner limiting membrane to the external limiting membrane. Limits of Agreement are equal to the mean difference ± Coefficient of Repeatability (CoR).

Mean overall retinal thickness was 217 ± 16µm at 0°, 296 ± 27µm at 2° and 350 ± 16µm at 5° nasal to foveal centre, with respective CoR values of 0.3, 3.2 and 0.5µm for inter-observer and 7.4, 8.5 and 7.6µm for inter-scan agreement (Figure 34).

Mean foveal width was 2550µm ± 322µm with mean difference of 0.60µm and CoR of 13µm for inter-investigator and mean difference of -0.70µm and CoR of 40µm for inter-scan agreement. Bland-Altman plots are presented in Figure 34.
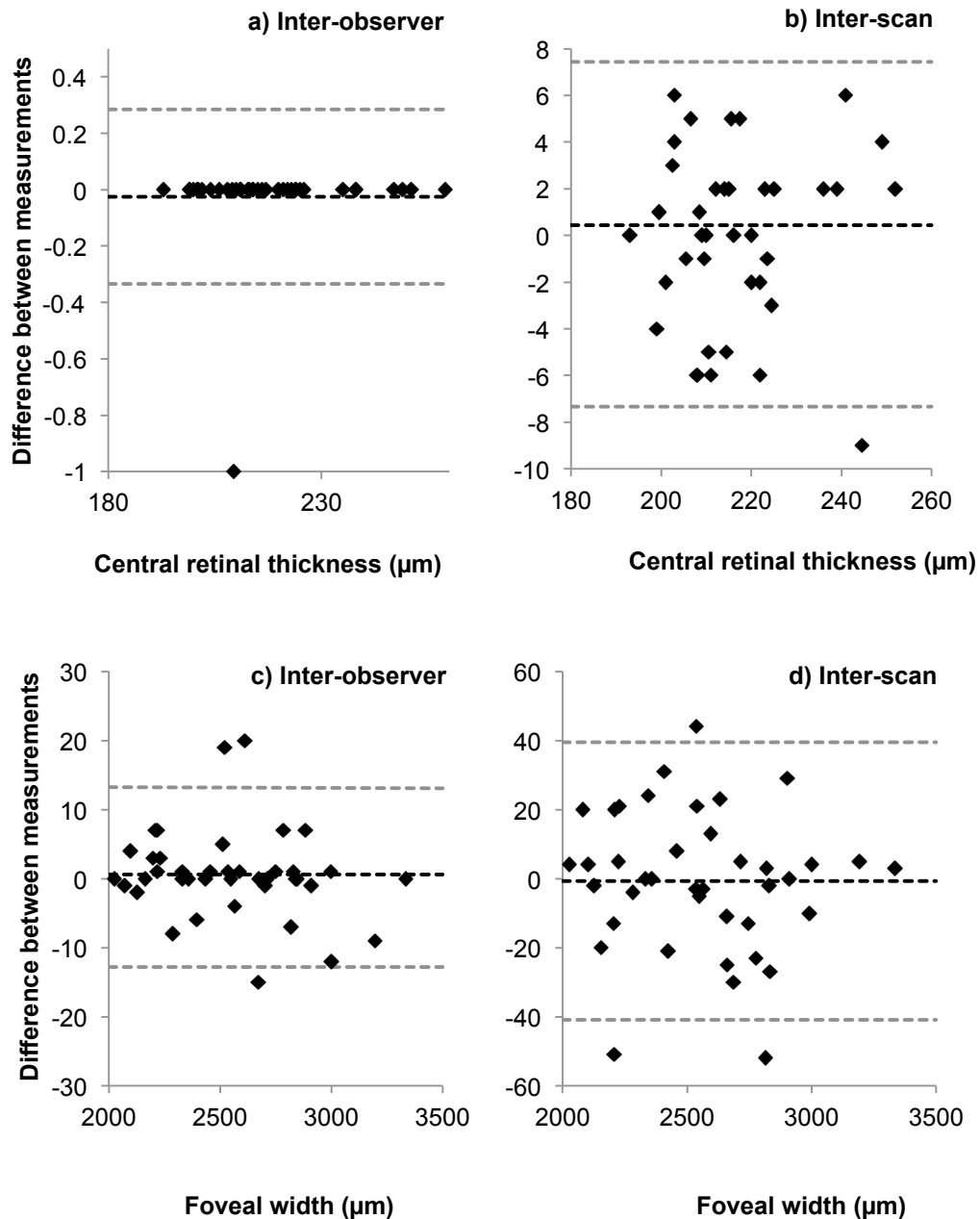
Figure 34 Bland-Altman plots to show a) Inter-observer agreement of central retinal thickness; b) Inter-scan agreement of central retinal thickness; c) Inter-observer agreement of foveal width; d) Inter-scan agreement of foveal width. All measurements presented in microns. Black dashed line indicates mean difference between values. Limits of agreement are represented by the upper and lower grey dashed lines respectively.

The automated measure of MFT showed a mean of 216 ± 15µm for the first scan and 217 ± 15µm for the repeated scan. MFT mean difference between scans was 0.33µm,

with CoR of 2.19 and LoA from -1.87 to 2.52μm. There was excellent correlation between automated MFT and the manual RT at 0° measurements taken from investigator B's analysis of the first scan (ρ = 0.97, P < 0.0005).

The mean thickness of the individual retinal layers at the foveal centre and at 2° and 5° eccentricity are given in Table 26. While there was no significant difference in thickness of all individual retinal layers at 2° nasal compared to temporal to fovea (P > 0.05) this was not true at 5° eccentricity, whereby the thickness of RT, RNFL, GCL, INL, ONL and IRL were significantly increased nasally compared to temporally.

		Eccentricity from foveal centre					
		2°			5°		
Retinal layer		**Mean**	**SD**	**P-value**	**Mean**	**SD**	**P-value**
Retina (total)	nasal	296	27	0.80	350	16	**<0.0005**
	temporal	298	19		321	14	
Retinal nerve	nasal	17	4	0.10	22	5	**<0.0005**
fibre layer	temporal	19	5		13	4	
Ganglion cell	nasal	26	9	0.99	60	5	**<0.0005**
layer	temporal	26	6		50	8	
Inner plexiform	nasal	29	7	0.23	47	5	0.15
layer	temporal	31	6		45	5	
Inner nuclear	nasal	25	7	0.06	42	5	**<0.0005**
layer	temporal	28	6		38	7	
Outer plexiform	nasal	28	7	0.97	29	5	0.84
layer	temporal	28	5		29	6	
Outer nuclear	nasal	80	12	0.43	72	9	**<0.0005**
layer	temporal	82	12		67	8	
Inner retinal	nasal	208	27	0.43	271	15	**<0.0005**
layer	temporal	212	19		241	14	
Photoreceptor	nasal	88	8	0.09	80	3	0.06
layer	temporal	85	6		79	3	
Retinal pigment	nasal	17	3	0.09	13	2	0.30
epithelium	temporal	16	3		13	2	

Table 26 Mean ±SD thickness of individual retinal layers at foveal centre and at 2° and 5° eccentricity nasal and temporal to fovea. P-value of independent t-test to investigate difference between nasal and temporal retinal thickness also presented.

4.3.4   Discussion

This study investigated Spectralis SD-OCT repeatability and reproducibility of manually derived and automated axial, as well as lateral foveal measurements in young healthy individuals. To our knowledge, this is the first report of repeatability and reproducibility of thickness measurements of each of eight individual retinal layers at the centre of the fovea as well as at two lateral positions derived using the newly available Spectralis segmentation software (version 6.0c). Manual measurements of RT at 0º (217 ± 16µm) and automated MFT (216 ± 15µm) in the current study compare well with those obtained in a study using the Spectralis OCT device in which a mean automated foveal thickness of 228 ± 11µm of forty subjects aged 19 to 50 years was reported (Carpineto et al., 2009). Our results show that inter-observer CoR values were less than 4µm for all individual layer thicknesses. The CoR values at 2° were greater than at 0° or 5° eccentricity with the greatest difference in the RT, RNFL, GCL and IRL, most likely due to software algorithm errors. Compared to inter-observer agreement, inter-scan CoR values were greater and varied across individual layers, up to a maximum of 15µm for the GCL at 5° eccentricity nasal to the foveal centre. The LoA for RT at 0º were narrower for inter-observer compared to inter-scan measurements (Figure 34). There was one outlier in each case that could not be explained. In agreement with an earlier report (Patel et al., 2008), there did not appear to be any relationship between mean central retinal thickness or foveal width and repeatability. It has been shown previously that retinal thickness measurements may be affected by OCT image quality below the acceptable range stated by the OCT manufacturer (Balasubramanian et al., 2009). This should be taken into account when examining individuals in whom the image quality is worse, for example due to cataract. Mean image quality of all scans in the current study was excellent at 38dB eliminating this source of error. We did not use the reference setting option to acquire the second scan. An earlier study showed that this is unlikely to affect the reproducibility of RNFL thickness in normal eyes (Langenegger et al., 2011); however, this should be confirmed for all retinal layers.

A strength of the present study is that all measurements were obtained from scans that had accounted for individual ocular biometry. Individual scan lengths are generated by the Spectralis software based on the subject's corneal curvature and refractive error as well as a non-modifiable pre-set axial length to minimise the effects of lateral magnification caused by the optics of the eye (Ctori et al., 2014), as described in section 4.2. While we did not perform a subjective refraction on each participant, it has

been shown that using an autorefractor to approximate refractive error is an accepted method (Pesudovs and Weisinger, 2004). In addition, optical defocus of two diopters has minimal effect on retinal thickness measurements obtained with the Spectralis (Balasubramanian et al., 2009).

It has been shown that the centre of the fovea assumed by OCT instruments and the retinal locus of fixation do not always correspond (Putnam et al., 2005, El-Ashry et al., 2008), with deviations of approximately 60 ± 50μm between fixation and the centre of the foveal avascular zone (Zeffren et al., 1990). In order to correlate some measure of visual function at fixation (e.g. visual acuity) or MP with retinal anatomy at the corresponding retinal locus, it may be more appropriate to manually locate the fixation point for foveal thickness measurements. Indeed, visual inspection of OCT images with manual identification of the foveal centre was the preferred method in a study quantifying foveal thickness and visual acuity in albinism (Mohammad et al., 2011). However, the repeatability of manually derived lateral and axial retinal measurements is less well documented: one study was based on manual measurements of a model eye (Folgar et al., 2014), while another study explored the repeatability of manual sub-foveal choroidal thickness measurements (Lee et al., 2013). We have shown excellent correlation between automated MFT and manually located RT at 0º measurements (ρ = 0.97, P < 0.0005). The low CoR values for RT at 0º (<1 μm inter-observer and <8μm inter-scan) show that the method of manually selecting the position at which to measure central retinal thickness is robust to inter-investigator and inter-scan variability. Additionally, in the current study, both investigators independently selected the same tomogram for analysis using the protocol described in the methods in all cases.

Repeatability of automated MFT and CFT has been shown to vary across OCT devices and also depend on the scan protocol employed (Eriksson and Alm, 2009). We have shown high reproducibility of automated macular thickness measurements (MFT) using the Spectralis to obtain high resolution 20° x 5° volume scans (49 B-scans 30 microns apart, ART 16 frames, 1024 A scans), indicated by the inter-scan CoR of 2.19μm. This is in accordance with a previous report in which the LoA were -2.49 to 3.77μm for inter-observer agreement of mean macular thickness measures using the Spectralis (Pierro et al., 2010). The inter-scan CoR of 3.7μm for CFT also compares well with a study in which a CoR value of 2.69μm for mean macular thickness across the central 1000μm diameter was reported using the Stratus OCT device (Polito et al., 2005). However, in an investigation involving fifty subjects with diabetic macula oedema, a higher CoR of 8.03μm was reported for Spectralis SD-OCT automated central subfield retinal

thickness measurements (Comyn et al., 2012). This suggests that ocular pathology increases the level at which true clinical change has occurred as opposed to measurement variability most likely due to fixation problems. In addition, the CoR for retinal thickness in subfields surrounding the foveal centre ranged from 3.97 to 7.23µm (Comyn et al., 2012). Caution must therefore be taken when considering the level at which clinical change is deemed to occur in individuals with retinal pathology and low vision (Comyn et al., 2012), and for retinal thickness changes occurring away from the centre of the fovea (Gilmore and Hudson, 2004).

To our knowledge there are no reports of repeatability of manually derived lateral SD-OCT scan measurements in healthy human eyes. We found a considerably large mean foveal width of 2550µm ± 322µm. Foveal pit diameters up to 2510µm have been reported using the Cirrus OCT (Wagner-Schuman et al., 2011) based on measuring the foveal pit from rim-to-rim using an automated MatLab algorithm (Dubis et al., 2009). Comparing foveal width between studies is challenging due to its variable definition. The mean foveal diameter of sixty healthy subjects was found to be 1244 ± 211µm measured between the points at which the nerve fibre layer ends, and 1371 ± 215µm when measured in the same subjects from foveal crest-to-crest (Nolan et al., 2008). Nevertheless we found a mean difference in foveal width of just 0.60µm between measurements obtained independently by the two investigators. This is much smaller than the difference of -14µm found in a study using the Cirrus OCT (Wagner-Schuman et al., 2011). Estimation of the reproducibility of lateral foveal width measurements obtained from two scans of the same participant acquired within one visit by investigator B yielded a CoR of 40µm. This relatively large inter-scan CoR should be taken into account when investigating differences in foveal diameter between individuals, or longitudinally with time. Of note, LoA were wider for inter-scan compared to inter-observer measures of foveal width. The three outliers in both cases could not be explained. Nonetheless, when investigating change over time in a clinical setting, a baseline scan image is usually set as a reference and repeated scans are subsequently compared to this. It is expected that this would improve the CoR for the lateral measurements (Fiore et al., 2015).

Few studies have quantitatively assessed both inner and outer retinal morphology of the foveal pit. An earlier study reported circular symmetry of the outer retina (from the ELM to Bruch's membrane) at low eccentricities (Srinivasan et al., 2008). Our results indicate that the individual inner and outer retinal layers are all symmetrical at low eccentricities. In contrast, at 5° eccentricity there were significant differences in

thickness of RT, RNFL, GCL, INL, ONL and IRL (Table 26). Asymmetry of the RNFL and GCL is not surprising given the distribution of the RNFL, with the thinnest peripapillary RNFL thickness found within the papillomacular bundle (Varma et al., 1996, Langenegger et al., 2011). The evaluation of inner and outer retinal layer symmetry in the current study may be useful in future investigations of foveal morphology (Matsumoto et al., 2009). Choroidal thickness (Lee et al., 2013) and the length of the photoreceptor layers (Mohammad et al., 2011) are increasingly being used as both diagnostic and visual prognostic indicators in a variety of retinal disease states such as albinism (Mohammad et al., 2011) and neuronal GCL loss has been evaluated in eyes of patients with multiple sclerosis (Saidha et al., 2011). Further work is needed however to estimate the reliability of measurements in eyes with macular pathology where poor fixation and disruptions in retinal morphology might make these measurements more variable (Meyer zu Westrup et al., 2014).

We estimated the measurement error of our manually derived axial and lateral retinal measurement methods. Measurement error may be caused by instrument and software algorithm errors as well as operator error. Our results show that manually finding the location at which to extract central retinal thickness measurements is robust to inter-investigator repeatability. We also showed good reproducibility of individual retinal layer thickness measurements obtained from two scans acquired within a single visit. The inter-investigator CoR values are actually smaller than the digital axial resolution of 3.9µm achievable with high resolution Spectralis SD-OCT (Heidelberg Engineering, 2013), indicating that there is very good repeatability of manual axial retinal thickness measurements between two observers looking at the same scan.

Conclusion

The findings show excellent repeatability and reproducibility of thickness measurements of each of eight individual retinal layers at manually derived axial and lateral foveal locations obtained using new Spectralis SD-OCT segmentation software in a young, healthy cohort. The inter-investigator CoR values for each retinal layer give the level at which thickness and foveal width variation is indicative of true difference as opposed to measurement variability (Table 24). The inter-scan CoR values signify the level at which change over time in axial and lateral measurements within an individual can be considered when the baseline reference scan feature of the Spectralis is not utilised (Table 25). The method of manually selecting the position at which to measure

central retinal thickness is robust to inter-investigator and inter-scan variability. Excellent correlation between automated and manually derived central retinal thickness measurements has been demonstrated. Additionally, the results show that the individual retinal layers are horizontally symmetrical at 2°, but not at 5° eccentricity. These findings could provide valuable information for future studies involving foveal morphology specifically examining the individual retinal layers.

4.4 The effect of ethnicity on the association between foveal morphology and macular pigment and its spatial distribution

4.4.1 Methods

OCT images were obtained from all participants included in the study described in Chapter 3, section 3.1.2. The area under the MP spatial profile curve from 0° to 3.8° was calculated i.e. MPODint (0 to 3.8), representing the total amount of MP present within the foveal pit. In addition, the slope of the MP spatial profile between 0° to 0.8°, 0.8° to 1.8° and 1.8° to 2.8° was calculated (Kirby et al., 2009).

Foveal morphology measurements

Infrared scanning laser ophthalmoscope fundus imaging and SD-OCT (Spectralis, Heidelberg Engineering, Heidelberg, Germany) imaging was performed on the test eye of each subject utilising the Automated Real Time eye-tracking feature. Mean keratometry and MSE measurements were obtained and incorporated into the Spectralis SD-OCT software as described previously (section 4.2). For each participant, a high resolution 20° x 10° volume scan (97 B-sections 30 microns apart, 16 frames including 1024 A-scans) and an additional 20° by 20° volume scan (25 B-sections, 240 microns apart, 9 frames including 512 A-scans) was acquired from the undilated test eye in a dark room (Paunescu et al., 2004, Nolan et al., 2008).

Measurements of foveal morphology were made according to the methods described in section 4.3.2 (Ctori and Huntjens, 2015). Specifically, the following foveal morphology variables were examined:

- Total, inner retinal layer and inner plexiform layer thickness at 0°, 0.8°, 1.8° and 3.8°;
- CFT corresponding to the average thickness of all points within the central ETDRS zone of 1000μm diameter;
- Total retinal volume derived from the 20° by 20° volume scan;
- Foveal width; and
- Foveal pit profile slope between 0° to 0.8°, 0.8° to 1.8° and 1.8° to 2.8° (Kirby et al., 2009).

Retinal thickness (RT and IRL) was also measured at retinal eccentricities corresponding to the locations where MPOD is measured by the MAP test i.e. 0°, 0.8°, 1.8°, 2.8° and 3.8°. The eccentricities in degrees were converted into microns based on each individual's Spectralis SD-OCT scan length as explained previously (section 4.2.2). For example, given that the scan length in microns generated by the Spectralis represents 20°, the lateral equivalent in microns of 0.8° would be given by 0.8*(scan length/20). Using the total retinal thickness values measured at 0°, 0.8° and 1.8°, the foveal pit profile slope was calculated between 0° to 0.8° and 0.8° to 1.8° ° (Kirby et al., 2009). The automated total volume measurement was also recorded from each 20° x 20° volume scan (Figure 35).
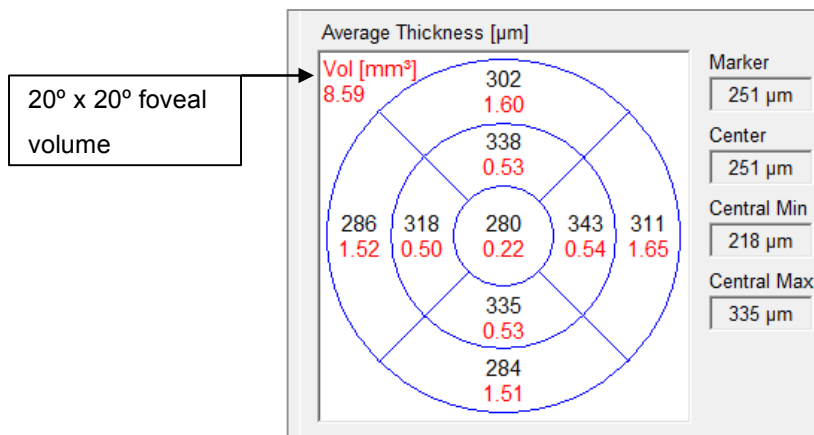
Figure 35 Screenshot of Spectralis SD-OCT thickness map to show 20° x 20° volume measurement.

Statistical analysis

All statistical analyses were performed using SPSS version 22.0 for Windows (SPSS Inc., Chicago, USA). Values in the text and tables are presented as the mean ± SD. Graphs were produced using either MS Excel or SPSS version 22. Error bars indicate the 95% confidence intervals.

Two-way ANCOVA evaluated the impact of ethnicity and gender confounders on foveal morphology parameters. One-way ANCOVA was used to explore the effect of the MP spatial profile phenotype (exponential, ring-like or central dip) on foveal parameters.

175

Adjusted mean differences with their 95% confidence intervals are provided. Unless otherwise stated bootstrapping was performed to provide robust confidence intervals. Pearson's product moment correlation coefficients were calculated to examine the association between retinal architecture parameters and MPOD measures. Preliminary analyses were performed to ensure no violation of the assumptions of normality, linearity and homoscedasticity. Statistical significance was accepted at the 95% confidence level ($P < 0.05$).

4.4.2   Results

In total, two hundred and twenty-six volunteers participated in the study, including seventy-six white, eighty South Asian and seventy black subjects. The demographics of the study sample have been presented in Chapter 3, section 3.1.3. Variations in MPOD and the MP spatial profile phenotype have also been described in Chapter 3.

Preliminary analyses

Visual graphical inspection indicated that retinal thickness measures (RT and IRL at 0º and CFT) foveal width and volume all followed a near normal distribution. Prior to investigating the variation in foveal anatomy between ethnic groups and association with MPOD, preliminary analyses were conducted to determine if there was any association of age, K, MSE and BMI with retinal thickness measures (RT and IRL at 0º and CFT) and foveal width.

The difference in age between the three ethnic groups has been described (Chapter 3, section 3.1.3). A Spearman's rank correlation analysis revealed no association between age and the foveal anatomy variables for the whole group and within each ethnic group ($P > 0.05$).

A one-way ANOVA indicated no statistically significant difference in mean K between the white (7.76 ± 0.26mm), South Asian (7.82 ± 0.25mm) and black ethnic groups (7.83 ± 0.28mm, $F_{(2)} = 1.40$, $P = 0.249$). Pearson's product moment correlation analysis indicated no association between keratometry and the foveal anatomy variables for the whole group and when tested per ethnicity ($P > 0.05$). The mean OCT scan length

generated for the entire study sample by the Spectralis SD-OCT was 6.05 ± 0.28mm, ranging from 5.1 to 7.6mm. There was no significant difference in scan length between the white (6.1 ±0.3mm), South Asian (6.1 ± 0.3mm) and black ethnic groups (6.0 ± 0.3mm, P > 0.05).

The range of MSE was -8.75 to +7.50DS in the white, -13.00 to +1.25DS in the South Asian and -7.75 to +1.75DS in the black ethnic groups. Mean MSE did not significantly vary between the three ethnic groups (Chapter 3, section 3.1.3). Spearman's rank correlation analysis for the whole group revealed no statistically significant association between MSE and the retinal thickness measures i.e. RT and IRL at 0° and CFT (P > 0.05). While this remained true for the South Asian and black ethnic groups, there was a significant weak to moderate negative correlation between MSE and retinal thickness in the white ethnic group (Table 27). A significant but weak to moderate positive correlation between MSE and foveal width was determined when the group was examined as a whole (ρ = 0.17, P = 0.01) as well as for the white and South Asian groups (Table 27). This finding was not statistically significant among the black ethnic group (ρ = 0.12, P = 0.34). Although the findings were not consistent for each ethnic group, due to the association of MSE and the foveal morphology measures, MSE was controlled for in subsequent analyses.

Partial correlation was used to explore the relationship between BMI and the foveal anatomy variables, controlling for MSE. No association between BMI and any of the foveal parameters was found when analysed for the whole group and per ethnic group (P > 0.05).

	White		**South Asian**		**Black**	
	ρ	P value	ρ	P value	ρ	P value
Retinal thickness at 0° (µm)	-0.22	0.06	-0.07	0.54	-0.02	0.86
Inner retinal layer at 0° (µm)	**-0.27**	**0.02**	0.01	0.95	-0.01	0.91
Central foveal thickness (µm)	**-0.24**	**0.04**	-0.15	0.20	-0.02	0.84
Foveal width (µm)	**0.25**	**0.03**	**0.25**	**0.02**	0.12	0.34

Table 27 Spearman's Rank Correlation Coefficient (ρ) analysis of mean spherical error with retinal thickness and foveal width. Central foveal thickness (CFT) corresponds to the average retinal thickness across the central area with diameter of 1000 microns.

Variations in foveal architecture between ethnic groups

An excellent correlation between the automated measure of MFT and the manually located RT and IRL at 0º has been demonstrated in section 4.2.3. However, the centre of the fovea assumed by OCT instruments and the retinal locus of fixation do not always correspond (Putnam et al., 2005, El-Ashry et al., 2008). For this reason, the manually located RT and IRL at 0º measurements were used for correlation with foveal morphology analysis as it was deemed to better represent fixation and therefore correspond to the location at which MP was measured at 0°.

A two way ANCOVA was conducted to investigate differences in foveal architecture between the white, South Asian and black ethnic groups and for male and female participants. The independent variables were ethnicity and gender. ANCOVA was performed using each of the following dependent variables: retinal thickness (RT at 0º, IRL at 0º and CFT) and foveal width and volume. Participants' MSE was used as the covariate in this analysis to control for individual differences. Preliminary checks were conducted to ensure that there was no violation of the assumptions of normality, linearity and homogeneity of regression slopes. Mean ± SD for foveal morphology parameters per ethnic group, per gender and for the whole group are presented in Table 28 and Table 29. Mean IRL thickness per ethnic group along with mean MPOD are presented graphically in Figure 36.

			White			South Asian			Black			Total		
				95% Confidence Interval			95% Confidence Interval			95% Confidence Interval			95% Confidence Interval	
				Lower	Upper		Lower	Upper		Lower	Upper		Lower	Upper
Retinal thickness at 0º (µm)	Male	Mean	239	230	247	223	218	228	218	211	224	226	222	230
		SD	22	14	27	15	10	18	15	11	18	19	15	23
	Female	Mean	225	221	230	218	215	222	213	209	217	219	217	222
		SD	18	13	22	14	10	18	13	10	16	16	14	18
	Total	Mean	229	225	234	220	217	223	215	212	218	222	219	224
		SD	20	16	24	14	11	17	14	12	16	17	15	19
Inner retinal thickness at 0º (µm)	Male	Mean	139	130	148	126	119	132	118	112	123	127	123	131
		SD	22	14	28	17	12	21	14	9	17	20	15	23
	Female	Mean	126	121	131	122	118	127	114	110	118	121	118	124
		SD	19	14	23	16	11	22	14	11	17	17	14	20
	Total	Mean	130	125	134	123	120	127	116	112	119	123	121	125
		SD	21	16	25	16	13	20	14	12	16	18	16	20
Central foveal thickness (µm)	Male	Mean	290	282	298	269	263	275	267	261	274	275	270	279
		SD	19	14	22	18	13	22	17	12	22	20	17	23
	Female	Mean	273	268	278	257	251	262	252	245	258	261	257	264
		SD	19	15	22	18	14	23	22	17	25	22	19	24
	Total	Mean	278	274	283	261	257	266	257	252	262	266	263	268
		SD	21	17	23	19	16	22	21	19	24	22	20	24

Table 28 Mean ± SD for retinal thickness parameters per ethnic group, per gender and for whole group.

			White			South Asian			Black			Total		
				95% Confidence Interval			95% Confidence Interval			95% Confidence Interval			95% Confidence Interval	
				Lower	Upper		Lower	Upper		Lower	Upper		Lower	Upper
Foveal	Male	Mean	2226	2116	2328	2417	2324	2514	2399	2314	2485	2354	2297	2415
width		SD	261	182	322	273	201	329	223	169	262	266	223	307
(µm)	Female	Mean	2308	2253	2362	2510	2443	2584	2477	2381	2574	2428	2382	2473
		SD	204	159	247	247	200	281	312	250	363	269	237	300
	Total	Mean	2282	2228	2334	2474	2420	2533	2449	2379	2518	2402	2363	2437
		SD	225	187	262	260	223	289	284	236	324	270	245	293
Foveal	Male	Mean	8.91	8.71	9.10	8.75	8.63	8.87	8.91	8.78	9.03	8.85	8.76	8.94
volume		SD	0.46	0.30	0.57	0.36	0.24	0.47	0.32	0.24	0.38	0.38	0.32	0.44
(μm^3)	Female	Mean	8.84	8.77	8.91	8.68	8.58	8.78	8.64	8.52	8.76	8.72	8.67	8.78
		SD	0.27	0.21	0.33	0.35	0.28	0.40	0.40	0.31	0.47	0.35	0.30	0.39
	Total	Mean	8.86	8.79	8.94	8.71	8.63	8.78	8.73	8.64	8.83	8.77	8.72	8.82
		SD	0.34	0.27	0.40	0.35	0.29	0.40	0.39	0.32	0.45	0.37	0.33	0.40

Table 29 Mean ± SD for foveal width and foveal volume (derived from 20° x 20° OCT scan) per ethnic group, per gender and for whole group.
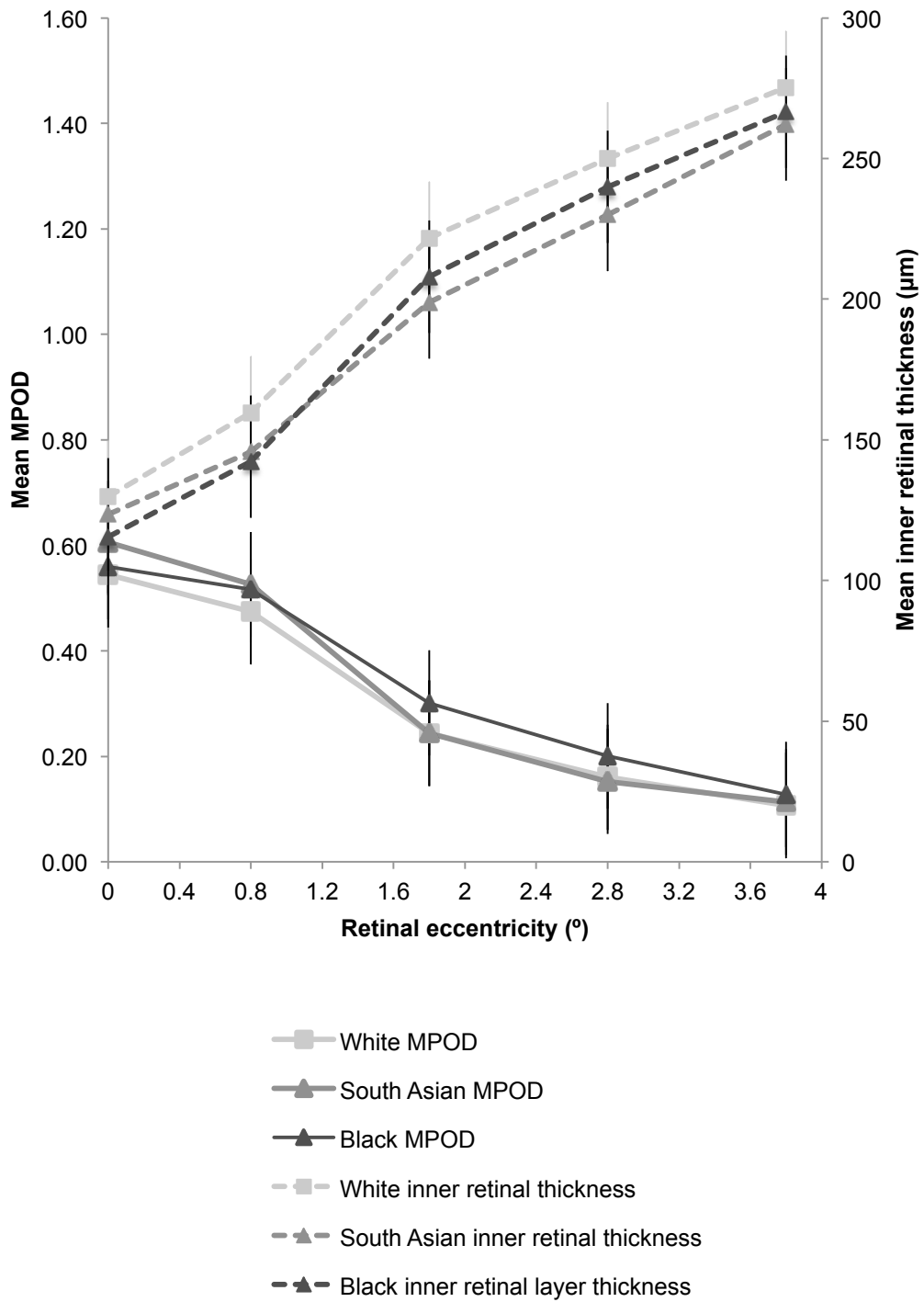
Figure 36 Graph to show variation in mean MPOD (primary y-axis) plotted against retinal eccentricity (x-axis) according to ethnicity with corresponding inner retinal thickness plotted on the secondary y-axis. Error bars indicate ±SD. Inner retinal layer thickness is significantly thinner and MPOD at 0° and 0.8° is significantly increased in South Asian and black compared to the white groups.

The results of the ANCOVA for the dependent variables RT and IRL thickness at 0º, CFT, foveal width and foveal volume, are presented in Table 30. After adjusting for MSE, there was no significant interaction effect between the independent variables ethnicity and gender. The main effects of ethnicity and gender were statistically significant for all foveal morphology dependent variables with a large effect size (partial eta squared > 0.1) for ethnicity and a smaller effect for gender. These results indicate that ethnicity explains more of the variation in foveal morphology than gender does. Post-hoc Tukey testing indicated that IRL thickness was larger in whites compared to South Asian (P = 0.009) and blacks (P = 0.001) with a trend towards a thicker IRL in males (Figure 37). These findings were replicated when the two-way ANCOVA was repeated for RT and IRL thicknesses at 0.8º and 1.8º. Foveal width was increased in South Asian (P = 0.001) and blacks (P = 0.003) compared to whites, while males had a tendency towards a narrower foveal width (Figure 38).

Dependent variable		df	F	P-value	Partial eta squared	Variance (%)
Retinal thickness at 0º (µm)	MSE	1	3.18	0.08	0.014	1.4
	Ethnicity	2	18.53	**< 0.0005**	**0.145**	**14.5**
	Gender	1	11.39	**< 0.0005**	**0.049**	**4.9**
Inner retinal thickness at 0º (µm)	MSE	1	2.68	0.10	0.012	1.2
	Ethnicity	2	14.352	**< 0.0005**	**0.116**	**11.6**
	Gender	1	7.65	**0.01**	**0.034**	**3.4**
Central foveal thickness	MSE	1	5.25	**0.02**	0.023	2.3
	Ethnicity	2	26.37	**< 0.0005**	**0.194**	**19.4**
	Gender	1	32.67	**< 0.0005**	**0.13**	**13**
Foveal width (µm)	MSE	1	10.01	**< 0.0005**	0.044	4.4
	Ethnicity	2	12.99	**< 0.0005**	**0.106**	**10.6**
	Gender	1	5.70	**0.02**	**0.025**	**2.5**
Foveal volume (µm³)	MSE	1	6.77	0.01	0.03	3.0
	Ethnicity	2	3.40	**0.04**	**0.03**	**3.0**
	Gender	1	7.73	**0.01**	**0.034**	**3.4**

Table 30 Results of two-way analysis of covariance for the independent variables: total and inner retinal layer thickness and foveal width, showing results of between-subjects effects of ethnicity and gender with mean spherical error as a covariate.
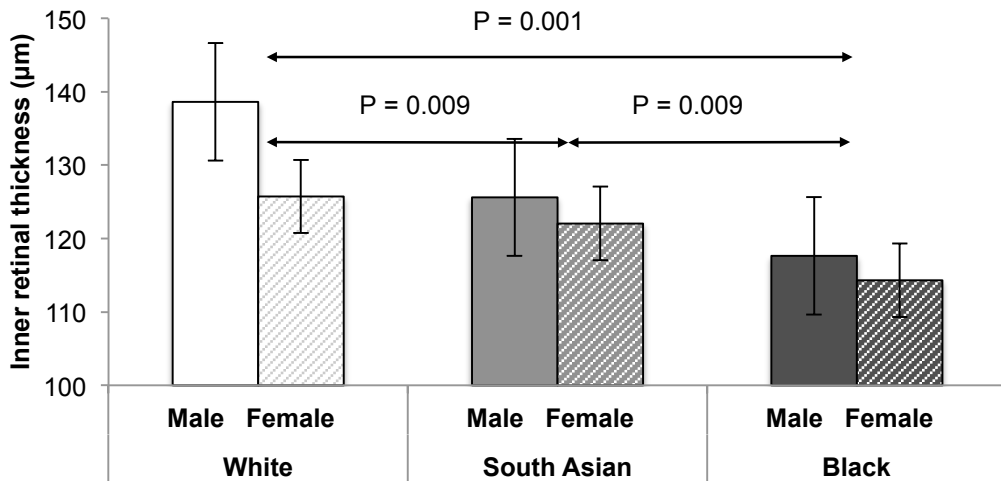
Figure 37 Bar chart to show difference in inner retinal thickness at 0° between the three ethnic groups and between males and females.
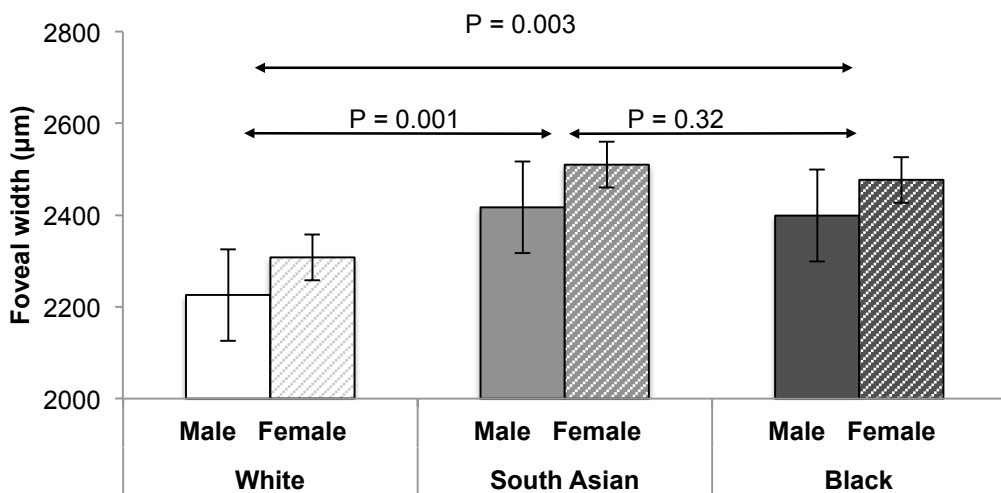
Figure 38 Bar chart to show difference in foveal width between the three ethnic groups and between males and females.

Mean ± SD values for IPL thickness at 0°, 0.8° and 1.8° for each ethnic group are provided in Table 31 and results of the ANCOVA are presented in Table 32. After adjusting for MSE, there was no significant interaction effect between the independent variables ethnicity and gender. The main effects of ethnicity and gender were statistically significant for IPL at 0°, 0.8° and 1.8°, with a small effect size (partial eta squared < 0.1) for ethnicity and gender for IPL at 0° and a larger effect size for ethnicity and gender for IPL at 0.8° and 1.8°. Males had a tendency towards thicker IPL. Post hoc analysis revealed a thicker IPL in whites compared to the South Asian and black groups (P < 0.0005).

Inner plexiform layer (µm)		White	South Asian	Black
0°	**Mean**	13	12	11
	SD	3	3	3
95% Confidence	**Lower**	12	12	11
Interval	**Upper**	13	13	12
0.8°	**Mean**	17	15	15
	SD	4	4	4
95% Confidence	**Lower**	16	14	14
Interval	**Upper**	18	16	15
1.8°	**Mean**	31	26	29
	SD	6	6	6
95% Confidence	**Lower**	30	25	28
Interval	**Upper**	33	27	30

Table 31 Inner plexiform layer thickness at 0°, 0.8° and 1.8° retinal eccentricity. Adjusted means provided.

Inner plexiform layer (µm)		df	F	P-value	Partial eta squared	Variance (%)
0°	**MSE**	1	0.62	0.43	0.003	0.3
	Ethnicity	2	5.49	**0.0005**	**0.05**	4.8
	Gender	1	8.02	**0.0050**	**0.04**	3.5
0.8°	**MSE**	1	6.55	**0.01**	**0.03**	2.9
	Ethnicity	2	13.85	**< 0.0005**	**0.11**	11.2
	Gender	1	17.19	**< 0.0005**	**0.07**	7.3
1.8°	**MSE**	1	28.93	**< 0.0005**	**0.12**	11.7
	Ethnicity	2	16.97	**< 0.0005**	**0.13**	13.4
	Gender	1	27.84	**< 0.0005**	**0.11**	11.3

Table 32 Results of two-way analysis of covariance for the independent variables: inner plexiform layer at 0°, 0.8° and 1.8° retinal eccentricity, showing tests of between-subjects effects of ethnicity and gender with mean spherical error as a covariate.

Association of MPOD with foveal architecture

The relationship between MPOD parameters and foveal morphology variables was investigated using Pearson's product moment correlation analysis. Preliminary checks

were conducted to ensure no violation of normality, linearity and homoscedasticity. Bootstrapping was performed to provide robust confidence intervals. Analyses were performed for the entire study group, followed by separate analyses based on ethnic and gender grouping. Specifically, the association between the following parameters was investigated:

- MPOD measured at single retinal eccentricities at 0°, 0.8° and 1.8° and the corresponding retinal thickness (RT and IRL and IPL);
- MPOD at 0° and foveal width;
- MPODint (0 to 1.8) and averaged retinal thickness (CFT),
- MPODint (0 to 3.8) and foveal width and volume;
- MP profile slope (0 to 0.8, 0.8 to 1.8, 1.8 to 2.8 and 2.8 to 3.8) and corresponding foveal pit profile slope.

The decision to explore the association between MPODint (0 to 1.8) and CFT was based on the following rationale: the CFT is a measure of the averaged retinal thickness across an area of diameter 1000µm. On average, 1.8° retinal eccentricity represented 545 ± 25µm; hence MPODint (0 to 1.8) represents approximately the same lateral extent. Similarly, 3.8° represented on average 1150 ± 52µm (around half the mean foveal width). For this reason the correlation between MPODint (0 to 3.8) and foveal width was explored. Furthermore, as MPODint (0 to 3.8) represents the overall amount of MP present (since MPOD is negligible at around 4° as demonstrated in Chapter 2, section 2.1.3), its correlation with the foveal volume as captured by the ETDRS grid covering an area of 20° x 20° was investigated.

Results of the Pearson product moment correlation analyses for MPOD and retinal thickness at 0° for each ethnic group are presented in Table 33. For whole group analysis, there was no association between MPOD and total retinal thickness at 0° (r = 0.12, P = 0.07). Although statistically significant, the correlation between MPOD and inner retinal thickness at 0° was weak (r = 0.18, P = 0.01). The strength of this association increased following separate ethnic group analysis (Figure 39). When the correlation analysis was repeated per gender grouping, there was no statistically significant correlation between MPOD and retinal thickness (total and inner retinal layers) at 0° for the male group (P > 0.05). On the other hand there was a statistically significant positive correlation between MPOD and IRL at 0° for the female group (r = 0.22, P = 0.007). There were no statistically significant correlations between MPOD at 0.8° and 1.8° and corresponding retinal thickness (RT and IRL) for whole group, ethnic

group and gender analysis (P > 0.05). No relationship between MPOD at 0º, 0.8º and 1.8º and corresponding IPL thickness was found for whole group and per gender analysis.

		RT at 0º	IRL at 0º	Foveal width
White	Pearson's r	0.16	**0.24**	0.05
	P-value	0.16	**0.03**	0.64
	Lower	-0.03	0.07	-0.19
	Upper	0.35	0.43	0.26
South Asian	Pearson's r	**0.23**	**0.23**	0.07
	P-value	**0.04**	**0.04**	0.55
	Lower	0.04	0.04	-0.10
	Upper	0.42	0.43	0.25
Black	Pearson's r	**0.34**	**0.38**	-0.10
	P-value	**0.004**	**0.001**	0.43
	Lower	0.11	0.16	-0.33
	Upper	0.52	0.56	0.12

Table 33 Correlation of MPOD at 0º with total and inner layer thickness at 0º and foveal width for each of the three ethnic groups. Lower and upper 95% bootstrapped confidence intervals are given.
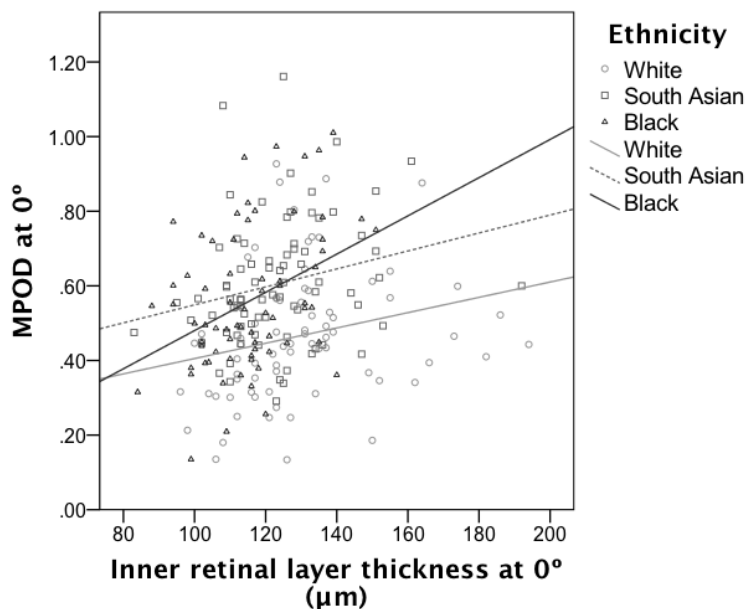
Figure 39 Scatterplot to show association of MPOD at 0º with inner retinal layer thickness at the corresponding retinal eccentricity per ethnic group.

There were no significant correlations between MPOD at 0° and foveal width when analysed for the whole sample, per ethnic group and per gender grouping (P > 0.05). Likewise, MPODint (0 to 1.8) was not related to CFT for whole group, per ethnic group and per gender group analysis (P > 0.05).

A weak positive but nonetheless statistically significant association between MPODint (0 to 3.8) and foveal width was determined for whole group analysis (r = 0.18, P = 0.008). This finding was not replicated when the analysis was repeated per ethnic group or per gender. No relationship between MPODint (0 to 3.8) and foveal volume was established in any case. In addition there were no significant associations between the MP profile slope (0 to 0.8, 0.8 to 1.8, 1.8 to 2.8 and 2.8 to 3.8) and corresponding foveal pit profile slope when the group was analysed as a whole, per ethnic group or by gender (P > 0.05).

Variations in foveal anatomy according to MP spatial profile phenotype

A one-way ANCOVA was performed to investigate whether foveal morphology measures varied according to MP spatial profile phenotype while controlling for MSE. There was no significant difference in retinal thickness (RT, IRL and IPL at 0°, 0.8° and 1.8°) (P> 0.05 for all). The lack of difference in IRL thickness between the three MP profile groups, in contrast to the significant variation in MPOD at 0° and 0.8° (P > 0.0005), is presented graphically in Figure 40. On the other hand foveal width was significantly increased in the ring-like MP profile group (2516 ± 295µm) compared to exponential (2389 ± 267 µm) and central dip profiles (2364 ± 270 µm) F(2) = 4.28, P = 0.015 (adjusted means provided). However, the effect size was small as indicated by a partial eta squared of 0.037. No difference in foveal volume was found between the three spatial profile groups (P = 0.78).
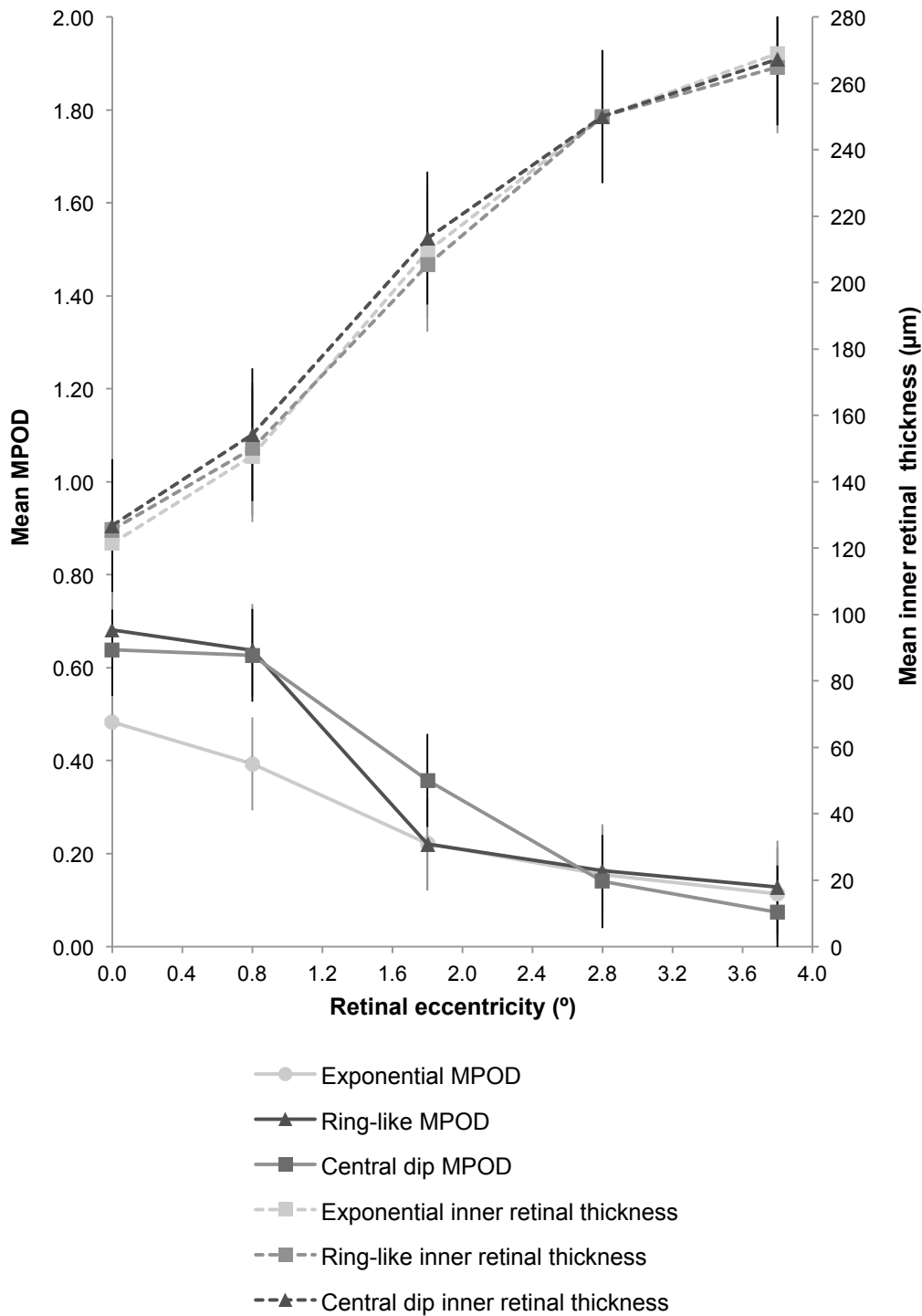
Figure 40 Graph to show variation in mean MPOD (primary y-axis) plotted against retinal eccentricity (x-axis) according to spatial profile phenotype with corresponding inner retinal thickness plotted on the secondary y-axis. Error bars indicate ±SD. Although MPOD at 0° and 0.8° is increased in the ring-like and central dip compared to the exponential spatial profile groups, there is no significant difference in inner retinal layer thickness between the groups.

Investigation of the association between MPOD parameters and foveal anatomy variables was repeated but this time the data was analysed per MP spatial profile grouping i.e. exponential, ring-like and central dip. There was a statistically significant moderate positive correlation between MPOD and total RT at 0° (r = 0.33, P = 0.04) and IRL at 0° (r = 0.42, P = 0.007) for the central dip group only (Figure 41). There were no other significant associations between MPOD at 0°, 0.8° and 1.8° and corresponding retinal thickness measures (RT, IRL and IPL).
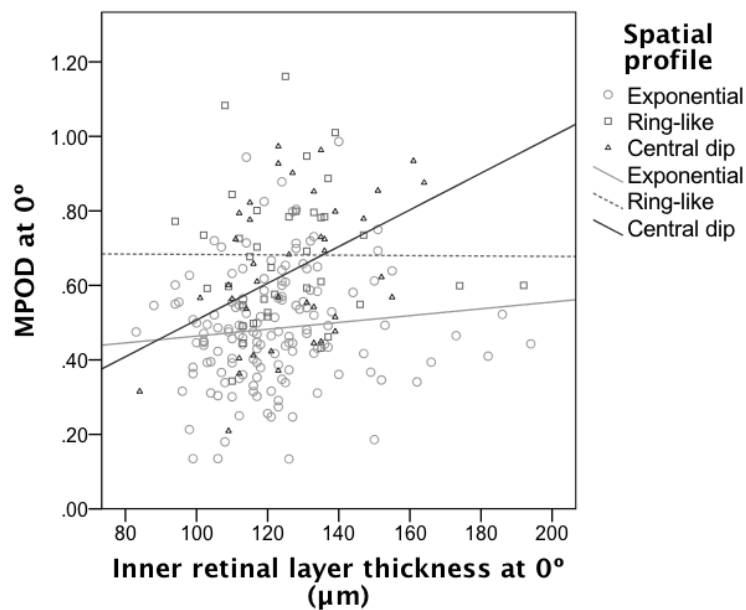
Figure 41 Scatterplot to show association of MPOD at 0° with inner retinal layer thickness at the corresponding retinal eccentricity per MP spatial profile phenotype group.

The following correlation analyses per MP spatial profile phenotype group revealed no significant associations (P > 0.05): MPOD at 0° and foveal width; MPODint (0 to 1.8) and averaged retinal thickness (CFT); and MPODint (0 to 3.8) foveal width and volume. There was a statistically significant moderate negative association between the MP profile slope and corresponding foveal pit profile slope between 0.8° to 1.8° (r = -0.4, P = 0.01), 1.8° to 2.8° (r = -0.33, P = 0.01) and 2.8) to 3.8° (r = -0.35, P = 0.01) for the central dip group only (Figure 42). This result indicates that a steeper decline in MPOD is associated with a shallower i.e. flatter foveal pit gradient for the central dip profile group (presented graphically in Figure 43).

189
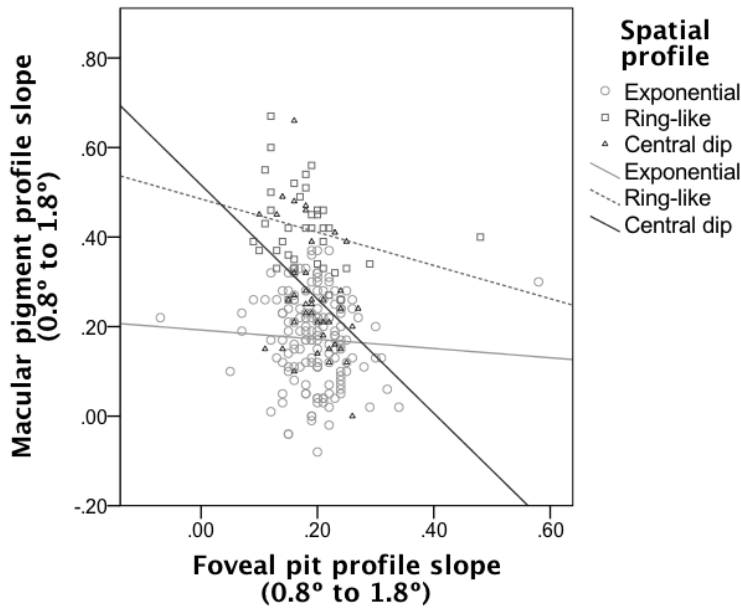
Figure 42 Scatterplot to show relationship between the macular pigment profile slope from 0.8° to 1.8° and corresponding foveal pit profile slope.
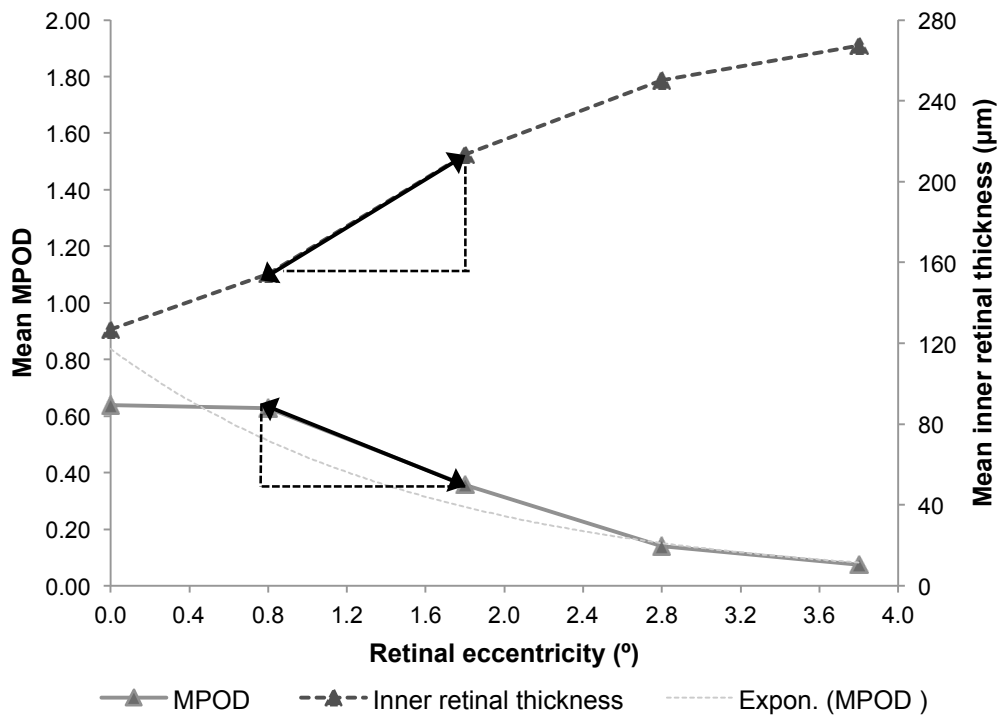
Figure 43 Mean MPOD with corresponding inner retinal thickness for the central dip profile group. The foveal pit profile slope and macular pigment profile slope from 0.8° to 1.8° is represented by the black arrows. A steeper decline in MPOD was associated with a shallower incline in inner retinal thickness from 0.8° to 1.8° retinal eccentricities for the central dip group.

Due to the apparent association between MPOD and retinal thickness at 0º in the central dip profile group the correlation analysis was conducted again but with the data split by ethnicity and MP spatial profile grouping. A Bonferroni correction was applied and significance was accepted at the P < 0.0157 level. A trend towards a strong positive correlation between MPOD at 0º and total retinal thickness at 0º (r = 0.79, P = 0.002) and inner retinal layer thickness at 0º (r = 0.70, P = 0.011) was evident in the South Asian central dip group, although this was based on twelve individuals. There were no other significant correlations.

4.4.3   Discussion

The study was conducted to investigate the relationship of MP parameters with foveal architecture between young healthy white, South Asian and black subjects. Variations in foveal morphology between the three ethnic groups were explored in the first instance. Age, corneal curvature and BMI had no significant effect on central retinal thickness or foveal width (P > 0.05). As MSE had a moderate negative association with IRL at 0º in the white ethnic group (ρ = -0.27, P = 0.02) it was controlled for in subsequent analyses. The results show that retinal thickness varied significantly with ethnicity and with gender. Around 12% of the variation in IRL thickness and 15% of the variation in RT was explained by ethnicity, while gender explained 3% of the variation in IRL thickness and 5% of the variation in RT. In the current investigation, South Asian and black subjects presented with a significantly thinner central retina (RT, IRL and CFT) compared to whites (P < 0.0005) (Table 28). This compares well with a recent study in which South Asian individuals had a significantly thinner central fovea compared to whites (243 ± 21µm vs. 250 ± 20µm, P = 0.04) (Pilat et al., 2014). A difference in central retinal thickness has also been confirmed comparing white and black ethnicities, in which African Caribbean subjects presented a thinner central retina (Asefzadeh et al., 2007, Kelty et al., 2008, Kashani et al., 2010, Girkin et al., 2011). This suggests that ethnicity may play a role in this aspect of foveal architecture. Whilst we found no significant difference in central retinal thickness between the South Asian and black ethnic groups, previous reports have suggested that macular thickness was significantly higher in white (273 ± 21µm, n = 28) and Asian subjects (280 ± 27µm, n = 11) as compared with black subjects (257 ± 17µm, n = 11, P = 0.007) (Grover et al., 2009). The difference in findings may be due to the limited sample size in the latter study. Of note, it has previously been reported that central retinal thickness is affected

by axial length (Wong et al., 2005, Tariq et al., 2010). However, this finding is inconsistent as no significant difference in macular thickness was found between low, mild and high myopic and emmetropic eyes (Wakitani et al., 2003, Kelty et al., 2008). Whilst we did not measure axial length, the three subject groups were matched for refractive error, thus minimising any potential influence. Of note, the findings of a mean CFT (278 ± 21μm) for the white ethnic group compares well with studies including similar cohorts using the Spectralis SD-OCT instrument (Grover et al., 2009), but are greater than reported by other researchers in which other TD-OCT instruments were employed (Liew et al., 2006, Kanis et al., 2007, van der Veen et al., 2009c). This variation is easily explained by the different retinal boundaries used by the inbuilt software to calculate these values (Grover et al., 2010), indicating that caution must be exercised when comparing absolute measurements between studies that have used different OCT instruments.

Foveal width presented significant variations between the white and non-white ethnic groups (P < 0.0005) as presented in Table 29. Mean foveal width was 2282 ± 204μm in white, 2474 ± 260μm in South Asian and 2449 ± 284μm in black individuals. The lack of consensus for a method for foveal width measurement makes direct comparisons of absolute measurements between studies difficult. Foveal width values for the white ethnic group reported in the current study are considerably wider in comparison to previous studies of white individuals in which values of 1402 ± 146μm for crest-to-crest (van der Veen et al., 2009c) and 1572 ± 381μm for nerve fibre layer-to-nerve fibre layer methods (Kirby et al., 2009) obtained with TD-OCT. However, our results compare well with a more recent study in which the foveal center was also identified as the deepest point of the foveal pit containing the central light reflex and foveal width was derived using the crest-to-crest method with the Spectralis SD-OCT, giving an average foveal width of 2474 ± 243μm based on forty-eight white and nine black individuals (Tick et al., 2011). The latter study included individuals aged 18 to 45 years and in agreement with the present findings, foveal width was found to be 21% wider in nine Afro-Caribbean subjects compared to forty-eight Europeans (P < 0.001) (Tick et al., 2011). A wider foveal pit diameter in Afro-Caribbean individuals (2070 ± 220μm, n = 30) compared to Caucasians (1880 ± 160μm; n = 30, P < 0.0001) has been found by other research groups (Wagner-Schuman et al., 2011), further suggesting there may be ethnicity related differences in foveal morphology. It is worth mentioning that foveal pit diameter is negatively correlated with axial length (r = -0.33, P < 0.001) (Tick et al., 2011); however, while scans were obtained using the Spectralis SD-OCT it does not seem that individual keratometry readings were included during image acquisition. It is

possible that the finding of an association between foveal width and axial length was confounded by the effect of ocular magnification that had not been accounted for. The effects of ocular magnification were minimised in the current study by incorporating each subject's K values into the OCT scan set-up (Ctori et al., 2014). Furthermore, although axial length was not measured, the three ethnic groups had similar refractive states thus minimizing this potential effect. To our knowledge this is the first report of increased foveal width in individuals of South Asian descent. Our results are in accordance with previous studies that have shown that overall foveal morphology varies with fundus pigmentation (Tick et al., 2011, Wagner-Schuman et al., 2011).

The effect of ethnicity, gender and MP spatial profile type on the relationship between MPOD and foveal morphology measures including retinal thickness, foveal width and foveal pit profile slope was investigated. No significant relationships were found with the exception of MPOD at 0° and corresponding retinal thickness. A significant positive association between MPOD at 0° and total retinal thickness at 0° was determined, but this was only present in the South Asian (r = 0.23) and black ethnic group (r = 0.34, P = 0.004) (Table 33). This is in agreement with the work by Nolan et al. (2008) whereby a lack of association between MPOD at 0.25° (measured by HFP) and averaged central foveal thickness in white subjects, but a positive and significant relationship in a non-white sample including South Asian, black and Hispanic subjects (r = 0.59, P < 0.01; n = 18) was found. However other studies have reported inconsistent findings. A positive correlation between central MPOD and central foveal thickness was demonstrated (van der Veen et al., 2009c), whereas others have found no relationship even when taking ethnicity into account (Kanis et al., 2007, Kirby et al., 2009, van der Veen et al., 2009c). In contrast a statistically significant negative correlation between central retinal thickness and MPOD at 0.5° (measured by HFP) was determined in a young healthy Caucasian cohort (r = -0.39, P = 0.01) (Kyle-Little et al., 2014).

The controversy surrounding the association of MPOD at 0° with corresponding retinal thickness may be due to the location of MP in the inner retina. It is conceivable that any relationship that may exist between MPOD and retinal thickness is merely due to variations in inner retinal thickness. Given the hypothesis that MP is associated with the Müller cell cone (Gass, 1999), an inverted conical area of Müller cells, it is reasonable to explore the association of MPOD with the thickness of the inner retinal layers in which Müller cells are located. For this reason an analysis to consider the association of MPOD and the inner retinal layer thickness at 0° was conducted. A weak to moderate positive relationship between MPOD and IRL at 0° was demonstrated

among the white (r = 0.24, P = 0.03), South Asian (r = 0.23, P = 0.04) and black ethnic groups (r= 0.38, P = 0.001) (Table 33). This finding may actually explain the inconsistency in previous reports, as it is possible that variations in total retinal thickness off set any underlying association. Since MP has specifically been identified in the IPL according to histology reports, the association of MPOD from 0º to 1.8º with the corresponding thickness of the IPL was analysed. However, no association was evident for whole group, per ethnic or gender group testing. It seems there is no immediate link between increased MPOD and increased thickness of the IPL. What is more, our results showed that the non-white ethnic groups presented with thinner total foveal thickness as well as inner retinal layer thickness along with increased central and integrated MPOD. One might have therefore expected to find a negative association between the two parameters and not a positive association. There are two possible explanations for this. One is that the Müller cell cone is thicker or denser in non-whites, despite an overall thinner inner retinal layer. The second explanation is that the relationship between MPOD and corresponding retinal thickness may be governed by the overall shape or profile of the foveal dip created by thickness of the individual retinal layers beyond the foveola towards 2° eccentricity. However, this does not appear to be straightforward. Recently, significantly thinner inner retinal layers in the central retina were found to be associated with increased MPOD at 1° and 2°, while there was no correlation with central MPOD (Meyer zu Westrup et al., 2014). This finding could not be confirmed in the present study. Further to this, the non-white ethnic groups presented with significantly increased foveal width and central and integrated MPOD. However, the hypothesis that a wider fovea is associated with increased MPOD was not supported by the study findings. In addition no association between measurements of foveal morphology (thickness and width and volume) and integrated measures of MPOD could be demonstrated.

The spatial density distribution of MP was also found to vary among the ethnic groups as described in Chapter 3. However, in agreement with an earlier investigation (Kirby et al., 2009), we found no significant variation in total or inner retinal thickness at 0º and 0.8º between subjects with exponential, ring-like or central dip MP spatial profiles. This suggests that increased retinal thickness is not responsible for the increased MPOD at 0° and 0.8° demonstrated in subjects with non-exponential MP spatial profiles. Inter-individual variations in the size and shape of the Müller cell cone may better explain the variations in MP distribution profiles. Indeed it has been postulated that the spatial arrangement of MPOD is created by the superimposition of the Henle fibre layer and the Müller cell cone (Meyer zu Westrup et al., 2014). It is possible that a

monotonic decline of MP is due to a continuum of these structures whereby there is no superimposition of the Henle fibre layer and the Müller cell cone. Non-exponential profiles may be a result of increased Müller cell cone thickness alone and a ring-like structure could be due to overlapping of the two structures.

Regarding the overall shape of the foveal pit, few studies have investigated the correlation between the gradient of the MP and foveal pit profiles. While not statistically significant, a positive trend between the slopes from 0.25° to 0.5° retinal eccentricity (r = 0.303, P = 0.25) was found by Kirby et al. (2009) involving sixteen individuals. In addition, a significant positive correlation between the MP and foveal pit profile slope (r = 0.821, P = 0.023) was determined in seven individuals presenting with a ring-like MP spatial profile (Kirby et al., 2009). In contrast, a relationship was not established in a recent study of seventy-nine individuals (Meyer zu Westrup et al., 2014). However the sample cohort, that included participants diagnosed with early AMD and an average age of 78 years, was dissimilar to the current study (healthy eyes) which may explain the contrasting findings. The authors did indeed comment that interpretation of OCT images was complicated by the presence of early AMD and caused problems regarding foveal morphology measurements, such as identification of the foveal rim. In the present study, no correlation between the MP profile slope and corresponding foveal pit profile slope was present for whole, ethnic and gender group testing. Interestingly, a significant negative association was revealed for the central dip group. Although the correlation was not strong, this finding suggests that a steeper decline in MPOD is associated with a shallower incline in the foveal pit profile slope.

A more complex foveal model is warranted to reveal subtle variations that exist between individuals. A recent study described the application of a detailed mathematical model of the foveal pit, based on OCT data (Ding et al., 2014). The fovea was reconstructed using MATLAB (The MathWorks, Inc. Natick, MA) tools based on the difference between a Gaussian and a polynomial fitting to the data. Following on from the work by Ding and colleagues (2014), it would be of great interest to apply sophisticated foveal pit modelling to the current data to evaluate the sensitivity of the model to population demographic differences. In addition, applying a similar approach to MPOD data would potentially enable analysis of the association between foveal structure and MP spatial distribution in a three-dimensional environment. Perhaps a "non-exponential" foveal model promotes non-exponential MP spatial profiles.

Our results imply that ethnic variations in MPOD and the different spatial distributions of MP cannot be explained by the differences observed in foveal morphology. That said, it is important to bear in mind that imaging of the retinal layers by SD-OCT is based on the optical properties of retinal tissue and the inbuilt algorithm to identify each layer. It has been proposed that the anatomical structures attributed to some of the hyper reflective bands may be incorrect and also may vary between devices (Spaide and Curcio, 2011). Furthermore, not all retinal layers identified by histological studies are distinguishable on SD-OCT images. The layer of Henle (the axons of the photoreceptor nuclei) has been visualised in vitro by histological examination (Hendrickson, 1992, Hendrickson et al., 2012). However, it cannot be delineated by standard SD-OCT imaging although a novel approach to achieve this has been described involving directionally altering the entry position of the SD-OCT beam through the subject's pupil (Lujan et al., 2011, Lujan et al., 2015). Given that this is the layer in which MP is at maximum concentration within the foveola (Chapter 1, section 1.1.2) it is simply not possible to measure variations of this layer in vivo by standard SD-OCT techniques. This in turn may explain the seeming lack of association of MP with foveal morphology.

Conclusion

This is the first study to consider the effect of ethnicity, gender and MP spatial profiles on the association between MP and its spatial density distribution and foveal morphology. In this study, South Asian and black individuals presented with higher MPOD at 0°, thinner central retinas and wider foveas compared to white individuals. If an increased MPOD at 0° was associated with increased retinal thickness then one would expect that relationship to be consistent across the three ethnic groups and for the group as a whole. This was not the case and the association between MPOD and IRL at 0° was actually stronger when the sample was analysed by ethnic grouping. Furthermore, in contrast to previous reports, a wider fovea was not associated with increased MPOD. Additionally, increased MPOD at 0.8° in ring-like profiles did not appear to be related to increased retinal thickness at the corresponding location. The results suggest that the spatial density distribution of MP is not a direct function of foveal morphology as measured in vivo by SD-OCT methods, but rather a feature of an individual's genetic makeup.

5 Conclusion

5.1   Conclusion

The main study in this thesis was a cross-sectional descriptive investigation of MP spatial density distribution and its relation to foveal morphology among three ethnic groups. The major findings of this work are summarised below:

- Deviations away from an exponential decline in MPOD from the centre of the fovea are real and reproducible;

- Applying the proposed objective classification method provides a reliable method of MP spatial profiling that is robust to test re-test variability when MPOD measurements are obtained using a HFP based method. However, it seems that central dips are not identified when applying this objective classification method to FAF imaging, most likely due to scan alignment;

- In the absence of a universal classification method that can be applied to all techniques of measuring MPOD we recommend that an integrated value of MPOD be reported;

- The amount of MP over the central retina area varies between different ethnic groups. Integrated measures of MP represented by MPODav and MPODint, as well as single central MPOD measurements were significantly increased in South Asian and black compared with white subjects;

- Non-exponential MP profiles were significantly more prevalent in South Asian and black compared with white subjects; a ring-like profile occurred more frequently in South Asians and a central dip was significantly increased in the black group. Integrated MPOD up to 1.8° was significantly increased in ring-like and central dip compared with an exponential profile, irrespective of ethnicity. This suggests that similar to the ring-like MP structure, a central dip represents enhanced retinal protection from harmful blue light;

- The effect of ocular magnification on scan length appears to be better accounted for when an individual's mean-K value is incorporated into the Spectralis SD-OCT software prior to imaging as opposed to using the device's default setting.

Performing scan acquisition using the subject's measured mean K value and the fundus image focussed according to their MSE is therefore recommended;

- We show excellent repeatability and reproducibility of thickness measurements of each of eight individual retinal layers at manually derived axial and lateral foveal locations obtained using new Spectralis SD-OCT segmentation software (version 6.0c) in a young, healthy cohort;

- South Asian and black individuals presented thinner central retinas and wider foveas compared to white individuals. However, foveal architecture provided no predictive values for the MP spatial profile while accounting for ethnic variations in retinal anatomy; and

- While non-exponential profiles were more common in the non-white ethnic groups, foveal architecture did not provide predictive values for these MP spatial profiles or indeed the average or integrated amounts of MP. The results suggest that the spatial density distribution of MP is not a direct function of foveal morphology as measured in vivo by SD-OCT methods.

In Chapter 2 it was shown that while several studies have reported on the different spatial profile phenotypes of MP, there is little agreement as to the definition of non-exponential profiles. Additionally, various methodologies are used to measure MPOD and consequently results are not easily interchangeable. Nevertheless, non-exponential profiles have previously been defined as those not exhibiting a typical exponential profile, but showing either: an annulus of higher MPOD described as a ring-like structure, where the central peak is surrounded by a ring of increased density (Dietzel et al., 2011b); or a central dip defined as MPOD at 0.25º not exceeding MPOD at 0.5º (Kirby et al., 2009, Nolan et al., 2012a); or a lack of central peak defined as a negative deviation from the expected exponential fit (Huntjens et al., 2014). The common theme to these definitions is a deviation away from the expected exponential decline. We therefore feel that the approach used in our work to classify the MP spatial profile phenotype is reasonable and allows systematic objective classification to be undertaken. The results of the preliminary study demonstrated that objective profiling is more reliable than subjective visual classification. It remains that in order for meaningful comparisons to be made between studies, a consensus for the definition and classification of the various MP spatial density presentations is required. Indeed, this was a topic of discussion at the recent Macular Carotenoids Conference (Downing

College, Cambridge, 2015) in which it was put forward that a working group be formed to agree on a unified reporting system for MPOD. Subsequently, future development of automated quantification of MP spatial profiles may serve as a potential diagnostic, prognostic and therapeutic tool for eye conditions such as AMD. Meanwhile, we recommend that integrated measures of MPODint and/or MPODav be reported in future studies to allow meaningful comparisons to be made. Both parameters were shown to be highly repeatable, despite a poor CoR for the most central MPOD values derived from FAF images. These values represent the amount of MP over a given area, for example the central 2º or 4º as opposed to a single central measurement. The advantage of reporting these values is that they can be derived from either HFP based methods or from two-wavelength FAF techniques and would enable comparison between studies that have used different MPOD measuring techniques.

In Chapter 3, MPOD parameters for three ethnic groups were compared within a single study, enabling MPOD measurements to be directly comparable. The findings showed that around 10% of the variance in the MPOD measurements was explained by ethnicity, highlighting the importance of taking ethnic background into account when reporting MPOD. To summarize, South Asians and blacks were found to have increased central MPOD as well as MPODav and MPODint over a central 2º retinal area, and an increased prevalence of non-exponential profiles. None of these findings were influenced by risk factors for AMD such as age, gender, or smoking. With regards to the MP spatial profile phenotype, the majority of ring-like profiles were found among the South Asians while central dips were significantly more common in blacks. Since "atypical" profiles may actually represent a more typical characteristic for a particular ethnic group or population, it is proposed that MP spatial profiles should not be described as typical (i.e. exponential) versus atypical as previously suggested by Berendschot and van Norren (2006) and also initially by our research group (Huntjens et al., 2014), but rather nomenclature of exponential versus non-exponential profile types be adopted instead.

A particularly interesting finding was that although around half of the black ethnic group had been born and raised in Africa or the Caribbean, there was no significant difference in any of the MPOD parameters measured between black individuals born and bread in the UK and those that had spent five or more childhood years in Africa or the Caribbean. This could imply that for the study sample there was little environmental influence on MPOD e.g. cumulative sunlight exposure. Further work is recommended to substantiate the hypothesis that MPOD does not increase in response to increased

environmental sunlight exposure, including gathering detailed information regarding sunlight exposure during childhood and adult years while taking into account the country of residence and ethnicity.

Another factor that varies according to the country of origin and residence is diet, whereby it has been shown that within Europe the specific intake of some carotenoids is related to particular foods eaten in different countries (including the UK, Republic of Ireland, Spain, France and The Netherlands) (O'Neill et al., 2001). This is of particular relevance to the present study as it has been shown that the traditional South Asian diet typically consisting of a diet rich in carotenoids may be altered after migration, particularly in young or second generation South Asians (Gilbert and Khokhar, 2008). Unfortunately dietary data was not collected for our study, which is a weakness of the investigation; future work comparing dietary data for different ethnic groups between different continents would be of great interest. However, this would require a culture specific validated food frequency questionnaire (FFQ). To the best of our knowledge, such a FFQ, specific for the three UK-based ethnic groups reported in our work (personal communication with Heather Clark of the Scottish Collaborative Group FFQ group, July 2013) have yet to be established. There is a report describing validation of a carotenoid FFQ for use in an African American population, although this was based on carotenoid content of fruits and vegetables only (Resnicow et al., 2000). An earlier study described validation of a FFQ for specific carotenoid intake among black women, but this included only six ethnic foods (Coates et al., 1991). Indeed, food composition tables contain a limited amount of ethnic food information, especially regarding complex recipes so that accurate calculation of carotenoid intake is not easily accessible (Vyas et al., 2003). A recent investigation identified the carotenoid rich foods present in a range of South Asian foods for incorporation into the UK national database (Khokhar et al., 2012). A similar study for foods consumed by other ethnicities would allow development of FFQs that could be used by multiple ethnic groups and would be of use not only to the field of MP, but also other diseases such as diabetes and cancer research.

Even though carotenoid dietary intake was not included in the study it is known that MPOD correlates with both dietary intake and blood serum levels of L and Z (Bone et al., 2000, Ciulla et al., 2001a, Nolan et al., 2007a). A genetic component has been suggested in carotenoid uptake (Hammond et al., 1995, Loane et al., 2010, Hammond et al., 2012, Hogg et al., 2012). There is evidence that carotenoid metabolism and its genetic coding plays a role in how MP is deposited in the retina (Meyers et al., 2013),

and it has been suggested that uptake and transport of L and Z may be affected by abnormalities in carotenoid metabolism (Wang et al., 2007). Moreover, variations in genetic coding for the retinal carotenoid binding proteins involved and affinity of L and Z to the lipoproteins involved in their transport may govern the delivery site for the carotenoids (Bhosale and Bernstein, 2005, Wang et al., 2007). However, the process of carotenoid metabolism is complex, involving competitive uptake of L and Z associated with beta-carotene (Fernández-García et al., 2012). In addition, the isomerisation of L to meso-Z at the centre of the fovea is a poorly understood mechanism (Bone et al., 1993, Bone et al., 1997, Nolan et al., 2013) but may be responsible for increased MPOD within the ring-like structures of MP. Such genetic factors may explain some of the variation seen between ethnic groups and warrants further investigation.

The use of self-reported ethnicity classification is a common method used in clinical studies. It has been demonstrated to yield a high correlation with genetic ancestry techniques and may have the added benefit of incorporating unknown environmental factors (Rosenberg et al., 2002). The perceived benefit of ethnicity in health research is the contribution to the understanding of the causes of disease. Notwithstanding, caution should be applied when describing results of such studies as being due to genetic factors (Bhopal and Donaldson, 1998). However, the aim of the PhD research study was to describe variations in MP profile phenotypes and potential association with foveal anatomy among different ethnic groups. Ascribing these features to genetic factors is beyond the capabilities of the research project and further studies are required to investigate the genetics that may be involved.

The hypothesis that there is a relationship between MP and its spatial density distribution and foveal anatomy was explored in Chapter 4. To our knowledge this has not been reported while taking into account the effect of ethnicity. As well as taking precautions to minimize the effect of ocular magnification (Ctori and Huntjens, 2014), our method of taking foveal measurements from Spectralis SD-OCT scans was shown to be repeatable (Ctori and Huntjens, 2015). It is known that the configuration of the foveal pit shows wide inter-individual variation among young, healthy adults. There is a structural continuum, ranging from a wide and deep foveal pit and with no obvious INL, to a shallower and narrower pit. The clinical relevance, if any, of the various configurations remains to be elucidated. Nonetheless, the present study showed that around 12% of the variation in inner retinal layer thickness and 15% of the variation in total retinal thickness was explained by ethnicity, whereby individuals of South Asian or

Afro-Caribbean descent presented with a thinner central retina than whites. There also appeared to be a gender effect in that it explained 3 to 5% of the variation, with females presenting thinner foveae than males. Similarly, foveal width significantly varied, with a narrower foveal pit diameter in white compared to non-white individuals. However, even though the spatial density distribution of MP and foveal architecture varied significantly between the ethnic groups, no consistent association between the retinal parameters measured and MPOD were established.

While our results imply that ethnic variations in MPOD and the different spatial distributions of MP cannot be explained by the differences observed in foveal morphology, imaging of the retinal layers by SD-OCT is based on the optical properties of retinal tissue and the inbuilt algorithm to identify each layer. Perhaps it is simply not possible to measure the subtle variations of the retinal layers in which MP is located in vivo by standard SD-OCT techniques. This would explain the seeming lack of association of MP with foveal morphology. As automated retinal layer algorithms improve, complex foveal modelling will become possible. This, along with objective MPOD measurement that incorporates a foveal marker would enable more sophisticated analysis of the association of MP and its spatial density distribution to be undertaken.

5.2   Future work

There are a number of possible opportunities to further extend the research presented within this thesis. Having described the presentation of MP and its spatial density distribution in young, healthy individuals of different ethnic backgrounds we recommend an investigation into ethnic variations in MP in eyes with disease. This would be of interest in subjects with AMD, in particular regarding the potential ethnic differences in manifestations of the condition such as polypoidal choroidal vasculopathy (Kawasaki et al., 2010, Laude et al., 2010). Does MP present differently in eyes with different types of AMD?

A recent study showed that macular oedema due to AMD (n = 30) or non-proliferative diabetic retinopathy (n = 21) did not appear to have any influence on maximum MPOD measured by one-wavelength FR (Thiele et al., 2015). The authors recommended follow-up measurements of MPOD in eyes with macular oedema. An extension to this work would be to analyse thickness of individual layers of the retina in eyes with macular oedema, especially since a positive correlation between MPOD and inner retinal layer thickness was demonstrated in our study. This approach could be applied to other longitudinal studies, using subjective two-wavelength FAF to measure MPOD, to address the following question: what happens to MP levels following anti-VEGF treatment for neovascular AMD?

Another eye disease that has received recent attention with regards to MP is glaucoma. There is emerging evidence that there are lower MP levels in patients with open angle glaucoma (Igras et al., 2013) and this is associated with mean deviation from the visual field analysis in glaucoma subjects i.e. individuals with global central visual field loss (Loughman, 2014). Further work to substantiate this would be of interest. Besides this, with suggestion that macular changes involving a reduced ganglion cell complex are associated with lower MPOD in patients with glaucoma (Siah et al., 2014), a longitudinal study of macular anatomy and its association with MP in glaucomatous eyes is merited. In particular, ethnicity should be taken into account given the increased prevalence of open-angle glaucoma in individuals of African descent and closed-angle glaucoma in those of Asian derivation (Quigley, 2006).

Relating the findings of the proposed studies back to visual function would be of great clinical value. According to the results of previous investigations, it is expected that visual function (as represented by high mesopic contrast acuity thresholds, contrast

sensitivity, glare disability and photostress recovery) would be significantly affected in subjects with lower MP levels (Kvansakul et al., 2006, Loughman et al., 2010, Hammond et al., 2013). In addition to assessing visual function using traditional visual acuity or contrast sensitivity tests, retinal sensitivity measurements could also be obtained with a microperimeter, especially as the technique of microperimetry has been shown to provide a reliable assessment of functional vision (Markowitz and Reyes, 2013, Hanout et al., 2015). However, baseline values for topographic macular sensitivity and correlations with ethnicity are yet to be established. We propose a study to investigate the relationship between macular sensitivity and thickness in healthy participants across ethnic groups. In addition, given that the prevalence of AMD varies significantly among ethnicities (Klein et al., 2013) we would like to investigate macular sensitivity in eyes with and without dry and wet AMD across these ethnic groups. These studies would be of value since microperimetry together with MP spatial density distribution could potentially be used as a predictor of AMD development and/or progression. Predicting those at risk of AMD will also has implications for targeting monitoring programs and for potential risk management.

Lastly, the newest area of interest regarding MP is in the field of its potential relationship with cognitive function and Alzheimer's disease. Lower levels of MP were observed in Alzheimer's patients in a recent exploratory study (Nolan et al., 2014). This finding appeared to be related to measures of visual function including best corrected visual acuity and contrast sensitivity. Following this, a randomized double blind clinical trial was conducted to investigate the potential benefit of macular carotenoid supplements on MP, vision and cognitive function. The results showed that augmentation of MP with macular carotenoid supplements (meso-Z, Z and L) lead to a clinically meaningful improvement in visual function (Nolan et al., 2015). Given our findings that MP levels do indeed vary with ethnicity and the recent report of an increased incidence of dementia in African Americans, with a 50 to 70% greater risk compared to whites and Asians (Whitmer et al., 2014), it is of great interest to investigate ethnic variations in MPOD among individuals with Alzheimer's disease.

This page is intentionally left blank

6 Appendix

6.1 Macular pigment spatial profiles in South Asian and white subjects

Macular Pigment Spatial Profiles in South Asian and White Subjects

Byki Huntjens, Tanveer Saida Asaria, Sheena Dhanani, Evgenia Konstantakopoulou, and Irene Ctori

Applied Vision Research Centre, The Henry Wellcome Laboratories for Vision Sciences, City University London, Northampton Square, London, United Kingdom

Correspondence: Byki Huntjens, Division of Optometry and Visual Science, School of Health Sciences, City University, Northampton Square, London EC1V 0HB; Byki.Huntjens.1@city.ac.uk.

PURPOSE. Variability in central macular pigment optical density (MPOD) has been reported among healthy individuals. These variations seem to be related to risk factors of AMD, such as female sex, smoking, and ethnicity. This study investigates variations in the spatial profiles of MPOD among ethnicities.

METHODS. Using heterochromatic flicker photometry (HFP), MPOD was measured at seven retinal locations in 54 healthy, young South Asian and 19 white subjects of similar age. Macular pigment spatial profiles were classified as either typical exponential, atypical ring-like, or atypical central dip.

RESULTS. Central MPOD was significantly greater in South Asian (0.56 ± 0.17) compared with white subjects (0.45 ± 0.18; $P = 0.015$). Integrated MPOD up to $1.8°$ (i.e., average MPOD [MPODav(0–1.8)]) was also significantly increased in South Asian (0.34 ± 0.09) compared to white subjects (0.27 ± 0.10; $P = 0.003$). Average MPOD(0–1.8) was significantly increased in all subjects presenting a ring-like profile (0.35 ± 0.08) or central dip profile (0.39 ± 0.09), compared with typical exponential profiles (0.28 ± 0.09; $P < 0.0005$). We found a statistically significant association between ethnicity and spatial profile type ($P = 0.008$), whereby an exponential profile was present in 79% of white compared with 41% of the South Asian subjects.

CONCLUSIONS. Central MPOD, MPODav(0–1.8), and the prevalence of atypical spatial profiles were significantly increased in South Asian compared with white subjects. Atypical profiles resulted in increased integrated MPOD up to $1.8°$, and may therefore offer enhanced macular protection from harmful blue light.

Keywords: macular pigment optical density, ethnicity, heterochromatic flicker photometry, macular pigment spatial profiles

The spatial profile of macular pigment (MP) optical density has been shown to vary considerably among subjects. The optical density of MP, measured in log units, typically peaks centrally and declines sharply with eccentricity away from the foveola.[1–3] Central MP optical density (MPOD) has been reported to be lower with age,[4] smoking,[5] in the presence of inflammation promoting conditions (e.g., diabetes),[6] in females,[7] and in the presence of light iris color.[8,9] Previous studies described MP spatial profiles with either a single peak decaying exponentially,[2,10,11] a central dip (i.e., without a central peak),[10,11] or exhibiting a secondary peak up to 2° eccentricity, also referred to as a subpeak, shoulder, bimodal, or ring-like structure.[2,10] Using psychophysical heterochromatic flicker photometry (HFP), Hammond et al.[2] found that the MP distribution of 32 Caucasian subjects was best described by an exponential fit. However, the authors also discovered that approximately 40% of subjects presented secondary subpeaks (defined as increments greater than 0.05 optical density units from the exponential fit) at 1° and 2°. More recent studies have shown similar bimodal MP spatial profiles in a significant proportion of subjects.[10,12–15] The presence of a parafoveal ring was also shown in 20% to 50% of subjects when using objective autofluorescence imaging (AFI) techniques.[10,15–17] Moreover,

using AFI, the frequency of ring-like profiles was found to be significantly greater in females and in nonsmokers,[15,16] and in healthy subjects (43%) compared with patients with age-related maculopathy (23%).[15] Similar findings have also been demonstrated in ethnicities with a low prevalence of AMD, whereby 86% of African subjects presented with secondary peaks versus 68% non-Hispanic, white subjects.[17] However, it was also suggested that the lack of a central peak could possibly have an adverse effect on the protective role of MP in AMD, as the prevalence of a central dip has been found to increase with age and smoking in Caucasian subjects.[11]

Several studies have investigated ethnic differences in central MPOD.[14,17–21] White subjects presented significantly lower mean central MPOD compared to South Asian,[18] African,[17,19] and non-white subjects, including Asian, black, and Hispanic ethnicities.[14] However, the central MPOD of white subjects did not differ greatly compared with Chinese subjects.[21] Additionally, in a study where darker iris color was linked to increased average MPOD over the central 1° area, the results implied that central MPOD was not related to ethnicity. However, possible differences in MP density due to race were minimized as only a small percentage of non-Caucasian (Asian and African American) subjects were included.[9] Published data

on MPOD variations between South Asian (from India, Pakistan, and Bangladesh) and white subjects is limited.[2,9,14,18] Using the HFP technique, Howells et al.[18] reported a significantly increased mean central MPOD in South Asian (0.43 ± 0.14 log units) versus white subjects (0.33 ± 0.13 log units; $P < 0.0005$), with increased MPOD in the Asian males compared with Asian females ($P < 0.01$). This was not true for the white subjects; while the males presented with lower central MPOD, this was not statistically significant ($P = 0.39$). Less is known about the ethnic differences in the distribution of MP away from the fovea. A study by Hammond et al.[2] found that MPOD distribution was not related to ethnicity.[9] Nolan et al.[14] also reported no association between the prevalence of a ring-like profile and ethnicity. However, both studies included limited numbers of non-White subjects (including South Asian) in comparison with the white group. To our knowledge, this is the first comparison study to investigate the prevalence of MP spatial profiles among South Asian and white subjects.

METHODS

Macular Pigment Measurements

Macular pigment optical density was assessed using a visual display unit based Macular Assessment Profile (MAP) test.[22] The MAP test uses HFP to measure MPOD at the center of the fovea ($0°$) and at six other retinal locations ($0.8°$, $1.8°$, $2.8°$, $3.8°$, $6.8°$, and $7.8°$ eccentricity from the fovea). Like other tests employing HFP techniques, the MAP test is based on the spectrally selective properties of MP. Two beams of light are produced optically by the phosphors of the MAP test display unit. The test beam is composed of short wavelength (SW) blue light, peaking at approximately 450 nm, which is maximally absorbed in the central retina by MP. The reference beam is of a longer wavelength (LW) light that is not absorbed by the MP.[23] A notch filter is used in front of the test eye to increase the separation between the test and the reference beam. When the luminance of these wavelengths is not equal, a counter phased sinusoidal pattern is produced and the stimulus appears to flicker.[1,24] A larger difference in luminance yields a stronger sensation of flicker.

The center stimulus is a disc of $0.36°$ diameter. The peripheral stimuli are sectors of an annulus, which are presented concentric to the fovea. Both the angular subtense and the width of the peripheral stimuli increase with eccentricity[22] to ensure greater flicker sensitivity in the peripheral retina. Although the test supports any selected meridian, all the measurements reported in this study were performed with the stimulus centered along the horizontal meridian. In addition, a static mirror symmetric stimulus was presented at the corresponding location in the visual field to minimize the subject's tendency to saccade to the flickering peripheral target.

During the MAP test, the luminance of the test beam is altered until the perception of flicker is canceled or minimized. In order to ascertain the range of luminance for which the perception of flicker is absent, the MAP test calculates a low and a high threshold using a double reversal technique. The average of the low and high values is computed to give the luminance of the test beam required to cancel the reference beam (the flicker null point). The test is repeated in a random order eight times (four high and four low thresholds) at each eccentricity and the average is calculated to give the mean luminance of the SW test beam required to achieve the flicker null point. Macular pigment optical density is calculated by comparing the mean luminance adjustment of this SW light in

the central retina with a reference point in the peripheral retina using the equation

$$\text{MPOD} = \log_{10}(\text{L}_i/\text{L}_o), \qquad (1)$$

where Li is the mean luminance of the SW test beam at location i and Lo is the average of the test beam luminance of the $6.8°$ and $7.8°$ peripheral locations (where MP levels are thought to be negligible[10]).

Study Protocol

The study took place at the Division of Optometry and Visual Science at City University London. Study data was collected from 54 South Asian and 19 white participants between May 2008 and November 2010. The average age of the South Asian participants was not statistically different from the average age of the white participants ($P = 0.068$). Ethnicity was self-reported as white or South Asian (born in India, Pakistan, or Bangladesh, or born in the United Kingdom (UK) from Indian, Pakistani, or Bangladeshi parents; hereafter referred to as Asian). All participants had LogMAR visual acuity greater than 0.3 log units in the eye being tested. Exclusion criteria were ocular pathology, including inflammation, AMD or cataract, (self-reported) pregnancy, current use of carotenoid supplementation, and/or medication that may affect retinal function. Participants completed a lifestyle and health questionnaire, providing information about general and ocular health, use of medication, nutritional supplementation, and smoking history. Prior to using the MAP test, each participant was given a practice run of the $0°$, $1.8°$, and $2.8°$ spatial locations. This provided a uniform introduction to the test and ensured complete dark adaptation.

Classification of MP Spatial Profiles

For each study participant, an exponential curve was fitted to the average absolute MPOD measurements at all retinal locations. The MP spatial profile presentation of each study participant was classified into typical exponential or atypical (nonexponential). The coefficient of repeatability (CoR; i.e., the average within-subject SD) was calculated from the eight repeated MPOD measurements at each eccentricity for both ethnicities. The exponential profile was classified by MPOD at $0°$, $0.8°$, and $1.8°$ being within one CoR of the value predicted by the exponential curve. All others were assumed atypical. We subclassified our atypical group into ring-like and central dip profiles. Using the method described by Hammond et al.,[2] a positive deviation greater than the MAP test CoR from the exponential curve at $0.8°$ and/or $1.8°$ was classified as a ring-like profile. A negative deviation from the exponential profile greater than the MAP test CoR from the exponential curve at $0°$ was considered to be a central dip profile (Fig. 1).[10]

Average Blue Light Transmittance (Tav) and Average MPOD (MPODav)

At each eccentricity measured by the MAP test, the transmittance (Ti) is a measure of the SW blue light-filtering capacity of the MP at location i and is given by

$$\text{T}_i = 10^{-\text{MPOD}_i}. \qquad (2)$$

The value of Ti was plotted against retinal eccentricity, and the trapezium rule was used to calculate the area under the curve (Tav), representing the integrated transmittance of the MP between eccentricities. Average blue light transmittance between $0°$ and $1.8°$ corresponding to a $3.6°$ diameter circular
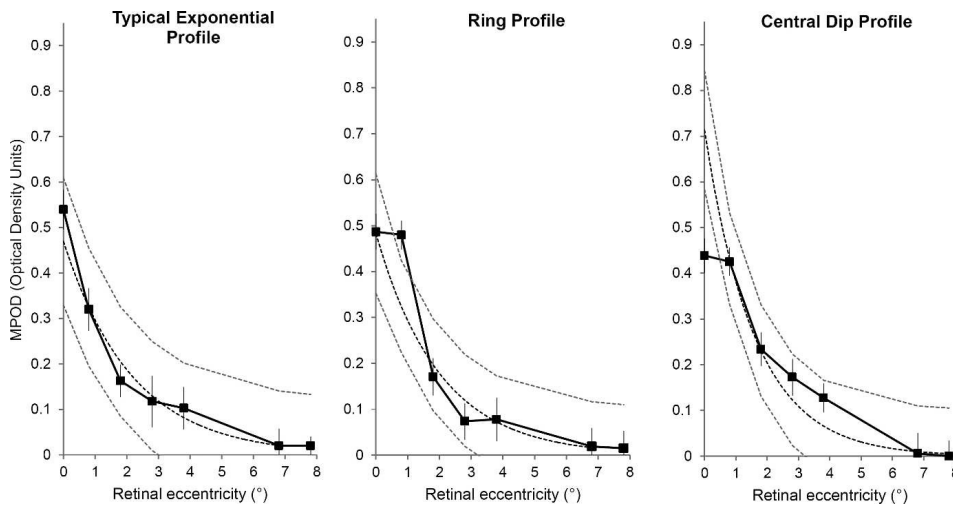
FIGURE 1. Macular pigment optical density as a function of eccentricity for three participants: examples of exponential, ring, and central dip profiles. All three graphs include the mean absolute MPOD values ± SD of eight measurements at each eccentricity. The *black dotted line* represents the exponential curve fitting to the mean absolute MPOD values. The *gray dashed lines* represent the MAP test measurement error according to the subject's ethnicity at each eccentricity from the exponential curve. Note the MPOD at 0.8° in the ring-like profile presents more than one coefficient of repeatability (CoR) above the expected exponential curve at 0.8°. The MPOD at 0° in the central dip profile shows more than one CoR below exponential curve.

aperture was calculated using the formula

$$T_{av(0-1.8)} =$$

$$\frac{0.5(T_0 + T_{0.8})(\pi 0.8^2 - 0) + 0.5(T_{0.8} + T_{1.8})(\pi 1.8^2 - \pi 0.8^2)}{\pi 1.8^2},$$ (3)

where $T_0 = 10^{-MPOD}$ at 0°, $T_{0.8} = 10^{-MPOD}$ at 0.8°, and $T_{1.8} = 10^{-MPOD}$ at 1.8°. The value of Tav(0–1.8) was used to calculate an average integrated MPOD between 0° and 1.8°:

$$MPOD_{av(0-1.8)} = -\log_{10}T_{av(0-1.8)}.$$ (4)

Ethical Approval and Consent

Ethical approval was obtained from the Optometry Research and Ethics Committee at City University London, and written informed consent was obtained from all subjects, conforming to the tenets of the Declaration of Helsinki.

Statistical Analysis

All statistical analyses were performed using SPSS version 19.0 for Windows (SPSS, Inc., Chicago, IL). Values in the text and tables are presented as the mean ± SD. Kolmogorov-Smirnov tests revealed no significant deviation from a normal distribution for MPOD at different spatial locations. Independent Student's *t*-tests and one-way, between-groups ANOVA analyzed the differences between the ethnic groups, sex, and smoking status. The Pearson χ^2 test and Mann-Whitney *U* test were used to assess any difference between categories and groups that showed an abnormal distribution. Analysis of the variance was used to investigate any differences between the three different

distribution profiles of MP. Statistical significance was accepted at the 95% confidence level ($P < 0.05$). Power statistics revealed that a sample size of 38, 19 subjects per group, was needed to detect a standardized difference of 0.91, using 80% power at 5% significance level.[25] This calculation was based on an estimated significant mean difference in MPOD of 0.1 with group SDs of 0.11 (based on the average MAP test coefficient of repeatability; Huntjens B, Asaria TS, Dhanani S, unpublished data, 2010).

RESULTS

Demographics between the ethnic groups, and mean MPOD measured at each eccentricity are summarized in Table 1. There was a significant difference between the two ethnic groups: the Asian group included fewer current smokers compared with the white group ($P = 0.039$). Age was not significantly correlated with central MPOD or any of the other spatial locations ($r = -0.110$; $P = 0.35$). Mean MPOD for individual eccentricities up to 2° showed a significant difference between the groups (Table 1). Average MPOD(0–1.8) (corresponding to integrated MPOD over the central 3.6° area) was significantly increased in Asian versus white subjects ($t[71] = 3.07$; $P = 0.003$). The significant difference in MPODav up to 1.8° between ethnicities was maintained with smoking as a covariant ($F[1,70] = 7.43$; $P = 0.008$).

Sex

When the group was considered as a whole ($n = 73$), females had higher central MPOD values (0.55 ± 0.19) compared with males (0.50 ± 0.16); however, this difference was not statistically significant ($t[71] = 1.25$; $P = 0.22$). A one-way, between-groups analysis was conducted to explore the impact

TABLE 1. Demographics and MPOD Results for All Subjects and Separate Ethnic Backgrounds

	All	**Asian**	**White**	**P Value**
Number	73	54	19	
Age, y				
Mean ± SD	21.3 ± 3.2	20.9 ± 3.2	22.4 ± 2.8	0.068
Range	16–34	18–34	16–28	
Sex				
Male	24 (33%)	14 (26%)	10 (53%)	0.065
Female	49 (67%)	40 (74%)	9 (47%)	
Current smoker?				
Yes	8 (12%)	3 (6%)	5 (26%)	0.039*
No	65 (88%)	51 (94%)	14 (74%)	
Mean ± SD MPOD, log units				
MPOD 0°	0.53 ± 0.18	0.56 ± 0.17	0.45 ± 0.18	0.015*
MPOD 0.8°	0.44 ± 0.14	0.46 ± 0.13	0.37 ± 0.14	0.010*
MPOD 1.8°	0.19 ± 0.08	0.20 ± 0.09	0.14 ± 0.07	0.007*
MPODav(0–1.8)	0.32 ± 0.10	0.34 ± 0.09	0.27 ± 0.10	0.003*

Independent *t*-tests and χ^2 tests were conducted to determine statistically significant differences in MP measurements between Asian and white participants.

*Statistical significance at the 0.05 level.

of sex on MPODav(0–1.8) between the ethnicities. Average MPOD(0–1.8) did not show a statistically significant difference between Asian males, Asian females, white males, and white females ($F[3,69] = 2.25$; $P = 0.06$).

FIGURE 2. The frequency of spatial profile types. The *upper graph* shows typical exponential versus atypical MP spatial profiles as a percentage of each ethnic group. The *lower graph* shows the prevalence of ethnicity within each of the spatial profile groups. On the *right side*, the prevalence of individual atypical profiles (ring and central dip) is shown for both ethnic groups. *Error bars* represent the 95% confidence interval for proportions.

Smoking Status

Among all participants, central MPOD was increased in nonsmokers (0.54 ± 0.18) when compared with current smokers (0.47 ± 0.17); however, this difference was not statistically significant ($t[71] = 1.01$; $P = 0.32$). Additionally, a one-way, between-groups analysis did not show a significant difference in MPODav(0–1.8) between smoking and nonsmoking Asian and white subjects ($F[3,69] = 2.69$; $P = 0.053$).

Spatial Profiles

When the group was considered as a whole, a typical exponential profile was seen in half of the group ($n = 37$), while 36 participants showed a nonexponential (i.e., atypical) profile. Pearson's χ^2 test using the appropriate continuity correction indicated a statistically significant association between ethnicity and spatial profile type ($\chi^2 [1, n = 73] = 6.75$, $P = 0.009$, Cramer's $V = 0.335$). The results show that within ethnicities, 79% of white subjects presented an exponential profile in comparison to 41% of the Asian subjects (Fig. 2). In showing an atypical profile, 98% of participants were of Asian phenotype. We also observed an interesting relationship between the ethnicities and the three spatial profiles of MP as described in the Methods. When the group was considered as a whole, an exponential profile occurred in half the group, a ring in 30% of the group and the central dip profile was present in 19% of the subjects. Furthermore, 82% of subjects showing a ring and 100% of subjects showing a central dip profile were of Asian descent (Fig. 2). The Pearson's χ^2 test indicated a statistically significant association between ethnicity and spatial profile type ($\chi^2 [2, n = 73] = 9.68$, $P = 0.008$, Cramer's $V = 0.364$).

We explored the relationship between spatial profile type and MPOD at individual spatial locations up to 2° and MPODav(0–1.8) (Table 2). Average MPOD(0–1.8) was significantly increased in participants that showed an atypical when compared with an exponential spatial profile ($t[71] = -4.56$; $P < 0.0005$). This was also true for MPOD at 0.8° and MPOD at 1.8°, but not for central MPOD ($t[67] = -1.35$; $P = 0.19$). When the same analysis was conducted for each ethnicity, identical statistically significant results were found for the Asian subjects

TABLE 2. Summary of MPOD Values Per Spatial Profile Type for All Participants

	Mean ± SD MPOD, Log Units				
	Typical Exponential, $n = 37$	Atypical, $n = 36$	MP Ring, $n = 22$	Central Dip, $n = 14$	P Value
MPOD 0°	0.51 ± 0.20	0.56 ± 0.15			0.19
MPOD 0.8°	0.36 ± 0.13	0.52 ± 0.11			<0.0005*
MPOD 1.8°	0.16 ± 0.06	0.22 ± 0.09			0.003*
MPODav(0-1.8)	0.28 ± 0.09	0.37 ± 0.08			<0.0005*
MPOD 0°	0.51 ± 0.20		0.57 ± 0.16	0.55 ± 0.14	0.43
MPOD 0.8°	0.36 ± 0.13†‡		0.52 ± 0.11	0.51 ± 0.11	<0.0005*
MPOD 1.8°	0.16 ± 0.06‡		0.19 ± 0.08‡	0.27 ± 0.10	<0.0005*
MPODav(0-1.8)	0.28 ± 0.09†‡		0.35 ± 0.08	0.39 ± 0.09	<0.0005*

* Indicates statistical significance at the 0.05 level.
† Statistically significantly different from ring-like profile.
‡ Statistically significantly different from central dip profile.

but not for white subjects. Analysis of the variance showed statistically significant differences for all MPOD values (Table 2) when all three spatial profiles (exponential, ring, and central dip) were considered, with the exception of central MPOD ($P = 0.43$). Post hoc analysis using the Tukey honest significant difference test indicated that the mean MPODav(0-1.8) for the exponential profile group (0.28 ± 0.09) was significantly decreased compared with the MP ring group (0.35 ± 0.08) and the central dip group (0.39 ± 0.09), but not between the two atypical profile groups. This was also true for MPOD at 0.8°. Interestingly, mean MPOD at 1.8° for the exponential group (0.16 ± 0.06) was not significantly different from the ring group (0.19 ± 0.08), but they were both significantly decreased from the subjects in the central dip group (0.27 ± 0.10; $P < 0.0005$).

DISCUSSION

Consistent with previous studies,[18,26] we found increased central MPOD in Asian (0.56 ± 0.17) versus white subjects (0.45 ± 0.18; $t[71] = 2.50$; $P = 0.015$). This is in agreement with the work of Howells et al.[18] where an average of 0.43 ± 0.14 in 117 Asian and 0.33 ± 0.13 in 52 white subjects was reported. Overall, their slightly lower average MPOD values compared with the present study are possibly due to the different HFP instruments used. However, the difference in central MPOD between the ethnicities is similar between the studies. In contrast, Raman et al.[26] reported a mean central MPOD (at 0.25° retinal eccentricity) of 0.63 ± 0.16 in 60 Asian subjects aged 20 to 29 years, and 0.72 ± 0.22 in 60 Asian subjects aged 30 to 39 years. These values are higher when compared with our results, which again may be due to the different HFP instruments. Furthermore, the Asian subjects were of South Indian origin living in India (Mumbai); however, similar to Howell's study,[19] the Asian subjects included in our study were of Indian, Pakistani, and Bangladeshi descent, the majority born and living in the UK (78%; 42 out of 54 Asian subjects). The country of origin and residence may be significant because of differences in diet. The traditional south Asian diet typically consisting of a diet rich in carotenoids may be altered after migration, particularly in the young or second generation Asians[27]; this may contribute to the lower MPOD levels found in our group.

The integrated transmittance of the MP between eccentricities was used to calculate the average MPOD up to 1.8°. Similar to central MPOD, mean MPODav(0-1.8) was significantly increased in Asian (0.34 ± 0.09) compared with white subjects

(0.27 ± 0.10; $t[71] = 3.07$; $P = 0.003$). Lower central MPOD has been associated with factors that may increase the risk of AMD, such as female sex[4,7,20,21,28,29] and smoking.[5,28] The relationship between spatial profiles and ethnicities, including covariates such as sex and smoking status, were difficult to establish in the present study due to the small sample size of each subgroup. Nonetheless, we did not find a sex association with MPOD, with central MPOD values of 0.55 ± 0.19 for the females compared with 0.50 ± 0.16 for the males ($P = 0.22$).

When the groups were analyzed by ethnicity, a similar trend was found for both Asian and white participants. Previous studies of Asian subjects with a similar age range to our study have reported that males have higher mean MPOD than females.[18,26] One study found this to be statistically significant.[18] The difference between MPODav(0-1.8) in nonsmokers (0.33 ± 0.09) compared with smokers (0.27 ± 0.11) did not reach statistical significance ($P = 0.15$). We note that the lack of a difference may be due to the small sample of smoking subjects (8 out of 73 subjects) and the short smoking history.

Our data suggest that atypical profiles (i.e., ring and central dip) occur more frequently in Asian compared with white subjects ($P = 0.009$). The average integrated MPOD up to 1.8° was significantly increased in Asian subjects presenting with atypical (0.38 ± 0.08) versus exponential profiles (0.29 ± 0.10; $t[52] = -3.86$; $P < 0.0005$). In white subjects, this finding was not significant (0.30 ± 0.07 and 0.26 ± 0.10, respectively; $t[17] = -0.85$; $P = 0.41$). Therefore, it seems that an atypical spatial profile is a representative characteristic of the Asian group, and indeed may be considered typical in this ethnic group. Since there was no significant difference between central MPOD in Asian ($t[35] = -0.71$; $P = 0.48$) or in white subjects presenting with an atypical profile compared with an exponential profile ($t[17] = 0.26$; $P = 0.80$), our results suggest that, compared with an individual MPOD measurement at a single retinal spatial location or an average of MPOD measurements at several retinal spatial locations, MPODav(0-1.8) provides a better representation of the amount of MP present. Although some of the subjects show a sizable decrease in MPOD at the fovea, many others do not. In spite of large variability in MPOD caused by averaging MPOD over the area of the stimulus and the variability in fixation accuracy during the HFP test, the results using a small central target (i.e., 0.36° diameter) suggest that a ring-like profile is possible. However, the main conclusion of the study based on the measured differences in short wavelength transmittance over the centre 3.6° has become more significant by analyzing the results in terms of area weighted central transmittance.

This is the first comparative study to investigate MP spatial profiles in Asian and white subjects. Several studies have reported on the different spatial distributions of MP; however, there is little consensus on the definition of an atypical profile. Additionally, there are various methodologies used to measure MP density and results are consequently not always interchangeable. The spatial profile of MP is normally described as following an exponential decline, although 20% to 50% of the population in studies where MP is measured by HFP and objective imaging techniques have shown a deviation from the exponential curve at 0° or at a location away from the central fovea.[10,15,16] The lack of spatial resolution in the measurement of central MPOD can be largely attributed to the size of the central target, as well as the subject's ability to maintain steady fixation. In comparison with other HFP techniques, the MAP test aims to minimize this effect by employing a very small central (0.36°) and static peripheral stimuli. A nonexponential spatial profile was found in 21% (4 out of 19) of white subjects and 59% (32 out of 54) of Asian subjects. Atypical profiles have been previously defined as those not exhibiting a typical exponential profile, but showing either a annulus of higher MP or ring, where the central peak is surrounded by a ring of increased density,[15] or a central dip (i.e., MPOD at 0.25° not visually exceeding MPOD at 0.5°,[13] or MPOD at 0.25° not exceeding MPOD at 0.5° by more than 0.04 optical density units[30]). The presence of a MP ring has been found significantly increased in ethnicities with low AMD prevalence,[17] suggesting it may enhance the MP's protective role. Wolf-Schnurrbusch et al.[17] showed significantly increased frequency of a parafoveal ring ($P < 0.0001$) and central MPOD ($P < 0.0001$) in African subjects, when compared with non-Hispanic white subjects. In contrast, since increased prevalence of a central dip was found to be associated with increased age and smoking, it was proposed that a central dip decreased the protective role of MP.[11]

Interestingly, when we considered the atypical spatial profiles in all participants, we found that MPOD values at 0.8° and 1.8° and MPODav(0–1.8) were increased in the profiles showing a ring or central dip, compared with the exponential profile. Table 2 shows that this was statistically significant, with the exception of central MPOD. There was no difference in central MPOD between the exponential, ring and surprisingly, the central dip profile groups. Unexpectedly, the mean MPOD at 1.8° for the group presenting a ring was not significantly different from the exponential group, but was significantly lower than for the central dip group ($P < 0.0005$). These results show that the central dip profile has more MPOD at or close to the location where the MP ring profile shows its additional peak. It seems that a central dip has not lost its peak, but possibly broadened its lateral distribution. We, therefore, propose that the presence of a central dip profile may actually offer increased integrated MPOD up to 1.8°, and therefore increased macular protection from harmful blue light. Moreover, our data suggest that there may be a disparity in the occurrence of MP spatial profiles amongst ethnicities. Not only were atypical spatial profiles more frequently present in Asian subjects ($P = 0.008$), but also the central dip was entirely absent in white subjects. This implies that there may be need for subclassification of MP spatial profiles other than typical (i.e., exponential) versus atypical, as previously suggested by Berendschot and van Norren.[10] Additionally, we propose using exponential versus nonexponential profile types, since atypical profiles for some ethnicities may represent typical characteristics for that group.

Considering previous reports of dietary differences between ethnicities,[31,32] our data support the hypothesis that the central dip could be the result of a high conversion of lutein to meso-zeaxanthin[33,34] resulting in an increased MPOD at the 0.8° and 1.8° locations. Additionally, there is supporting evidence that lutein and zeaxanthin supplementation increases MPOD in the human foveal and parafoveal areas.[35-37] The distribution of zeaxanthin (centrally) and lutein (more peripherally) within the macula may suggests that an exponential or atypical ring profile represent a relative enrichment of zeaxanthin, while an atypical central dip profile represents a relative enrichment of lutein. However, Zeimer et al.[38] suggested that lutein and zeaxanthin supplementation in AMD and control subjects might amplify, not create, atypical MP spatial profiles. A limitation of our study was that we did not measure lutein and zeaxanthin dietary intake. Neither could we relate these differences in spatial profiles to the iris color, or family history of AMD, since we did not collect this data. While not controlled for in our study, iris color and dietary intake of carotenoids may be the largest source of variation between our two groups. Nonetheless, our results have shown an uneven distribution of MP spatial profile types between white and Asian subjects, which confirms the need for wider-scale studies, including other ethnic phenotypes, iris color, and dietary intake of carotenoids.

CONCLUSIONS

This is the first study to investigate the prevalence of different MP spatial distributions for Asian and white subjects. Our results show that central MPOD was significantly increased in our 54 Asian subjects, compared with 19 white subjects of similar age. We classified spatial distributions of macular pigment into typical exponential and atypical (nonexponential) profiles. Atypical profiles were significantly more prevalent in Asian compared with white subjects. Additionally, we noted that ring and central dip spatial profiles varied between the ethnicities, whereby the prevalence of central dip was significantly increased in Asian group. Additionally, integrated MPOD up to 1.8° was significantly increased in a central dip compared with an exponential profile. This suggests that, similar to a MP ring, a central dip represents enhanced retinal protection from harmful blue light.

References

1. Snodderly DM, Auran JD, Delori FC. The macular pigment. II. Spatial distribution in primate retinas. *Invest Ophthalmol Vis Sci*. 1984;25:674–685.

2. Hammond BR, Wooten BR, Snodderly DM. Individual variations in the spatial profile of human macular pigment. *J Opt Soc Am A Opt Image Sci Vis*. 1997;14:1187–1196.

3. Bone RA, Landrum JT, Fernandez L, Tarsis SL. Analysis of the macular pigment by HPLC: retinal distribution and age study. *Invest Ophthalmol Vis Sci*. 1988;29:843–849.

4. Beatty S, Murray IJ, Henson DB, Carden D, Koh HH, Boulton ME. Macular pigment and risk for age-related macular degeneration in subjects from a northern European population. *Invest Ophthalmol Vis Sci*. 2001;42:439–446.

5. Hammond BR, Wooten BR, Snodderly DM. Cigarette smoking and retinal carotenoids: implications for age-related macular degeneration. *Vision Res*. 1996;36:3003–3009.

6. Mares JA, LaRowe TL, Snodderly DM, et al. Predictors of optical density of lutein and zeaxanthin in retinas of older women in the Carotenoids in Age-Related Eye Disease Study, an ancillary study of the Women's Health Initiative. *Am J Clin Nutr*. 2006;84:1107–1122.

7. Hammond BR, Curran-Celentano J, Judd S, et al. Sex differences in macular pigment optical density: relation to plasma carotenoid concentrations and dietary patterns. *Vision Res*. 1996;36:2001–2012.

8. Ciulla TA, Curran-Celantano J, Cooper DA, et al. Macular pigment optical density in a midwestern sample. *Ophthalmology*. 2001;108:730–737.

9. Hammond BR, Fuld K, Snodderly DM. Iris color and macular pigment optical density. *Exp Eye Res*. 1996;62:715–720.

10. Berendschot TT, van Norren D. Macular pigment shows ringlike structures. *Invest Ophthalmol Vis Sci*. 2006;47:709–714.

11. Kirby ML, Beatty S, Loane E, et al. A central dip in the macular pigment spatial profile is associated with age and smoking. *Invest Ophthalmol Vis Sci*. 2010;51:6722–6728.

12. Elsner AE, Burns SA, Beausencourt E, Weiter JJ. Foveal cone photopigment distribution: small alterations associated with macular pigment distribution. *Invest Ophthalmol Vis Sci*. 1998;39:2394–2404.

13. Kirby ML, Galea M, Loane E, Stack J, Beatty S, Nolan JM. Foveal anatomic associations with the secondary peak and the slope of the macular pigment spatial profile. *Invest Ophthalmol Vis Sci*. 2009;50:1383–1391.

14. Nolan JM, Stringham JM, Beatty S, Snodderly DM. Spatial profile of macular pigment and its relationship to foveal architecture. *Invest Ophthalmol Vis Sci*. 2008;49:2134–2142.

15. Dietzel M, Zeimer M, Heimes B, Pauleikhoff D, Hense HW. The ringlike structure of macular pigment in age-related maculopathy: results from the Muenster Aging and Retina Study (MARS). *Invest Ophthalmol Vis Sci*. 2011;52:8016–8024.

16. Delori FC, Goger DG, Keilhauer C, Salvetti P, Staurenghi G. Bimodal spatial distribution of macular pigment: evidence of a gender relationship. *J Opt Soc Am A Opt Image Sci Vis*. 2006; 23:521–538.

17. Wolf-Schnurrbusch UEK, Roosli N, Weyermann E, Heldner MR, Hohne K, Wolf S. Ethnic differences in macular pigment density and distribution. *Invest Ophthalmol Vis Sci*. 2007;48: 3783–3787.

18. Howells O, Eperjesi F, Bartlett H. Macular pigment optical density in young adults of South Asian origin. *Invest Ophthalmol Vis Sci*. 2013;54:2711–2719.

19. Iannaccone A, Mura M, Gallaher KT, et al. Macular pigment optical density in the elderly: findings in a large biracial Midsouth population sample. *Invest Ophthalmol Vis Sci*. 2007;48:1458–1465.

20. Lam RF, Rao SK, Fan DSP, Lau FTC, Lam DSC. Macular pigment optical density in a Chinese sample. *Curr Eye Res*. 2005;30: 729–735.

21. Tang CY, Yip H, Poon M, Yau W, Yap MKH. Macular pigment optical density in young Chinese adults. *Ophthalmic Physiol Opt*. 2004;24:586–593.

22. Barbur JL, Konstantakopoulou E, Rodriguez-Carmona M, Harlow JA, Robson AG, Moreland JD. The Macular Assessment Profile test—a new VDU-based technique for measuring the spatial distribution of the macular pigment, lens density and rapid flicker sensitivity. *Ophthalmic Physiol Opt*. 2010;30: 470–483.

23. Snodderly DM, Brown PK, Delori FC, Auran JD. The macular pigment. I. Absorbance spectra, localization, and discrimination from other yellow pigments in primate retinas. *Invest Ophthalmol Vis Sci*. 1984;25:660–673.

24. Bone RA, Landrum JT. Heterochromatic flicker photometry. *Arch Biochem Biophys*. 2004;430:137–142.

25. Bland M. *An Introduction to Medical Statistics*. 3rd ed. London: Oxford University Press; 2000.

26. Raman R, Rajan R, Biswas S, Vaitheeswaran K, Sharma T. Macular pigment optical density in a South Indian population. *Invest Ophthalmol Vis Sci*. 2011;52:7910–7916.

27. Gilbert PA, Khokhar S. Changing dietary habits of ethnic groups in Europe and implications for health. *Nutr Rev*. 2008; 66:203–215.

28. Hammond BR, Caruso-Avery M. Macular pigment optical density in a southwestern sample. *Invest Ophthalmol Vis Sci*. 2000;41:1492–1497.

29. Broekmans WMR, Berendschot TTJM, Klöpping-Ketelaars IAA, et al. Macular pigment density in relation to serum and adipose tissue concentrations of lutein and serum concentrations of zeaxanthin. *Am J Clin Nutr*. 2002;76:595–603.

30. Nolan JM, Akkali MC, Loughman J, Howard AN, Beatty S. Macular carotenoid supplementation in subjects with atypical spatial profiles of macular pigment. *Exp Eye Res*. 2012;101:9–15.

31. O'Neill ME, Carroll Y, Corridan B, et al. A European carotenoid database to assess carotenoid intakes and its use in a five-country comparative study. *Br J Nutr*. 2001;85:499–507.

32. Wang LH, Tam CF, Yang HL, Chen YC, Davis R, Schwartz MEA. Comparison of eye-health nutrients, lutein (l)/zeaxanthin (z) intakes and l/z rich food choices between college students living in Los Angeles and Taiwan. *Coll Stud J*. 2008;42:1118–1133.

33. Connolly EE, Beatty S, Thurnham DI, et al. Augmentation of macular pigment following supplementation with all three macular carotenoids: an exploratory study. *Curr Eye Res*. 2010;35:335–351.

34. Kraats JVD, Kanis MJ, Genders SW, Norren DV. Lutein and zeaxanthin measured separately in the living human retina with fundus reflectometry. *Invest Ophthalmol Vis Sci*. 2008; 49:5568–5573.

35. Richer SP, Stiles W, Graham-Hoffman K, et al. Randomized, double-blind, placebo-controlled study of zeaxanthin and visual function in patients with atrophic age-related macular degeneration: the Zeaxanthin and Visual Function Study (ZVF) FDA IND# 78, 973. *Optometry*. 2011;82:667–680.

36. Schalch W, Cohn W, Barker FM, et al. Xanthophyll accumulation in the human retina during supplementation with lutein or zeaxanthin—the LUXEA (LUtein Xanthophyll Eye Accumulation) Study. *Arch Biochem Biophys*. 2007;458:128–135.

37. Trieschmann M, Beatty S, Nolan JM, et al. Changes in macular pigment optical density and serum concentrations of its constituent carotenoids following supplemental lutein and zeaxanthin: the LUNA Study. *Exp Eye Res*. 2007;84:718–728.

38. Zeimer M, Dietzel M, Hense HW, Heimes B, Austermann U, Pauleikhoff D. Profiles of macular pigment optical density and their changes following supplemental lutein and zeaxanthin: new results from the LUNA Study. *Invest Ophthalmol Vis Sci*. 2012;53:4852–4859.

6.2 The effects of ocular magnification on Spectralis spectral domain optical coherence tomography scan length

BASIC SCIENCE

The effects of ocular magnification on Spectralis spectral domain optical coherence tomography scan length

Irene Ctori · Stephen Gruppetta · Byki Huntjens

Abstract

Purpose The purpose of this study was to assess the effects of incorporating individual ocular biometry measures of corneal curvature, refractive error, and axial length on scan length obtained using Spectralis spectral domain optical coherence tomography (SD-OCT).

Methods Two SD-OCT scans were acquired for 50 eyes of 50 healthy participants, first using the Spectralis default keratometry (K) setting followed by incorporating individual mean-K values. Resulting scan lengths were compared to predicted scan lengths produced by image simulation software, based on individual ocular biometry measures including axial length.

Results Axial length varied from 21.41 to 29.04 mm. Spectralis SD-OCT scan lengths obtained with default-K ranged from 5.7 to 7.3 mm, and with mean-K from 5.6 to 7.6 mm. We report a stronger correlation of simulated scan lengths incorporating the subject's mean-K value (ρ=0.926, P<0.0005) compared to Spectralis default settings (ρ=0.663, P<0.0005).

Conclusions Ocular magnification appears to be better accounted for when individual mean-K values are incorporated into Spectralis SD-OCT scan acquisition versus using the device's default-K setting. This must be considered when taking area measurements and lateral measurements parallel to the retinal surface.

I. Ctori · S. Gruppetta · B. Huntjens (✉)
Applied Vision Research Centre, The Henry Wellcome Laboratories
for Vision Sciences, City University London, Northampton Square,
London EC1V 0HB, UK
e-mail: Byki.Huntjens.1@city.ac.uk

I. Ctori
e-mail: Irene.Ctori.2@city.ac.uk

S. Gruppetta
e-mail: Steve.Gruppetta.1@city.ac.uk

Introduction

Optical coherence tomography (OCT) allows a direct cross-sectional view of the human retina [1] correlating well with retinal histology [2]. SD-OCT provides increased acquisition speed and higher image resolution compared to older time-domain OCT techniques [3, 4]. OCT technology is increasingly employed in the clinical diagnosis of ocular pathology such as age-related macular degeneration [5], macular holes [6], vitreomacular traction [7], and glaucoma [8]. Quantitative evaluation of retinal thickness using both automatic and manual measuring techniques is useful for clinical diagnosis and in designing treatment protocols [9–11]. It is known that segmentation algorithms employed by individual OCT instruments result in variability in retinal thickness measurements, complicating comparisons across different platforms [12, 13]. In addition, ocular magnification of retinal images is affected by refractive error, corneal curvature, refractive index, axial length, and anterior chamber depth [14, 15]. The distance from the eye to the measuring device can also influence the magnification effect [16]. In the case of OCT scan images, ocular magnification may affect lateral measurements i.e., those made parallel to the retinal plane [17]. The optical setup of the OCT instrument, as well as the software program for calculating image size, will govern image size calculation in computerized fundus imaging [18]. If lateral measurements such as drusen diameter, geographical atrophy area in dry age-related macular degeneration, or foveal width measurements are to be used for establishing diagnosis and treatment protocols, the potential impact of ocular

🖄 Springer

6.3 Repeatability of foveal measurements using Spectralis optical coherence tomography segmentation software

PLOS | ONE

Repeatability of Foveal Measurements Using Spectralis Optical Coherence Tomography Segmentation Software

Irene Ctori, Byki Huntjens*

Applied Vision Research Centre, The Henry Wellcome Laboratories for Vision Sciences, City University London, Northampton Square, London, EC1V 0HB, United Kingdom

* Byki.Huntjens.1@city.ac.uk

Abstract

Purpose

To investigate repeatability and reproducibility of thickness of eight individual retinal layers at axial and lateral foveal locations, as well as foveal width, measured from Spectralis spectral domain optical coherence tomography (SD-OCT) scans using newly available retinal layer segmentation software.

Methods

High-resolution SD-OCT scans were acquired for 40 eyes of 40 young healthy volunteers. Two scans were obtained in a single visit for each participant. Using new Spectralis segmentation software, two investigators independently obtained thickness of each of eight individual retinal layers at 0°, 2° and 5° eccentricities nasal and temporal to foveal centre, as well as foveal width measurements. Bland-Altman Coefficient of Repeatability (CoR) was calculated for inter-investigator and inter-scan agreement of all retinal measurements. Spearman's ρ indicated correlation of manually located central retinal thickness (RT_0) with automated minimum foveal thickness (MFT) measurements. In addition, we investigated nasal-temporal symmetry of individual retinal layer thickness within the foveal pit.

Results

Inter-scan CoR values ranged from 3.1µm for axial retinal nerve fibre layer thickness to 15.0µm for the ganglion cell layer at 5° eccentricity. Mean foveal width was 2550µm ± 322µm with a CoR of 13µm for inter-investigator and 40µm for inter-scan agreement. Correlation of RT_0 and MFT was very good ($\rho = 0.97$, $P < 0.0005$). There were no significant differences in thickness of any individual retinal layers at 2° nasal compared to temporal to fovea ($P > 0.05$); however this symmetry could not be found at 5° eccentricity.

221

Conclusions

We demonstrate excellent repeatability and reproducibility of each of eight individual retinal layer thickness measurements within the fovea as well as foveal width using Spectralis SD-OCT segmentation software in a young, healthy cohort. Thickness of all individual retinal layers were symmetrical at 2°, but not at 5° eccentricity away from the fovea.

Introduction

The arrival of Optical Coherence Tomography (OCT) has changed the way that retinal pathology is diagnosed and managed. OCT imaging allows non-invasive cross-sectional imaging of the human retina [1]. Good correlation with retinal histology [2–4] pertains OCT technology to the clinical diagnosis of a variety of ocular pathologies [5–8] based on quantitative evaluation of retinal thickness measurements in-vivo [9–11]. Newer spectral domain (SD-OCT) methods offer faster acquisition time and improved image resolution compared to older time-domain OCT techniques [12,13]. In addition, automated retinal thickness measurement techniques are a time-efficient way to investigate retinal thickness change over time [14]. Repeatability and reproducibility of automated total retinal thickness measurements using SD-OCT has been demonstrated in healthy individuals [15,16] as well as those with ocular pathology [17–22]. This has enabled the definition of levels at which true clinical change can be distinguished from measurement variability. However, OCT instruments employ a variety of segmentation algorithms within their software platforms so that measurements cannot be directly compared between instruments [23,24]. It is therefore important to establish the repeatability and reproducibility of retinal measurements for each OCT device being used for clinical diagnosis and treatment protocol designs [9–11].

According to the configuration of the Spectralis SD-OCT (Heidelberg Engineering, Heidelberg, Germany), one pixel represents 3.9μm axially and 6μm laterally [25]. It features Automatic Real Time (ART), a setting that improves image quality by averaging multiple B-scans to reduce noise and Tru-Track, an eye-tracking device that improves scan reproducibility [26]. Compared to other OCT instruments, the Spectralis SD-OCT presents the highest reproducibility of automated crude central foveal thickness measurement [27,22]. Very recently, Heidelberg Engineering launched an update to the Spectralis SD-OCT Heidelberg Eye Explorer mapping software (version 6.0c) that allows automatic segmentation of individual retinal layers.

This study reports inter-investigator and inter-scan repeatability of thickness of eight individual retinal layers including the inner and outer plexiform and nuclear layers along with combined inner retinal layer thickness and overall retinal thickness at manually derived axial and lateral foveal locations. Repeatability of foveal width measurements is also investigated. All measurements are derived from Spectralis SD-OCT scans using the newly available Spectralis retinal layer segmentation software.

Methods

Study protocol

The study included 40 healthy volunteers and took place at the Division of Optometry and Visual Science, City University London from October to December 2013. The inclusion criterion was logMAR visual acuity better than 0.3 log units in the eye being tested. Exclusion criteria

were ocular pathology including corneal disease, macular disease and fundus myopicus, medication that may affect retinal function and previous eye surgery, including refractive laser correction. For each volunteer, the eye with the best logMAR acuity was selected as the test eye. Mean spherical error (MSE), calculated as sphere plus half of the cylinder[28] (average of five autorefractor readings), and mean keratometry measurements (average of three horizontal and vertical readings) were obtained using the Topcon TRK-1P autorefractor (Topcon, Tokyo, Japan). Two experienced investigators (A and B) each derived foveal measurements from Spectralis SD-OCT scans, using the techniques described below. Investigators A and B both obtained measurements from the first scan of each participant (1A and 1B respectively), and investigator B took measurements from the second scan (2B). For repeat measurements, each investigator was masked to their initial or the other investigator's results. Tomograms were measured in a random order to minimize this potential source of bias.

SD-OCT scan acquisition

All scans were obtained without pupil dilation [29–31] in a dark room using the Spectralis SD-OCT device. As recommended by manufacturer instructions, each participant's mean keratometry value was inserted into the Spectralis software prior to scan acquisition [32]. Two consecutive 20° x 5° volume scans (49 B-scans 30 microns apart, ART 16 frames including 1024 A scans) were taken for the test eye within a single visit, without setting the first scan as a reference. The participant was instructed to sit back from the device between scans. Each time, the investigator focused the infrared fundus image according to the participant's MSE. Central fixation was monitored via the live fundus image and scan quality was accepted above 25 decibels (dB), in accordance with the manufacturer guidelines.

Foveal measurements

Foveal measurements from each SD-OCT scan were performed using the inbuilt Spectralis mapping software, Heidelberg Eye Explorer (version 6.0c). The new Spectralis segmentation software was used to obtain individual retinal layer thickness measurements including: overall retinal thickness (RT), retinal nerve fibre layer (RNFL), ganglion cell layer (GCL), inner plexiform layer (IPL), inner nuclear layer (INL), outer plexiform layer (OPL), outer nuclear layer (ONL), retinal pigment epithelium (RPE), inner retinal layer (IRL) and photoreceptor layer (PR). Measures of foveal width were also evaluated, as well as the correlation of manual and automated measures of central retinal thickness. In addition, we explored the horizontal symmetry from the foveal centre of the thickness of the individual retinal layers.

No manual adjustments to B-scan retinal layer segmentation were made prior to measurements being taken. For each scan, the foveal centre was identified as the frame including the brightest foveal reflex [33,34]. As suggested by Mohammad *et al.*, when a bright reflex was absent or present in two or more frames, the frame containing the thickest outer segment layer was chosen [35]. At the point where the software caliper bisected the foveal reflex, individual layer thickness (RT, RNFL, GCL, IPL, INL, OPL, ONL, RPE, IRL and PR) was recorded in microns (Fig 1A). The software displays overall retinal thickness as the vertical distance between the vitreoretinal interface and Bruch's membrane (Fig 1B).

Thickness of each retinal layer was also measured at 2° and 5° eccentricity away from the fovea. In order to locate these lateral positions on the tomogram, the eccentricities in degrees were converted into microns based on each individual's OCT scan length. For example, given that the scan length (in millimeters, mm) generated by the Spectralis represents 20°, the lateral equivalent in microns of 2° would be 2*(scan length/20). The inbuilt software caliper was set at the appropriate lateral distance perpendicular to the vertical caliper bisecting the foveal reflex

Fig 1. 1a and b. Central retinal thickness and layer segmentation by Spectralis SD-OCT software. The Spectralis software displays overall retinal thickness as the vertical distance between the vitreoretinal interface and Bruch's membrane. Using the thickness profile, the foveal reflex was bisected by the software caliper, and the thickness of the individual layers was recorded in microns (a). Segmentation of the individual retinal layers can be seen in the lower image (b).

and thickness of each retinal layer recorded from the retinal thickness profile (Fig 2). Lateral measurements were taken nasal to the fovea for all tomograms. In addition, temporal retinal thickness measurements were also obtained for the first scan of each participant to assess horizontal symmetry.

Using the inbuilt manual calipers, foveal width was measured in microns as the horizontal distance between foveal crests [11,30,33,36], identified as the maximum retinal thickness nearest to the foveal reflex on the nasal and temporal side (Fig 3A and 3B).
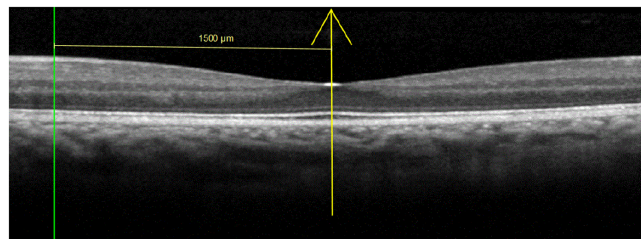
Fig 2. Positioning of software caliper for lateral retinal thickness measurement.

Fig 3. a and b. Measurement of foveal width. Maximum retinal thickness nearest to the foveal reflex on nasal (a) and temporal side identified from the thickness profile. Foveal width was measured in microns using the inbuilt manual calipers (b).

The Spectralis mapping software also generates automated measures of retinal thickness based on analyses of the central and inner 1000, 3000 and 6000μm subfields as defined by the Early Treatment Diabetic Retinopathy Study [37]. From this, the central minimum retinal thickness value was recorded as the minimum foveal thickness (MFT) for each scan. Central foveal thickness of each retinal layer (CFT), corresponding to the average thickness of all points within the central ETDRS zone of 1000μm diameter, was also recorded.

Ethical approval and consent

Approval for the study was obtained from the Optometry Research & Ethics Committee City University London. All subjects gave written informed consent conforming to the tenets of the Declaration of Helsinki.

Statistical analysis

All statistical analyses were performed using SPSS version 22.0 for Windows (SPSS Inc., Chicago, USA). Values in the text and tables are presented as the mean ± standard deviation (SD). Preliminary analyses were performed to ensure no violation of the assumptions of normality, linearity and homoscedasticity. The CoR was calculated as *1.96s*, where *s* is the SD of the difference between pairs of measurements [38]. Limits of agreement (LoA) were calculated as the

225

Table 1. Inter-observer agreement of thickness of retinal layers in microns.

I)	Eccentricity from foveal centre (degrees)					
II)	0		2		5	
Retinal layer	Mean difference	CoR	Mean difference	CoR	Mean difference	CoR
III) Retina	-0.025	0.31	-0.425	3.20	-0.075	0.52
IV) Retinal nerve fibre layer	-0.025	0.31	0.225	3.91	-0.10	0.74
V) Ganglion cell layer	-0.05	0.43	-0.35	2.41	-0.025	0.31
VI) Inner plexiform layer	0.025	0.31	-0.10	1.07	-0.025	0.31
VII) Inner nuclear layer	0.125	1.27	-0.15	1.14	0.00	0.44
VIII) Outer plexiform layer	0.025	0.54	0.075	1.03	-0.025	0.54
IX) Outer nuclear layer	-0.125	1.73	-0.075	2.36	0.00	0.44
X) Inner retinal layer	-0.025	0.70	-0.475	3.20	-0.075	0.93
Photoreceptor layer	-0.05	0.43	-0.025	1.13	0.075	0.93
XI) Retinal pigment epithelium	0.00	0.77	0.05	1.08	0.025	0.31

Retinal thickness refers to thickness from the inner limiting membrane to the external limiting membrane. Limits of Agreement are equal to the mean difference ± Coefficient of Repeatability (CoR).

mean difference between two sets of data ± CoR. The LoA indicate the range within which 95% of the differences between measurements will lie [38–40].

We calculated the inter-investigator agreement of the thickness of each retinal layer and also foveal width measurements from the first scan (1A versus 1B). The inter-scan CoR for the same retinal measurements taken by investigator B was also calculated (1B versus 2B). We determined the correlation of manual location of central retinal thickness (RT_0) and MFT using Spearman's Rank Correlation coefficient, ρ. The independent t-test was used to assess difference between nasal and temporal retinal layer thickness. Statistical significance was accepted at $P < 0.05$.

Results

The study group included 40 participants (12 males and 28 females) with a mean age of 21.1 ± 3.1 years (range 18 to 36 years). Mean MSE was -1.70 ± 2.32DS (ranging from -10.00DS to +0.50DS) and mean keratometry was 7.83 ± 0.30mm (ranging from 7.16 to 9.05mm). There was no significant difference in mean image quality between scan 1 (38 ± 4dB) and scan 2 (38 ± 3dB; P = 1.00).

Repeatability of thickness of individual retinal layer measurements are presented in Table 1 (inter-investigator) and Table 2 (inter-scan), with the mean difference and CoR values for each layer at 0°, 2° and 5° nasal eccentricity as well as the CFT given. Mean overall retinal thickness was 217 ± 16µm at 0°, 296 ± 27µm at 2° and 350 ± 16µm at 5° nasal to foveal centre, with respective CoR values of 0.3, 3.2 and 0.5µm for inter-observer and 7.4, 8.5 and 7.6µm for inter-scan agreement. Mean foveal width was 2550µm ± 322µm with mean difference of 0.60µm and CoR of 13µm for inter-investigator and mean difference of -0.70µm and CoR of 40µm for inter-scan agreement. Bland-Altman plots are presented in Fig 4.

The automated measure of MFT showed a mean of 216 ± 15µm for the first scan and 217 ± 15µm for the repeated scan. MFT mean difference between scans was 0.33µm, with CoR of 2.19 and LoA from -1.87 to 2.52µm. There was excellent correlation between automated

Table 2. Inter-scan agreement of thickness of retinal layers in microns at 0, 2 and 5° from foveal centre.

XII)								
XIII)	**Eccentricity from foveal centre (degrees)**							
	0		**2**		**5**		**CFT**	
Retinal layer	**Mean difference**	**CoR**	**Mean difference**	**CoR**	**Mean difference**	**CoR**	**Mean difference**	**CoR**
XIV) Retina	-0.35	7.4	-0.423	8.46	0.5	7.57	-0.08	3.7
XV) Retinal nerve fibre layer	0.18	3.1	0.75	8.42	-0.85	10.0	-0.05	1.6
XVI) Ganglion cell layer	-0.43	4.4	-1.00	7.13	-0.83	15.0	-0.18	1.8
XVII) Inner plexiform layer	-0.53	5.7	0.03	7.29	-0.20	9.2	-0.32	3.6
XVIII) Inner nuclear layer	-0.23	5.0	0.75	9.74	0.35	14.1	-0.03	2.0
XIX) Outer plexiform layer	-0.90	8.9	-0.25	10.7	0.80	14.8	-0.2	6.0
XX) Outer nuclear layer	1.85	14.7	0.63	13.9	-0.28	4.92	-0/05	6.9
XXI) Inner retinal layer	0.18	12.0	0.63	14.1	-0.03	7.97	-0.20	7.7
Photoreceptor layer	-0.13	13.2	0.53	12.5	1.05	7.36	0.53	4.9
XXII) Retinal pigment epithelium	0.15	11.6	0.08	8.54	0.45	4.57	0.18	2.1

Retinal thickness refers to thickness from the inner limiting membrane to the external limiting membrane. Limits of Agreement are equal to the mean difference ± Coefficient of Repeatability (CoR).

doi:10.1371/journal.pone.0129005.t002

MFT and the manual RT_0 measurements taken from investigator B's analysis of the first scan ($\rho = 0.97$, P < 0.0005).

The mean thickness of the individual retinal layers at the foveal centre and at 2° and 5° eccentricity are given in Table 3. While there was no significant difference in thickness of all individual retinal layers at 2° nasal compared to temporal to fovea (P > 0.05) this was not true at 5° eccentricity, whereby the thickness of RT, RNFL, GCL, INL, ONL and IRL were significantly increased nasally compared to temporally (Table 3).

Discussion

We investigated Spectralis SD-OCT repeatability and reproducibility of manually derived and automated axial, as well as lateral foveal measurements in young healthy individuals. To our knowledge, this is the first report of repeatability and reproducibility of thickness measurements of each of eight individual retinal layers at the centre of the fovea as well as at two lateral positions derived using the newly available Spectralis segmentation software. Manual measurements of RT_0 (217 ± 16μm) and automated MFT (216 ± 15μm) in the current study compare well with those obtained in a study using the Spectralis OCT device in which a mean automated foveal thickness of 228 ± 11μm of forty subjects aged 19 to 50 years was reported [23]. Our results show that inter-observer CoR values were less than 4μm for all individual layer thicknesses. The CoR values at 2° were greater than at 0° or 5° eccentricity with the greatest difference in the RT, RNFL, GCL and IRL, most likely due to software algorithm errors. Compared to inter-observer agreement, inter-scan CoR values were greater and varied across individual layers, up to a maximum of 15μm for the GCL at 5° eccentricity nasal to the foveal centre. LoA for RT_0 were narrower for inter-observer compared to inter-scan measurements (Fig 4). There was one outlier in each case that could not be explained. In agreement with an earlier report [19], there did not appear to be any relationship between mean central retinal thickness or foveal width and repeatability. It has been shown previously that retinal thickness measurements may be affected by OCT image quality below the acceptable range stated by the OCT manufacturer [41]. This should be taken into account when examining individuals in whom the image quality is worse, for example due to cataract. Mean image quality of all scans

227
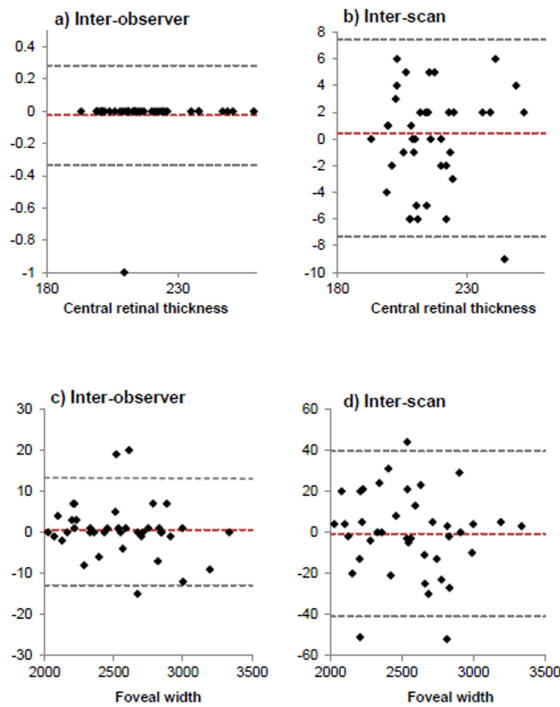
Fig 4. a-d. Bland-Altman plots to show a) Inter-observer agreement of central retinal thickness; b) Inter-scan agreement of central retinal thickness; c) Inter-observer agreement of foveal width; d) Inter-scan agreement of foveal width. All measurements presented in microns. Red line indicates mean difference, d between values. Limits of Agreement (d+1.96s) represented by upper and lower grey dashed lines respectively.

in the current study was excellent at 38dB eliminating this source of error. We did not use the reference setting option to acquire the second scan. An earlier study showed that this may unlikely affect the reproducibility of RNFL thickness in normal eyes [42]; however, this should be confirmed for all retinal layers.

A strength of our study is that all measurements were obtained from scans that had individual ocular biometry taken into account. Individual scan lengths are generated by the Spectralis software based on the subject's corneal curvature and refractive error as well as a non-modifiable pre-set axial length to minimise the effects of lateral magnification caused by the optics of the eye [32]. While we did not perform a subjective refraction on each participant, it has been shown that using an autorefractor to approximate refractive error is an accepted method [43]. In addition, optical defocus of two diopters has minimal effect on retinal thickness measurements obtained with the Spectralis [41].

It has been shown that the centre of the fovea assumed by OCT instruments and the retinal locus of fixation do not always correspond [44,45], with deviations of approximately 60 ± 50μm between fixation and the centre of the foveal avascular zone [46]. In order to

Table 3. Mean thickness of individual retinal layers at foveal centre and at 2 and 5 degrees eccentricity nasal and temporal to fovea.

| | | Eccentricity from foveal centre (degrees) | | | | | |
| | | 2 | | | 5 | | |
Retinal layer		Mean+SD		P-value	Mean+SD		P-value
Retina	nasal	296	27	0.80	350	16	**<0.0005**
	temporal	298	19		321	14	
XXIII) Retinal nerve fibre layer	nasal	17	4	0.10	22	5	**<0.0005**
	temporal	19	5		13	4	
Ganglion cell layer	nasal	26	9	0.99	60	5	**<0.0005**
	temporal	26	6		50	8	
Inner plexiform layer	nasal	29	7	0.23	47	5	0.15
	temporal	31	6		45	5	
Inner nuclear layer	nasal	25	7	0.06	42	5	**<0.0005**
	temporal	28	6		38	7	
Outer plexiform layer	nasal	28	7	0.97	29	5	0.84
	temporal	28	5		29	6	
Outer nuclear layer	nasal	80	12	0.43	72	9	**<0.0005**
	temporal	82	12		67	8	
XXIV) Inner retinal layer	nasal	208	27	0.43	271	15	**<0.0005**
	temporal	212	19		241	14	
Photoreceptor layer	nasal	88	8	0.09	80	3	0.06
	temporal	85	6		79	3	
Retinal pigment epithelium	nasal	17	3	0.09	13	2	0.30
	temporal	16	3		13	2	

P-value of independent t-test between nasal and temporal shown.

correlate some measure of visual function at fixation (e.g. visual acuity or macular pigment) with retinal anatomy at the corresponding retinal locus, it may be more appropriate to manually locate the fixation point for foveal thickness measurements. Indeed, visual inspection of OCT images with manual identification of the foveal centre was the preferred method in a study quantifying foveal thickness and visual acuity in albinism [35]. However, the repeatability of manually derived lateral and axial retinal measurements is less well documented: one study was based on manual measurements of a model eye [24], while another study explored the repeatability of manual sub-foveal choroidal thickness measurements [10]. We have shown excellent correlation between automated MFT and manually located RT_0 measurements (ρ = 0.97, P < 0.0005). The low CoR values for RT_0 (<1 µm inter-observer and <8µm inter-scan) show that the method of manually selecting the position at which to measure central retinal thickness is robust to inter-investigator and inter-scan variability. Additionally, in the current study, both investigators independently selected the same tomogram for analysis using the protocol described in the methods in all cases.

Repeatability of automated MFT and CFT has shown to vary across OCT devices and also depend on the scan protocol employed [47]. We have shown high reproducibility of automated macular thickness measurements (MFT) using the Spectralis to obtain high resolution 20° x 5° volume scans (49 B-scans 30 microns apart, ART 16 frames, 1024 A scans), indicated by the inter-scan CoR of 2.19µm. This is in accordance with a previous report in which the LoA were -2.49 to 3.77µm for inter-observer agreement of mean macular thickness measures using the

229

Spectralis [27]. The inter-scan CoR of 3.7μm for CFT also compares well with a study in which a CoR value of 2.69μm for mean macular thickness across the central 1000μm diameter was reported using the Stratus OCT device [31]. However, in an investigation involving 50 subjects with diabetic macula oedema, a higher CoR of 8.03μm was reported for Spectralis SD-OCT automated central subfield retinal thickness measurements [18]. This suggests that ocular pathology increases the level at which true clinical change has occurred as opposed to measurement variability most likely due to fixation problems. In addition, the CoR for retinal thickness in subfields surrounding the foveal centre ranged from 3.97 to 7.23μm [18]. Caution must therefore be taken when considering the level at which clinical change is deemed to occur in individuals with retinal pathology and low vision [18], and for retinal thickness changes occurring away from the centre of the fovea [48].

To our knowledge there are no reports of repeatability of manually derived lateral SD-OCT scan measurements in human subjects. We found a considerably large mean foveal width of 2550μm ± 322μm. Foveal pit diameters up to 2510μm have been reported using the Cirrus OCT [49] based on measuring the foveal pit from rim-to-rim using an automated MatLab algorithm [50]. Comparing foveal width between studies is challenging due to its variable definition. The mean foveal diameter of sixty healthy subjects was found 1244 ± 211μm measured between the points at which the nerve fibre layer ends, and 1371 ± 215μm when measured in the same subjects from foveal crest-to-crest [30]. Nevertheless we found a mean difference in foveal width of just 0.60μm between measurements obtained independently by the two investigators. This is much smaller than the difference of -14μm found in a study using the Cirrus OCT [49]. Estimation of the reproducibility of lateral foveal width measurements obtained from two scans of the same participant acquired within one visit by investigator B yielded a CoR of 40μm. This relatively large inter-scan CoR should be taken into account when investigating differences in foveal diameter between individuals, or longitudinally with time. Of note, LoA were wider for inter-scan compared to inter-observer measures of foveal width. The three outliers in both cases could not be explained. Nonetheless, when investigating change over time in a clinical setting a baseline scan image is usually set as a reference and repeated scans are subsequently compared to this. It is expected that this would improve the CoR for the lateral measurements [51].

Few studies have quantitatively assessed both inner and outer retinal morphology of the foveal pit. An earlier study reported circular symmetry of the outer retina (from the external limiting membrane to Bruch's membrane) at low eccentricities [52]. Our results indicate that the individual inner and outer retinal layers are all symmetrical at low eccentricities. In contrast, at 5° eccentricity there were significant differences in thickness of RT, RNFL, GCL, INL, ONL and IRL (Table 3). Asymmetry of the RNFL and GCL is not surprising given the distribution of the RNFL, with the thinnest peripapillary RNFL thickness found within the papillomacular bundle [42,53]. The evaluation of inner and outer retinal layer symmetry in the current study may be useful in future investigations of foveal morphology [54]. Choroidal thickness [10] and the length of the photoreceptor layers [35] are increasingly being used as both diagnostic and visual prognostic indicators in a variety of retinal disease states such as albinism [35]; and neuronal GCL loss has been evaluated in eyes of patients with multiple sclerosis [55]. Further work is needed however to estimate the reliability of measurements in eyes with macular pathology where poor fixation and disruptions in retinal morphology might make these measurements more variable [56].

We estimated the measurement error of our manually derived axial and lateral retinal measurement methods. Measurement error may be caused by instrument and software algorithm errors as well as operator error. Our results show that manually finding the location at which to extract central retinal thickness measurements is robust to inter-investigator repeatability.

We also showed good reproducibility of individual retinal layer thickness measurements obtained from two scans acquired within a single visit. The inter-observer CoR values are actually smaller than the digital axial resolution of 3.9μm achievable with high resolution Spectralis SD-OCT (Spectralis technical guidelines) [25], indicating that there is very good repeatability of manual axial retinal thickness measurements between two observers looking at the same scan.

Conclusion

Our findings show excellent repeatability and reproducibility of thickness measurements of each of eight individual retinal layers at manually derived axial and lateral foveal locations obtained using new Spectralis SD-OCT segmentation software in a young, healthy cohort. The inter-observer CoR values for each retinal layer give an indication of the level at which thickness and foveal width variation is indicative of true difference as opposed to measurement variability. The inter-scan CoR values signify the level at which change over time in axial and lateral measurements within an individual can be considered when the baseline reference scan feature of the Spectralis is not utilised. The method of manually selecting the position at which to measure central retinal thickness is robust to inter-investigator and inter-scan variability. We have demonstrated excellent correlation between automated and manually derived central retinal thickness measurements. Additionally, we have shown that the individual retinal layers are horizontally symmetrical at 2°, but not at 5° eccentricity. These results could provide valuable information for future studies involving foveal morphology specifically examining the individual retinal layers.

Acknowledgments

Author Contributions

Conceived and designed the experiments: IC BH. Performed the experiments: IC BH. Analyzed the data: IC BH. Wrote the paper: IC BH.

References

1. Huang D, Swanson EA, Lin CP, Schuman JS, Stinson WG, Chang W, et al. Optical coherence tomography. Science. 1991; 254(5035):1178–81. PMID: 1957169

2. Anger EM, Unterhuber A, Hermann B, Sattmann H, Schubert C, Morgan JE, et al. Ultrahigh resolution optical coherence tomography of the monkey fovea. Identification of retinal sublayers by correlation with semithin histology sections. Exp Eye Res. 2004; 78(6):1117–25. PMID: 15109918

3. Vajzovic L, Hendrickson AE, O'Connell RV, Clark LA, Tran-Viet D, Possin D, et al. Maturation of the human fovea: Correlation of spectral-domain optical coherence tomography findings with histology. Am J Ophthalmol. 2012; 154(5):779–89. doi: 10.1016/j.ajo.2012.05.004 PMID: 22898189

4. Spaide RF, Curcio CA. Anatomical correlates to the bands seen in the outer retina by optical coherence tomography: Literature review and model. Retina. 2011; 31(8):1609. doi: 10.1097/IAE.0b013e3182247535 PMID: 21844839

5. Regatieri CV, Branchini L, Duker JS. The role of spectral-domain OCT in the diagnosis and management of neovascular age-related macular degeneration. Ophthalmic Surg Lasers. 2011; 42:S56.

6. Oh J, Smiddy WE, Flynn HW, Gregori G, Lujan B. Photoreceptor inner/outer segment defect imaging by spectral domain OCT and visual prognosis after macular hole surgery. Invest Ophthalmol Vis Sci. 2010; 51(3):1651–8. doi: 10.1167/iovs.09-4420 PMID: 19850825

231

7. Mojana F, Cheng L, Bartsch D-UG, Silva GA, Kozak I, Nigam N, et al. The role of abnormal vitreomacular adhesion in age-related macular degeneration: Spectral optical coherence tomography and surgical results. Am J Ophthalmol. 2008; 146(2):218–27. doi: 10.1016/j.ajo.2008.04.027 PMID: 18538742

8. Moreno-Montañés J, Olmo N, Alvarez A, García N, Zarranz-Ventura J. Cirrus high-definition optical coherence tomography compared with stratus optical coherence tomography in glaucoma diagnosis. Invest Ophthalmol Vis Sci. 2010; 51(1):335–43. doi: 10.1167/iovs.08-2988 PMID: 19737881

9. Chakravarthy U, Williams M. The Royal College of Ophthalmologists guidelines on AMD: Executive summary. Eye. 2013; 27:1429–31. doi: 10.1038/eye.2013.233 PMID: 24158023

10. Lee S, Fallah N, Forooghian F, Ko A, Pakzad-Vaezi K, Merkur AB, et al. Comparative analysis of repeatability of manual and automated choroidal thickness measurements in nonneovascular age-related macular degeneration. Invest Ophthalmol Vis Sci. 2013; 54(4):2864–71. doi: 10.1167/iovs.12-11521 PMID: 23538060

11. Chiu SJ, Izatt JA, O'Connell RV, Winter KP, Toth CA, Farsiu S. Validated automatic segmentation of AMD pathology including drusen and geographic atrophy in SD-OCT images. Invest Ophthalmol Vis Sci. 2012; 53(1):53–61. doi: 10.1167/iovs.11-7640 PMID: 22039246

12. Leung CK, Cheung CY, Weinreb RN, Lee G, Lin D, Pang CP. Comparison of macular thickness measurements between time domain and spectral domain optical coherence tomography. Invest Ophthalmol Vis Sci. 2008; 49(11):4893–7. doi: 10.1167/iovs.07-1326 PMID: 18450592

13. Nassif N, Cense B, Hyle Park B, Yun SH, Chen TC, Bouma BE, et al. *In vivo* human retinal imaging by ultra high-speed spectral domain optical coherence tomography. Optics Letters. 2004; 29(5):480–2. PMID: 15005199

14. Seigo MA, Sotirchos ES, Newsome S, Babiarz A. In vivo assessment of retinal neuronal layers in multiple sclerosis with manual and automated optical coherence tomography segmentation techniques. J Neurol. 2012; 259(10):2119–30. doi: 10.1007/s00415-012-6466-x PMID: 22418995

15. Tan CSH, Li KZ, Lim TH. A novel technique of adjusting segmentation boundary layers to achieve comparability of retinal thickness and volumes between spectral domain and time domain optical coherence tomography. Invest Ophthalmol Vis Sci. 2012; 53(9):5515–9. doi: 10.1167/iovs.12-9868 PMID: 22786905

16. Wolf-Schnurrbusch UEK, Ceklic L, Brinkmann CK, Iliev ME, Frey M, Rothenbuehler SP, et al. Macular thickness measurements in healthy eyes using six different optical coherence tomography instruments. Invest Ophthalmol Vis Sci. 2009; 50(7):3432–7. doi: 10.1167/iovs.08-2970 PMID: 19234346

17. Krebs I, Smretschnig E, Moussa S, Brannath W, Womastek I, Binder S. Quality and reproducibility of retinal thickness measurements in two spectral-domain optical coherence tomography machines. Invest Ophthalmol Vis Sci. 2011; 52(9):6925–33. doi: 10.1167/iovs.10-6612 PMID: 21791591

18. Comyn O, Heng LZ, Ikeji F, Bibi K, Hykin PG, Bainbridge JW, et al. Repeatability of Spectralis OCT measurements of macular thickness and volume in diabetic macular edema. Invest Ophthalmol Vis Sci. 2012; 53(12):7754–9. doi: 10.1167/iovs.12-10895 PMID: 23111610

19. Patel PJ, Chen FK, Ikeji F, Xing W, Bunce C, Da Cruz L, et al. Repeatability of stratus optical coherence tomography measures in neovascular age-related macular degeneration. Invest Ophthalmol Vis Sci. 2008; 49(3):1084–8. doi: 10.1167/iovs.07-1203 PMID: 18326734

20. Patel PJ, Chen FK, Ikeji F, Tufail A. Intersession repeatability of optical coherence tomography measures of retinal thickness in early age-related macular degeneration. Acta Ophthalmol. 2011; 89 (3):229–34. doi: 10.1111/j.1755-3768.2009.01659.x PMID: 19845557

21. Pinilla IMDP, Garcia-Martin EMD, Fernandez-Larripa SMD, Fuentes-Broto LP, Sanchez-Cano AIP, Abecia EMDP. Reproducibility and repeatability of cirrus and spectralis fourier-domain optical coherence tomography of healthy and epiretinal membrane eyes. Retina. 2013; 33(7):1448–55. doi: 10.1097/IAE.0b013e3182807683 PMID: 23538575

22. Bressler SB. Reproducibility of spectral-domain optical coherence tomography retinal thickness measurements and conversion to equivalent time-domain metrics in diabetic macular edema. JAMA Ophthalmol. 2014; 132(9):1113. doi: 10.1001/jamaophthalmol.2014.1698 PMID: 25058482

23. Carpineto P, Nubile M, Toto L, Aharrh Gnama A, Marcucci L, Mastropasqua L, et al. Correlation in foveal thickness measurements between spectral-domain and time-domain optical coherence tomography in normal individuals. Eye. 2009; 24(2):251–8. doi: 10.1038/eye.2009.76 PMID: 19390564

24. Folgar FA, Yuan EL, Farsiu S, Toth CA. Lateral and axial measurement differences between spectral-domain optical coherence tomography systems. J Biomed Opt. 2014. doi: 10.1117/1. JBO.19.1.016014

25. Heidelberg Engineering. Spectralis HRA + OCT User manual software version 5.7. 2013.

232

26. Menke MN, Dabov S, Knecht P, Sturm V. Reproducibility of retinal thickness measurements in healthy subjects using spectralis optical coherence tomography. Am J Ophthalmol. 2009; 147(3):467–72. doi: 10.1016/j.ajo.2008.09.005 PMID: 19026403

27. Pierro L, Giatsidis SM, Mantovani E, Gagliardi M. Macular thickness interoperator and intraoperator reproducibility in healthy eyes using 7 optical coherence tomography instruments. Am J Ophthalmol. 2010; 150(2):199–204. doi: 10.1016/j.ajo.2010.03.015 PMID: 20570233

28. Thibos L, Wheeler W, Horner D. Power vectors: An application of fourier analysis to the description and statistical analysis of refractive error. Optom Vis Sci. 1997; 74(6): 367–75. PMID: 9255814

29. Paunescu LA, Schuman JS, Price LL, Stark PC, Beaton S, Ishikawa H, et al. Reproducibility of nerve fiber thickness, macular thickness, and optic nerve head measurements using Stratus OCT. Invest Ophthalmol Vis Sci. 2004; 45(6):1716–24. PMID: 15161831

30. Nolan JM, Stringham JM, Beatty S, Snodderly DM. Spatial profile of macular pigment and its relationship to foveal architecture. Invest Ophthalmol Vis Sci. 2008; 49(5):2134–42. doi: 10.1167/iovs.07-0933 PMID: 18436846

31. Polito A, Del Borrello M, Isola M, Zemella N, Bandello F. Repeatability and reproducibility of fast macular thickness mapping with stratus optical coherence tomography. Arch Ophthalmol. 2005; 123 (10):1330–7. PMID: 16219723

32. Ctori I, Gruppetta S, Huntjens B. The effects of ocular magnification on Spectralis spectral domain optical coherence tomography scan length. Graefes Arch Clin Exp Ophthalmol. 2014. doi: 10.1007/s00417-014-2915-9

33. Tick S, Rossant F, Ghorbel I, Gaudric A, Sahel JA, Chaumet-Riffaud P, et al. Foveal shape and structure in a normal population. Invest Ophthalmol Vis Sci. 2011; 52(8):5105–10. doi: 10.1167/iovs.10-7005 PMID: 21803966

34. Hammer DX, Iftimia NV, Ferguson RD, Bigelow CE, Ustun TE, Barnaby AM, et al. Foveal fine structure in retinopathy of prematurity: An adaptive optics fourier domain optical coherence tomography study. Invest Ophthalmol Vis Sci. 2008; 49(5):2061–70. doi: 10.1167/iovs.07-1228 PMID: 18223243

35. Mohammad S, Gottlob I, Kumar A, Thomas M, Degg C, Sheth V, et al. The functional significance of foveal abnormalities in albinism measured using spectral-domain optical coherence tomography. Ophthalmology. 2011; 118(8):1645–52. doi: 10.1016/j.ophtha.2011.01.037 PMID: 21570122

36. van der Veen RLP, Ostendorf S, Hendrikse F, Berendschot TTJM. Macular pigment optical density relates to foveal thickness. Eur J Ophthalmol. 2009; 19(5):836–41. PMID: 19787606

37. Early Treatment Diabetic Retinopathy Study research group. Photocoagulation for diabetic macular edema. Early Treatment Diabetic Retinopathy Study Report No.1. Arch Ophthalmol. 1985; 103:1796–806 doi: 10.1001/archopht.1985.01050120030015 PMID: 2866759

38. Bland JM, Altman DG. Statistical methods for assessing agreement between two methods of clinical measurement. Lancet. 1986; 1(8476):307–10. PMID: 2868172

39. Bland JM, Altman DG. Measuring agreement in method comparison studies. Statistical methods in medical research. 1999; 8(2):135–60. PMID: 10501650

40. McAlinden C, Khadka J, Pesudovs K. Statistical methods for conducting agreement (comparison of clinical tests) and precision (repeatability or reproducibility) studies in optometry and ophthalmology. Ophthalmic Physiol Opt. 2011; 31(4):330–8. doi: 10.1111/j.1475-1313.2011.00851.x PMID: 21615445

41. Balasubramanian M, Bowd C, Vizzeri G, Weinreb RN, Zangwill LM. Effect of image quality on tissue thickness measurements obtained with spectral-domain optical coherence tomography. Opt Express. 2009; 17(5):4019–36. PMID: 19259243

42. Langenegger SJ, Funk J, Töteberg-Harms M. Reproducibility of retinal nerve fiber layer thickness measurements using the eye tracker and the retest function of spectralis SD-OCT in glaucomatous and healthy control eyes. Invest Ophthalmol Vis Sci. 2011; 52(6):3338–44. doi: 10.1167/iovs.10-6611 PMID: 21330656

43. Pesudovs K, Weisinger HS. A comparison of autorefractor performance. Optom Vis Sci. 2004; 81 (7):554–8. PMID: 15252356

44. Putnam NM, Hofer HJ, Doble N, Chen L, Carroll J, Williams DR. The locus of fixation and the foveal cone mosaic. J Vision. 2005; 5(7):632–9. doi: 10.1167/5.7.3

45. El-Ashry M, Hegde V, James P, Pagliarini S. Analysis of macular thickness in British population using optical coherence tomography (OCT): An emphasis on interocular symmetry. Curr Eye Res. 2008; 33:693–9. doi: 10.1080/02713680802323140 PMID: 18696345

46. Zeffren BS, Applegate RA, Bradley A, van Heuven WA. Retinal fixation point location in the foveal avascular zone. Invest Ophthalmol Vis Sci. 1990; 31(10):2099–105. PMID: 2211007

233

47. Eriksson U, Alm A. Repeatability in and interchangeability between the macular and the fast macular thickness map protocols: A study on normal eyes with Stratus optical coherence tomography. Acta Ophthalmol. 2009; 87(7):725–30. doi: 10.1111/j.1755-3768.2008.01345.x PMID: 18937816

48. Gilmore ED, Hudson c. Eccentricity and measurement variability and repeatability with the retinal thickness analyser. Br J Ophthalmol. 2004; 88:62–5. PMID: 14693775

49. Wagner-Schuman M, Dubis AM, Nordgren RN, Lei Y, Odell D, Chiao H, et al. Race- and sex-related differences in retinal thickness and foveal pit morphology. Invest Ophthalmol Vis Sci. 2011; 52(1):625–34. doi: 10.1167/iovs.10-5886 PMID: 20861480

50. Dubis AM, McAllister JT, Carroll J. Reconstructing foveal pit morphology from optical coherence tomography imaging. Br J Ophthalmol. 2009; 93:1223–7. doi: 10.1136/bjo.2008.150110 PMID: 19474001

51. Fiore T, Lupidi M, Androudi S, Giansanti F, Fruttini D, Cagini C. Repeatability of retinal macular thickness measurements in healthy subjects and diabetic patients with clinically significant macular edema: Evaluation of the follow-up system of Spectralis optical coherence tomography. Ophthalmologica. 2015. doi: 10.1159/000380832

52. Srinivasan VJ, Monson BK, Wojtkowski M, Bilonick RA, Gorczynska I, Chen R, et al. Characterization of outer retinal morphology with high-speed, ultrahigh-resolution optical coherence tomography. Invest Ophthalmol Vis Sci. 2008; 49(4):1571–9. doi: 10.1167/iovs.07-0838 PMID: 18385077

53. Varma R, Skaf M, Barron E. Retinal nerve fiber layer thickness in normal human eyes. Ophthalmology. 1996; 103(12):2114–9. PMID: 9003346

54. Matsumoto H, Sato T, Kishi S. Outer nuclear layer thickness at the fovea determines visual outcomes in resolved central serous chorioretinopathy. Am J Ophthalmol. 2009; 148(1):105–10. doi: 10.1016/j.ajo.2009.01.018 PMID: 19327740

55. Saidha S, Syc SB, Durbin MK, Eckstein C, Oakley JD, Meyer SA, et al. Visual dysfunction in multiple sclerosis correlates better with optical coherence tomography derived estimates of macular ganglion cell layer thickness than peripapillary retinal nerve fiber layer thickness. Mult Scler. 2011; 17(12):1449–63. doi: 10.1177/1352458511418630 PMID: 21865411

56. Meyer zu Westrup V, Dietzel M, Pauleikhoff D, Hense H-W. The association of retinal structure and macular pigment distribution. Invest Ophthalmol Vis Sci. 2014; 55(2):1169–75. doi: 10.1167/iovs.13-12903 PMID: 24474270

234

6.4   Participant information sheet

CITY UNIVERSITY LONDON
EST 1894

Division of Optometry and Visual Science
Tait Building
Northampton Square
London EC1V 0HB

INFORMATION SHEET

Title of study:
An investigation of ethnic differences in the spatial profile of macular pigment and its relation to foveal anatomy.

Invitation
We would like to invite you to take part in a research study. Before you decide whether you would like to participate it is important that you understand why the research is being done and what it would involve for you. Please take time to read the following sheet carefully and discuss it with others if you wish. Ask us if there is anything that is not clear or if you would like more information.

What is the purpose of the study?
Age-related macular degeneration (AMD) is one of the leading causes of irreversible blindness in the western world. It is characterized by a degenerative disorder of the central area of the retina (the macula), causing significant visual loss. Risk factors for developing AMD have been identified and include ethnicity and levels of macular pigment (MP).

Repeated exposure to blue light and free radicals is associated with the prevalence of AMD. It is thought that the function of MP is the neutralisation of free radicals and the filtering of harmful blue light. In this way, MP is thought to protect the macula, thus reducing the likelihood of AMD.

It has been shown that the amount of MP varies between individuals. It has also been suggested that the density and distribution of MP varies between ethnicities. However, there is little research regarding the effect of ethnicity on the variations in the amount of MP between individuals. Levels of MP may also be associated with the thickness of the macula and other retinal anatomical features.

The aim of the main study is to investigate the effect of ethnicity on MP levels in relation to the anatomy of the retina.

Within the main study are three sub-studies:
- Repeatability of the MAP test (used to determine MP)
- Repeatability of OCT scan measurements (used for retinal anatomy)
- Gender differences in retinal anatomy in an adult South Asian population

Why have I been invited?
We would like to invite 100 White, 100 South Asian (born in, or parents from Bangladesh/Pakistan/India) and 100 Black participants aged between 18 and 40 years old to take part in this study.

Do I have to take part?
Taking part in this study is voluntary and you can withdraw at any time. You should ask questions if there are aspects that you do not understand or if you need further information. It is up to you to decide whether or not to take part. If you do decide to take part you will be asked to sign a consent form, but you are still free to withdraw at any time and without giving a reason.

CITY UNIVERSITY
LONDON
EST 1894

(For students) Will my grades be affected?
Volunteering, deciding not to participate, or withdrawing from the study at any time will not affect your grades.

What will happen if I take part?
If you decide to take part, you will visit City University London to take part in vision tests. Typically, this will be one visit that is expected to last approximately 45 minutes. We are also looking to repeat the measurements in a smaller group of around 40 people. If you wish to participate in any of the sub-studies, a second appointment (about a week later) will be arranged for you. The second visit will last around 10 to 20 minutes.

You will also be given a health and lifestyle questionnaire to complete and bring with you to the visit. The researcher may contact you by email, text or telephone to remind you of your appointments.

What do I have to do?
At the beginning of the first visit you will sign a consent form agreeing to take part in the study. The researcher will go over the health and lifestyle questionnaire with you in case of any questions. Your visual acuity, the length of the eye and your spectacle prescription will be measured, as well as your height and weight. **If you wear contact lenses, it would be preferable for you to wear your glasses for the visit. Alternatively, bring a contact lens case (with suitable storage solution), as you will need to remove your contact lenses for some of the measurements.**

Your MP levels will be measured using the MAP test (developed at City University). For this, you are asked to observe a VDU screen. A flickering target is presented. The researcher alters the intensity of the test beam until you are no longer seeing any flicker. The macula will be imaged using a digital imaging device (Spectralis OCT). This is a non-invasive technique that takes a scan of the retina and measures the thickness of the retinal layers.

For the repeatability study, the second visit will involve visual acuity measurement, followed by one MAP test measurement.

How long will the research study last?
This study will take place between 1st September 2013 and 1st October 2015. Irene Ctori will book appointments. Please email ▮▮▮▮▮▮▮▮▮▮▮▮

Where is the research taking place?
Division of Optometry and Visual Science
Tait Building, Northampton Square, City University London

What are the possible disadvantages and risks of taking part?
We know of no risks involved by taking part in this study.

What are the possible benefits of taking part?
Whilst the knowledge gained from this study may be of no immediate benefit to you; the results will provide a better understanding of the presentation of macular pigment in different ethnicities.

CITY UNIVERSITY LONDON
EST 1894

Division of Optometry and Visual Science
Tait Building
Northampton Square
London EC1V 0HB

What will happen when the research study stops?
All collected data will be kept securely in accordance with the University and Data Protection Act guidelines. Disposal of data after the obligatory retention period will be done in a secure manner according to the University policy.

Will my taking part in the study be kept confidential?
Your identity will be recorded against the findings but will not be stored on any computer. This information will be kept in a locked filing cabinet in the Optometry and Visual Science Division, City University London. Only the investigators will have access to this information. Your identity is needed in case we wish to contact you at a later date. All data will be anonymised. The results obtained will be analysed and probably published but your identity will never be unveiled.

What will happen to results of the research study?
We aim to publish the findings in an internationally peer reviewed journal. You will be given an oral summary of any significant results. Please note that although these procedures may give you useful information about your vision, they are not a full eye test that can be used for diagnostic purposes, and are no substitute for regular visits to your optometrist.

What will happen if I don't want to carry on with the study?
You are free to withdraw from the study without an explanation or penalty at any time.

Who has reviewed the study?
City University London Optometry Proportionate Review Research Ethics Committee has approved this study.

What if there is a problem?
If you would like to complain about any aspect of the study, City University London has established a complaints procedure via the Secretary to the University's Senate Research Ethics Committee. To complain about the study, you need to phone 020 7040 3040. You can then ask to speak to the Secretary to Senate Research Ethics Committee and inform them that the name of the project is: "An investigation of ethnic differences in the spatial profile of macular pigment and its relation to foveal anatomy''.

You could also write to the Secretary at:

Secretary to Senate Research Ethic Committee
Research Office, E214
City University London
Northampton Square, London EC1V 0HB
Email:

Further information and contact details
In case you have any further queries regarding this study, please feel free to contact Irene Ctori by email

Thank you for taking the time to read this information sheet.

6.5 Participant's consent form

CITY UNIVERSITY LONDON
EST 1894

Division of Optometry and Visual Science
Tait Building
Northampton Square
London EC1V 0HB

Consent Form

Title of study: An investigation of ethnic differences in the spatial profile of macular pigment and its relation to foveal anatomy.

Please initial box

1.	I agree to take part in the above City University London research project. I have had the project explained to me, and I have read the participant information sheet, which I may keep for my records. I understand this will involve: • Completing questionnaires asking me about my general health, regular medication, family history, age, ethnicity, gender, and smoking status. • Allowing the researcher to measure my height and weight. • Allowing the researcher to measure my visual acuity, eye length (IOL Master), corneal curvature (keratometry) and refractive error (autorefractor). • Allowing the researcher to test my macular pigment (using the MAP test). • Allowing the researcher to take macular scans (with OCT). • Allowing the researcher to remind me of my appointments (by email, text or telephone).	
2.	I understand that my participation is voluntary, that I can choose not to participate in part or all of the project, and that I can withdraw at any stage of the project without being penalized or disadvantaged in any way.	
3.	This information will be held and processed for the following purpose(s): • Publication in peer reviewed journals • Presentation at conferences I understand that any information I provide is confidential, and that no information that could lead to the identification of any individual will be disclosed in any reports on the project, or to any other party. No identifiable personal data will be published. The identifiable data will not be shared with any other organisation. I understand that the data will be de-identified to protect my identity from being made public.	
4.	I agree to City University London recording and processing this information about me. I understand that this information will be used only for the purposes set out in this statement and my consent is conditional on the University complying with its duties and obligations under the Data Protection Act 1998.	
5.	I agree to take part in the above study.	

_____   _____
Name of Participant   Signature

Date:

6.6   Health and lifestyle questionnaire

CITY UNIVERSITY LONDON
EST 1894

Division of Optometry and Visual Science
Tait Building
Northampton Square
London EC1V 0HB

Title of study: An investigation of ethnic differences in the spatial profile of macular pigment and its relation to foveal anatomy.

Health and Lifestyle Questionnaire

Should you need any advice on completing the questionnaire please email:

Please bring this completed questionnaire with you to your visit. If you wear contact lenses, remember to bring a contact lens case with solution, or preferably wear your glasses.

1.   PERSONAL DETAILS

First name: ..………………………………..…………………….

Surname: ..………………………………..…………………….

Gender: Male   Female

Age: ……….   Date of Birth _ _ /_ _ /_ _ _ _

Contact address for correspondence:

....
....

Telephone number:

....

Email address:

....

Go to Question 2.

CITY UNIVERSITY LONDON

Division of Optometry and Visual Science
Tait Building
Northampton Square
London EC1V 0HB

2. ETHNICITY

Choose one option that best describes your ethnic group or background.

(From Office of National Statistics)

a. White

English / Welsh / Scottish / Northern Irish / British
Irish
Gypsy or Irish Traveller
Other White background (please describe):

b. Mixed / Multiple ethnic groups

White and Black Caribbean
White and Black African
White and Asian
Other Mixed background (please describe):

c. Asian or Asian British

Indian
Pakistani
Bangladeshi
Other Asian background (please describe):

d. Black or Black British

African
Caribbean
Other Black background, please describe:

e. Other ethnic group

Chinese
Other ethnic group (please describe):

3. GENERAL HEALTH

3.a. Medical conditions

i. Do you suffer from any medical conditions?   Yes   No
If yes, please state:
....
....

ii. Do you suffer from epilepsy?   Yes   No

iii. Are you pregnant?   Yes   No

CITY UNIVERSITY LONDON

3.b.   Medication

i.   Do you take any regular medication?   Yes   No
If yes, please state:
....
....

ii.   Do you regularly use any eye drops?   Yes   No
If yes, please state:
....
....

3.c.   Supplements

i.   Do you take any supplements/vitamins?   Yes   No
If yes, please state:
....
....

ii.   Have you ever taken any macular pigment supplements?
(Such as MacuShield or PreserVision)   Yes   No

If yes, go to questions iii and iv.   If no, go to question 3.d.

iii.   State the name or brand of supplement below:
....

iv.   How long have you used the supplement for?
....

3.d. Smoking status

i.   Do you smoke?   Yes   No

If yes, go to questions ii and iii.   If no, go to question iv.

ii.   How many cigarettes do you smoke per day?   …………….................

iii.   Approximately how many years have you smoked for? …….……………

iv.   Have you smoked in the past?   Yes   No

If yes, go to questions v to vii.   If no, go to question 3.e.

v.   How many cigarettes per day did you smoke? ……………..…………….

vi.   How many years did you smoke for?..

vii.   When did you stop smoking? ……………………………..………………..

CITY UNIVERSITY LONDON
EST 1894

3.e.   Alcohol consumption
On average, how many units of alcohol do you consume per week?
…………………………………………………………………...………………..

(From: www.nhs.uk/Livewell/alcohol/Pages/alcohol-units.aspx)

A small glass red/white/rosé wine (125ml)	= 1.5 units
A standard glass red/white/rosé wine (175ml)	= 2.1 units
A large glass red/white/rosé wine (250ml)	= 3 units
A pint low strength lager/beer/cider	= 3 units
A bottle (330ml) of lager/beer/cider	= 1.7 units
A can (440ml) lager/beer/cider	= 2 units
A bottle alcopop (275ml)	= 1.5 units
A single small (25ml) shot of spirits*	= 1 unit
A single large (35ml) shot of spirits*	= 1.4 units
*gin, rum, vodka, whisky, tequila, Sambuca	

3.e.   Diet
Which of the following best describes your dietary background over the last 2 years?

Meat eater   Vegetarian   Vegan

4.   EYE HEALTH

4.a.   Do you wear glasses or contact lenses?   Yes   No

If yes, go to questions i and ii.   If no, go to question 4.b.

i.   Do you wear glasses or contact lenses:
□ Full time   □ Part-time   □ Occasional use only

4.b.   Do you suffer from any eye conditions?
(Not including refractive error)   Yes   No

If yes, go to questions i and ii.   If no, go to question 4.c.

i.   What is the name of the condition (if known)?......................................

ii.   How does your eye condition affect your vision?
....
....

4.c.   Have you ever had refractive surgery?   Yes   No

4.d.   What colour eyes do you consider yourself as having?

Light (blue, green, grey)   Dark (brown, hazel)

CITY UNIVERSITY LONDON

5. FAMILY HISTORY

5.a. Do you have any family history of age-related macular degeneration (AMD)?   Yes   No

If yes, go to questions i and ii.   If no, go to question 6.

i. Which family member has AMD?
   Mother / Father   Brother / Sister
   Other (give details)…………………………………………………………...

ii. If known, please indicate which type:
   Dry AMD   Wet AMD

6. GENERAL INFORMATION

6.a Country of residence
i. Have you always lived in the UK?   Yes   No

If you have lived abroad for more than a year please give details:
ii. Where?   …………………………...……………………….................
iii. When?   …………………………...……………………….................
iv. For how long? …………………………...……………………….................

6.b. Sun exposure, skin and hair type

i. Approximately how many hours a week do you spend outdoors (exposed to daylight) in:

Autumn/Winter? ……   Spring/Summer? ……..

ii. Do you wear sunglasses in bright conditions?   Yes   No

iii. Please indicate which of the following best describes your skin type:
   skin type I: always burns, never tans
   skin type II: usually burns, tans less than average
   skin type III: sometimes mild burns, tans about average
   skin type IV: rarely burns, tans more than average
   skin type V: brown skinned
   skin type VI: black skinned

iv. Please indicate your (un-dyed) hair colour:
   light blonde   dark blonde   red
   brown   black

-------THE END-------

Health and Lifestyle Questionnaire   irene.ctori.2@city.ac.uk   5

6.7 List of publications and presentations

Publications

Ctori, I and Huntjens, B. 2015. The effect of ethnicity on the association between macular pigment distribution and foveal anatomy in healthy individuals. European Journal of Ophthalmology, 25 (4): e59-e73. *[Abstract]*

Ctori, I and Huntjens, B. 2015. Repeatability of foveal measurements using Spectralis OCT segmentation software." *PloS One,* 10 (6), e0129005.

Ctori, I; Grupetta, S; Huntjens, B. 2014. The effects of ocular magnification on Spectralis spectral domain optical coherence tomography scan length. *Graefe's Archive for Clinical and Experimental Ophthalmology*, 253 (5), 733-738.

Huntjens, B; Asaria, TS; Dhanani, S; Konstantakopoulou, E; **Ctori, I.** 2014**.** Macular pigment spatial profiles in South Asian and white subjects. *Investigative Ophthalmology and Visual Science*, 55:1440-1446.

Ctori, I and Huntjens, B. 2014. Variations in macular pigment, its spatial profile and crystalline lens optical density. A study of south Asian and white individuals. *Ophthalmic and Physiological Optics*, 34(6):694. *[Abstract]*

Ctori, I and Huntjens, B. 2014. Does foveal anatomy influence macular pigment and its spatial profile? A bi-racial study. *Acta Ophthalmologica*, 92(s253) *[Abstract]*

Huntjens, B and **Ctori, I**. 2014. Variations and repeatability of macular pigment and its spatial profiles in South Asian and white subjects. *Acta Ophthalmologica,* 92(s253) *[Abstract]*

Presentations

British Congress of Optometry and Vision Science, City University London, September 2015
Poster presentation "Macular pigment spatial distribution and its association with foveal anatomy. Does ethnicity matter?

Macular Carotenoids Conference, Cambridge, July 2015

Poster presentation "The effect of ethnicity on the association between macular pigment distribution and foveal anatomy in healthy individuals"

City University London, Learning Enhancement and Development Symposium, March 2015

Oral presentation "Classification of the macular pigment spatial profile. Are our eyes deceiving us?"

City University London, 3-Minute Thesis Competition, March 2015

Oral Presentation "Variations in macular pigment: the eye's internal sunglasses"

City University London, School of Health Science Colloquial Session, November 2014

Oral presentation "Does the anatomy of the fovea influence the distribution of macular pigment? A study of two ethnic groups"

European Association for Vision and Eye Research, Nice, October 2014

Oral presentation "Does foveal anatomy influence macular pigment and its spatial profile? A bi-racial study"

Poster presentation "Variations and repeatability of macular pigment and its spatial profiles in South Asian and white subjects"

British Congress of Optometry and Vision Science, Cardiff University, September 2014

Poster presentation "Variations in macular pigment, its spatial profile and crystalline lens optical density. A study of South Asian and white individuals"

City University London, School of Health Science Annual Research Symposium, April 2014

Oral presentation "The relationship of the macular pigment spatial profile and foveal anatomy between South Asian and white females"

City University London, School of Health Science Annual Research Symposium, April 2013

Poster presentation "An investigation of ethnic differences in the spatial profile of macular pigment"

This page is intentionally left blank

7 References

Abell, R. G., Hewitt, A. W., Andric, M., Allen, P. L. & Verma, N. 2014. The use of heterochromatic flicker photometry to determine macular pigment optical density in a healthy Australian population. *Graefe's Archive for Clinical and Experimental Ophthalmology,* 252 (3), 417-421.

Almeida, M. S. & Carvalho, L. A. 2007. Different schematic eyes and their accuracy to the in vivo eye: a quantitative comparison study. *Brazilian Journal of Physics,* 37, 378-387.

Anger, E. M., Unterhuber, A., Hermann, B., Sattmann, H., Schubert, C., Morgan, J. E., Cowey, A., Ahnelt, P. K. & Drexler, W. 2004. Ultrahigh resolution optical coherence tomography of the monkey fovea. Identification of retinal sublayers by correlation with semithin histology sections. *Experimental Eye Research,* 78 (6), 1117-1125.

Asefzadeh, B., Cavallerano, A. A. & Fisch, B. M. 2007. Racial differences in macular thickness in healthy eyes. *Optometry and Vision Science,* 84 (10), E941-E945.

Atchinson, D. A. & Smith, G. 2000. *Schematic eyes.* Oxford: Butterworth Heinemann.

Balasubramanian, M., Bowd, C., Vizzeri, G., Weinreb, R. N. & Zangwill, L. M. 2009. Effect of image quality on tissue thickness measurements obtained with spectral-domain optical coherence tomography *Optics Express,* 17 (5), 4019-4036.

Barbur, J. L., Konstantakopoulou, E., Rodriguez-Carmona, M., Harlow, J. A., Robson, A. G. & Moreland, J. D. 2010. The Macular Assessment Profile test - a new VDU-based technique for measuring the spatial distribution of the macular pigment, lens density and rapid flicker sensitivity. *Ophthalmic and Physiological Optics,* 30 (5), 470-483.

Barker, F. M., Snodderly, D. M., Johnson, E. J., Schalch, W., Koepcke, W., Gerss, J. & Neuringer, M. 2011. Nutritional manipulation of primate retinas, V: effects of lutein, zeaxanthin, and n-3 fatty acids on retinal sensitivity to blue-light-induced damage. *Investigative Ophthalmology and Visual Science,* 52 (7), 3934-3942.

Bartlett, H., Acton, J. & Eperjesi, F. 2010a. Clinical evaluation of the MacuScope macular pigment densitometer. *The British Journal of Ophthalmology,* 94 (3), 328-331.

Bartlett, H. & Eperjesi, F. 2011. Apparent motion photometry: evaluation and reliability of a novel method for the measurement of macular pigment. *The British Journal of Ophthalmology,* 95 (5), 662-665.

Bartlett, H., Stainer, L., Singh, S., Eperjesi, F. & Howells, O. 2010b. Clinical evaluation of the MPS 9000 macular pigment screener. *The British Journal of Ophthalmology,* 94 (6), 753-756.

Bayraktar, S., Bayraktar, Z. & Yilmaz, Ö. F. 2001. Influence of scan radius correction for ocular magnification and relationship between scan radius with retinal nerve fiber layer thickness measured by optical coherence tomography. *Journal of Glaucoma,* 10 (3), 163-169.

Beatty, S., Koh, H. H., Carden, D. & Murray, I. J. 2000a. Macular pigment optical density measurement: a novel compact instrument. *Ophthalmic and Physiological Optics,* 20 (2), 105-111.

Beatty, S., Koh, H. H., Henson, D. & Boulton, M. 2000b. The role of oxidative stress in the pathogenesis of age-related macular degeneration. *Survey of Ophthalmology,* 45 (2), 115-134.

Beatty, S., Murray, I. J., Henson, D. B., Carden, D., Koh, H. H. & Boulton, M. E. 2001. Macular pigment and risk for age-related macular degeneration in subjects from a Northern European population. *Investigative Ophthalmology and Visual Science,* 42 (2), 439-446.

Bennett, A. G., Rudnicka, A. R. & Edgar, D. F. 1994. Improvements on Littmann's method of determining the size of retinal features by fundus photography. *Graefe's Archive for Clinical and Experimental Ophthalmology,* 232 (6), 361-367.

Berendschot, T. T. J. M., DeLint, P. J. & Norren, D. v. 2003. Fundus reflectance - historical and present ideas. *Progress in Retinal and Eye Research,* 22 (2), 171-200.

Berendschot, T. T. J. M. & van Norren, D. 2004. Objective determination of the macular pigment optical density using fundus reflectance spectroscopy. *Archives of Biochemistry and Biophysics,* 430 (2), 149-155.

Berendschot, T. T. J. M. & van Norren, D. 2005. On the age dependency of the macular pigment optical density. *Experimental Eye Research,* 81 (5), 602-609.

Berendschot, T. T. J. M. & van Norren, D. 2006. Macular pigment shows ringlike structures. *Investigative Ophthalmology and Visual Science,* 47 (2), 709-714.

Bernstein, P. S., Ahmed, F., Liu, A., Allman, S., Sheng, X., Sharifzadeh, M., Ermakov, I. & Gellermann, W. 2012. Macular pigment imaging in AREDS 2 participants: an ancillary study of AREDS 2 subjects enrolled at the Moran Eye Center. *Investigative Ophthalmology and Visual Science,* 53 (10), 6178-6186.

Bernstein, P. S., Khachik, F., Carvalho, L. S., Muir, G. J., Zhao, D. Y. & Katz, N. B. 2001. Identification and quantitation of carotenoids and their metabolites in the tissues of the human eye. *Experimental Eye Research,* 72 (3), 215-223.

Bernstein, P. S., Yoshida, M. D., Katz, N. B., McClane, R. W. & Gellermann, W. 1998. Raman detection of macular carotenoid pigments in intact human retina. *Investigative Ophthalmology and Visual Science,* 39 (11), 2003-2011.

Bhopal, R. & Donaldson, L. 1998. White, European, Western, Caucasian, or what? Inappropriate labeling in research on race, ethnicity, and health. *American Journal of Public Health,* 88 (9), 1303-1307.

Bhosale, P., Serban, B., Zhao, D. Y., & Bernstein, P. S. 2007. Identification and metabolic transformations of carotenoids in ocular tissues of the Japanese quail Coturnix japonica. *Biochemistry*, *46* (31), 9050-9057.

Bhosale, P. & Bernstein, P. S. 2005. Synergistic effects of zeaxanthin and its binding protein in the prevention of lipid membrane oxidation. *Biochimica et Biophysica Acta,* 1740 (2), 116-121.

Bhosale, P., Zhao, D. Y. & Bernstein, P. S. 2007. HPLC measurement of ocular carotenoid levels in human donor eyes in the lutein supplementation era. *Investigative Ophthalmology and Visual Science,* 48 (2), 543-549.

Bird, A. C., Bressler, N. M., Bressler, S. B., Chisholm, I. H., Coscas, G., Davis, M. D., de Jong, P. T. V. M., Klaver, C. C. W., Klein, B. E. K., Klein, R., Mitchell, P., Sarks, J. P., Sarks, S. H., Soubrane, G., Taylor, H. R. & Vingerling, J. R. 1995. An international classification and grading system for age-related maculopathy and age-related macular degeneration. *Survey of Ophthalmology,* 39 (5), 367-374.

Bland, J. M. & Altman, D. G. 1986. Statistical methods for assessing agreement between two methods of clinical measurement. *Lancet,* 1 (8476), 307-310.

Bland, J. M. & Altman, D. G. 1999. Measuring agreement in method comparison studies. *Statistical Methods in Medical Research,* 8 (2), 135-160.

Boettner, E. A. & Wolter, J. R. 1962. Transmission of the ocular media. *Investigative Ophthalmology and Visual Science,* 1 (6), 776-783.

Bone, R. A., Brener, B. & Gibert, J. C. 2007. Macular pigment, photopigments, and melanin: distributions in young subjects determined by four-wavelength reflectometry. *Vision Research,* 47 (26), 3259-3268.

Bone, R. A., Gibert, J. C. & Mukherjee, A. 2012. Light distributions on the retina: relevance to macular pigment photoprotection. *Acta Biochimica Polonica,* 59 (1), 91-96.

Bone, R. A. & Landrum, J. T. 2004. Heterochromatic flicker photometry. *Archives of Biochemistry and Biophysics,* 430 (2), 137-142.

Bone, R. A., Landrum, J. T. & Cains, A. 1992. Optical density spectra of the macular pigmentin vivo andin vitro. *Vision Research,* 32 (1), 105-110.

Bone, R. A., Landrum, J. T., Dixon, Z., Chen, Y. & Llerena, C. M. 2000. Lutein and zeaxanthin in the eyes, serum and diet of human subjects. *Experimental Eye Research,* 71 (3), 239-245.

Bone, R. A., Landrum, J. T., Fernandez, L. & Tarsis, S. L. 1988. Analysis of the macular pigment by HPLC: retinal distribution and age study. *Investigative Ophthalmology and Visual Science,* 29 (6), 843-849.

Bone, R. A., Landrum, J. T., Fiedes, L. M., Gomez, C. M., Kilburn, M. D., Menendez, E., Vidal, I. & Wang, W. 1997. Distribution of lutein and zeaxanthin stereoisomers in the human retina. *Experimental Eye Research,* 64 (2), 211-218.

Bone, R. A., Landrum, J. T., Hime, G. W., Cains, A. & Zamor, J. 1993. Stereochemistry of the human macular carotenoids. *Investigative Ophthalmology and Visual Science,* 34 (6), 2033-2040.

Bourne, R. R. A., Stevens, G. A., White, R. A., Smith, J. L., Flaxman, S. R., Price, H., Jonas, J. B., Keeffe, J., Leasher, J., Naidoo, K., Pesudovs, K., Resnikoff, S. & Taylor, H. R. 2013. Causes of vision loss worldwide, 1990–2010: a systematic analysis. *The Lancet Global Health,* 1 (6), e339-e349.

Brantley, M. A., Osborn, M. P., Sanders, B. J., Rezaei, K. A., Lu, P., Li, C., Milne, G. L., Cai, J. & Sternberg, P. 2012. Plasma biomarkers of oxidative stress and genetic variants in age-related macular degeneration. *American Journal of Ophthalmology,* 153 (3), 460-467.

Bremner, F. D. & Smith, S. E. 2006. Pupil abnormalities in selected autonomic neuropathies. *Journal of Neuro-Ophthalmology,* 26 (3), 209-219.

Bressler, S. B. 2014. Reproducibility of spectral-domain optical coherence tomography retinal thickness measurements and conversion to equivalent time-domain metrics in diabetic macular edema. *JAMA Ophthalmology,* 132 (9), 1113.

Bressler, S. B., Munoz, B., Solomon, S. & West, S. K. 2008. The prevalence of age-related macular degeneration and fundus characteristics of AMD in blacks and whites: the Salisbury Eye Evaluation (SEE) project. *Archives of Ophthalmology,* 126 (2), 241-245.

Broekmans, W., Berendschot, T., Klöpping-Ketelaars, I., de Vries, A., Goldbohm, R., Tijburg, L., Kardinaal, A. & van Poppel, G. 2002. Macular pigment density in relation to serum and adipose tissue concentrations of lutein and serum concentrations of zeaxanthin. *The American Journal of Clinical Nutrition,* 76 (3), 595-603.

Bron, A. J., Tripathi, R. & Tripathi, B. 1997. 'The eyeball and its dimensions', *Wolff's anatomy of the eye and orbit.* London: Chapman and Hall Medical, 211-232.

Bunce, C. & Wormald, R. 2006. Leading causes of certification for blindness and partial sight in England and Wales. *BMC Public Health,* 10.1186/1471-2458-6-58.

Bunce, C., Xing, W. & Wormald, R. 2010. Causes of blind and partial sight certifications in England and Wales: April 2007-March 2008. *Eye,* 24 (11), 1692-1699.

Canovas, R., Lima, V. C., Garcia, P., Morini, C., Prata, T. S. & Rosen, R. B. 2010. Comparison between macular pigment optical density measurements using two-wavelength autofluorescence and heterochromatic flicker photometry techniques. *Investigative Ophthalmology and Visual Science,* 51 (6), 3152-3156.

Carpineto, P., Nubile, M., Toto, L., Aharrh Gnama, A., Marcucci, L., Mastropasqua, L. & Ciancaglini, M. 2009. Correlation in foveal thickness measurements between spectral-domain and time-domain optical coherence tomography in normal individuals. *Eye,* 24 (2), 251-258.

Chakravarthy, U. & Williams, M. 2013. The Royal College of Ophthalmologists Guidelines on AMD: Executive summary. *Eye,* 27 (12), 1429-1431.

Chakravarthy, U., Wong, T. Y., Fletcher, A., Piault, E., Evans, C., Zlateva, G., Buggage, R., Pleil, A. & Mitchell, P. 2010. Clinical risk factors for age-related macular degeneration: a systematic review and meta-analysis. *BMC Ophthalmology,* 10.1186/1471-2415-10-31.

Chang, M. A., Bressler, S. B., Muñoz, B. & West, S. K. 2008. Racial differences and other risk factors for incidence and progression of age-related macular degeneration: Salisbury Eye Evaluation (SEE) project. *Investigative Ophthalmology and Visual Science,* 49 (6), 2395-2402.

Chen, S. J., Cheng, C. Y., Peng, K. L., Li, A. F., Hsu, W. M., Liu, J. H. & Chou, P. 2008. Prevalence and associated risk factors of age-related macular degeneration in an elderly Chinese population in Taiwan: the Shihpai eye study. *Investigative Ophthalmology and Visual Science,* 49 (7), 3126-3133.

Chiu, S. J., Izatt, J. A., O'Connell, R. V., Winter, K. P., Toth, C. A. & Farsiu, S. 2012. Validated automatic segmentation of AMD pathology including drusen and geographic atrophy in SD-OCT images. *Investigative Ophthalmology and Visual Science,* 53 (1), 53-61.

Chucair, A. J., Rotstein, N. P., SanGiovanni, J. P., During, A., Chew, E. Y. & Politi, L. E. 2007. Lutein and zeaxanthin protect photoreceptors from apoptosis induced by oxidative stress: Relation with docosahexaenoic acid. *Investigative Ophthalmology and Visual Science,* 48 (11), 5168-5177.

Cicerone, C. M. & Nerger, J. L. 1989. The relative numbers of long-wavelength-sensitive to middle-wavelength-sensitive cones in the human fovea centralis. *Vision Research,* 29 (1), 115-128.

Ciulla, T. A., Curran-Celantano, J., Cooper, D. A., Hammond, B. R., Danis, R. P., Pratt, L. M., Riccardi, K. A. & Filloon, T. G. 2001a. Macular pigment optical density in a midwestern sample. *Ophthalmology,* 108 (4), 730-737.

Ciulla, T. A. & Hammond, B. R. 2004. Macular pigment density and aging, assessed in the normal elderly and those with cataracts and age-related macular degeneration. *American Journal of Ophthalmology,* 138 (4), 582-587.

Ciulla, T. A., Hammond, B. R., Yung, C. W. & Pratt, L. M. 2001b. Macular pigment optical density before and after cataract extraction. *Investigative Ophthalmology and Visual Science,* 42 (6), 1338-1341.

Clemons, T. E., Milton, R. C., Klein, R. S. J. M. & Ferris, L. 2005. Risk factors for the incidence of advanced age-related macular degeneration in the age-related eye disease study (AREDS): AREDS report no. 19. *Ophthalmology,* 112 (4), 533-539.

Coates, R. J., Eley, J. W., Block, G., Gunter, E. W., Sowell, A. L., Grossman, C. & Greenberg, R. S. 1991. An evaluation of a food frequency questionnaire for assessing dietary intake of specific carotenoids and vitamin E among low-income black women. *American Journal of Epidemiology,* 134 (6), 658-671.

Comyn, O., Heng, L. Z., Ikeji, F., Bibi, K., Hykin, P. G., Bainbridge, J. W. & Patel, P. J. 2012. Repeatability of Spectralis OCT measurements of macular thickness and volume in diabetic macular edema. *Investigative Ophthalmology and Visual Science,* 53 (12), 7754-7759.

Congdon, N., O'Colmain, B., Klaver, C. C., Ronald Klein, R., Muñoz, B., Friedman, D. S., Kempen, J., Taylor, H. R., Mitchell, P. & Hyman, L. 2004. Causes and prevalence of visual impairment among adults in the United States. *Archives of Ophthalmology,* 122 (4), 477-485.

Connolly, E. E., Beatty, S., Thurnham, D. I., Loughman, J., Howard, A. N., Stack, J. & Nolan, J. M. 2010. Augmentation of macular pigment following supplementation with all three macular carotenoids: an exploratory study. *Current Eye Research,* 35 (4), 335-351.

Cruickshanks, K. J., Klein, R. & Klein, B. E. K. 1993. Sunlight and age-related macular degeneration: the Beaver Dam Eye Study. *Archive of Ophthalmology,* 111 (4), 514-518.

Cruickshanks, K. J., Klein, R., Klein, B. E. K. & Nondahl, D. M. 2001. Sunlight and the 5-year incidence of early age-related maculopathy - the Beaver Dam Eye Study. *Archives of Ophthalmology,* 119, 246-250.

Ctori, I., Gruppetta, S. & Huntjens, B. 2014. The effects of ocular magnification on Spectralis spectral domain optical coherence tomography scan length. *Graefe's Archive for Clinical and Experimental Ophthalmology,* 253 (5), 733-738.

Ctori, I. & Huntjens, B. 2015. Repeatability of foveal measurements using Spectralis optical coherence tomography segmentation software. *PloS One,* 10 (6), e0129005.

Curcio, C. A., Allen, K. A., Sloan, K. R., Lerea, C. L., Hurley, J. B., Klock, I. B. & Milam, A. H. 1991. Distribution and morphology of human cone photoreceptors stained with anti‐blue opsin. *Journal of Comparative Neurology,* 312 (4), 610-624.

Curcio, C. A., Sloan, K. R., Kalina, R. E. & Hendrickson, A. E. 1990. Human photoreceptor topography. *Journal of Comparative Neurology,* 292 (4), 497-523.

Davey, P. G., Carusone, F., Alvarez, S., Vyas, P., Greenan, J., Thamsopit, T., Zaczyk, S., Shah, R. & Lievens, C. 2014. Association of Macular Pigment Optical Density (MPOD) and age in ocular healthy adults of different ethnicities - A preliminary report. *Investigative Ophthalmology and Visual Science,* 55 (13), 3492-3492.

Davies, N. P., Morland, A. B. 2002. Color matching in diabetes: optical density of the crystalline lens and macular pigments. *Investigative Ophthalmology and Visual Science*, 43 (1), 281–289.

de Kinkelder, R., van der Veen, R. L. P., Verbaak, F. D., Faber, D. J., van Leeuwen, T. G. & Berendschot, T. T. J. M. 2010. Macular pigment optical density measurements: evaluation of a device using heterochromatic flicker photometry. *Eye,* 25 (1), 105-112.

Delcourt, C., Cougnard-Grégoire, A., Boniol, M. & Carrière, I. 2014. Lifetime exposure to ambient ultraviolet radiation and the risk for cataract extraction and age-related macular degeneration: the Alienor Study. *Investigative Ophthalmology and Visual Science,* 55 (11), 7619-7627.

Delori, F., Greenberg, J. P., Woods, R. L., Fischer, J., Duncker, T., Sparrow, J. & Smith, R. T. 2011. Quantitative measurements of autofluorescence with the scanning laser ophthalmoscope. *Investigative Ophthalmology and Visual Science,* 52 (13), 9379-9390.

Delori, F. C. 2004. Autofluorescence method to measure macular pigment optical densities fluorometry and autofluorescence imaging. *Archives of Biochemistry and Biophysics,* 430 (2), 156-162.

Delori, F. C., Dorey, C. K., Staurenghi, G., Arend, O., Goger, D. G. & Weiter, J. J. 1995. In vivo fluorescence of the ocular fundus exhibits retinal pigment epithelium

lipofuscin characteristics. *Investigative Ophthalmology and Visual Science,* 36 (3), 718-729.

Delori, F. C., Goger, D. G. & Dorey, C. K. 2001a. Age-related accumulation and spatial distribution of lipofuscin in RPE of normal subjects. *Investigative Ophthalmology and Visual Science,* 42 (8), 1855-1866.

Delori, F. C., Goger, D. G., Hammond, B. R., Snodderly, D. M. & Burns, S. A. 2001b. Macular pigment density measured by autofluorescence spectrometry: comparison with reflectometry and heterochromatic flicker photometry. *Journal of the Optical Society of America A,* 18 (6), 1212-1230.

Delori, F. C., Goger, D. G., Keilhauer, C., Salvetti, P. & Staurenghi, G. 2006. Bi-modal spatial distribution of macular pigment: evidence of a gender relationship. *Journal of the Optical Society of America A,* 23 (3), 521-538.

Delori, F. C. & Pflibsen, K. P. 1989. Spectral reflectance of the human ocular fundus. *Applied Optics,* 28 (6), 1061-1077.

DeMarco, P., Pokorny, J. & Smith, V. C. 1992. Full-spectrum cone sensitivity functions for X-chromosome-linked anomalous trichromats. *Journal of the Optical Society of America A,* 9 (9), 1465-1476.

Dennison, J. L., Stack, J., Beatty, S. & Nolan, J. M. 2013. Concordance of macular pigment measurements obtained using customized heterochromatic flicker photometry, dual-wavelength autofluorescence, and single-wavelength reflectance. *Experimental Eye Research,* 116 (0), 190-198.

Dietzel, M., Zeimer, M., Heimes, B., Claes, B., Pauleikhoff, D. & Hense, H. W. 2011a. Determinants of macular pigment optical density and its relation to age-related maculopathy: results from the Muenster Aging and Retina Study (MARS). *Investigative Ophthalmology and Visual Science,* 52 (6), 3452-3457.

Dietzel, M., Zeimer, M., Heimes, B., Pauleikhoff, D. & Hense, H. W. 2011b. The ringlike structure of macular pigment in age-related maculopathy: results from the Muenster Aging and Retina Study (MARS). *Investigative Ophthalmology and Visual Science,* 52 (11), 8016-8024.

Ding, Y., Spund, B., Glazman, S., Shrier, E. M., Miri, S., Selesnick, I. & Bodis-Wollner, I. 2014. Application of an OCT data-based mathematical model of the foveal pit in Parkinson disease. *Journal of Neural Transmission,* 121 (11), 1367-1376.

Distler, C. & Dreher, Z. 1996. Glia cells of the monkey retina II. Müller cells. *Vision Research,* 36 (16), 2381-2394.

Dubis, A. M., Hansen, B. R., Cooper, R. F., Beringer, J., Dubra, A. & Carroll, J. 2012. Relationship between the foveal avascular zone and foveal pit morphology. *Investigative Ophthalmology and Visual Science,* 53 (3), 1628-1636.

Dubis, A. M., McAllister, J. T. & Carroll, J. 2009. Reconstructing foveal pit morphology from optical coherence tomography imaging. *British Journal of Ophthalmology,* 93, 1223-1227.

Early Treatment Diabetic Retinopathy Study research group 1985. Photocoagulation for diabetic macular edema. Early Treatment Diabetic Retinopathy Study Report No.1. *Archives of Ophthalmology,* 103 (12), 1796-1806.

Egan, C. A., Robson, A. G. & Moreland, J. D. 2009. Comparison of motion photometry and 2-wavelength fundus autofluorescence assessments of macular pigment spatial profiles in healthy subjects. *Investigative Ophthalmology and Visual Science,* 50 (13), 1714.

El-Ashry, M., Hegde, V., James, P. & Pagliarini, S. 2008. Analysis of macular thickness in British population using optical coherence tomography (OCT): an emphasis on interocular symmetry. *Current Eye Research,* 33 (8), 693-699.

Elsner, A. E., Burns, S. A., Beausencourt, E. & Weiter, J. J. 1998. Foveal cone photopigment distribution: small alterations associated with macular pigment distribution. *Investigative Ophthalmology and Visual Science,* 39 (12), 2394-2404.

Engles, M., Wooten, B. R. & Hammond, B. R. 2007. Macular pigment: A test of the acuity hypothesis. *Investigative Ophthalmology and Visual Science,* 48 (6), 2922-2931.

Eriksson, U. & Alm, A. 2009. Repeatability in and interchangeability between the macular and the fast macular thickness map protocols: a study on normal eyes with Stratus optical coherence tomography. *Acta Ophthalmologica,* 87 (7), 725-730.

Faul, F., Erdfelder, E., Buchner, A. & Lang, A. G. 2009. Statistical power analyses using G*Power 3.1: tests for correlation and regression analyses. *Behavior Research Methods,* 41 (4), 1149-1160.

Faul, F., Erdfelder, E., Lang, A.-G. & Buchner, A. 2007. G*Power 3: a flexible statistical power analysis program for the social, behavioral, and biomedical sciences. *Behavior Research Methods,* 39 (2), 175-191.

Feigl, B., Morris, C. P., Voisey, J., Kwan, A. & Zele, A. J. 2014. The relationship between BCMO1 gene variants and macular pigment optical density in persons with and without age-related macular degeneration. *PloS One* [Online], 10.1371/journal.pone.0089069.

Fernández-García, E., Carvajal-Lérida, I., Jarén-Galán, M., Garrido-Fernández, J., Pérez-Gálvez, A. & Hornero-Méndez, D. 2012. Carotenoids bioavailability from foods: from plant pigments to efficient biological activities. *Food Research International,* 46 (2), 438-450.

Field, A. P. 2013. *Discovering statistics using IBM SPSS.* London: SAGE.

Fiore, T., Lupidi, M., Androudi, S., Giansanti, F., Fruttini, D. & Cagini, C. 2015. Repeatability of retinal macular thickness measurements in healthy subjects and diabetic patients with clinically significant macular edema: evaluation of the follow-up system of Spectralis optical coherence tomography. *Ophthalmologica,* 233 (3-4), 186-191.

Fitzpatrick, T. B. 1988. The validity and practicality of sun-reactive skin types I through VI. *Archives of Dermatology,* 124 (6), 869-871.

Fletcher, A. E., Bentham, G. C., Agnew, M., Young, I. S., Augood, C. B. S., Chakravarthy, U., de Jong, P. T. V. M., Rahu, M., Seland, J., Soubrane, G., Tomazzoli, L., Topouzis, F., Vingerling, J. R. & Vioque, J. 2008. Sunlight

exposure, antioxidants, and age-related macular degeneration. *Archives of Ophthalmology,* 126 (10), 1396-1403.

Folgar, F. A., Yuan, E. L., Farsiu, S. & Toth, C. A. 2014. Lateral and axial measurement differences between spectral-domain optical coherence tomography systems. *Journal of Biomedical Optics,* 10.1117/1. JBO.19.1.016014.

Friedman, D. S., Colmain, B. J., Muñoz, B., Tomany, S. C., McCarty, C., de Jong, P. T., Nemesure, B., Mitchell, P. & Kempen, J. 2004. Eye Diseases Prevalence Research Group. Prevalence of age-related macular degeneration in the United States. *Archives of Ophthalmology,* 122 (4), 564-572.

Garway-Heath, D. F., Rudnicka, A. R., Lowe, T., Foster, P. J., Fitzke, F. W. & Hitchings, R. A. 1998. Measurement of optic disc size: equivalence of methods to correct for ocular magnification. *British Journal of Ophthalmology,* 82 (6), 643-649.

Gass, J. D. M. 1999. Müller cell cone, an overlooked part of the anatomy of the fovea centralis: hypotheses concerning its role in the pathogenesis of macular hole and foveomacular retinoschisis. *Archives of Ophthalmology,* 117 (6), 821-823.

Ghasemi, A. & Zahediasl, S. 2012. Normality tests for statistical analysis: a guide for non-statisticians. *International Journal of Endocrinology and Metabolism,* 10 (2), 486-489.

Gilbert, P. A. & Khokhar, S. 2008. Changing dietary habits of ethnic groups in Europe and implications for health. *Nutrition Reviews,* 66 (4), 203-215.

Gilmore, E. D. & Hudson, c. 2004. Eccentricity and measurement variability and repeatability with the retinal thickness analyser. *British Journal of Ophthalmology,* 88 (1), 62-65.

Girkin, C. A., McGwin Jr, G., Sinai, M. J., Sekhar, G. C., Fingeret, M., Wollstein, G., Varma, R., Greenfield, D., Liebmann, J., Araie, M., Tomita, G., Maeda, N. & Garway-Heath, D. F. 2011. Variation in optic nerve and macular structure with age and race with spectral-domain optical coherence tomography. *Ophthalmology,* 118 (12), 2403-2408.

Grover, S., Murthy, R. K., Brar, V. S. & Chalam, K. V. 2009. Normative data for macular thickness by high-definition spectral-domain optical coherence tomography (Spectralis). *American Journal of Ophthalmology,* 148 (2), 266-271.

Grover, S., Murthy, R. K., Brar, V. S. & Chalam, K. V. 2010. Comparison of retinal thickness in normal eyes using Stratus and Spectralis optical coherence tomography. *Investigative Ophthalmology and Visual Science,* 51 (5), 2644-2647.

Hagen, S., Krebs, I., Glittenberg, C. & Binder, S. 2010. Repeated measures of macular pigment optical density to test reproducibility of heterochromatic flicker photometry. *Acta Ophthalmologica,* 88 (2), 207-211.

Hammer, D. X., Iftimia, N. V., Ferguson, R. D., Bigelow, C. E., Ustun, T. E., Barnaby, A. M. & Fulton, A. B. 2008. Foveal fine structure in retinopathy of prematurity: an adaptive optics fourier domain optical coherence tomography study. *Investigative Ophthalmology and Visual Science,* 49 (5), 2061-2070.

Hammer, M. & Schweitzer, D. 2002. Quantitative reflection spectroscopy at the human ocular fundus. *Physics in Medicine and Biology,* 47 (2), 179-191.

Hammond, B. R. & Caruso-Avery, M. 2000. Macular pigment optical density in a Southwestern sample. *Investigative Ophthalmology and Visual Science,* 41 (6), 1492-1497.

Hammond, B. R., Ciulla, T. A. & Snodderly, D. M. 2002. Macular pigment density Is reduced in obese subjects. *Investigative Ophthalmology and Visual Science,* 43 (1), 47-50.

Hammond, B. R., Curran-Celentano, J., Judd, S., Fuld, K., Krinsky, N. I., Wooten, B. R. & Snodderly, D. M. 1996a. Sex differences in macular pigment optical density: relation to plasma carotenoid concentrations and dietary patterns. *Vision Research,* 36 (13), 2001-2012.

Hammond, B. R., Fletcher, L. M. & Elliott, J. G. 2013. Glare disability, photostress recovery, and chromatic contrast: relation to macular pigment and serum lutein and zeaxanthin. *Investigative Ophthalmology and Visual Science,* 54 (1), 476-481.

Hammond, B. R. & Fuld, K. 1992. Interocular differences in macular pigment density. *Investigative Ophthalmology and Visual Science,* 33 (2), 350-355.

Hammond, B. R., Fuld, K. & Curran-Celentano, J. 1995. Macular pigment density in monozygotic twins. *Investigative Ophthalmology and Visual Science,* 36 (12), 2531-2541.

Hammond, B. R., Fuld, K. & Snodderly, D. M. 1996b. Iris color and macular pigment optical density. *Experimental Eye Research,* 62, 715-720.

Hammond, B. R., Johnson, E. J., Russell, R. M., Krinsky, N. I., Yeum, K. J., Edwards, R. B. & Snodderly, D. M. 1997a. Dietary modification of human macular pigment density. *Investigative Ophthalmology and Visual Science,* 38 (9), 1795-1801.

Hammond, B. R., Jr., Wooten, B. R. & Snodderly, D. M. 1997b. Density of the human crystalline lens is related to the macular pigment carotenoids, lutein and zeaxanthin. *Optometry and Vision Science,* 74 (7), 499-504.

Hammond, B. R. & Wooten, B. R. 2005. CFF thresholds: relation to macular pigment optical density. *Ophthalmic and Physiological Optics,* 25 (4), 315-319.

Hammond, B. R., Wooten, B. R. & Smollon, B. 2005. Assessment of the validity of in vivo methods of measuring human macular pigment optical density. *Optometry and Vision Science,* 82 (5), 387-404.

Hammond, B. R., Wooten, B. R. & Snodderly, D. M. 1996c. Cigarette smoking and retinal carotenoids: implications for age-related macular degeneration. *Vision Research,* 36 (18), 3003-3009.

Hammond, B. R., Wooten, B. R. & Snodderly, D. M. 1997c. Individual variations in the spatial profile of human macular pigment. *Journal of the Optical Society of America A,* 14 (6), 1187-1196.

Hammond, C. J., Liew, S. H. M., Van Kuijk, F. J., Beatty, S., Nolan, J. M., Spector, T. D. & Gilbert, C. E. 2012. The heritability of macular response to supplemental lutein and zeaxanthin: a classic twin study. *Investigative Ophthalmology and Visual Science,* 53 (8), 4963-4968.

Handelman, G. J., Dratz, E. A., Reay, C. C. & van Kuijk, J. G. 1988. Carotenoids in the human macula and whole retina. *Investigative Ophthalmology and Visual Science,* 29 (6), 850-855.

Handelman, G. J., Snodderly, D. M., Krinsky, N. I., Russett, M. D. & Adler, A. J. 1991. Biological control of primate macular pigment. Biochemical and densitometric studies. *Investigative Ophthalmology and Visual Science,* 32 (2), 257-267.

Hanout, M., Horan, N. & Do, D. V. 2015. Introduction to microperimetry and its use in analysis of geographic atrophy in age-related macular degeneration. *Current Opinion in Ophthalmology,* 26 (3), 149-156.

Heidelberg Engineering 2013. *Spectralis HRA + OCT User manual software version 5.7.* Germany: Heidelberg Engineering.

Hendrickson, A. 1992. A morphological comparison of foveal development in man and monkey. *Eye,* 6 (2), 136-144.

Hendrickson, A., Possin, D., Vajzovic, L. & Toth, C. A. 2012. Histologic development of the human fovea from midgestation to maturity. *American Journal of Ophthalmology,* 154 (5), 767-778.

Hirakawa, M., Tanaka, M., Tanaka, Y., Okubo, A., Koriyama, C., Tsuji, M., Akiba, S., Miyamoto, K., Hillebrand, G., Yamashita, T. & Sakamoto, T. 2008. Age-related maculopathy and sunlight exposure evaluated by objective measurement. *British Journal of Ophthalmology,* 92 (5), 630-634.

Hogg, R. E., Anderson, R. S., Stevenson, M. R., Zlatkova, M. B. & Chakravarthy, U. 2007. In vivo macular pigment measurements: a comparison of resonance Raman spectroscopy and heterochromatic flicker photometry. *British Journal of Ophthalmology,* 91 (4), 485-490.

Hogg, R. E., Ong, E. L., Chamberlain, M., Dirani, M., Baird, P. N., Guymer, R. H. & Fitzke, F. 2012. Heritability of the spatial distribution and peak density of macular pigment: a classical twin study *Eye,* 26 (9), 1217-1225.

Howells, O., Eperjesi, F. & Bartlett, H. 2011. Measuring macular pigment optical density in vivo: a review of techniques. *Graefe's Archive for Clinical and Experimental Ophthalmology,* 249 (3), 315-347.

Howells, O., Eperjesi, F. & Bartlett, H. 2013. Macular pigment optical density in young adults of South Asian origin. *Investigative Ophthalmology and Visual Science,* 54 (4), 2711-2719.

Huang, D., Swanson, E. A., Lin, C. P., Schuman, J. S., Stinson, W. G., Chang, W., Hee, M. R., Flotte, T., Gregory, K. & Puliafito, C. A. 1991. Optical coherence tomography. *Science,* 254 (5035), 1178-1181.

Huntjens, B., Asaria, T. S., Dhanani, S., Konstantakopoulou, E. & Ctori, I. 2014. Macular pigment spatial profiles in South Asian and white subjects. *Investigative Ophthalmology and Visual Science,* 55 (3), 1440-1446.

Iannaccone, A., Mura, M., Gallaher, K. T., Johnson, E. J., Todd, W. A., Kenyon, E., Harris, T. L., Harris, T., Satterfield, S., Johnson, K. C. & Kritchevsky, S. B. 2007. Macular pigment optical density in the elderly: findings in a large biracial midsouth population sample. *Investigative Ophthalmology and Visual Science,* 48 (4), 1458-1465.

Igras, E., Loughman, J., Ratzlaff, M. & O'Caoimh, R. 2013. Evidence of lower macular pigment optical density in chronic open angle glaucoma. *British Journal of Ophthalmology,* 97 (8), 994-998.

Jarrett, S. G. & Boulton, M. E. 2012. Consequences of oxidative stress in age-related macular degeneration. *Molecular Aspects of Medicine,* 33 (4), 399-417.

Jin, G. F., Hurst, J. S. & Godley, B. F. 2001. Rod outer segments mediate mitochondrial DNA damage and apoptosis in human retinal pigment epithelium. *Current Eye Research,* 23 (1), 11-19.

Johnson, E. J., Maras, J. E., Rasmussen, H. M. & Tucker, K. L. 2010. Intake of lutein and zeaxanthin differ with age, sex, and ethnicity. *Journal of the American Dietetic Association,* 110 (9), 1357-1362.

Junghans, A., Sies, H. & Stahl, W. 2001. Macular pigments lutein and zeaxanthin as blue light filters studied in liposomes. *Archives of Biochemistry and Biophysics,* 391 (2), 160-164.

Kanis, M. J., Berendschot, T. T. J. M. & van Norren, D. 2007. Interocular agreement in melanin and macular pigment optical density. *Experimental Eye Research,* 84 (5), 934-938.

Kashani, A. H., Zimmer-Galler, I. E., Shah, S. M., Dustin, L., Do, D. V., Eliott, D., Haller, J. A. & Nguyen, Q. D. 2010. Retinal thickness analysis by race, gender, and age using Stratus OCT. *American Journal of Ophthalmology,* 149 (3), 496-502.

Kawasaki, R., Wang, J. J., Ji, G., Taylor, B., Oizumi, T., Daimon, M., Kato, T., Kawata, S., Kayama, T., Tano, Y., Mitchell, P., Yamashita, H. & Wong, T. Y. 2008. Prevalence and risk factors for age-related macular degeneration in an adult Japanese population: the Funagata Study. *Ophthalmology,* 115 (8), 1376-1381.

Kawasaki, R., Yasuda, M., Song, S. J., Chen, S. J., Jonas, J. B., Wang, J. J., Mitchell, P. & Wong, T. Y. 2010. The prevalence of age-related macular degeneration in Asians: A systematic review and meta-analysis. *Ophthalmology,* 117 (5), 921-927.

Kelty, P. J., Payne, J. F., Trivedi, R. H., Kelty, J., Bowie, E. M. & Burger, B. M. 2008. Macular thickness assessment in healthy eyes based on ethnicity using Stratus OCT optical coherence tomography. *Investigative Ophthalmology and Visual Science,* 49 (6), 2668-2672.

Kennedy, C. J., Rakoczy, P. E. & Constable, I. J. 1995. Lipofuscin of the retinal pigment epithelium: A review. *Eye,* 9 (6), 763-771.

Khachik, F., Bernstein, P. S. & Garland, D. L. 1997. Identification of lutein and zeaxanthin oxidation products in human and monkey retinas. *Investigative Ophthalmology and Visual Science,* 38 (9), 1802-1811.

259

Khan, J. C., Shahid, H., Thurlby, D. A., Bradley, M., Clayton, D. G., Moore, A. T., Bird, A. C. & Yates, J. R. W. 2006a. Age related macular degeneration and sun exposure, iris colour, and skin sensitivity to sunlight. *British Journal of Ophthalmology,* 90 (1), 29-32.

Khan, J. C., Thurlby, D. A., Shahid, H., Clayton, D. G., Yates, J. R. W., Bradley, M., Moore, A. T. & Bird, A. C. 2006b. Smoking and age related macular degeneration: the number of pack years of cigarette smoking is a major determinant of risk for both geographic atrophy and choroidal neovascularisation. *The British Journal of Ophthalmology,* 90 (1), 75-80.

Khandhadia, S. & Lotery, A. 2010. Oxidation and age-related macular degeneration: insights from molecular biology. *Expert Reviews in Molecular Medicine,* 12, e34.

Khokhar, S., Roe, M. & Swan, G. 2012. Carotenoid and retinol composition of South Asian foods commonly consumed in the UK. *Journal of food composition and analysis,* 25 (2), 166-172.

Kim, S. R., Nakanishi, K., Itagaki, Y. & Sparrow, J. R. 2006. Photooxidation of A2-PE, a photoreceptor outer segment fluorophore, and protection by lutein and zeaxanthin. *Experimental Eye Research,* 82 (5), 828-839.

Kirby, M. L., Beatty, S., Loane, E., Akkali, M. C., Connolly, E. E., Stack, J. & Nolan, J. M. 2010. A central dip in the macular pigment spatial profile is associated with age and smoking. *Investigative Ophthalmology and Visual Science,* 51 (12), 6722-6728.

Kirby, M. L., Beatty, S., Stack, J., Harrison, M., Greene, I., McBrinn, S., Carroll, P. & Nolan, J. M. 2011. Changes in macular pigment optical density and serum concentrations of lutein and zeaxanthin in response to weight loss. *British Journal of Nutrition,* 105 (7), 1036-1046.

Kirby, M. L., Galea, M., Loane, E., Stack, J., Beatty, S. & Nolan, J. M. 2009. Foveal anatomic associations with the secondary peak and the slope of the macular pigment spatial profile. *Investigative Ophthalmology & Visual Science,* 50 (3), 1383-1391.

Klein, B. E. K., Howard, K. P., Iyengar, S. K., Sivakumaran, T. A., Meyers, K. J., Cruickshanks, K. J. & Klein, R. 2014. Sunlight exposure, pigmentation, and incident age-related macular degeneration. *Investigative Ophthalmology and Visual Science,* 55 (9), 5855-5861.

Klein, R., Chou, C. F., Klein, B. E., Zhang, X., Meuer, S. M. & Saaddine, J. B. 2011. Prevalence of age-related macular degeneration in the US population. *Archives of Ophthalmology,* 129 (1), 75-80.

Klein, R., Klein, B. E. K., Knudtson, M. D., Wong, T. Y., Cotch, M. F., Liu, K., Burke, G., Saad, M. F. & Jacobs Jr, D. R. 2006. Prevalence of age-related macular degeneration in 4 racial/ethnic groups in the multi-ethnic study of atherosclerosis. *Ophthalmology,* 113 (3), 373-380.

Klein, R., Li, X., Kuo, J. Z., Klein, B. E. K., Cotch, M. F., Wong, T. Y., Taylor, K. D. & Rotter, J. I. 2013. Associations of candidate genes to age-related macular degeneration among racial/ethnic groups in the multi-ethnic study of atherosclerosis. *American Journal of Ophthalmology,* 156 (5), 1010-1020.

Krebs, I., Smretschnig, E., Moussa, S., Brannath, W., Womastek, I. & Binder, S. 2011. Quality and reproducibility of retinal thickness measurements in two spectral-domain optical coherence tomography machines. *Investigative Ophthalmology and Visual Science,* 52 (9), 6925-6933.

Kvansakul, J., Rodriguez -Carmona, M., Edgar, D. F., Barker, F. M., Köpcke, W., Schalch, W. & Barbur, J. L. 2006. Supplementation with the carotenoids lutein or zeaxanthin improves human visual performance. *Ophthalmic and Physiological Optics,* 26 (4), 362-371.

Kyle-Little, Z., Zele, A. J., Morris, P. & Feigl, B. 2014. The effect of BCMO1 gene variants on macular pigment optical density in young healthy Caucasians. *Frontiers in Nutrition,* 1.

Lam, A. K. C., Chan, R. & Pang, P. C. K. 2001. The repeatability and accuracy of axial length and anterior chamber depth measurements from the IOLMaster™. *Ophthalmic and Physiological Optics,* 21 (6), 477-483.

Lam, R. F., Rao, S. K., Fan, D. S., Lau, F. T. & Lam, D. S. 2005. Macular pigment optical density in a Chinese sample. *Current Eye Research,* 30 (9), 799-805.

Landis, J. R. & Koch, G. G. 1977. The measurement of observer agreement for categorical data. *Biometrics,* 33 (1), 159-174.

Landrum, J. T. 2001. Lutein, zeaxanthin, and the macular pigment. *Archives of Biochemistry and Biophysics,* 385 (1), 28.

Langenegger, S. J., Funk, J. & Töteberg-Harms, M. 2011. Reproducibility of retinal nerve fiber layer thickness measurements using the eye tracker and the retest function of spectralis SD-OCT in glaucomatous and healthy control eyes. *Investigative Ophthalmology and Visual Science,* 52 (6), 3338-3344.

Laude, A., Cackett, P. D., Vithana, E. N., Yeo, I. Y., Wong, D., Koh, A. H., Wong, T. Y. & Aung, T. 2010. Polypoidal choroidal vasculopathy and neovascular age-related macular degeneration: same or different disease? *Progress in Retinal and Eye Research,* 29 (1), 19-29.

Lee, S., Fallah, N., Forooghian, F., Ko, A., Pakzad-Vaezi, K., Merkur, A. B., Kirker, A. W., Albiani, D. A., Young, M., Sarunic, M. V. & Beg, M. F. 2013. Comparative analysis of repeatability of manual and automated choroidal thickness measurements in nonneovascular age-related macular degeneration. *Investigative Ophthalmology and Visual Science,* 54 (4), 2864-2871.

Leffondré, K., Abrahamowicz, M., Siemiatycki, J. & Rachet, B. 2002. Modeling smoking history: a comparison of different approaches. *American Journal of Epidemiology,* 156 (9), 813-823.

Leung, C. K., Cheng, A. C. K., Chong, K. K. L., Leung, K. S., Mohamed, S., Lau, C. S. L., Cheung, C. Y. L., Chu, G. C., Lai, R. Y. K., Pang, C. C. P. & Lam, D. S. C. 2007. Optic disc measurements in myopia with optical coherence tomography and confocal scanning laser ophthalmoscopy. *Investigative Ophthalmology and Visual Science,* 48 (7), 3178-3183.

Leung, C. K., Cheung, C. Y., Weinreb, R. N., Lee, G., Lin, D., Pang, C. P. & Lam, D. S. C. 2008. Comparison of macular thickness measurements between time

domain and spectral domain optical coherence tomography. *Investigative Ophthalmology and Visual Science,* 49 (11), 4893-4897.

Liew, S. H. M., Gilbert, C. E., Spector, T. D., Mellerio, J., Kuijk, F. J. V., Beatty, S., Fitzke, F., Marshall, J. & Hammond, C. J. 2006. Central retinal thickness is positively correlated with macular pigment optical density. *Experimental Eye Research,* 82 (5), 915-920.

Liew, S. H. M., Gilbert, C. E., Spector, T. D., Mellerio, J., Marshall, J., van Kuijk, F. J., Beatty, S., Fitzke, F. & Hammond, C. J. 2005. Heritability of macular pigment: a twin study. *Investigative Ophthalmology and Visual Science,* 46 (12), 4430-4436.

Loane, E., McKay, G. J., Nolan, J. M. & Beatty, S. 2010. Apolipoprotein E genotype is associated with macular pigment optical density. *Investigative Ophthalmology and Visual Science,* 51 (5), 2636-2643.

Loane, E., Stack, J., Beatty, S. & Nolan, J. M. 2007. Measurement of macular pigment optical density using two different heterochromatic flicker photometers. *Current Eye Research,* 32 (6), 555-564.

Loughman, J. 2014. The relationship between macular pigment and visual function among glaucoma subjects: a baseline evaluation of the Macular Pigment and Glaucoma Trial. *Investigative Ophthalmology and Visual Science,* 55 (13), 3489.

Loughman, J., Akkali, M. C., Beatty, S., Scanlon, G., Davison, P. A., O'Dwyer, V., Cantwell, T., Major, P., Stack, J. & Nolan, J. M. 2010. The relationship between macular pigment and visual performance. *Vision Research,* 50 (13), 1249-1256.

Lujan, B. J., Roorda, A., Croskrey, J. A., Dubis, A. M., Cooper, R. F., Bayabo, J.-K., Duncan, J. L., Antony, B. J. & Carroll, J. 2015. Directional optical coherence tomography provides accurate outer nuclear layer and Henle fiber layer measurements. *Retina,* 35 (8), 1511–1520.

Lujan, B. J., Roorda, A., Knighton, R. W. & Carroll, J. 2011. Revealing Henle's fiber layer using spectral domain optical coherence tomography. *Investigative Ophthalmology and Visual Science,* 52 (3), 1486-1492.

Ma, L., Yan, S. F., Huang, Y. M., Lu, X. R., Qian, F., Pang, H. L., Xu, X. R., Zou, Z. Y., Dong, P. C., Xiao, X., Wang, X., Sun, T. T., Dou, H. L. & Lin, X. M. 2012. Effect of lutein and zeaxanthin on macular pigment and visual function in patients with early age-related macular degeneration. *Ophthalmology,* 119 (11), 2290-2297.

Mackey, D. A., Wilkinson, C. H., Kearns, L. S. & Hewitt, A. W. 2011. Classification of iris colour: review and refinement of a classification schema. *Clinical and experimental ophthalmology,* 39 (5), 462-471.

Malinow, M. R., Feeney-Burns, L., Peterson, L. H., Klein, M. L. & Neuringer, M. 1980. Diet-related macular anomalies in monkeys. *Investigative Ophthalmology and Visual Science,* 19 (8), 857-863.

Mares, J. A., LaRowe, T. L., Snodderly, D. M., Moeller, S. M., Gruber, M. J., Klein, M. L., Wooten, B. R., Johnson, E. J. & Chappell, R. J. 2006. Predictors of optical density of lutein and zeaxanthin in retinas of older women in the Carotenoids in

Age-Related Eye Disease Study, an ancillary study of the Women's Health Initiative. *The American Journal of Clinical Nutrition,* 84 (5), 1107-1122.

Markowitz, S. N. & Reyes, S. V. 2013. Microperimetry and clinical practice: an evidence-based review. *Canadian Journal of Ophthalmology / Journal Canadien d'Ophtalmologie,* 48 (5), 350-357.

Matsumoto, H., Sato, T. & Kishi, S. 2009. Outer nuclear layer thickness at the fovea determines visual outcomes in resolved central serous chorioretinopathy. *American Journal of Ophthalmology,* 148 (1), 105-110.

McAlinden, C., Khadka, J. & Pesudovs, K. 2011. Statistical methods for conducting agreement (comparison of clinical tests) and precision (repeatability or reproducibility) studies in optometry and ophthalmology. *Ophthalmic and Physiological Optics,* 31 (4), 330-338.

Menke, M. N., Dabov, S., Knecht, P. & Sturm, V. 2009. Reproducibility of retinal thickness measurements in healthy subjects using spectralis optical coherence tomography. *American Journal of Ophthalmology,* 147 (3), 467-472.

Meyer zu Westrup, V., Dietzel, M., Pauleikhoff, D. & Hense, H.-W. 2014. The association of retinal structure and macular pigment distribution. *Investigative Ophthalmology and Visual Science,* 55 (2), 1169-1175.

Meyers, K. J., Johnson, E. J., Bernstein, P. S., Iyengar, S. K., Engelman, C. D., Karki, C. K., Liu, Z., Igo, R. P., Truitt, B. & Klein, M. L. 2013. Genetic determinants of macular pigments in women of the Carotenoids in Age-Related Eye Disease Study. *Investigative Ophthalmology and Visual Science,* 54 (3), 2333-2345.

Mohammad, S., Gottlob, I., Kumar, A., Thomas, M., Degg, C., Sheth, V. & Proudlock, F. A. 2011. The functional significance of foveal abnormalities in albinism measured using spectral-domain optical coherence tomography. *Ophthalmology,* 118 (8), 1645-1652.

Mojana, F., Cheng, L., Bartsch, D.-U. G., Silva, G. A., Kozak, I., Nigam, N. & Freeman, W. R. 2008. The role of abnormal vitreomacular adhesion in age-related macular degeneration: spectral optical coherence tomography and surgical results. *American Journal of Ophthalmology,* 146 (2), 218-227.

Moreland, J. D. 2004. Macular pigment assessment by motion photometry. *Archives of Biochemistry and Biophysics,* 430 (2), 143-148.

Moreland, J. D., Robson, A. G. & Kulikowski, J. J. 2001. Macular pigment assessment using a colour monitor. *Color Research and Application,* 26 (S1), S261-S263.

Moreno-Montañés, J., Olmo, N., Alvarez, A., García, N. & Zarranz-Ventura, J. 2010. Cirrus high-definition optical coherence tomography compared with stratus optical coherence tomography in glaucoma diagnosis. *Investigative Ophthalmology and Visual Science,* 51 (1), 335-343.

Murray, I. J., Carden, D. & Makridaki, M. 2011. The repeatability of the MPS 9000 macular pigment screener. *British Journal of Ophthalmology,* 95 (3), 431-432.

Nangia, V., Jonas, J. B., Kulkarni, M. & Matin, A. 2011. Prevalence of age-related macular degeneration in rural central India: the Central India Eye and Medical Study. *Retina,* 31 (6), 1179-1185.

Nassif, N., Cense, B., Hyle Park, B., Yun, S. H., Chen, T. C., Bouma, B. E., Tearney, G. J. & Boer, J. F. d. 2004. *In vivo* human retinal imaging by ultra high-speed spectral domain optical coherence tomography. *Optics Letters,* 29 (5), 480-482.

Neelam, K., Ho, H., Yip, C. C., Li, W. & Eong, K.-G. A. 2014. The spatial profile of macular pigment in subjects from a Singapore Chinese population. *Investigative Ophthalmology and Visual Science,* 55 (4), 2376-2383.

Neelam, K., Nolan, J., Loane, E., Stack, J., O'Donovan, O., Au-Eong, K. G. & Beatty, S. 2006. Macular pigment and ocular biometry. *Vision Research,* 46 (13), 2149-2156.

Nerger, J. L. & Cicerone, C. M. 1992. The ratio of L cones to M cones in the human parafoveal retina. *Vision Research,* 32 (5), 879-888.

Neuringer, M., Sandstrom, M. M., Johnson, E. J. & Snodderly, D. M. 2004. Nutritional manipulation of primate retinas, I: effects of lutein or zeaxanthin supplements on serum and macular pigment in xanthophyll-free rhesus monkeys. *Investigative Ophthalmology and Visual Science,* 45 (9), 3234-3243.

Ng, M., Freeman, M. K., Fleming, T. D., Robinson, M., Dwyer-Lindgren, L., Thomson, B., Wollum, A., Sanman, E., Wulf, S. & Lopez, A. D. 2014. Smoking prevalence and cigarette consumption in 187 countries, 1980-2012. *JAMA,* 311 (2), 183-192.

Nirmalan, P. K., Katz, J., Robin, A. L., Tielsch, J. M., Namperumalsamy, P., Kim, R., Narendran, V., Ramakrishnan, R., Krishnadas, R., Thulasiraj, R. D. & Suan, E. 2004. Prevalence of vitreo retinal disorders in a rural population of Southern India: the Aravind Comprehensive Eye Study. *Archives of Ophthalmology,* 122 (4), 581-586.

Nolan, J. M., Meagher, K., Kashani, S., & Beatty, S. 2013. What is meso-zeaxanthin, and where does it come from? *Eye*, 27 (8), 899–905.

Nolan, J. M., Akkali, M. C., Loughman, J., Howard, A. N. & Beatty, S. 2012a. Macular carotenoid supplementation in subjects with atypical spatial profiles of macular pigment. *Experimental Eye Research,* 101, 9-15.

Nolan, J. M., Feeney, J., Kenny, R. A., Cronin, H., O'Regan, C., Savva, G. M., Loughman, J., Finucane, C., Connolly, E., Meagher, K. & Beatty, S. 2012b. Education Is positively associated with macular pigment: The Irish Longitudinal Study on Ageing (TILDA). *Investigative Ophthalmology and Visual Science,* 53 (12), 7855-7861.

Nolan, J. M., Kenny, R., O'Regan, C., Cronin, H., Loughman, J., Connolly, E. E., Kearney, P., Loane, E. & Beatty, S. 2010. Macular pigment optical density in an ageing Irish population: the Irish longitudinal study on ageing. *Ophthalmic Research,* 44 (2), 131-139.

Nolan, J. M., Loskutova, E., Howard, A. N., Moran, R., Mulcahy, R., Stack, J., Bolger, M., Dennison, J., Akuffo, K. O. & Owens, N. 2014. Macular pigment, visual function, and macular disease among subjects with Alzheimer's disease: an exploratory study. *Journal of Alzheimer's Disease,* 42 (4), 1191-1202.

Nolan, J. M., O'Donovan, O., Kavanagh, H., Stack, J., Harrison, M., Muldoon, A., Mellerio, J. & Beatty, S. 2004. Macular pigment and percentage of body fat. *Investigative Ophthalmology and Visual Science,* 45 (11), 3940-3950.

Nolan, J. M., O'Reilly, P., Loughman, J., Stack, J., Loane, E., Connolly, E. & Beatty, S. 2009. Augmentation of macular pigment following implantation of blue light filtering intraocular lenses at the time of cataract surgery. *Investigative Ophthalmology and Visual Science,* 50 (10), 4777-4785.

Nolan, J. M., Stack, J., O'Connell, E. & Beatty, S. 2007a. The relationships between macular pigment optical density and its constituent carotenoids in diet and serum. *Investigative Ophthalmology and Visual Science,* 48 (2), 571-582.

Nolan, J. M., Stack, J., O'Donovan, O., Loane, E. & Beatty, S. 2007b. Risk factors for age-related maculopathy are associated with a relative lack of macular pigment. *Experimental Eye Research,* 84 (1), 61-74.

Nolan, J. M., Stringham, J. M., Beatty, S. & Snodderly, D. M. 2008. Spatial profile of macular pigment and its relationship to foveal architecture. *Investigative Ophthalmology and Visual Science,* 49 (5), 2134-2142.

Nolan, J. M., Loskutova, E., Howard, A., Mulcahy, R., Moran, R., Stack, J., Bolger, M., Coen, R.F., Dennison, J., Akuffo, K.O., Owens, N., Poere, R., Thurnham, D. & Beatty, S. 2015. The impact of supplemental macular carotenoids in Alzheimer's disease: a randomized clinical trial. *J Alzheimers Dis*; 44 (4), 1157-1169.

O'Beirne, R. 2014. The macular pigment optical density spatial profile and increasing age. *Graefe's Archive for Clinical and Experimental Ophthalmology,* 252 (3), 383-388.

O'Neill, M. E., Carroll, Y., Corridan, B., Olmedilla, B., Granado, F., Blanco, I., Van den Berg, H., Hininger, I., Rousell, A. M., Chopra, M., Southon, S. & Thurnham, D. I. 2001. A European carotenoid database to assess carotenoid intakes and its use in a five-country comparative study. *British Journal of Nutrition,* 85 (4), 499-507.

Obana, A. 2014. Effect of age and other factors on macular pigment optical density measured with resonance Raman spectroscopy. *Graefe's Archive for Clinical and Experimental Ophthalmology,* 252 (8), 1221-1228.

Obana, A., Hiramitsu, T., Gohto, Y., Ohira, A., Mizuno, S., Hirano, T., Bernstein, P. S., Fujii, H., Iseki, K., Tanito, M. & Hotta, Y. 2008. Macular carotenoid levels of normal subjects and age-related maculopathy patients in a Japanese population. *Ophthalmology,* 115 (1), 147-157.

Odell, D., Dubis, A. M., Lever, J. F., Stepien, K. E. & Carroll, J. 2011. Assessing errors inherent in OCT-derived macular thickness maps. *Journal of Ophthalmology* [Online], 10.1155/2011/692574.

Office for National Statistics. 2011. Ethnicity and National Identity in England and Wales 2011 [Online]. Available: http://www.ons.gov.uk/ons/rel/census/2011-census/key-statistics-for-local-authorities-in-england-and-wales/rpt-thnicity.html-tab-Ethnicity-in-England-and-Wales [Accessed 22 April 2015].

Office for National Statistics 2013. *Harmonised Concepts and Questions for Social Data Sources. Primary Standards. Ethnic group. Version 3.2. pp 1- 24.*

Oh, J., Smiddy, W. E., Flynn, H. W., Gregori, G. & Lujan, B. 2010. Photoreceptor inner/outer segment defect imaging by spectral domain OCT and visual prognosis after macular hole surgery. *Investigative Ophthalmology and Visual Science,* 51 (3), 1651-1658.

Ooto, S., Hangai, M., Tomidokoro, A., Saito, H., Araie, M., Otani, T., Kishi, S., Matsushita, K., Maeda, N., Shirakashi, M., Abe, H. i., Ohkubo, S., Sugiyama, K., Iwase, A. & Yoshimura, N. 2011. Effects of age, sex, and axial length on the three-dimensional profile of normal macular layer structures. *Investigative Ophthalmology and Visual Science,* 52 (12), 8769-8779.

Organisciak, D. T. & Vaughan, D. K. 2010. Retinal light damage: mechanisms and protection. *Progress in Retinal and Eye Research,* 29 (2), 113-134.

Pallant, J. 2010. *SPSS survival manual.* England: Open University Press.

Pascolini, D. & Mariotti, S. P. 2012. Global estimates of visual impairment: 2010. *British Journal of Ophthalmology,* (96), 614-618.

Patel, N. B., Wheat, J. L., Rodriguez, A., Tran, V. & Harwerth, R. S. 2012. Agreement between retinal nerve fiber layer measures from Spectralis and Cirrus spectral domain OCT. *Optometry and Vision Science,* 89 (5), E652-66.

Patel, P. J., Chen, F. K., Ikeji, F. & Tufail, A. 2011. Intersession repeatability of optical coherence tomography measures of retinal thickness in early age-related macular degeneration. *Acta Ophthalmologica,* 89 (3), 229-234.

Patel, P. J., Chen, F. K., Ikeji, F., Xing, W., Bunce, C., Da Cruz, L. & Tufail, A. 2008. Repeatability of stratus optical coherence tomography measures in neovascular age-related macular degeneration. *Investigative Ophthalmology and Visual Science,* 49 (3), 1084-1088.

Paunescu, L. A., Schuman, J. S., Price, L. L., Stark, P. C., Beaton, S., Ishikawa, H., Wollstein, G. & Fujimoto, J. G. 2004. Reproducibility of nerve fiber thickness, macular thickness, and optic nerve head measurements using Stratus OCT. *Investigative Ophthalmology and Visual Science,* 45 (6), 1716-1724.

Peachey, N. S., Alexander, K. R., Derlacki, D. J. & Fishma, G. A. 1992. Light adaptation, rods, and the human cone flicker ERG. *Visual Neuroscience,* 8 (02), 145-150.

Pease, P. L., Adams, A. J. & Nuccio, E. 1987. Optical density of human macular pigment. *Vision Research,* 27 (5), 705-710.

Pesudovs, K. & Weisinger, H. S. 2004. A comparison of autorefractor performance. *Optometry and Vision Science,* 81 (7), 554-558.

Pierro, L., Giatsidis, S. M., Mantovani, E. & Gagliardi, M. 2010. Macular thickness interoperator and intraoperator reproducibility in healthy eyes using 7 optical coherence tomography instruments. *American Journal of Ophthalmology,* 150 (2), 199-204.

Pilat, A. V., Proudlock, F. A., Mohammad, S. & Gottlob, I. 2014. Normal macular structure measured with optical coherence tomography across ethnicity. *British Journal of Ophthalmology,* 98 (7), 941-945.

Pinilla, I. M. D. P., Garcia-Martin, E. M. D., Fernandez-Larripa, S. M. D., Fuentes-Broto, L. P., Sanchez-Cano, A. I. P. & Abecia, E. M. D. P. 2013. Reproducibility and repeatability of cirrus and spectralis fourier-domain optical coherence tomography of healthy and epiretinal membrane eyes. *Retina,* 33 (7), 1448-1455.

Polito, A., Del Borrello, M., Isola, M., Zemella, N. & Bandello, F. 2005. Repeatability and reproducibility of fast macular thickness mapping with stratus optical coherence tomography. *Archives of Ophthalmology,* 123 (10), 1330-1337.

Powner, M. B., Gillies, M. C., Tretiach, M., Scott, A., Guymer, R. H., G.S., H. & Fruttiger, M. 2010. Perifoveal muller cell depletion in a case of macular telangiectasia Type 2. *Ophthalmoogy,* 117 (12), 2407-2416.

Putnam, C. M. & Bassi, C. J. 2015. Macular pigment spatial distribution effects on glare disability. *Journal of Optometry* [Online], 10.1016/j.optom.2014.12.004.

Putnam, N. M., Hofer, H. J., Doble, N., Chen, L., Carroll, J. & Williams, D. R. 2005. The locus of fixation and the foveal cone mosaic. *Journal of Vision,* 5 (7), 632-639.

Quigley, H. A. 2006. The number of people with glaucoma worldwide in 2010 and 2020. *British Journal of Ophthalmology,* 90 (3), 262-267.

Raman, R., Biswas, S., Gupta, A., Kulothungan, V. & Sharma, T. 2012a. Association of macular pigment optical density with risk factors for wet age-related macular degeneration in the Indian population. *Eye,* 26 (7), 950-957.

Raman, R., Biswas, S., Vaitheeswaran, K. & Sharma, T. 2012b. Macular pigment optical density in wet age-related macular degeneration among Indians *Eye,* 26 (8), 1052-1057.

Raman, R., Rajan, R., Biswas, S., Vaitheeswaran, K. & Sharma, T. 2011. Macular pigment optical density in a South Indian population. *Investigative Ophthalmology and Visual Science,* 52 (11), 7910-7916.

Rapp, L. M., Maple, S. S. & Choi, J. H. 2000. Lutein and zeaxanthin concentrations in rod outer segment membranes from perifoveal and peripheral human retina. *Investigative Ophthalmology and Visual Science,* 41 (5), 1200-1209.

Rauscher, F. M., Sekhon, N., Feuer, W. J. & Budenz, D. L. 2009. Myopia affects retinal nerve fiber layer measurements as determined by optical coherence tomography. *Journal of Glaucoma,* 18 (7), 501-505.

Razali, N. M. & Wah, Y. B. 2011. Power comparisons of Shapiro-Wilk, Kolmogorov-Smirnov, Lilliefors and Anderson-Darling tests. *Journal of Statistical Modeling and Analytics,* 2 (1), 21-33.

Regatieri, C. V., Branchini, L. & Duker, J. S. 2011. The role of spectral-domain OCT in the diagnosis and management of neovascular age-related macular degeneration. *Ophthalmic Surgery, Lasers & Imaging: the Official Journal of the International Society for Imaging in the Eye,* 42, S56.

Resnicow, K., Odom, E., Wang, T., Dudley, W. N., Mitchell, D., Vaughan, R., Jackson, A. & Baranowski, T. 2000. Validation of three food frequency questionnaires and 24-hour recalls with serum carotenoid levels in a sample of African-American adults. *American Journal of Epidemiology,* 152 (11), 1072-1080.

Richer, S. P. 2011. Randomized, double-blind, placebo-controlled study of zeaxanthin and visual function in patients with atrophic age-related macular degeneration. *Optometry,* 82 (11), 667-680.

Robinson, A. E. & de Sa, V. R. 2012. Spatial properties of flicker adaptation. *Vision Research,* 70, 2-6.

Robson, A. G., Moreland, J. D., Pauleikhoff, D., Morrissey, T., Holder, G. E., Fitzke, F. W., C Bird, A. & van Kuijk, F. J. G. M. 2003. Macular pigment density and distribution: comparison of fundus autofluorescence with minimum motion photometry. *Vision Research,* 43 (16), 1765-1775.

Robson, A. G. & Parry, N. R. 2008. Measurement of macular pigment optical density and distribution using the steady-state visual evoked potential. *Visual Neuroscience,* 25 (4), 575-583.

Röck, T., Wilhelm, B., Bartz-Schmidt, K. U. & Röck, D. 2014. The influence of axial length on confocal scanning laser ophthalmoscopy and spectral-domain optical coherence tomography size measurements: a pilot study. *Graefe's Archive for Clinical and Experimental Ophthalmology,* 252 (4), 589-593.

Rodriguez-Carmona, M., Kvansakul, J., Harlow, J. A., Köpcke, W., Schalch, W. & Barbur, J. L. 2006. The effects of supplementation with lutein and/or zeaxanthin on human macular pigment density and colour vision. *Ophthalmic and Physiological Optics,* 26 (2), 137-147.

Roorda, A. & Williams, D. 1999. The arrangement of the three cone classes in the living human eye. *Nature,* 397 (6719), 520-522.

Rosenberg, N. A., Pritchard, J. K., Weber, J. L., Cann, H. M., Kidd, K. K., Zhivotovsky, L. A. & Feldman, M. W. 2002. Genetic structure of human populations. *Science,* 298 (5602), 2381-2385.

Rudnicka, A. R., Burk, R. O. W., Edgar, D. F. & Fitzke, F. W. 1998. Magnification characteristics of fundus imaging systems. *Ophthalmology,* 105 (12), 2186-2192.

Saidha, S., Syc, S. B., Durbin, M. K., Eckstein, C., Oakley, J. D., Meyer, S. A., Conger, A., Frohman, T. C., Newsome, S. & Ratchford, J. N. 2011. Visual dysfunction in multiple sclerosis correlates better with optical coherence tomography derived estimates of macular ganglion cell layer thickness than peripapillary retinal nerve fiber layer thickness. *Multiple Sclerosis Journal,* 17 (12), 1449-1463.

Sanchez-Cano, A., Baraibar, B., Pablo, L. E. & Honrubia, F. M. 2008. Magnification characteristics of the optical coherence tomograph Stratus OCT 3000. *Ophthalmic and Physiological Optics,* 28 (1), 21-28.

Sasamoto, Y., Gomi, F., Sawa, M., Tsujikawa, M. & Hamasaki, T. 2010. Macular pigment optical density in central serous chorioretinopathy. *Investigative Ophthalmology and Visual Science,* 51 (10), 5219-5225.

Savini, G., Barboni, P., Parisi, V. & Carbonelli, M. 2012. The influence of axial length on retinal nerve fibre layer thickness and optic-disc size measurements by spectral-domain OCT. *British Journal of Ophthalmology,* 96 (1), 57-61.

Schachat, A. P., Hyman, L., Leske, M. C., Connell, M. S. & Wu, S. Y. 1995. Features of age-related macular degeneration in a black population. *Archive of Ophthalmology,* 113 (6), 728-735.

Schalch, W., Cohn, W., Barker, F. M., Köpcke, W., Mellerio, J., Bird, A. C., Robson, A. G., Fitzke, F. F. & van Kuijk, F. J. G. M. 2007. Xanthophyll accumulation in the human retina during supplementation with lutein or zeaxanthin - The LUXEA (LUtein Xanthophyll Eye Accumulation) study. *Archives of Biochemistry and Biophysics,* 458 (2), 128-135.

Schalch, W., Rodriguez-Carmona, M., Harlow, J. A., Barbur, J. L. & Koepcke, W. 2004. Macular pigment optical density (MPOD) measurements using visual displays - a new method and first results. *Investigative Ophthalmology and Visual Science,* 45 (5), 1296-1296.

Seddon, J. M., Sahagian, C. R., Glynn, R. J., Sperduto, R. D. & Gragoudas, E. S. 1990. Evaluation of an iris color classification system. The eye disorders case-control study group. *Investigative Ophthalmology and Visual Science,* 31 (8), 1592-1598.

Seigo, M. A., Sotirchos, E. S., Newsome, S. & Babiarz, A. 2012. In vivo assessment of retinal neuronal layers in multiple sclerosis with manual and automated optical coherence tomography segmentation techniques. *Journal of Neurology,* 259 (10), 2119-2130.

Sharifzadeh, M., Bernstein, P. S. & Gellermann, W. 2006. Nonmydriatic fluorescence-based quantitative imaging of human macular pigment distributions. *Journal of the Optical Society of America A,* 23 (10), 2373-2387.

Siah, W. F., Loughman, J. & O'Brien, C. J. 2014. The relationship between macular pigment and glaucoma-related structural parameters: a baseline evaluation of the Macular Pigment and Glaucoma Trial. *Investigative Ophthalmology and Visual Science,* 55 (13), 3490-3490.

Sim, J. & Wright, C. C. 2005. The Kappa statistic in reliability studies: use, interpretation, and sample size requirements. *Physical Therapy,* 85 (3), 257-268.

Snodderly, D. M., Auran, J. D. & Delori, F. C. 1984a. The macular pigment II. Spatial distribution in primate retinas. *Investigative Ophthalmology and Visual Science,* 25 (6), 674-685.

Snodderly, D. M., Brown, P. K., Delori, F. C. & Auran, J. D. 1984b. The macular pigment I. Absorbance spectra, localization, and discrimination from other yellow pigments in primate retinas. *Investigative Ophthalmology and Visual Science,* 25 (6), 660-673.

Snodderly, D. M., Handelman, G. J. & Adler, A. J. 1991. Distribution of individual macular pigment carotenoids in central retina of macaque and squirrel monkeys. *Investigative Ophthalmology and Visual Science,* 32 (2), 268-279.

Snodderly, D. M., Mares, J. A., Wooten, B. R., Oxton, L., Gruber, M. & Ficek, T. 2004. Macular pigment measurement by heterochromatic flicker photometry in older subjects: the Carotenoids and Age-Related Eye Disease Study. *Investigative Ophthalmology and Visual Science,* 45 (2), 531-538.

Song, H., Chui, T. Y. P., Zhong, Z., Elsner, A. E. & Burns, S. A. 2011. Variation of cone photoreceptor packing density with retinal eccentricity and age. *Investigative Ophthalmology and Visual Science,* 52 (10), 7376-7384.

Song, W. K., Lee, S. C., Lee, E. S., Kim, C. Y. & Kim, S. S. 2010. Macular thickness variations with sex, age, and axial length in healthy subjects: a spectral domain optical coherence tomography study. *Investigative Ophthalmology and Visual Science,* 51 (8), 3913-3918.

Spaide, R. F. & Curcio, C. A. 2011. Anatomical correlates to the bands seen in the outer retina by optical coherence tomography: literature review and model. *Retina,* 31 (8), 1609-1619.

Srinivasan, V. J., Monson, B. K., Wojtkowski, M., Bilonick, R. A., Gorczynska, I., Chen, R., Duker, J. S., Schuman, J. S. & Fujimoto, J. G. 2008. Characterization of outer retinal morphology with high-speed, ultrahigh-resolution optical coherence tomography. *Investigative Ophthalmology and Visual Science,* 49 (4), 1571-1579.

Stockman, A. & Sharpe, L. T. 2000. The spectral sensitivities of the middle- and long-wavelength-sensitive cones derived from measurements in observers of known genotype. *Vision Research,* 40 (13), 1711-1737.

Stringham, J. M., Fuld, K. & Wenzel, A. J. 2003. Action spectrum for photophobia. *Journal of the Optical Society of America A,* 20 (10), 1852-1858.

Stringham, J. M., Fuld, K. & Wenzel, A. J. 2004. Spatial properties of photophobia. *Investigative Ophthalmology and Visual Science,* 45 (10), 3838-3848.

Stringham, J. M. & Hammond, B. R. 2007. The glare hypothesis of macular pigment function. *Optometry and Vision Science,* 84 (9), 859-864.

Stringham, J. M. & Hammond, B. R. 2008. Macular pigment and visual performance under glare conditions. *Optometry and Vision Science,* 85 (2), 82-88.

Stringham, J. M., Hammond, B. R., Nolan, J. M., Wooten, B. R., Mammen, A., Smollon, W. & Snodderly, D. M. 2008. The utility of using customized heterochromatic flicker photometry (cHFP) to measure macular pigment in patients with age-related macular degeneration. *Experimental Eye Research,* 87 (5), 445-453.

Stringham, J. M., Hammond, B. R., Wooten, B. R. & Snodderly, D. M. 2006. Compensation for light loss resulting from filtering by macular pigment: relation to the s-cone pathway. *Optometry and Vision Science,* 83 (12), 887-894.

Sujak, A., Gabrielska, J., Grudzinski, W., Borc, R., Mazurek, P. & Gruszecki, W. I. 1999. Lutein and zeaxanthin as protectors of lipid membranes against oxidative damage: the structural aspects. *Archives of Biochemistry and Biophysics,* 371 (2), 301-307.

Tan, C. S. H., Li, K. Z. & Lim, T. H. 2012. A novel technique of adjusting segmentation boundary layers to achieve comparability of retinal thickness and volumes

270

between spectral domain and time domain optical coherence tomography. *Investigative Ophthalmology and Visual Science,* 53 (9), 5515-5519.

Tan, J. C., Poinoosawmy, D., Fitzke, F. W. & Hitchings, R. A. 2004. Magnification changes in scanning laser tomography. *Journal of Glaucoma,* 13 (2), 137-141.

Tang, C. Y., Yip, H., Poon, M., Yau, W. & Yap, M. K. H. 2004. Macular pigment optical density in young Chinese adults. *Ophthalmic and Physiological Optics,* 24 (6), 586-593.

Tariq, A., Mahroo, O. A., Williams, K. M., Liew, S. H. M., Beatty, S., Gilbert, C. E., Van Kuijk, F. J. & Hammond, C. J. 2014. The heritability of the ring-like distribution of macular pigment assessed in a twin study. *Investigative Ophthalmology and Visual Science,* 55 (4), 2214-2219.

Tariq, Y. M., Samarawickrama, C., Pai, A., Burlutsky, G. & Mitchell, P. 2010. Impact of ethnicity on the correlation of retinal parameters with axial length. *Investigative Ophthalmology & Visual Science,* 51 (10), 4977-4982.

Thibos, L., Wheeler, W. & Horner, D. 1997. Power vectors: an application of fourier analysis to the description and statistical analysis of refractive error. *Optometry and Vision Science,* 74 (6), 367-375.

Thiele, S., Rauscher, F. G., Wiedemann, P. & Dawczynski, J. 2015. Influence of macular oedema on the measurement of macular pigment optical density. *Graefe's Archive for Clinical and Experimental Ophthalmology,* 10.1007/s00417-015-3079-y.

Tick, S., Rossant, F., Ghorbel, I., Gaudric, A., Sahel, J. A., Chaumet-Riffaud, P. & Paques, M. 2011. Foveal shape and structure in a normal population. *Investigative Ophthalmology and Visual Science,* 52 (8), 5105-5110.

Tomany, S. C., Cruickshanks, K. J., Klein, R., Klein, B. E. K. & Knudtson, M. D. 2004. Sunlight and the 10-year incidence of age-related maculopathy: the Beaver Dam eye study. *Archives of Ophthalmology,* 122 (5), 750-757.

Trieschmann, M., Beatty, S., Nolan, J. M., Hense, H. W., Heimes, B., Austermann, U., Fobker, M. & Pauleikhoff, D. 2007. Changes in macular pigment optical density and serum concentrations of its constituent carotenoids following supplemental lutein and zeaxanthin: the LUNA study. *Experimental Eye Research,* 84 (4), 718-728.

Trieschmann, M., Heimes, B., Hense, H. W. & Pauleikhoff, D. 2006. Macular pigment optical density measurement in autofluorescence imaging: comparison of one- and two-wavelength methods. *Graefe's Archive for Clinical and Experimental Ophthalmology,* 44, 1565-1574.

Trieschmann, M., Spital, G., Lommatzsch, A., van Kuijk, E., Fitzke, F., Bird, A. C. & Pauleikhoff, D. 2003. Macular pigment: quantitative analysis on autofluorescence images. *Graefe's Archive for Clinical and Experimental Ophthalmology,* 241 (12), 1006-1012.

Trieschmann, M., van Kuijk, F. J., Alexander, R., Hermans, P., Luthert, P., Bird, A. C. & Pauleikhoff, D. 2008. Macular pigment in the human retina: histological evaluation of localization and distribution. *Eye,* 22, 132-137.

Vajzovic, L., Hendrickson, A. E., O'Connell, R. V., Clark, L. A., Tran-Viet, D., Possin, D., Chiu, S. J., Farsiu, S. & Toth, C. A. 2012. Maturation of the human fovea: correlation of spectral-domain optical coherence tomography findings with histology. *American Journal of Ophthalmology,* 154 (5), 779-789.

van de Kraats, J., Berendschot, T. T. J. M., Valen, S. & van Norren, D. 2006. Fast assessment of the central macular pigment density with natural pupil using the macular pigment reflectometer. *Journal of Biomedical Optics,* 11 (6), 064031-064031.

van de Kraats, J., Kanis, M. J., Genders, S. W. & van Norren, D. 2008. Lutein and zeaxanthin measured separately in the living human retina with fundus reflectometry. *Investigative Ophthalmology and Visual Science,* 49 (12), 5568-5573.

van den Berg, T. J. T. P., Ijspeert, J. K. & de Waard, P. W. T. 1991. Dependence of intraocular straylight on pigmentation and light transmission through the ocular wall. *Vision Research,* 31 (7–8), 1361-1367.

van der Veen, R., Berendschot, T. T. J. M., Hendrikse, F., Carden, D., Makridaki, M. & Murray, I. 2009a. A new desktop instrument for measuring macular pigment optical density based on a novel technique for setting flicker thresholds. *Ophthalmic and Physiological Optics,* 29 (2), 127-137.

van der Veen, R. L., Berendschot, T. T. J. M., Makridaki, M., Hendrikse, F., Carden, D. & Murray, I. J. 2009b. Correspondence between retinal reflectometry and a flicker- based technique in the measurement of macular pigment spatial profiles. *Journal of Biomedical Optics,* 14 (6), 064046.

van der Veen, R. L. P., Ostendorf, S., Hendrikse, F. & Berendschot, T. T. J. M. 2009c. Macular pigment optical density relates to foveal thickness. *European Journal of Ophthalmology,* 19 (5), 836-841.

Varma, R., Skaf, M. & Barron, E. 1996. Retinal nerve fiber layer thickness in normal human eyes. *Ophthalmology,* 103 (12), 2114-2119.

Verkicharla, P. K., Mallen, E. A. H. & Atchison, D. A. 2013. Repeatability and comparison of peripheral eye lengths with two instruments. *Optometry and Vision Science,* 90 (3), 215-222.

Visser, N., Berendschot, T., Verbakel, F., de Brabander, J. & Nuijts, R. 2012. Comparability and repeatability of corneal astigmatism measurements using different measurement technologies. *Journal of Cataract and Refractive Surgery,* 38 (10), 1764-1770.

Vyas, A., Greenhalgh, A., Cade, J., Sanghera, B., Riste, L., Sharma, S. & Cruickshank, K. 2003. Nutrient intakes of an adult Pakistani, European and African-Caribbean community in inner city Britain. *Journal of Human Nutrition and Dietetics,* 16 (5), 327-337.

Wagner-Schuman, M., Dubis, A. M., Nordgren, R. N., Lei, Y., Odell, D., Chiao, H., Weh, E., Fischer, W., Sulai, Y., Dubra, A. & Carroll, J. 2011. Race- and sex-related differences in retinal thickness and foveal pit morphology. *Investigative Ophthalmology and Visual Science,* 52 (1), 625-634.

Wakitani, Y., Sasoh, M., Sugimoto, M., Ito, Y., Ido, M. & Uji, Y. 2003. Macular thickness measurements in healthy subjects with different axial lengths using optical coherence tomography. *Retina,* 23 (2), 177-182.

Wang, W., Connor, S. L., Johnson, E. J., Klein, M. L., Hughes, S. & Connor, W. E. 2007. Effect of dietary lutein and zeaxanthin on plasma carotenoids and their transport in lipoproteins in age-related macular degeneration. *American Journal of Clinical Nutrition,* 85 (3), 762-769.

Weale, R. A. 1988. Age and the transmittance of the human crystalline lens. *The Journal of Physiology,* 395 (1), 577-587.

Werner, J. S., Bieber, M. L. & Schefrin, B. E. 2000. Senescence of foveal and parafoveal cone sensitivities and their relations to macular pigment density. *Journal of the Optical Society of America A,* 17 (11), 1918-1932.

Werner, J. S., Donnelly, S. K. & Kliegl, R. 1987. Aging and human macular pigment density: appended with translations from the work of Max Schultze and Ewald Hering. *Vision Research,* 27 (2), 257-268.

Whitmer, R. A., Mayeda, E. R., Quesenberry, C. P., Lu, W., & Glymour, M. 2014. Ethnic and racial disparities in ten-year cumulative prevalence of dementia and alzheimer's disease. *Alzheimer's & Dementia: The Journal of the Alzheimer's Association*, *10* (4), 152.

Wolf-Schnurrbusch, U. E. K., Ceklic, L., Brinkmann, C. K., Iliev, M. E., Frey, M., Rothenbuehler, S. P., Enzmann, V. & Wolf, S. 2009. Macular thickness measurements in healthy eyes using six different optical coherence tomography instruments. *Investigative Ophthalmology and Visual Science,* 50 (7), 3432-3437.

Wolf-Schnurrbusch, U. E. K., Röösli, N., Weyermann, E., Heldner, M. R., Höhne, K. & Wolf, S. 2007. Ethnic differences in macular pigment density and distribution. *Investigative Ophthalmology and Visual Science,* 48 (8), 3783-3787.

Wong, A. C., Chan, C. W. & Hui, S. P. 2005. Relationship of gender, body mass index, and axial length with central retinal thickness using optical coherence tomography. *Eye,* 19, 292-297.

Wooten, B. R. & Hammond, B. R. 2002. Macular pigment: Influences on visual acuity and visibility. *Progress in Retinal and Eye Research,* 21 (2), 225-240.

Wooten, B. R. & Hammond, B. R. 2005. Spectral absorbance and spatial distribution of macular pigment using heterochromatic flicker photometry. *Optometry and Vision Science,* 82 (5), 378-386.

Wooten, B. R., Hammond, B. R., Land, R. I. & Snodderly, D. M. 1999. A practical method for measuring macular pigment optical density. *Investigative Ophthalmology and Visual Science,* 40 (11), 2481-2489.

World Health Organization. 2015. *Obesity and overweight* [Online]. Available: http://www.who.int/mediacentre/factsheets/fs311/en/ [Accessed 14th June 2015 2015].

World Health Organization Expert Consultation 2004. Appropriate body-mass index for Asian populations and its implications for policy and intervention strategies. *The Lancet,* 363 (9403), 157-163.

Wustemeyer, H., Moessner, A., Jahn, C. & Wolf, S. 2003. Macular pigment density in healthy subjects quantified with a modified confocal scanning laser ophthalmoscope. *Graefe's Archive of Clinical and Experimental Ophthalmology,* 241 (8), 647-651.

Yam, J. S. & Kwok, A. H. 2014. Ultraviolet light and ocular diseases. *International Ophthalmology,* 34 (2), 383-400.

Yamada, M., Hiratsuka, Y., Roberts, C. B., Pezzullo, M. L., Yates, K., Takano, S., Miyake, K. & Taylor, H. R. 2010. Prevalence of visual impairment in the adult Japanese population by cause and severity and future projections. *Ophthalmic Epidemiology,* 17 (1), 50-57.

Yeum, K. J., Taylor, A., Tang, G. & Russell, R. M. 1995. Measurement of carotenoids, retinoids, and tocopherols in human lenses. *Investigative Ophthalmology and Visual Science,* 36 (13), 2756-2761.

Yu, J., Johnson, E. J., Shang, F., Lim, A., Zhou, H., Cui, L., Xu, J., Snellingen, T., Liu, X., Wang, N. & Liu, N. 2012. Measurement of macular pigment optical density in a healthy Chinese population sample. *Investigative Ophthalmology and Visual Science,* 53 (4), 2106-2111.

Yuodelis, C. & Hendrickson, A. 1986. A qualitative and quantitative analysis of the human fovea during development. *Vision Research,* 26 (6), 847-855.

Zeffren, B. S., Applegate, R. A., Bradley, A. & van Heuven, W. A. 1990. Retinal fixation point location in the foveal avascular zone. *Investigative Ophthalmology and Visual Science,* 31 (10), 2099-2105.

Zeimer, M., Dietzel, M., Hense, H. W., Heimes, B., Austermann, U. & Pauleikhoff, D. 2012. Profiles of macular pigment optical density and their changes following supplemental lutein and zeaxanthin: New results from the LUNA study. *Investigative Ophthalmology and Visual Science,* 53 (8), 4852-4859.